

1998

Modeling the fate and transport of agricultural pollutants and their environmental impact on surface and subsurface water quality

Se-Woong Chung
Iowa State University

Follow this and additional works at: <https://lib.dr.iastate.edu/rtd>

 Part of the [Environmental Sciences Commons](#), and the [Hydrology Commons](#)

Recommended Citation

Chung, Se-Woong, "Modeling the fate and transport of agricultural pollutants and their environmental impact on surface and subsurface water quality" (1998). *Retrospective Theses and Dissertations*. 11914.
<https://lib.dr.iastate.edu/rtd/11914>

This Dissertation is brought to you for free and open access by the Iowa State University Capstones, Theses and Dissertations at Iowa State University Digital Repository. It has been accepted for inclusion in Retrospective Theses and Dissertations by an authorized administrator of Iowa State University Digital Repository. For more information, please contact digirep@iastate.edu.

INFORMATION TO USERS

This manuscript has been reproduced from the microfilm master. UMI films the text directly from the original or copy submitted. Thus, some thesis and dissertation copies are in typewriter face, while others may be from any type of computer printer.

The quality of this reproduction is dependent upon the quality of the copy submitted. Broken or indistinct print, colored or poor quality illustrations and photographs, print bleedthrough, substandard margins, and improper alignment can adversely affect reproduction.

In the unlikely event that the author did not send UMI a complete manuscript and there are missing pages, these will be noted. Also, if unauthorized copyright material had to be removed, a note will indicate the deletion.

Oversize materials (e.g., maps, drawings, charts) are reproduced by sectioning the original, beginning at the upper left-hand corner and continuing from left to right in equal sections with small overlaps. Each original is also photographed in one exposure and is included in reduced form at the back of the book.

Photographs included in the original manuscript have been reproduced xerographically in this copy. Higher quality 6" x 9" black and white photographic prints are available for any photographs or illustrations appearing in this copy for an additional charge. Contact UMI directly to order.

UMI

A Bell & Howell Information Company
300 North Zeeb Road, Ann Arbor MI 48106-1346 USA
313/761-4700 800/521-0600



**Modeling the fate and transport of agricultural pollutants and their environmental
impact on surface and subsurface water quality**

by

Se-Woong Chung

A dissertation submitted to the graduate faculty
in partial fulfillment of the requirements for the degree of

DOCTOR OF PHILOSOPHY

Major: Civil Engineering (Environmental Engineering)

Major Professor: Ruochuan Gu

Iowa State University

Ames, Iowa

1998

Copyright © Se-Woong Chung, 1998. All rights reserved.

UMI Number: 9911588

**UMI Microform 9911588
Copyright 1999, by UMI Company. All rights reserved.**

**This microform edition is protected against unauthorized
copying under Title 17, United States Code.**

UMI
300 North Zeeb Road
Ann Arbor, MI 48103

Graduate College
Iowa State University

This is to certify that the Doctoral dissertation of

Se-Woong Chung

has met the dissertation requirements of Iowa State University

Signature was redacted for privacy.

Major Professor

Signature was redacted for privacy.

For the Major Program

Signature was redacted for privacy.

For the Graduate College

TABLE OF CONTENTS

LIST OF FIGURES	v
LIST OF TABLES	ix
ABSTRACT	xii
CHAPTER 1. GENERAL INTRODUCTION	1
Background	1
Problem Statement	3
Objectives	6
Dissertation Organization	6
References	7
CHAPTER 2. TWO-DIMENSIONAL MODELING OF THE FATE AND TRANSPORT OF TOXIC CONTAMINANTS IN A RESERVOIR	9
Abstract	9
Introduction	9
Previous Studies	11
Model Development	12
Model Application	22
Results and Discussion	29
Conclusions	49
References	50
Notations	53
CHAPTER 3. ESTIMATING TIME-VARIABLE KINETIC TRANSFORMATION RATE OF ATRAZINE IN A RESERVOIR	56
Abstract	56
Introduction	56
Description of Study Site	61
Method	64
Results and Discussion	72
Conclusions	84
References	85
Notations	88
CHAPTER 4. PREDICTION OF THE FATE AND TRANSPORT OF ATRAZINE WITH A 2D RESERVOIR TOXIC MODEL	90
Abstract	90
Introduction	90

Method	93
Model Application	99
Results and Discussion	108
Conclusions	120
References	121
Notations	125
CHAPTER 5. VALIDATION OF EPIC FOR TWO WATERSHEDS IN SOUTHWEST IOWA	127
Abstract	127
Introduction	127
Materials and Methods	130
Results and Discussion	139
Summary and Conclusions	151
Acknowledgments	152
References	152
CHAPTER 6. USE OF EPIC FOR ASSESSING THE ENVIRONMENTAL IMPACT OF ALTERNATIVE AGRICULTURAL MANAGEMENT SYSTEMS	157
Abstract	157
Introduction	157
Materials and Methods	159
Results and Discussion	166
Summary and Conclusions	182
References	183
CHAPTER 7. GENERAL CONCLUSIONS	186
Model Development	186
Effects of Flow Regime on the MITC Degradation	186
The Fate and Transport of Atrazine	187
Evaluation of EPIC Model	188
Contribution	190
Future Research	190
References	191
APPENDIX. SOURCE PROGRAM OF THE 2D RESERVOIR TOXIC SUBMODEL	193
ACKNOWLEDGMENTS	207

LIST OF FIGURES**CHAPTER 2. TWO-DIMENSIONAL MODELING OF THE FATE AND TRANSPORT OF TOXIC CONTAMINANTS IN A RESERVOIR**

- Figure 1. Map of the spill site and sampling stations in the Shasta Reservoir. 13
- Figure 2. Schematic of transport and transformation processes of a toxic substance in a reservoir system. 17
- Figure 3. Flow chart of the 2D reservoir toxic model. 20
- Figure 4. The fraction of dissolved form to the total MITC concentration in water as a function of sediments concentration and fraction of organic carbon. 26
- Figure 5. The first-order hydrolysis reaction rate and half-life of MITC in water as a function of pH. 27
- Figure 6. The inflow boundary MITC concentrations that measured at the upper head of the Shasta Reservoir (Doney Creek) during the spill. 28
- Figure 7. The (a) flow velocity vector field and (b) contour of reservoir water temperature in the Shasta Reservoir during the spill at 9:00 a.m. on 7/23/91. 30
- Figure 8. Contours of the simulated (a) MITC concentrations and (b) concentration difference between tracer and MITC that represents the amount of contaminant reduction by physico-chemical reactions. 31
- Figure 9. Observed and simulated MITC concentrations at selected sampling stations during the spill. 35
- Figure 10. The linear relationships of observed and simulated MITC concentrations versus time during the early stage of the spill. 36
- Figure 11. Observed MITC and simulated tracer and MITC concentrations at Stations 9 and 16 (downstream of the artificial mixing device). 37
- Figure 12. The spatial distributions of tracer (top) and MITC (bottom) concentrations in (a) the interflow regime and (b) the overflow
-

	regime after 10 days (7/26/91) in the Shasta Reservoir.	39
Figure 13.	The longitudinal profiles of maximum tracer and MITC concentrations in (a) the interflow and (b) overflow regimes after 10 days.	41
Figure 14.	The spatial distributions of tracer concentrations in a hypothetical reservoir after 20 days in the (a) interflow and (b) overflow for different values of Richardson number.	46
Figure 15.	The spatial distributions of MITC concentrations in a hypothetical reservoir after 20 days in the (a) interflow and (b) overflow for different values of Richardson number.	47
Figure 16.	Maximum concentrations of tracer and MITC versus distance for (a) low Ri (0.17), (b) medium Ri (2.82), and (c) high Ri (68.3).	48
 CHAPTER 3. ESTIMATING TIME-VARIABLE KINETIC TRANSFORMATION RATE OF ATRAZINE IN A RESERVOIR		
Figure 1.	Atrazine and its degradation products.	58
Figure 2.	Map of study site and the location of sampling stations.	62
Figure 3.	Schematic description of the mass balance model for atrazine in the Saylorville Reservoir, Iowa.	65
Figure 4.	Comparison of model results with observed atrazine concentrations.	75
Figure 5.	Relations of time-variable atrazine half-life to (a) the daily hours of sunlight and (b) water temperature.	77
Figure 6.	Estimated annual atrazine mass budget in the Saylorville Reservoir, Iowa.	79
Figure 7.	The fraction of dissolved atrazine to total concentrations as a function of sediments concentrations and organic carbon fraction in water.	81
Figure 8.	Saylorville reservoir water quality response to changes in atrazine use.	83

CHAPTER 4. PREDICTION OF THE FATE AND TRANSPORT OF ATRAZINE WITH A 2D RESERVOIR TOXIC MODEL

Figure 1.	Map of the Saylorville Reservoir, vicinity area, and sampling Stations.	94
Figure 2.	The finite difference grid system of the Saylorville Reservoir: (a) plan view, (b) vertical view, and (c) cross sectional view.	101
Figure 3.	Comparison of elevation-capacity curve obtained from model bathymetry data with project elevation-capacity curve of the Saylorville Reservoir.	103
Figure 4.	Daily precipitation, inflow, outflow, and storage of the Saylorville Reservoir during the study period.	104
Figure 5.	Estimated monthly-distributed flow (Q_d), atrazine mass loading (M_d), and concentration (C_d) in 1978 for the Saylorville Reservoir.	107
Figure 6.	Observed and simulated reservoir water surface elevations.	109
Figure 7.	Seasonal reservoir circulation patterns during (a) early spring, (b) late spring, (c) summer, and (d) fall.	111
Figure 8.	Observed river water and reservoir surface water temperatures on 3/21, 5/24, 7/25, and 9/26.	112
Figure 9.	Simulated and observed seasonal thermal structures of the Saylorville Reservoir during (a) early spring, (b) late spring, (c) summer, and (d) fall.	114
Figure 10.	Simulated and observed spatial distributions of atrazine in the Saylorville Reservoir during (a) early spring, (b) late spring, (c) summer, and (d) fall.	116
Figure 11.	Observed and simulated (a) water temperatures and (b) atrazine concentrations versus time at three depths (surface, middle, and bottom) in the reservoir.	118
Figure 12.	Observed and simulated depth-mean (a) water temperatures and (b) atrazine concentrations versus time in the reservoir.	119

CHAPTER 5. VALIDATION OF EPIC FOR TWO WATERSHEDS IN SOUTHWEST IOWA

- Figure 1. Annual precipitation, observed and simulated surface runoff and seepage flows for (a) Watershed 2 and (b) Watershed 3 during the validation period. 143
- Figure 2. Observed and simulated annual leached $\text{NO}_3\text{-N}$ for (a) Watersheds 2 and (b) Watershed 3 during the validation period. 147
- Figure 3. Observed and simulated annual $\text{NO}_3\text{-N}$ runoff loss for (a) Watershed 2 and (b) Watershed 3 during the validation period. 148
- Figure 4. Observed and simulated annual crop yield for (a) Watersheds 2 and (b) Watershed 3 during the validation period. 150

CHAPTER 6. USE OF EPIC FOR ASSESSING THE ENVIRONMENTAL IMPACT OF ALTERNATIVE AGRICULTURAL MANAGEMENT SYSTEMS

- Figure 1. Observed and simulated monthly subsurface drain flows under (a) moldboard, (b) chisel plow, and (c) no-till systems for 1990-1992 at Nashua, Iowa. 169
- Figure 2. Observed and simulated daily subsurface drain flows under no-till and continuous corn rotation for 1990 at Nashua, Iowa. 170
- Figure 3. Observed and simulated monthly leached $\text{NO}_3\text{-N}$ under (a) moldboard, (b) chisel plow, and (c) no-till systems for 1990-1992 at Nashua, Iowa. 173
- Figure 4. Observed and simulated daily $\text{NO}_3\text{-N}$ losses under no-till and continuous corn rotation for 1990 at Nashua, Iowa. 175
- Figure 5. Observed and simulated crop yields under (a) continuous corn and (b) soybean-corn rotation systems for 1990-1992 at Nashua, Iowa. 180

LIST OF TABLES

CHAPTER 2. TWO-DIMENSIONAL MODELING OF THE FATE AND TRANSPORT OF TOXIC CONTAMINANTS IN A RESERVOIR	
Table 1. Physical and chemical properties of methyl isothiocyanate (MITC).	24
Table 2. The effects of flow dilution and physico-chemical reactions on total MITC reduction versus time in various reservoir flow regimes.	33
Table 3. Effects of reservoir flow regime on the fate and transport of the toxic contaminant, MITC, in the late stage of the spill.	42
Table 4. Reservoir flow regimes and inflow conditions used in the hypothetical case study.	44
CHAPTER 3. ESTIMATING TIME-VARIABLE KINETIC TRANSFORMATION RATE OF ATRAZINE IN A RESERVOIR	
Table 1. Atrazine half-life values documented in the previous studies.	59
Table 2. Description of sampling stations.	63
Table 3. Input parameters used for estimating time-variable kinetic transformation rate of atrazine in the Saylorville Reservoir.	68
Table 4. Monthly input data used for mass balance model at the study site.	69
Table 5. Physical and chemical properties of atrazine.	71
Table 6. Estimated atrazine half-life values for each month.	73
Table 7. Scenarios for different atrazine uses in the upstream watershed of the Saylorville Reservoir, IA.	82
CHAPTER 4. PREDICTION OF THE FATE AND TRANSPORT OF ATRAZINE WITH A 2D RESERVOIR TOXIC MODEL	

Table 1.	Time-variable kinetic transformation rate and half-life of atrazine.	97
Table 2.	Hydrodynamics and transport model coefficients used in the model.	108
CHAPTER 5. VALIDATION OF EPIC FOR TWO WATERSHEDS IN SOUTHWEST IOWA		
Table 1.	Properties by layer for the Monona soil.	132
Table 2.	Results of the univariate normality test for the observed annual hydrologic and environmental state variables.	138
Table 3.	Model parameters for conventional and ridge till systems in Treynor, IA.	140
Table 4.	Observed and simulated annual hydrologic variable summary statistics for the 1988-93 calibration period.	141
Table 5.	Observed and simulated annual hydrologic variable summary statistics for the 1976-1987 validation period.	142
Table 6.	Parametric model evaluation statistics for the simulated hydrologic variables over the 1976-1987 validation period.	144
Table 7.	Observed and simulated annual environmental summary statistics for the 1976-1987 validation period.	145
Table 8.	Non-parametric model evaluation statistics for the simulated environmental variables for the 1976-87 validation period.	149
CHAPTER 6. USE OF EPIC FOR ASSESSING THE ENVIRONMENTAL IMPACT OF ALTERNATIVE AGRICULTURAL MANAGEMENT SYSTEMS		
Table 1.	Soil properties used in the simulations for Nashua site, Iowa.	161
Table 2.	Observed and simulated annual total subsurface drain flows (mm).	168
Table 3.	Observed and simulated annual total leached nitrogen (kg/ha).	172
Table 4.	The statistics used to evaluate the performance of EPIC model.	176

Table 5.	The results of t-test used to assess the model reliability for tillage effects.	178
Table 6.	The results of t-test used to assess the model reliability for crop rotation effects.	181

ABSTRACT

This dissertation contains five journal papers describing the modeling efforts that devoted to understand the fate and transport processes of agricultural chemicals (pesticides and fertilizer) in aquatic environments and their impacts on surface and subsurface water quality. The main tasks were (1) to develop and apply a two-dimensional (2D) reservoir toxic model, as a sub-model of the CE-QUAL-W2, for simulating toxic substances and (2) to evaluate the performance and reliability of a field-scale nonpoint source model, Erosion Productivity Impact Calculator (EPIC), as a tool for agricultural policy analysis.

The 2D toxic model was developed using finite difference numerical solutions to the laterally integrated hydrodynamics, mass transport, and transformation equations. It was applied to the Shasta Reservoir, California to investigate the effects of reservoir flow regime on the persistence and behavior of a spilled toxic compound, methyl isothiocyanate (MITC). The results showed that the interflow that developed during the spill in the Shasta Reservoir slowed down the physico-chemical decay processes of MITC due to a reduced volatilization in deep layers. The amount of chemical loss through kinetic degradation processes was insignificant in the early stage of the spill, but the importance of these processes increased with time as the turbulent mixing diminished. In the late stage, the physico-chemical reactions became a dominant pathway that reduces the contaminant concentrations. A case study demonstrated that reservoir flow regime substantially affects the persistence of the volatile toxic contaminant in the stratified reservoir. The overflow regime resulted in a reduced toxic contamination level (less persistent), shorter plume length, and longer response time compare to the interflow. These differences may be considered in water quality management as water intake structures and recreational activities are mostly located downstream near the dam.

The model was also tested and validated using field data for a herbicide, atrazine [2-chloro-4-ethylamino-6-isopropylamino-1,3,5-triazine], collected from the Saylorville Reservoir, Iowa. The seasonal half-life of atrazine in the Saylorville Reservoir was estimated with a mass balance concept and used as input for the 2D toxic model. The half-life varied

monthly from 2 to 58 days depending upon environmental conditions. An inverse relation was found between the half-life and the daily hours of sunlight, showing the significance of photodegradation at the study site. The fate and transport of atrazine were investigated using seasonal flow circulation patterns, thermal structures, and spatial and temporal distributions of atrazine concentrations. In general, no strong thermal stratification in the Saylorville Reservoir was noticed from both observed and simulated results. The effect of flow short-circuiting on the transport of atrazine was notable during summer and resulted in less mixing near the surface of the reservoir. The model accurately simulated the temporal variations of observed atrazine concentrations and captured the peak concentrations. The use of monthly half-life led to more accurate predictions of atrazine concentration because of time-varying environmental conditions such as temperature and sunlight. The assumption of steady transformation rate over the entire periods resulted in a 40% overestimation in predicting peak concentrations.

The EPIC model was tested at two field sites in Iowa. The model's performance was evaluated through simulations of subsurface drain flow, nitrogen loss, and crop yield in response to various tillage and crop rotation systems. Based on the EPIC evaluation study, it is concluded that standard tabulated curve number values should be adequately reduced to represent the impacts of residue cover on the partition of precipitation between surface runoff and infiltration. The results showed that EPIC is sensitive to variations in tillage and cropping practices and can be used to estimate long-term environmental indicators in response to different management systems. However, clear discrepancies occurred between some model estimates and corresponding measured values, e.g., under-prediction of peak flows and nitrogen losses during storm events. Two potential sources of these errors include: (1) the lack of a preferential flow component, and (2) nitrogen transformation routines that may not adequately reflect all of the processes that occur in the field. EPIC also showed a limited capability to reproduce tillage and crop rotation effects on crop yield.

CHAPTER 1. GENERAL INTRODUCTION

Background

The great production efficiency of modern agriculture has heavily relied on the use of various agricultural chemicals such as herbicides, fungicides, insecticides, and chemical fertilizers. Even though modern agriculture is credited with providing plentiful low-cost supplies of food, it has also been accused of creating numerous environmental problems (Canter 1986). When these chemicals first began to use, concern about the environmental consequences was minimal. In the mid-1960's, however, small groups of people and government agencies were awakened to its new significance that some agricultural chemicals were damaging the environment, and may be affecting human as well. The United States Environmental Protection Agency (EPA) recognized the harmful effects of some persistent chemicals (i.e., DDT, DDE, aldrin, and dieldrin) and eventually banned their use in 1970's. Thereafter, chemical manufacturers began to produce new chemicals that were more effective and thought to be environmentally sound.

Although modern agricultural chemicals are less persistent in the nature and their impacts on human health are not well understood, the public has shown a great deal of concern because their extensive transport and intensive use in agricultural lands are likely to bear various environmental risks either by intended or unintended ways. For instance, some accidental spills of toxic pesticides into river and reservoir systems seriously affected fisheries and local water supply systems in a short time period (Capel et al 1988; Chatterjee 1991). Chemical spill into a surface water system is not a matter of frequent incident, but the environmental and economic losses are fatal for a community. In the Midwest of United States, the agricultural pollutants are the major non-point source that contaminating river and reservoir water quality. The occurrences of significant level of nitrate and pesticides concentrations in groundwater, rivers, and reservoirs are seriously concerned because of not only for its potential adverse impacts on aquatic organisms and human health but also for economic perspectives (Thurman et al. 1991; Goolsby et al 1993; Hallberg 1996). Since these chemicals are not easily eliminated from drinking water by conventional water treatment

processes, tap water concentrations are similar to raw water concentrations unless an advanced treatment process such as ion exchange and carbon filtration is employed (Hallberg 1996).

Agricultural chemicals can reach surface and subsurface water system through various pathways: surface runoff, seepage flow, artificial drain flow, aerial drift during application and redeposition in waters upon volatilization, precipitation, and accidental spill. Their fate, transport, and exposure level in the environment depend upon various factors: chemical own properties such as solubility, sorption potential, volatility, and persistence; application amount; agricultural management practices; weather; and hydrologic conditions of watershed. Conway and Pretty (1991) reported the average nitrogen fertilizer applications to arable and permanent crops in U.S. is about 75 kg-N/ha. In Iowa, an average of 137 kg-N/ha was applied to corn fields as fertilizer in 1990. Atrazine, one of the most intensively used herbicides in corn cropping area, is the most frequently detected chemical with highest concentrations in 76 Midwestern reservoirs. A survey of pesticides used in Iowa crop production in 1990 showed that 61% of the corn crop land (roughly 3 million ha) in Iowa was treated with atrazine, corresponding to an application of 3.4 million kg of active ingredient. The United States Department of Agriculture (USDA)'s 1992 National Resource Inventory (NRI) data revealed that about 152 and 718 thousand tons of nitrogen lost from agricultural lands of Iowa and Corn Belt area, respectively, through leaching and runoff (Babcock et al. 1997). The loss of Atrazine was about 10 and 95 thousand kilograms for the same areas, respectively. Therefore, the important research questions are "What is the fate of these off-site chemicals and how persistent in the environment?" and "What are the environmental impacts of these chemicals on the ecosystem and human health?".

Over the past decades, studies have been conducted to investigate the fate and transport processes of these agricultural pollutants in the nature and so as to develop better management practices for minimizing their adverse impacts on the environment. A great number of experimental studies have provided essential data and important answers towards understanding these processes, but they are often site-specific to some degree and

prohibitively costly to perform in all cases to directly extend experimental results from a small number of hypothetical scenarios to all conceivable situations.

Therefore, mathematical simulation models, as a proxy for experimental approaches, are increasingly used to enhance the understanding of these processes and assess the impacts of the off-site transport of these pollutants on economic and environmental outcomes. The concept, capabilities, and limitations of these mathematical models are well documented in Donigian and Huber (1991) and Wurbs (1995). The main uses of these models were to (1) identify the fate of chemicals by quantifying their transport and kinetics of physico-chemical reactions, (2) to determine the level of contaminant exposure concentrations to aquatic organisms and humans, and (3) to predict future environmental impacts under various loading scenarios or pollutant control alternatives (Schnoor 1996). Some models have been effectively used and played an important role to provide adequate information for decision makers and environmental policy makers, but there still remains great challenges to validate the models against more field data and enhance the capabilities of the models. These challenges are becoming more significant since environmental controls become more costly to implement and the consequences of misjudgment (or a faulty policy) can be fatal for regional economics as well as environments. Therefore, a great portion of responsibility rests with environmental engineers to develop, test, validate, and improve these environmental models for better predicting the fate and transport processes of various pollutants and assessing their impacts on water quality.

Problem Statement

In this study, two mathematical models: a laterally integrated two-dimensional (2D) hydrodynamics and transport model, CE-QUAL-W2 (Cole and Buchak 1994), and the Erosion Productivity Impact Calculator, EPIC model (Williams 1995) are introduced and studied in compliance with the need for improvement. The first model can be classified into in-stream water quality and the second one into nonpoint source and watershed processes. Since agricultural pollutants move through watersheds and eventually enter surface waters (river, reservoir or lake) and groundwater, both types of models are required to fully

understand the fate and transport processes along the entire pathway of pollutants in overland flow, surface runoff, groundwater and stream flow. Although an ultimate goal may be directed to the linking of these models to assess the impacts of various agricultural management practices on in-stream water quality, this dissertation focused on several issues related to improvement and enhancement of the model capabilities. The following paragraphs describe the motives and problem statement of this dissertation.

Once a toxic chemical spill or runoff entering a surface waterbody, its fate and transport processes are governed by various factors including flow conditions, chemical and biological conditions of the waterbody, weather, and properties of the toxicant. In a reservoir, the processes can be furthermore complicated if the waterbody is stratified, and inflow forms a density current due to the temperature difference between river and ambient waters. The fate processes can be heavily influenced by various flow regimes, i.e., overflow, plunge flow, underflow, and interflow. Some chemicals are potentially more degradable through volatilization, photolysis, and oxidation if inflow forms an overflow regime because sufficient turbulence, sunlight, and oxygen are available near the surface of the reservoir. Therefore, a simulation model should be able to accurately predict both the hydrodynamics of reservoir and the kinetic processes of contaminants because the effects of reservoir flow regime on the persistence of toxic contaminants are sometimes significant.

The CE-QUAL-W2 model has been widely used for the modeling of temperature and conventional contaminants, i.e., dissolved oxygen and nutrient, in reservoirs. However, the use of model for the fate and transport of toxic contaminants such as pesticides has been limited because of the lack of a toxic modeling component. Chung and Gu (1998) applied the model to simulate and analyze the transport of a toxic pesticide that spilled into the Shasta Reservoir, California in 1991. The model accurately predicted the field measurements of water temperature and field observations of plume intruding depth and thickness. But, the model application was only limited to the transport and mixing processes of the pesticide. The chemical was treated as a conservative tracer by assuming that the level of degradation by kinetic reaction processes may not be significant under the deep reservoir environments with low level of turbulence, lights, and oxygen after plunging. The study laid an important

assignment for the development of a toxic submodel to better understand the kinetics and behavior of the spilled chemical under various flow regimes and enhance the versatility of the reservoir model. A full understanding of the effects of flow regimes on the fate and transport of a toxic spill in a reservoir is important in engineering practice. When a flow regime is undesirable for more degradation, mixing, and longer travel time, one ought to know methods of calculating and management by which it can be prevented. If a flow regime is desirable for contamination control, one should be able to choose or alter the involved variables such as water temperature so that the flow pattern can be created or established.

The EPIC model (Williams 1995) was originally developed by the United States Department of Agriculture. EPIC has been applied for studies ranging from farm-level to multiple states, such as the 1985 Resources Conservation Act analysis. The model was basically designed to simulate the impacts of erosion upon soil productivity. However, current version of EPIC has incorporated many advanced functions related to water quality and global climate/CO₂ change, which has resulted in the model being renamed to Environmental Policy Integrated Climate (Williams et al. 1996). Environmental indicators that can be output from EPIC include the transport and fate of nutrients from fertilizer and manure applications on eroded sediment, in runoff, and in leached water, pesticide leaching and runoff, the impact of atmospheric carbon levels on crop yield, sequestration of carbon in soil, and erosion losses due to water and wind. Recently, the EPIC model has been adopted within the Resources and Agricultural Police System (RAPS), an integrated modeling system designed to evaluate the economic and environmental impacts of agricultural policies for the North Central United States (Babcock et al. 1997; Gassman et al. 1998). The main uses of EPIC within RAPS is to provide nitrogen loss, soil erosion, and crop yield indicators in response to variations in tillage and crop rotation. Thus, an important aspect that may limit the use of EPIC in the RAPS is whether the model realistically replicate the impact of alternative agricultural management systems on the environmental and economic indicators. Although EPIC has been tested and validated on various sites and conditions, there is still a need to test the model with particular conditions of the study region and to further improve its prediction capabilities.

Objectives

The main goals of this dissertation are (1) to develop and apply a 2D reservoir toxic model for simulating the fate and transport of toxic pollutants in surface water and investigating the effects of flow regimes on reservoir water quality and (2) to evaluate the performance and reliability of EPIC model in simulating environmental and economic impacts of alternative agricultural management systems. Five independent sub-studies were performed to achieve the goals by setting the following specific objectives.

The specific objectives for the first goal are:

- to develop and test a 2D toxic substance simulation model as a submodel of the CE-QUAL-W2;
- to investigate the effects of reservoir flow regimes on the fate and transport of a pesticide that spilled into a stratified reservoir using the 2D toxic model;
- to estimate time-variable kinetic transformation rates of atrazine in the Saylorville Reservoir of Iowa using a mass balance model; and
- to investigate the fate and transport of atrazine in the Saylorville Reservoir, in particular, for the occurrence and persistence of peak concentrations, by predicting the longitudinal and vertical contamination levels of atrazine using the 2D toxic model.

The specific objectives for the second goal are:

- to validate EPIC performance in simulating the impact of two different tillage systems on water balance, nitrogen loss, sediment, and crop yield using long-term field data sets collected at southwestern Iowa.
- to assess the performance and reliability of EPIC in simulating subsurface drain flow, nitrogen loss, and crop yield in response to various tillage and cropping systems using field data collected at northeast of Iowa.

Dissertation Organization

This dissertation consists of General Introduction, five journal papers, and General Conclusions. Research was performed to achieve the above specific objectives. The first paper is an extension work of previous studies (Chung 1997; Chung and Gu 1998), and

contains the details of the 2D toxic model development and its application to the analysis of the 1991 spill in the Shasta Reservoir, California, and a case study to examine the effects of flow regimes on the fate of toxic contaminant and reservoir water quality. The second paper describes the construction processes of the mass balance model for estimating time-variable kinetic transformation rates of atrazine in the Saylorville Reservoir, Iowa and the impact of a different agricultural management system on the atrazine contamination levels in the reservoir. This research was performed to provide an adequate input parameters for the application of the 2D toxic model in this site. The third paper contains the details about the application of the 2D toxic model for simulating the fate and transport of atrazine in the Saylorville Reservoir. Simulated flow velocities, thermal structures, and atrazine concentrations were used to investigate the seasonal transport and fate processes of atrazine, and compared with field data collected earlier. The fourth and fifth papers describe the results of EPIC validation study in the two sites of Iowa, respectively. The fourth paper is accepted by the Journal of Environmental Quality.

References

- Babcock, B.A., J. T. Campbell, P.W. Gassman, P. D. Mitchell, T. Otake, M. Siemers, T.M. Hurley. 1997. RAPS 1997: Agricultural and Environmental Outlook. Center for Agricultural and Rural Development, Iowa State University, Ames, Iowa.
- Canter, L. W. 1986. Environmental Impacts of Agricultural Production Activities. Lewis Publications, Inc. Michigan, USA.
- Capel, P. D., W. Giger, P. Reichert, O. Wanner. 1988. Accidental input of pesticides into the Rhine River. *J. Environ. Sci. Technol.*, 22 (9): 992-997.
- Chatterjee, P., 1991. California suffers its worst chemical spill., *New Scientist* 10, Aug. p12.
- Chung, S. W. 1997. Contaminated density currents in a stratified reservoir. In Proceeding of the John F. Kennedy Student Paper Competition and Specialty Seminar Summaries. The 27th Congress of the International Association for Hydraulic Research. Aug. 10-15, San Francisco, California. pp. 37-42.
- Chung, S. W., and R. Gu. 1998. Two-dimensional simulations of contaminant currents in a stratified reservoir. *J. Hydr. Engrg.*, ASCE, 124(7):704-711.
-

- Cole, T. M., and E. M. Buchak. 1994. CE-QUAL-W2: A two-dimensional, laterally averaged, hydrodynamic and water quality model, version 2.0 user manual. Army Engineer Waterways Experiment Station, Vicksburg, Miss.
- Conway, G. R., and J. N. Pretty. 1991. *Unwelcome Harvest – Agriculture and Pollution*, Earthscan Publications, Ltd., London, England.
- Donigian, Jr. A. S., and W. C. Huber. 1991. Modeling of nonpoint source water quality in urban and non-urban areas. EPA/600/3-91/039. U.S. Environmental Protection Agency, Athens, GA.
- Gassman, P. W., J. Wu, P. D. Mitchell, B. A. Babcock, T. M. Hurley, and S. W. Chung. 1998. Impact of U.S. agricultural policy on regional nitrogen losses. In *Proceeding of 3rd International Conference on Diffuse Pollution (Poster Papers)*, 31 Aug.-4 Sept., Edinburg, Scotland. International Association of Water Quality, London, England. pp. 115-122.
- Goolsby, D. A. and W. A. Battaglin. 1993. Occurrence, distribution, and transport of agricultural chemicals in surface waters of the Midwestern United States. In Goolsby, D. A., L. L. Boyer, and G. E. Mallard ed., *Selected Papers on Agricultural Chemicals in Water Resources of the Midcontinental United States*. U.S. Geological Survey. Denver, CO.
- Hallberg, G. R. 1996. Water quality and watersheds: an Iowa perspective. *Proceedings of the Agriculture and Environment -Building Local Partnerships-*. Iowa State University, Ames, IA.
- Schnoor, J. L. 1996. *Environmental Modeling: Fate and transport of pollutants in water, air, and soil.*, John Wiley & Sons, New York, USA.
- Thurman, E. M., D. A. Goolsby, M. T. Meyer and D. W. Kolpin. 1991. Herbicides in surface waters of the Midwestern United States: The effect of spring flush. *Environ. Sci. Technol.* 25:1794-1796.
- Williams, J.R. 1995. The EPIC Model. In: *Computer Models of Watershed Hydrology* (Ed.: V.P. Singh). Water Resources Publications, Highlands Ranch, Colorado.
- Williams, J. R., M. A. Nearing, A. D. Nick, E. L. Skidmore, and M. R. Savabi. 1996. Using soil erosion models for global change studies. *J. Soil and Water Conser.* 51:381-385.
- Wurbs, R. A. 1995. *Water management models: A guide to software*. Prentice Hall, Inc. Englewood Cliffs, NJ.

CHAPTER 2. TWO-DIMENSIONAL MODELING OF THE FATE AND TRANSPORT OF TOXIC CONTAMINANTS IN A RESERVOIR

A paper to be submitted to the Journal of Water Resources Planning and Management

Se-Woong Chung and Ruochuan Gu

Abstract

In a stratified reservoir, the fate and transport of toxic pollutants can be significantly affected by flow regimes or circulation patterns. Accurate predictions of hydrodynamics and kinetics of physico-chemical and biological processes are important to contamination control and remediation management in case of a toxic chemical spill into the reservoir. A two-dimensional toxic submodel was developed and incorporated into a laterally integrated hydrodynamics and transport model. The model was applied to the Shasta Reservoir, California to investigate the effect of flow regimes on the fate and transport of a volatile toxicant (MITC) during a spill. Results showed that an interflow slowed down the degradation of MITC due to a reduced volatilization in deep layers and resulted in a longer persistence of the toxicant than an overflow did. The amount of chemical loss through kinetic processes was insignificant compare to that by transport and mixing processes in the early stage of the spill, but the importance of these processes increased with time as the turbulent mixing diminished. In the late stage, the effect of flow regime on the persistence of the toxic contaminant became significant because the reduction of MITC concentrations was primarily accomplished by physico-chemical reactions. In the overflow, the toxic plume moved more slowly in the reservoir and experienced greater chemical loss (kinetic degradation) than in the interflow. The model can be used to assist in spill control, field sampling and contamination remediation, and reservoir management including closure of water intakes.

Introduction

The production efficiency of modern agriculture is in part attributed to the use of various agricultural pesticides such as insecticides, fungicides, and herbicides. Use of these

chemicals is expected to continue due to an increasing food demand in the world. However, their extensive transport, intensive use, and accumulation in agricultural lands has also caused various environmental pollution either by acute or chronic exposures. For example, accidental spills of toxic pesticides into rivers and reservoirs severely affected fisheries and local water supply systems in a short time period (Capel et al 1988; Chatterjee 1991). In the Midwest of United States, the occurrences of peak pesticide concentrations during late spring and early summer due to short-term runoff events are seriously concerned because of its potential adverse impacts on aquatic organisms and human health (Thurman et al. 1991; Goolsby et al 1993; Hallberg 1996). The contamination levels of some pesticides in streams and reservoirs occasionally exceed their maximum contamination levels (MCL) for drinking water. Chemical spill into a reservoir is not a matter of frequent incident, but the environmental and economic losses can be fatal for a community, in particular, if the community is heavily rely on the reservoir for water supply. Therefore, adequate understanding about the fate of off-site transported toxic chemicals in a reservoir during a peak loading period is crucial to protect the scarce water resources from various pollution.

Once a toxic chemical spill or runoff entering a surface waterbody, its fate and transport processes are governed by various factors including flow conditions, chemical and biological conditions of the waterbody, weather, and properties of the toxicant. In a reservoir, the processes can be furthermore complicated if the waterbody is stratified, and inflow forms a density current due to the temperature difference between river and ambient waters. The fate processes can be heavily influenced by various reservoir flow regimes, i.e., overflow, plunge flow, underflow, and interflow, depending upon its physico-chemical properties. Some chemicals are potentially more degradable through volatilization, photolysis, and oxidation if inflow forms an overflow regime because sufficient turbulence, sunlight, and oxygen are available near the surface of a reservoir. Therefore, a prediction tool for reservoir hydrodynamics and kinetics of toxic substances is needed for providing prompt information about the persistence and exposure level of a toxic chemical during a spill or runoff.

The objectives of this study are to develop a two-dimensional (2D) reservoir toxic model, test the model against field data, and apply the model to investigate the effect of

reservoir flow regimes on the fate and transport of a volatile toxic compound during a spill event. The toxic model was constructed, by developing a toxic submodel and incorporating into an existing hydrodynamics and transport model, to simulate unsteady vertical and longitudinal distribution of a toxic chemical in light of various transfer and transformation processes. The model was tested against the field data collected from the Shasta Reservoir, California, during a spill event. Observed and simulated concentrations were used to analyze the fate and transport processes of the spilled pesticide, methyl isothiocyanate (MITC), under various flow regimes, plunging flow, underflow, and interflow. A case study was attempted to examine the effect of two different flow regimes, interflow and overflow, on the degradation of MITC. The development of the toxic model enhances the versatility of the original reservoir model and provides an effective tool for describing and predicting the behavior of toxic contaminants in a stratified reservoir.

Previous Studies

The effects of flow regimes on reservoir water quality were studied as early as 1947 (Churchill 1947). Thereafter, many researchers have investigated the influence of reservoir flow regimes on dissolved oxygen (Kim et al. 1983; Martin 1988) and nutrient dynamics (Martin and Arneson 1978; Gloss et. al 1980; Carmack and Gary 1982; Kennedy and Walker 1990). However, their influence on toxic chemicals was rarely studied due to the limited field data and the lack of mathematical model that requires reliable hydrodynamics and reaction kinetics. Over the past decade several reservoir water quality models have been developed: WQRRS (USACE Hydrologic Engineering Center 1985), HEC-5Q (USACE Hydrologic Engineering Center 1986), MINLAKE (Riley and Stefan 1987), and WASP5 (Ambrose et al. 1993). WQRRS, HEC-5Q, and MINLAKE are one-dimensional (1D) models that developed to simulate the vertical distribution of water temperature and conventional constituents such as dissolved oxygen and nutrient in a lake and reservoir. WASP5 is a recent model that designed to simulate various pollutants in most type of surface water system (Ambrose et al. 1987, 1993). However, the model employs a compartmental approximation and its hydrodynamic submodel (DYNHYD5) solves the 1D equations of continuity and

momentum. Therefore, WASP5 is not pertinent for a stratified waterbody (Ambrose et al. 1993). To simulate the fate and transport processes of a toxic chemical taking into account flow regime effects in a stratified reservoir, a mathematical model should be able to accurately simulate both the reservoir hydrodynamics and kinetics of chemical reaction processes. Therefore, an unsteady, two-dimensional (in the longitudinal and vertical directions) model is required for this purpose.

The laterally integrated 2D hydrodynamics and transport model, CE-QUAL-W2 (Cole and Buchak 1994), has been broadly used for the modeling of water temperature and conventional constituents in reservoirs not only in the United States but also in many other countries (Gordon 1980, Kim et. al 1983, Martin 1988, Bath and Timm 1994). Its application for toxic contaminants, however, has been limited due to the lack of a toxic modeling component. Chung and Gu (1998) applied the model to simulate and analyze the transport of a toxic pesticide that spilled into the Shasta Reservoir, California in 1991 (Figure 1) by treating the toxicant as a conservative substance. The model accurately predicted the field measurements of water temperature and field observations of plume intruding depth and thickness. However, the application was only bounded to the transport and mixing processes of a tracer. To understand the effectiveness of physico-chemical reaction processes and behavior of the toxic contaminant under various flow regimes, the development of a toxic submodel is necessary.

Model Development

Governing Equations

A stationary sediment bed condition was assumed because it is quite valid in reservoirs and lakes of relatively great depth to which wind effect does not extend. Toxic substances may decay in the adsorbed particulate form, but decay was assumed to occur only in the dissolved phase to simplify the processes (Schnoor, 1996). A linear sorption-desorption kinetics was adopted because chemical concentrations in reservoir water are mostly environmentally relevant, i.e., less than one-half water solubility. An instantaneous local equilibrium was assumed for sorption process since the time scale for sorption reactions is

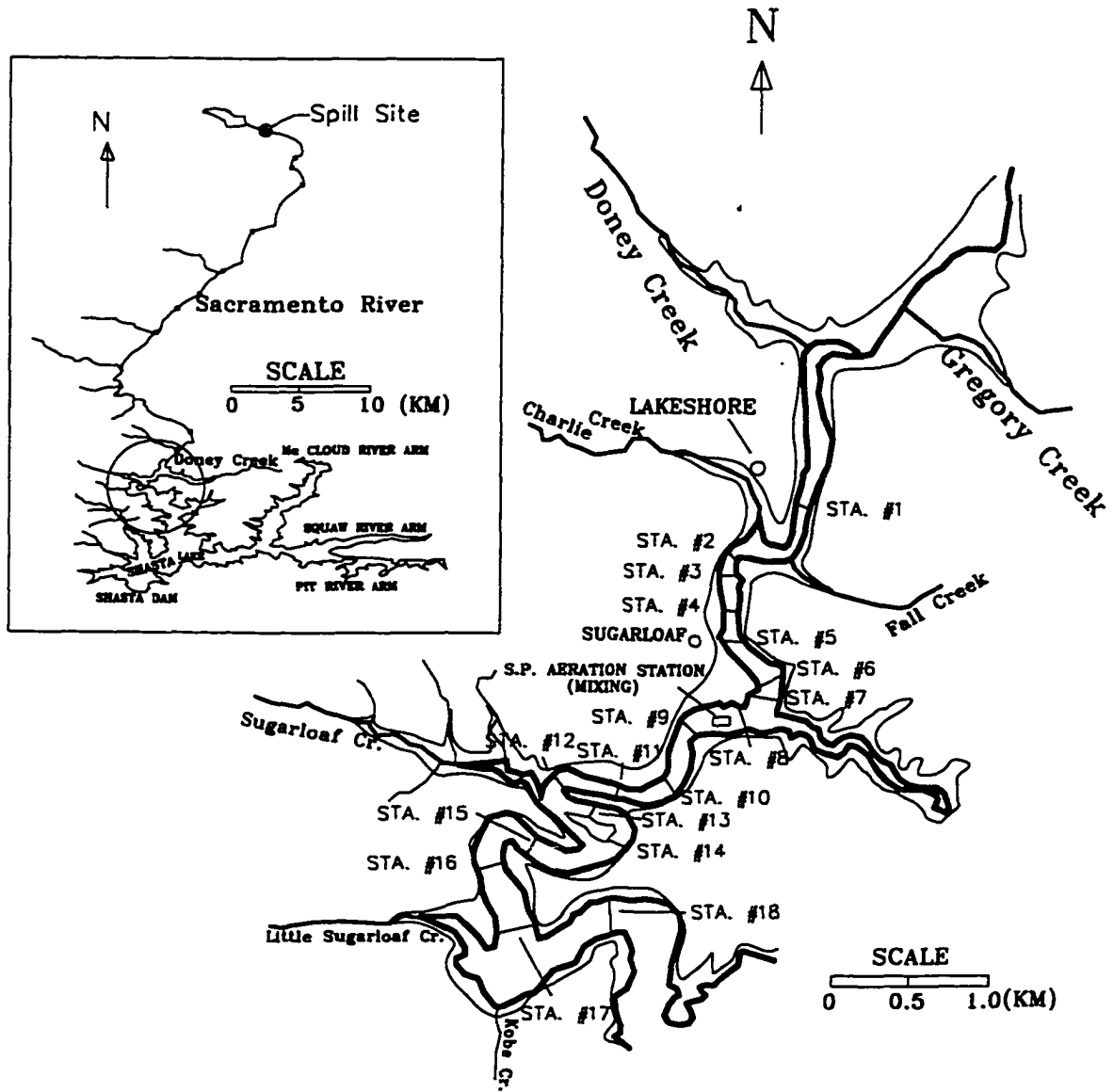


Figure 1. Map of the spill site and sampling stations in the Shasta Reservoir.

much smaller than that of other kinetic and macroscopic transport (advection and diffusion) processes in reservoirs (Thomann and Mueller 1987; Schnoor et al. 1992).

With the assumptions, total chemical concentrations in the water column ($C_{t,w}$) and bed sediments ($C_{t,b}$) are formulated by considering the mass conservation in water column:

$$\begin{aligned} \frac{\partial(BC_{t,w})}{B\partial t} + \frac{\partial(UBC_{t,w})}{B\partial x} + \frac{\partial(WBC_{t,w})}{B\partial z} - \frac{\partial}{B\partial x}(BD_x \frac{\partial C_{t,w}}{\partial x}) - \frac{\partial}{B\partial z}(BD_z \frac{\partial C_{t,w}}{\partial z}) \\ = \frac{K_f}{y}(f_{d,b}C_{t,b} / \phi - f_{d,w}C_{t,w}) - (K_P + K_H + K_O + K_B)f_{d,w}C_{t,w} \\ + \frac{k_l}{z}\{(C_a / H) - f_{d,w}C_{t,w}\} - \frac{v_s}{z}f_{p,w}C_{t,w} + \Phi_{NPS} \end{aligned} \quad (1)$$

$$\begin{aligned} \frac{\partial(BC_{t,b})}{B\partial t} = -\frac{K_f}{y}(f_{d,b}C_{t,b} / \phi - f_{d,w}C_{t,w}) - (K_H + K_O + K_B)f_{d,b}C_{t,b} \\ + \frac{v_s}{z}f_{p,w}C_{t,w} \end{aligned} \quad (2)$$

where subscripts t, d and p denote the total, dissolved, and particulate phases of a chemical, respectively; subscripts a, w and b denote air, water, and bed, respectively; f_d and f_p are the fractions of dissolved and particulate chemicals to the total chemical; t is time; x is longitudinal Cartesian coordinate (positive to the right); B is waterbody width; U and W are longitudinal and vertical flow velocities; D_x is longitudinal constituent dispersion coefficient; D_z is vertical constituent dispersion coefficient; K_f is diffusive exchange rate between water column and pore water of the bed; ϕ is the porosity of the bed sediments; K_P is photolysis rate constant; K_H is hydrolysis rate constant; K_O is oxidation rate constant; K_B is biotransformation rate constant; H is Henry's constant; C_a is vapor phase concentration; Φ_{NPS} is the nonpoint source (NPS) mass flow rate per unit volume; v_s is the net settling velocity of sorbed chemical; z is the depth of water from water surface; and y is the distance from bottom of a reservoir. The first term of right hand side (RHS) in (1) is the diffusive exchange of dissolved toxicant between sediment and water column. The second term is the degradation of dissolved toxicant due to photolysis, hydrolysis, oxidation, and microbial decay. The third term is the air-water exchange of the toxicant due to volatilization. The

fourth term is the net settling of the chemical in the particulate phase. The model uses a net settling velocity as an input for sediments that does not explicitly account for particle type, grain size, density, viscosity, and turbulence. The last term is the external NPS loading. The second term of RHS in (2) is the degradation of dissolved toxicant in bed sediment due to hydrolysis, oxidation, and microbial decay. Chemical kinetic reaction rates and model input parameters can be determined from field and laboratory experiments, estimation using chemical properties, and previous literature (Lyman et al., 1982; Schnoor et al. 1987)

Sediment transport for water column and reservoir bed were formulated using the 2D laterally integrated advection-diffusion equations:

$$\frac{\partial(BC_s)}{B\partial t} + \frac{\partial(UBC_s)}{B\partial x} + \frac{\partial(WBC_s)}{B\partial z} - \frac{\partial}{B\partial x}(BD_x \frac{\partial C_s}{\partial x}) - \frac{\partial}{B\partial z}(BD_z \frac{\partial C_s}{\partial z}) = -\frac{v_s}{\Delta z} C_{ss} - K_{dt} \gamma_{om} C_{dt} - \frac{v_{dt}}{\Delta z} C_{dt} + q_l \quad (3)$$

$$\frac{\partial(BC_b)}{B\partial t} + \frac{\partial(u_b BC_b)}{B\partial x} + \frac{\partial(w_b BC_b)}{B\partial z} = \frac{v_s}{\Delta z} C_{ss} + \frac{v_{dt}}{\Delta z} C_{dt} - \gamma_{om} K_s C_b + q_b \quad (4)$$

where C_s is sediment concentration including inorganic and organic (detritus) sediments in water column; q_l is lateral mass flow rate of sediments per unit volume for water column; v_{ss} is net settling velocity of suspended solids; C_{ss} is suspended solids concentration; Δz is cell thickness; K_{dt} is detritus decay rate; v_{dt} is net detritus settling rate; and C_{dt} is detritus concentration in water column; u_b and w_b are longitudinal and vertical bed load velocities; C_b is the total bed sediment concentration; γ_{om} is rate multiplier for organic matter; K_s is organic bed sediment decay rate; and q_b is lateral mass flow rate of sediments per unit volume for bed sediments. By assuming a stationary bed condition (i.e., u_b and $w_b = 0$), equation (4) simplified to:

$$\frac{\partial(BC_b)}{B\partial t} = \frac{v_s}{\Delta z} C_{ss} + \frac{v_{dt}}{\Delta z} C_{dt} - \gamma_{om} K_s C_b + q_b \quad (5)$$

Physical, Chemical and Biological Processes

The schematic description of transport and transformation processes of toxic substances in a reservoir system is presented in Figure 2. A partition coefficient (K) was used to determine the fractions of dissolved and particulate chemical forms to the total chemical based on the linear sorption-desorption kinetics. There are three different equilibrium phase partitioning models that are available to calculate a partition coefficient (Bierman, 1994); conventional two phases model, three phases model, and particle interaction model by Di Toro (1985). The two phases and particle interaction models were incorporated into the model because it is too difficult for the three phases model to separate and characterize the third phase (non separable particles plus dissolved organic carbon) (Bierman, 1994). Thus, the distribution of the toxicant between particulate and dissolved phases was determined dependent upon the partition coefficient of a chemical and the sediment concentration in a waterbody.

Dissolved chemical in water column may transfer to interstitial water in the bottom sediment by diffusion process in the initial stages of a chemical spill, or vice versa may occur during the recovery phase depending on the gradient of dissolved chemical concentrations. The mass-transfer between bottom sediment and overlying water column was estimated as a function of molecular weight (M) of a chemical and porosity of bed sediments using the equation by Di Toro et al. (1981) as follows:

$$K_f = 19\phi(M)^{-\frac{2}{3}} \quad (6)$$

The amount of chemical loss due to photolysis was computed as a function of the quantity and wavelength distribution of incident light, the light absorption characteristics of the chemical, and the efficiency at which absorbed light procedures a chemical reaction. A first-order reaction constant was used to estimate the rate of photolysis (Thomann and Mueller, 1987):

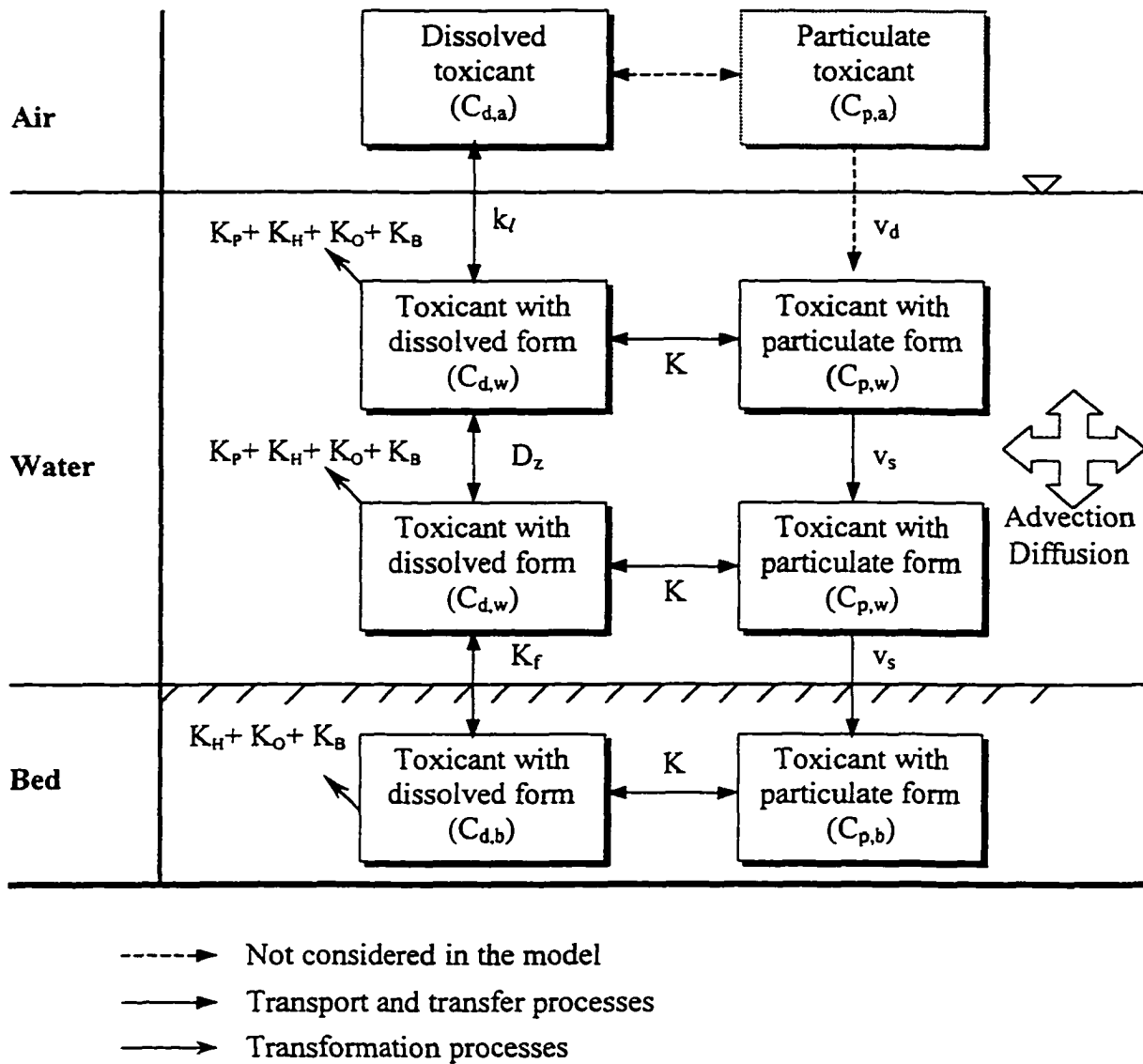


Figure 2. Schematic of transport and transformation processes of a toxic substance in a reservoir system.

$$K_p = K_{do} \frac{I_o}{I_o'} \frac{D}{D_o} \left\{ \frac{1 - \exp[-K_e(\lambda_{max}) \cdot z]}{K_e(\lambda_{max}) \cdot z} \right\} \quad (7)$$

where K_{do} is the direct near surface photolysis rate; I_o is the daily amount of incoming solar radiation at the water surface; I_o' is the light intensity at which K_{do} was measured; D is the radiance distribution function; D_o is the radiance distribution function near the surface; and $K_e(\lambda_{max})$ is the net light extinction coefficient at λ_{max} , the wavelength of the maximum light absorption. Extinction coefficients for water, inorganic, and organic sediments were used to calculate a net light extinction coefficient, K_e (Cole and Buchak 1994).

Hydrolysis is a major decay process in which a chemical compound reacts with water molecules and results in a cleavage of a chemical bond. A new compound with either the hydrogen or hydroxyl bond may be formed. Generally, hydrolysis is a second-order reaction because of dependence on the molar concentrations of $[H^+]$, $[OH^-]$, or water mediators (Schnoor, 1996; Thomann and Mueller, 1987). A pseudo-first-order rate constant $K_H = K_n + K_a[H^+] + K_b[OH^-]$ was used, where K_n is the neutral hydrolysis rate, K_a is the acid catalyzed hydrolysis rate, and K_b is the base catalyzed hydrolysis rate. Arrhenius function was used to adjust the rate with temperature.

Toxic chemicals can be oxidized by a reaction with either dissolved oxygen or free radicals such as peroxy radicals $ROO\cdot$, alkoxy radicals $RO\cdot$, hydrogen peroxide H_2O_2 , and hydroxyl radicals $\cdot OH$ in natural waters (Schnoor, 1996). A pseudo-first-order reaction rate constant was used to compute degradation of a chemical by oxidation assuming that the rate of free radical formation (oxidant) is relatively constant (steady state). The rate was adjusted using Arrhenius function depending on water temperature.

Biotransformation is the microbially mediated decay processes by which a chemical is degraded by bacteria and fungi. It may occur with oxygen (aerobic) or without oxygen (anaerobic). The model was designed to treat the biotransformation process either by second-order or by pseudo-first-order kinetic reactions based on the Monod equation:

$$\frac{dC_d}{dt} = -\frac{1}{y_B} \frac{dC_B}{dt} = \frac{\mu_{\max}}{y_B} \left(\frac{C_d}{K_x + C_d} \right) C_B \quad (8)$$

where C_B is the bacterial concentration; y_B is the bacterial yield coefficient; μ_{\max} is the maximum specific growth rate; and K_x is the half-saturation constant. The biotransformation rate was adjusted with water temperature

Two-film theory (Whitman 1923; Mackay 1982; O'Connor 1983) was used to compute the gaseous transfer of chemical from air to water and water to air. The transfer rate was proportional to the concentration gradient between the chemical in water column and in the overlying atmosphere. The conductivity was influenced by both physico-chemical properties of a chemical and environmental conditions at the air-water interface. The overall volatilization transfer coefficient, k_l , was given as follows:

$$\frac{1}{k_l} = \frac{1}{K_l} + \frac{1}{K_g H} \quad (9)$$

where K_l is the liquid film coefficient and K_g is the gas film coefficient. The k_l value was computed as a function of the chemical characteristics (H , K_l and K_g), water velocity, and wind speed. Since the transfer coefficient for the open bodies of water such as reservoir and lake are largely affected by wind, O'Connor (1983) and Mackay (1982) equations were incorporated into the model to estimate the liquid and gas film transfer coefficients.

Numerical Method and Programming Procedure

The governing equations were solved using the finite-difference solution method as used in the laterally integrated hydrodynamics and mass transport model, CE-QUAL-W2 (Cole and Buchak 1994). The dependent variables are water surface elevation, pressure, density, horizontal and vertical velocities, and toxicant concentration. The independent variables are longitudinal distance, flow depth, and time. The flow chart in Figure 3 briefly describes the overall algorithms of the model and the way how the toxic submodel was linked to the original model. The free water surface elevation and horizontal momentum are computed simultaneously in the model based on an implicit finite-difference scheme, which

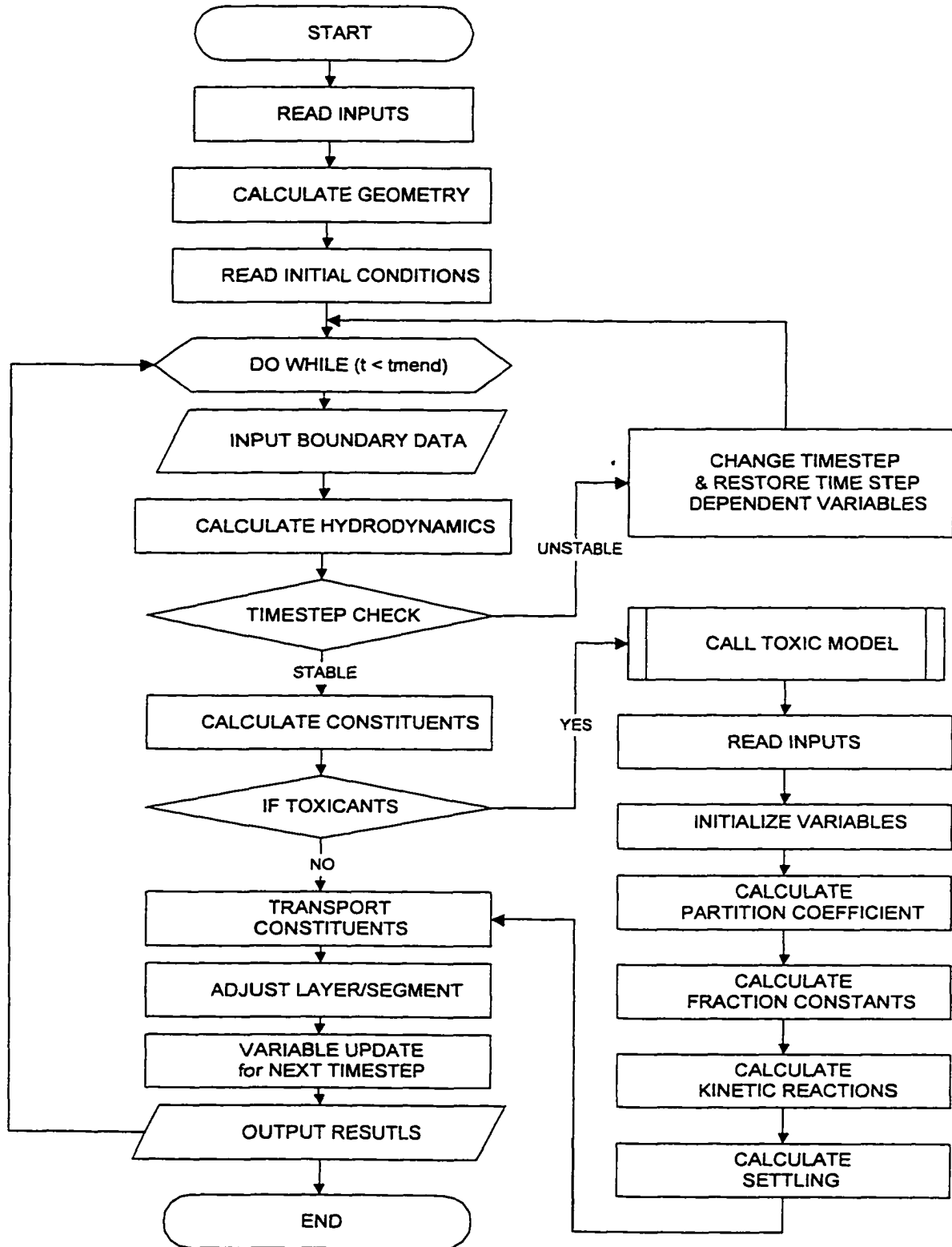


Figure 3. Flow chart of the 2D reservoir toxic model.

allows the use of reasonable time scale for field application over entire stratification cycles (Martin 1988; Cole and Buchak 1994). The equations for toxicant and sediment transport were solved using the explicit QUICKEST (Quadratic Upstream Interpolation for Convective Kinematics with Estimated Streaming Terms) finite difference scheme (Leonard 1979) that was used for temperature simulation in CE-QUAL-W2 (Cole and Buchak 1994). Vertical turbulent transfer of toxic contaminants was determined from the vertical shear of horizontal velocity and a density gradient dependent Richardson number function (Cole and Buchak 1994). The toxic sub-program was created and linked using the Microsoft Fortran Powerstation program. Minimum change in the original model was attempted to incorporate the toxic model. The physical, chemical, and biological properties of a toxic chemical and its kinetic reaction rates need to be provided through an input file. The model can compute the various degradation processes either independently by providing individual kinetic reaction rates or collectively by providing a lumped transformation rate or half-life value. A time-variable half-life value can also be specified in the model.

Boundary and Initial Conditions

The model generates the vertical and longitudinal distributions of a toxic chemical in response to time-varying boundary conditions that include the flows and contaminant loadings from upstream, tributaries, and distributed NPS; the discharges of contaminant through outflow and lateral withdrawals; surface precipitation and evaporation; and meteorological changes over time. The time-varying flows and mass loadings can be defined as either a step function or linearly interpolated value between two data points. The distributed NPS loading of toxicants from a watershed can be produced with the help of field- or watershed- scale NPS models.

The initial toxic substance and sediment concentrations in the water column can be specified as either a uniform value, a single vertical profile for all segments, or a vertical profile for each segment. In bed sediment, they can be specified as either a uniform value or a longitudinal profile for each bottom layer. If non-uniform initial conditions are preferred, a grid-wide vertical or longitudinal profiles should be provided as an input file.

Model Application

The model was applied to the Shasta Reservoir spill for investigating the physical and chemical reactions of MITC under various flow regimes. In the previous study (Chung and Gu 1998), MITC was treated as a conservative tracer. The justification for the assumption was that the level of MITC degradation by kinetic processes (hydrolysis, photolysis, and volatilization) is insignificant in the deep and cold reservoir environments with low level of turbulence, lights, and oxygen. In the present application, dilution of contaminant concentration due to mixing, reduction due to physico-chemical reactions, and reduction by artificial mixing were quantified using observed and simulated MITC concentrations.

Spill and Site Descriptions

On July 14, 1991, approximately 49,000 to 72,000 liters of VAPAM liquid formulation were estimated to have spilled into the Sacramento River, California (Figure 1) (Rosario et al. 1994; Gu et. al 1996). VAPAM, sodium methyl dithiocarbamate (Na-MDTC), is a pesticide with a fungicidal, nematicidal and herbicidal action (Worthing 1987). The parent compound Na-MDTC decomposes into more stable products, primarily the far more toxic chemical methyl isothiocyanate (MITC, $\text{CH}_3\text{N}=\text{C}=\text{S}$) in water. During traveling the long Sacramento River, which provided good environments such as high level of lights and oxygen for the chemical reactions, Na-MDTC transformed into more toxic MITC through oxidation and photolysis (Wang et al. 1997). The LC_{50} (96-h) of MITC, that the lethal concentration at which 50% mortality occurs from 96 hours exposure time, for bluegill is $130 \mu\text{g/l}$ (Worthing 1987), indicating the strong toxicity of the chemical. A great number of fish died during the spill. A large portion of the MITC was vaporized into the air and impaired human health in the vicinity of the spill site (Chatterjee 1991). The residual MITC, eventually, entered into the Shasta Reservoir at midnight of July 16.

Water sampling activities were conducted by the California Regional Water Quality Control Board in order to keep track of the spill after it entered the Shasta Reservoir (Figure 1). The spill managers marked the contaminant plume with the red dye rhodamine WT to track its progress in the reservoir because the plume plunged into the reservoir due to the temperature difference between the incoming river water and the ambient water. The field

measurements also served to determine the contamination level of the waterbody and the speed at which the plume was moving in the river and reservoir towards the Shasta Dam. An artificial mixing device was installed at the distance of about 2.6 km downstream from the head of reservoir to mix the contaminant plume with the reservoir water after the chemical spill. The device stirred up the plume with gigantic pumps, and shot great gusts of air into the plume.

The reservoir was stratified during the spill period. The observed temperatures in the reservoir showed that vertical and longitudinal variations were significant, but lateral variations are generally small in the upper reach from the head of the reservoir to its confluence with the Squaw River arm (Chung 1996). Water temperatures in the reservoir were in the range of 19 to 27.5 °C in the epilimnion and 7 to 16 °C in the hypolimnion. The river flow entering the reservoir averaged 7.5 m³/s with a temperature of 18-24 °C during the spill. Under these conditions, the contaminated river flow plunged after entering the reservoir and formed an underflow and interflow during the spill period (Chung and Gu 1998).

Degradation Processes of MITC

The degradation of MITC due to physico-chemical reactions is dependent upon the chemical properties and environmental conditions of the reservoir such as the level of turbulence, temperature, dissolved oxygen, and solar radiation that are all function of water depth in a stratified reservoir. MITC is a volatile toxic chemical that has high solubility (7600 mg/L) but low adsorption potential (Octanol-water partition coefficient, $K_{ow} = 23.5$) in water. The main physical and chemical properties of MITC are shown in Table 1. In general, MITC is known to be volatile and reactive when exposed to elevated temperature, oxygen level, and sunlight. However, its fate and transformations in surface waters are not well understood (Rosario et al. 1994).

Previous studies concluded that the primary pathways of MITC degradation in surface water are volatilization and hydrolysis (Rosario et al. 1994; Tomlin 1994; Wang et al. 1997). Direct photolysis rate of MITC in surface water is a function of water depth (Zepp and Cline 1977). Draper and Wakeham (1993) found that MITC is resistant to photodegradation in water. No detectable MITC photolysis occurred after 5 hours of irradiation in their laboratory

Table 1. Physical and chemical properties^a of methyl isothiocyanate (MITC).

Property	Unit	Value
Molecular weight	g/mol	73
Solubility	mg/l	7600
Vapor pressure at 20 °C	kPa	2.7
Henry's constant	atm-m ³ /mol	0.26×10 ⁻³
Octanol-water partition K _{ow}	-	23.5
Specific gravity at 20 °C	g/cm ³	1.048
Diffusivity in water ^b	cm ² /sec	1.26×10 ⁻⁶
Diffusivity in air ^b	cm ² /sec	0.109

^aC. Tomlin (1994).

^bCalculated as a function of molecular weight.

experiments. Therefore, the MITC degradation by photolysis was assumed insignificant during the spill, although this may lead underestimation of chemical degradation to some extent. The sorption of MITC onto suspended solids was negligible in the reservoir because of a low suspended solids concentration in this site and highly soluble characteristics of MITC (Wang et al. 1997). The fraction of dissolved MITC, f_d , was estimated as a function of partition coefficient, suspended solids concentrations, and the fraction of organic matter (Figure 4). More than 97% of MITC remained dissolved form because the suspended solids concentration was far below 1000 mg/l during the spill.

Therefore, MITC concentrations were degraded in the simulations by volatilization and hydrolysis as well as flow dilution. The rate of volatilization from water to air was computed using two-resistance theory. The rate was influenced by both chemical properties such as molecular weight, Henry's constant, and environmental conditions at the air-water interface, i.e., turbulence controlled by wind speed and current velocity, and water depth. The hydrolysis of MITC through the reaction with water molecules is a strong function of the pH level of water (Tomlin 1994) (Figure 5). The first-order hydrolysis rate constant (K_h) for MITC was obtained from its half life ($t_{1/2}$) value in the neutral water (490 hours at pH = 7) using the relation of $K_h = 0.693/t_{1/2}$.

Boundary and Initial Conditions

The time-varying MITC boundary concentrations were specified at the upper end of the computational domain, Doney Creek (Figure 6). Sampling was conducted on an hourly basis during from midnight of July 16, when the plume arrived at Doney Creek, to 10:10 a.m. next day. Only three measurements were taken from then until noon July 19. The peak concentration (C_p) passed Doney Creek at 5:00 a.m. on July 17. Most of the chemical plume had entered the reservoir by 10:00 a.m. on July 17. The measured concentrations at the reservoir head varied with time, from 2 mg/l at midnight on July 16 to 35 mg/l (peak) at 5:00 a.m. and 5 mg/l at 10:00 a.m. on July 17, and dropped to a non-detectable level (< 0.001 mg/l) at noon on July 19. Initial and boundary conditions for flows, temperature, and weather conditions were set based on the observed data. A detail information for modeling approach and input data was documented in the previous publication (Chung and Gu 1998).

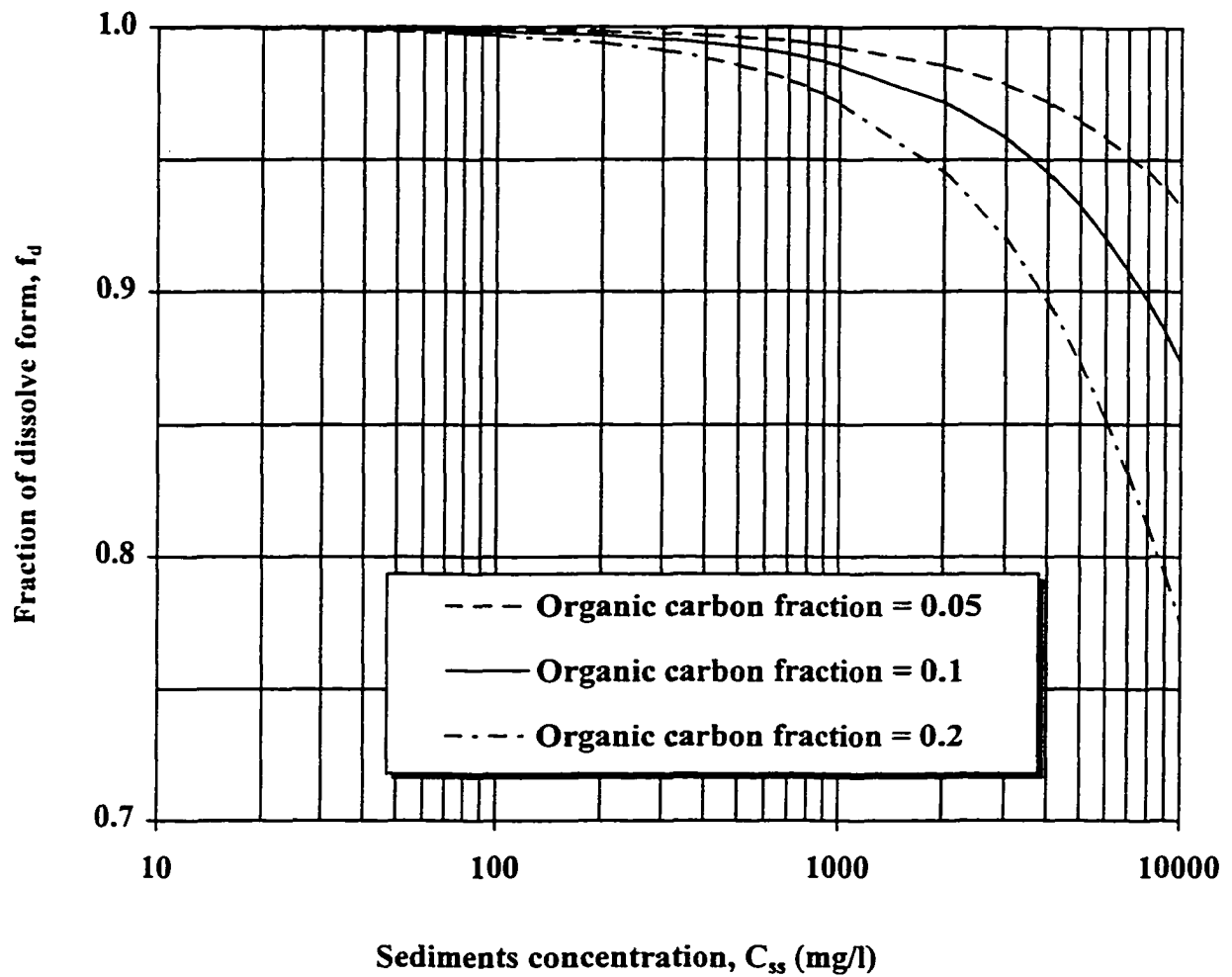


Figure 4. The fraction of dissolved form to the total MITC concentration in water as a function of sediments concentration and fraction of organic carbon.

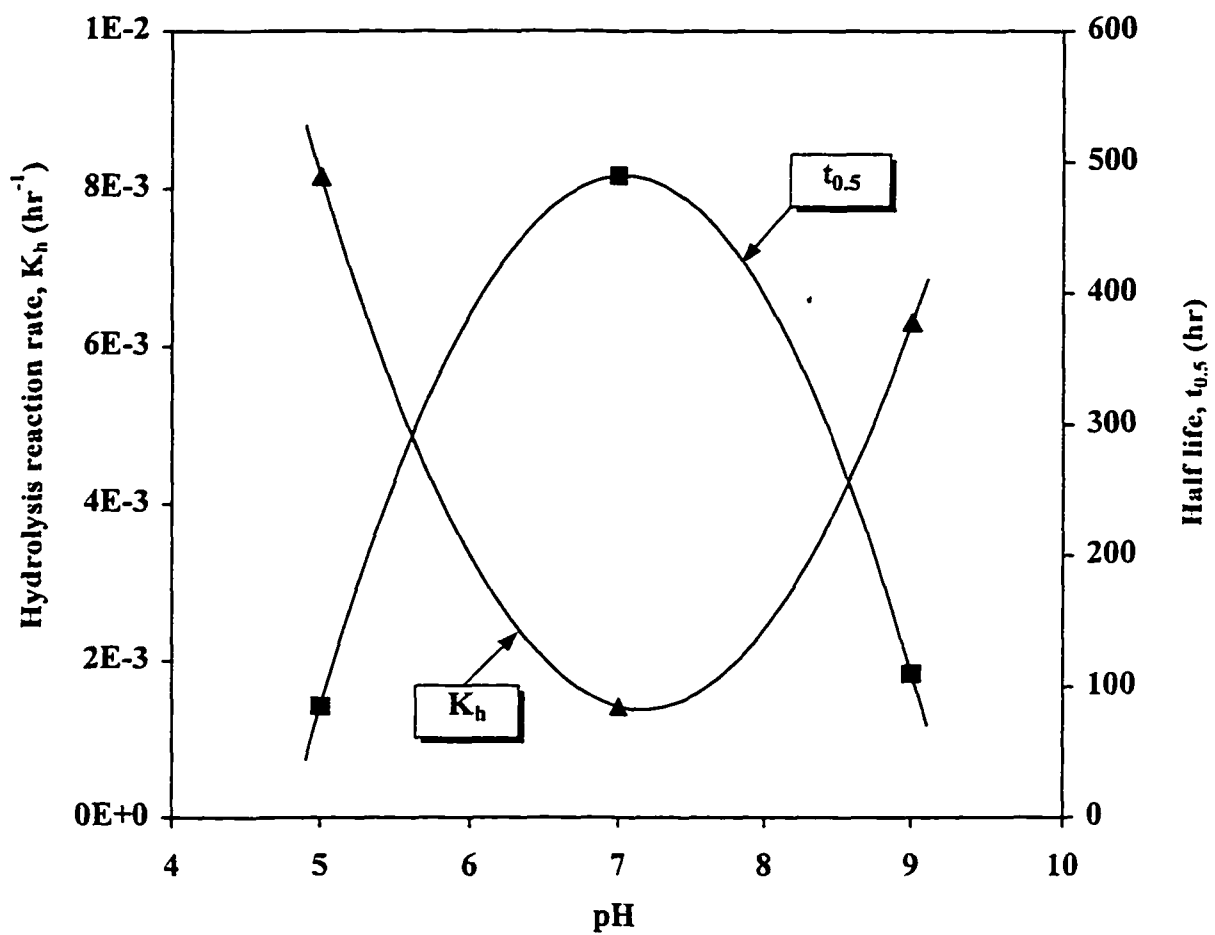


Figure 5. The first-order hydrolysis reaction rate and half-life of MITC in water as a function of pH.

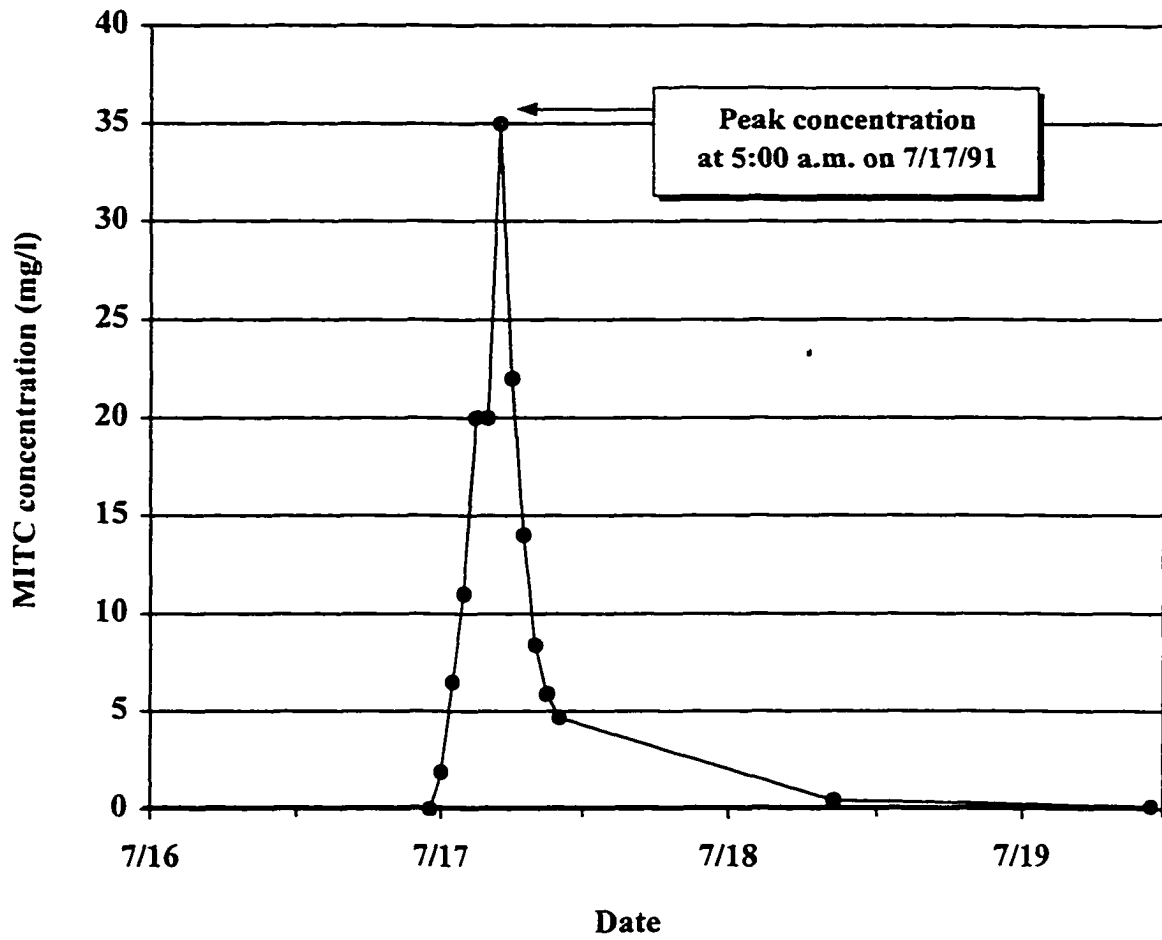


Figure 6. The inflow boundary MITC concentrations that measured at the upper head of the Shasta Reservoir (Doney Creek) during the spill.

Results and Discussion

Reservoir Flow Regimes

Flow velocities and water temperature were used to depict the reservoir circulation and mixing patterns during the spill. Figures 7a and 7b show flow velocity vectors and contour of water temperature, respectively during the spill period at 9:00 a.m. on July 23. It should be noted in the vector plot that only part of the reservoir (near inflow boundary) is plotted due to the large spatial variations in velocities between upstream and downstream. The direction and magnitude of the vectors represent the residual velocity of longitudinal and vertical components. The contaminated plume formed an underflow and interflow after plunging near the head of the reservoir (about 0.8 km downstream from the head) due to the temperature difference between inflow and ambient water. The vector plot obviously shows a considerable vertical motion of the plume within the underflow region driven by the density-induced negative buoyancy forces. The interflow created at the depth of 8 to 10 meters below the water surface when the plume detached from the reservoir bottom. The temperature contour shows that the inflow with lower temperature (18 to 24 °C) than the ambient water (26 to 28 °C) plunged into the reservoir and traveled along the reservoir bottom until it reached its equilibrium temperature (21 - 22 °C) about 8 m below the water surface. Both the velocity vector fields and temperature contour demonstrated that the model successfully captured the behavior of various flow regimes, plunge flow, underflow, and interflow after the contaminated river water entered the reservoir.

Fate and Transport of MITC

Longitudinal and vertical distributions of MITC concentration in the reservoir are presented in Figure 8 using iso-concentration contours that obtained after 2, 30, and 60 hours from the time the peak passed the upstream inflow boundary. The contaminant degradation due to physico-chemical reaction processes, which was obtained by subtracting the concentrations of MITC from concentrations of a tracer (a conservative matter), are also given to determine the effectiveness of these processes in the total MITC reduction in the various flow regimes. As expected, more chemical losses occurred by kinetic reactions near the core of the plume where peak or maximum concentrations were located than plume edge

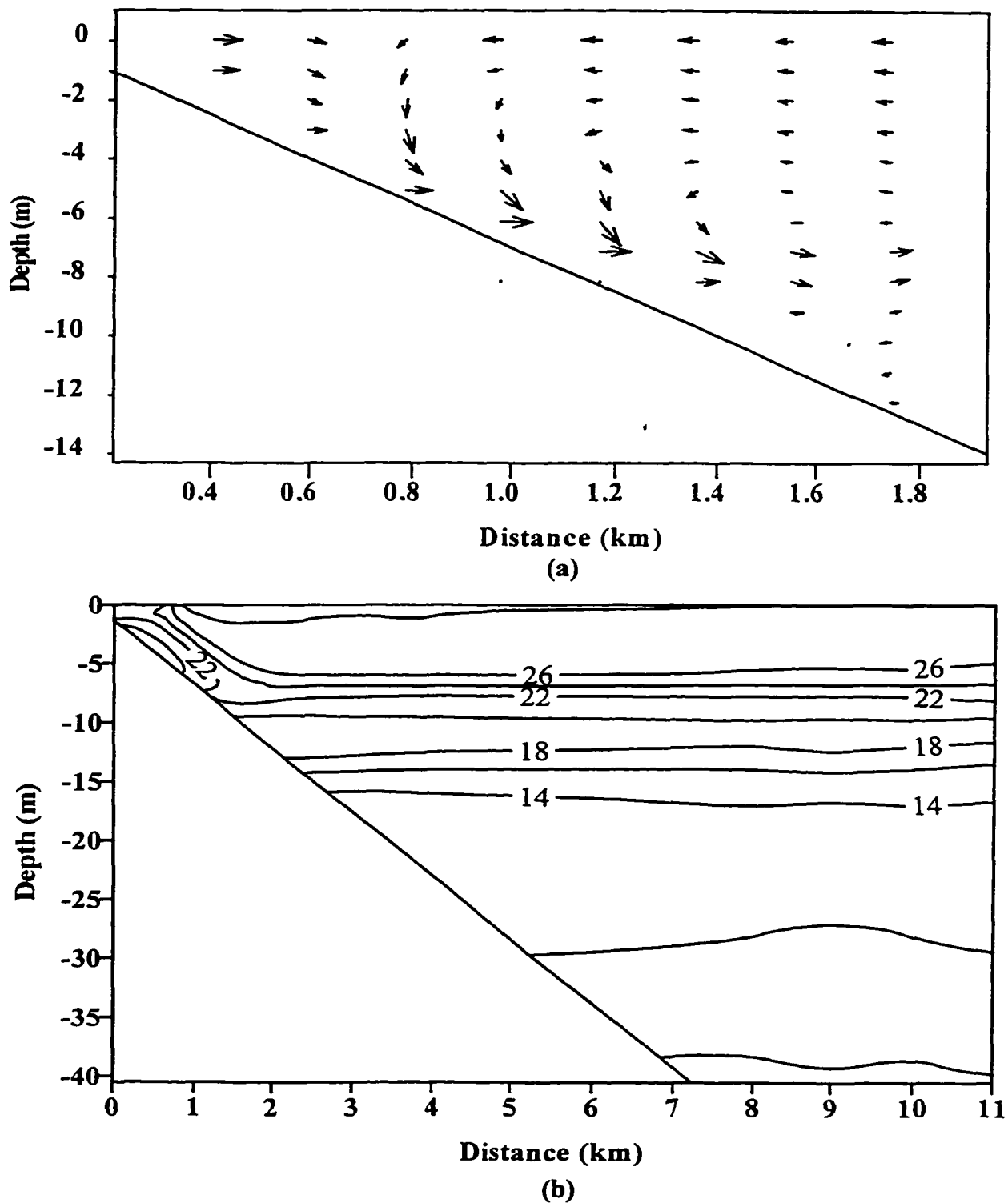


Figure 7. The (a) flow velocity vector field and (b) contour of reservoir water temperature in the Shasta Reservoir during the spill at 9:00 a.m. on 7/23/91.

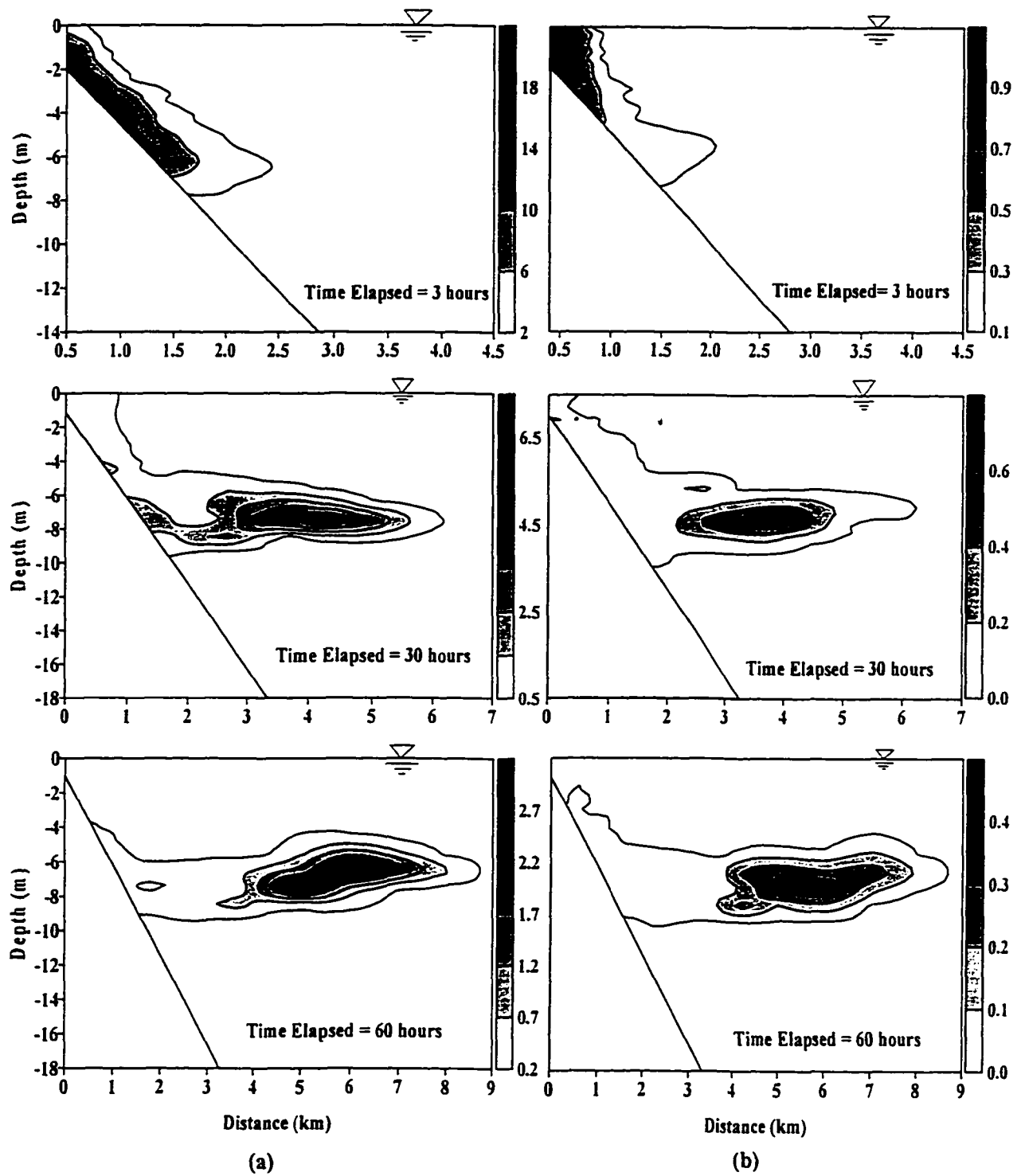


Figure 8. Contours of the simulated (a) MITC concentrations and (b) concentration difference between tracer and MITC that represents the amount of contaminant reduction by physico-chemical reactions.

because the chemical decay rate is first-order function to the chemical concentration. The amount of the toxicant degradation by reactions in the plunge flow and underflow was greater than in the interflow regime. This is mainly attributed to the sufficient turbulence that developed near the surface of the reservoir by wind and flow velocities that accelerated volatilization of the contaminant. The contribution of chemical reactions to the total MITC reduction decreased as the plume plunged and formed the underflow and interflow in the deep reservoir environments where the strong stratification limits the gaseous transfer of the contaminant from water to air. In the interflow regime, the reduction of concentrations was mainly achieved by hydrolysis of the chemical and mixing with ambient water rather than by volatilization.

The effectiveness of chemical reactions in the total concentration reduction, E_R , was quantitatively analyzed using the predicted maximum chemical concentrations at different times or in different flow regimes (Table 2). In Table 2, C_{tracer} and C_{mitc} denote the predicted maximum tracer and MITC concentrations in the reservoir after time t (hours), respectively. The total concentration reduction after time t was obtained by subtracting C_{mitc} from the peak concentration at the inflow boundary, C_o . The total reduction rate (R_T), which was defined by $100 \times (C_o - C_{\text{mitc}}) / C_o$, increased exponentially with time. More than 80% of the chemical concentration reduction was accomplished within 30 hours after the peak passed the upper boundary of the reservoir. A dilution index (I_D) and a reaction index (I_R) were used to separate the contributions of flow dilution by mixing processes and chemical decay by physico-chemical reaction processes during the spill period. The I_D and I_R values can be varied from 0 to 100%, and their sum should be always equal to 100%. The index value 100% indicates that the reduction of chemical concentrations totally accomplished by the dilution (if $I_D = 100\%$) or reactions (if $I_R = 100\%$) during time t . Therefore, these indices designate the accumulated contribution of each process. The E_R value was used to determine the effectiveness of physico-chemical reactions for a local time period. A large E_R value indicates a great effectiveness of chemical reactions at time t .

The I_R value in the plunge flow region reached as much as about 7% due to the high chemical concentrations and flow turbulence that accelerated the MITC loss through

Table 2. The effects of flow dilution and physico-chemical reactions on total MITC reduction versus time in various reservoir flow regimes.

t (hrs.)	Flow regime	C_{tracer} (mg/l)	C_{mitc} (mg/l)	$C_o - C_{\text{mitc}}$ (mg/l)	R_T (%)	I_D (%)	I_R (%)	E_R (%)
(1)	(2)	(3)	(4)	(5)	(6)	(7)	(8)	(9)
0	Inflow	35.0	35.0	0.0	0.0	-	-	-
3	Plunge flow	22.9	22.0	13.0	37.1	93.1	6.9	3.9
12	Underflow	9.9	9.1	25.9	74.0	96.9	3.1	8.1
30	Interflow	5.6	5.0	30.0	85.7	98.0	2.0	10.7
57	Interflow	3.4	3.0	32.0	91.4	98.7	1.3	11.8
81	Interflow	2.8	2.4	32.5	92.8	99.1	0.9	14.3

(1) Time elapsed after the peak passed the upstream boundary (Doney Creek).

(2) Reservoir flow regime.

(3) Peak tracer concentration (dilution effect).

(4) Peak MITC concentration (dilution and physico-chemical reactions effect).

(5) Total reduction of peak MITC concentration.

(6) Total MITC reduction rate, $R_T = 100 \times (C_o - C_{\text{mitc}}) / C_o$

(7) Dilution index, $I_D = 100 \times (C_o - C_{\text{tracer}}) / (C_o - C_{\text{mitc}})$

(8) Reaction index, $I_R = 100 \times (C_{\text{tracer}} - C_{\text{mitc}}) / (C_o - C_{\text{mitc}})$

(9) Effectiveness of chemical reactions at time t, $E_R = 100 \times (C_{\text{tracer},t} - C_{\text{mitc},t}) / C_{\text{tracer},t}$

volatilization. The I_r decreased to 2-3% in the underflow and to less than 1% after 81 hours in the interflow, but the E_r value increased with time as the turbulent mixing decreased. The results suggest that although the reduction of the contaminant concentrations was primarily attained by flow dilution due to transport and mixing processes (i.e., $I_D > 90\%$) in the early stage of the spill, the influence of the physico-chemical reaction processes on the chemical reduction can be more significant in the late stage of the spill. If so, it is possible that the persistence of the spilled chemical in the reservoir is more likely dependent upon the decay processes rather than the turbulent mixing processes in the late stage. A long persistence of the high level of MITC concentrations ($C_{mitc} = 2.4$ mg/l after 81 hours) in the reservoir has a significant meaning for the reservoir ecosystem and water supply because the LC_{50} for bluegill is 130 μ g/l.

Observed and simulated MITC concentrations at different stations are presented in Figure 9. The results show that the contribution of chemical reactions to the total MITC reduction was not significant during the spill. The model results were slightly improved after taking into account the chemical reactions. The large deviation between observed and simulated MITC concentration at the Station 1 may have two reasons. First, inaccurate prediction of wind mixing effects in the epilimnion due to lack of wind direction data in this site. Second, a continuous break down of small amount of residual Na-MDTC near the reservoir surface. Using natural log scales and linear relationships between $\ln(C/C_0)$ and $\ln(t)$ Figure 10 shows the observed MITC and simulated tracer and MITC concentrations versus time. The slopes obtained from the linear regressions for the tracer and MITC concentrations represent the dilution rate (q) and the combined rate of dilution and kinetic reactions ($q + k$), respectively. Thus, the difference (0.025 hr^{-1}) between q and $q + k$ is the overall MITC kinetic reaction rate (k) during this period. The ratio of overall kinetic reaction rate to dilution rate (k/q) was about 4% along the various flow regimes. This is well agreed with the results obtained in Table 2, $I_r = 0.9 - 6.9\%$.

The influence of artificial mixing device on the additional mixing of spilled plume was estimated using the observed and simulated maximum MITC concentrations at sampling Stations 9 and 16 (Figure 11). The results indicate that the artificial mixing device reduced

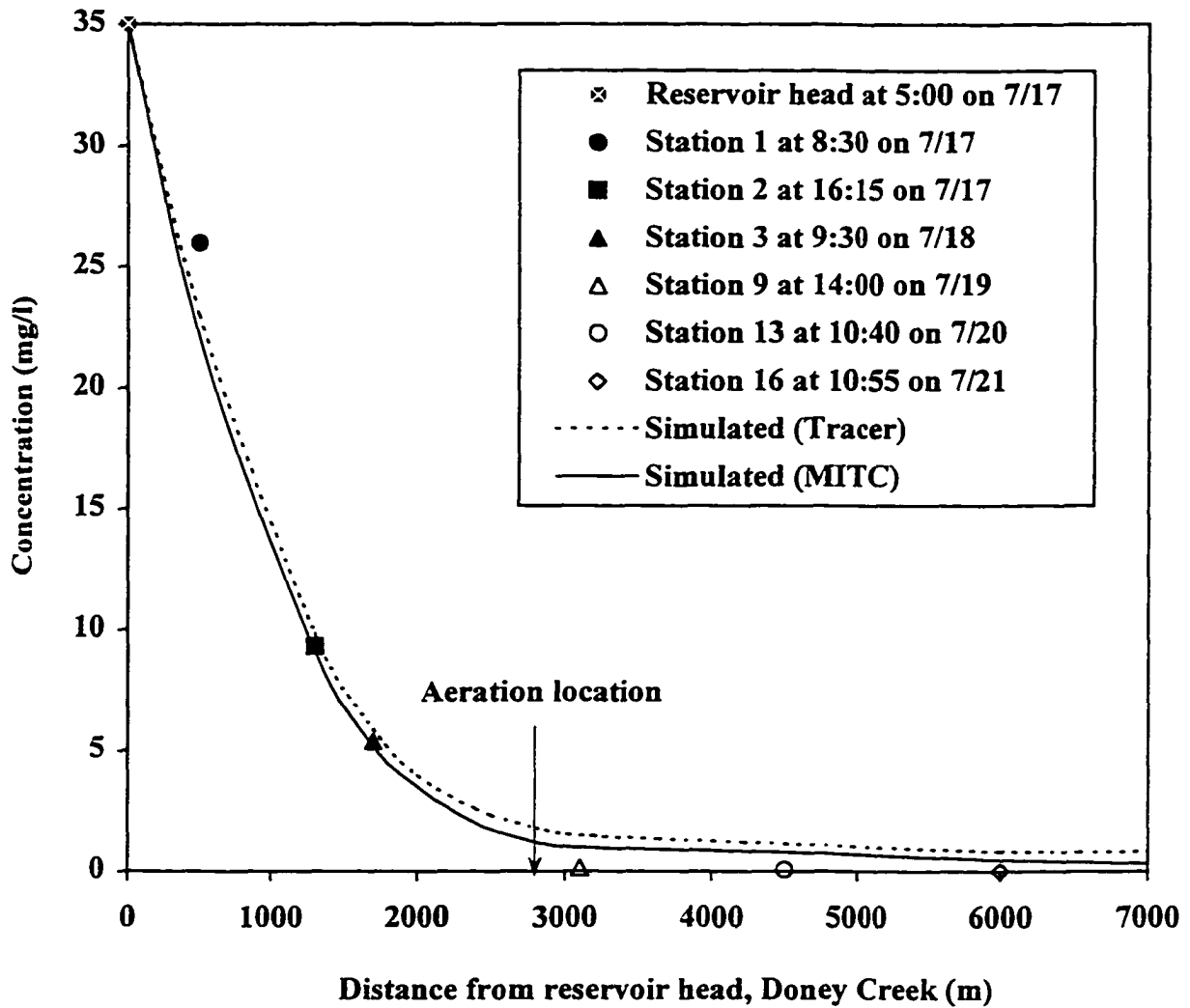


Figure 9. Observed and simulated MITC concentrations at selected sampling stations during the spill.

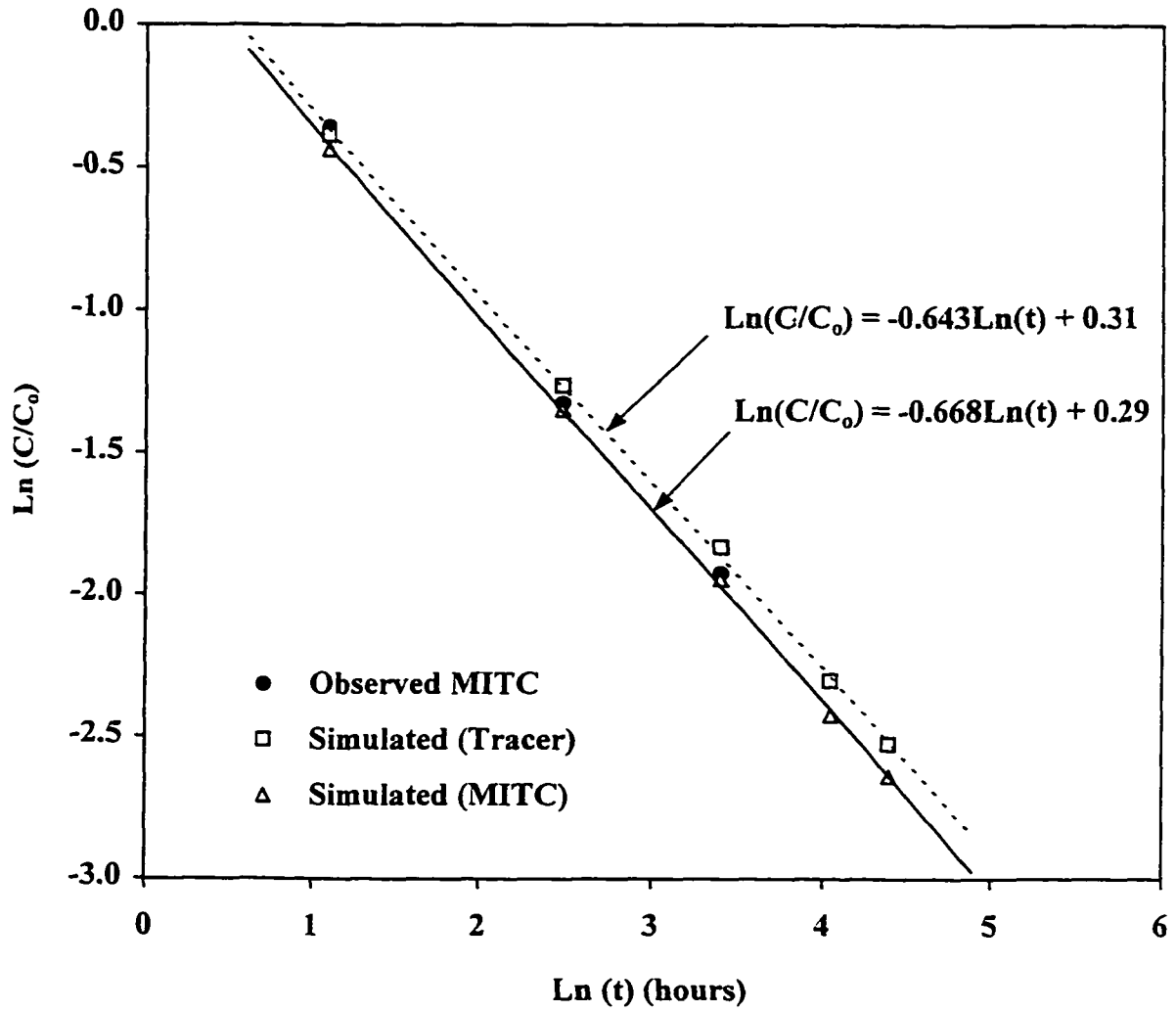


Figure 10. The linear relationships of observed and simulated MITC concentrations versus time during the early stage of the spill.

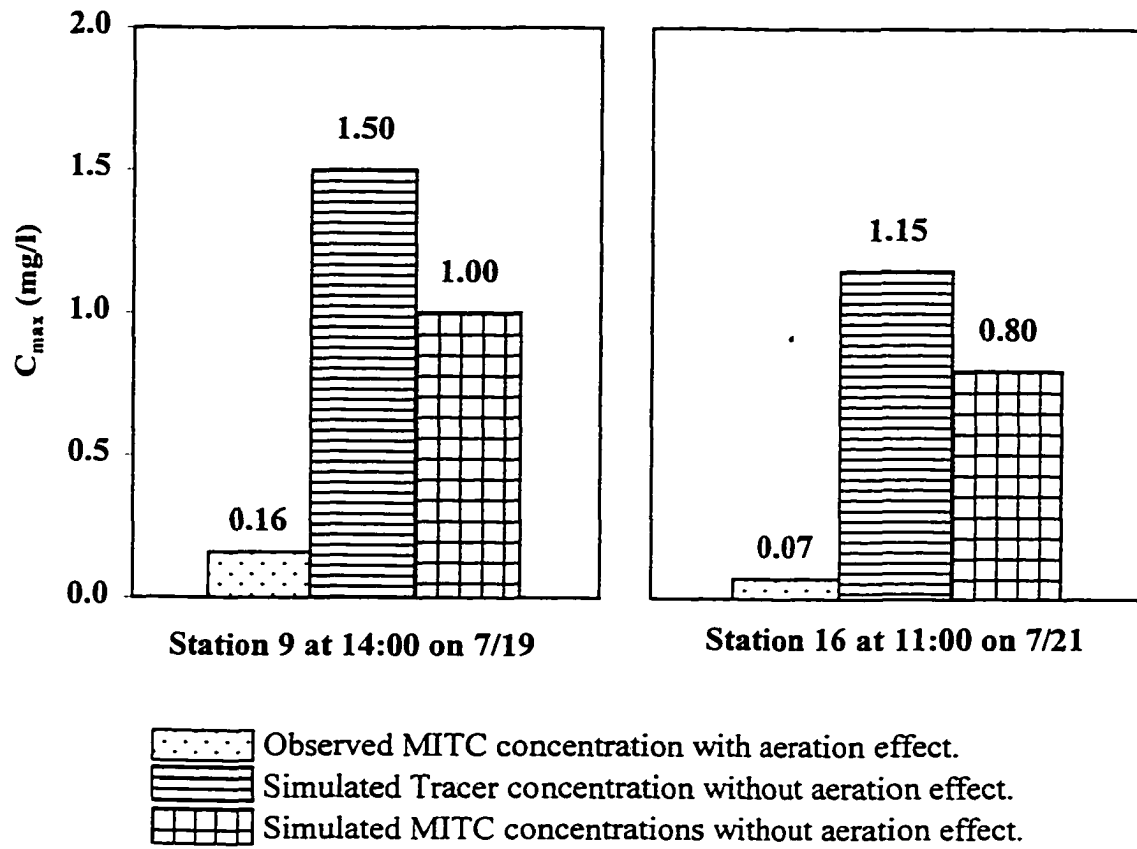


Figure 11. Observed MITC and simulated tracer and MITC concentrations at Stations 9 and 16 (downstream of the artificial mixing device).

the chemical concentrations additionally about 0.84 and 0.73 mg/l at Stations 9 and 16, respectively. These are notable reductions if the toxicity of the chemical, $LC_{50} = 0.13$ mg/l for bluegill, is considered. About 0.5 and 0.35 mg/l reduction in MITC concentrations were due to chemical reactions at Stations 9 and 16. The artificial mixing device effectively contributed to the reduction of MITC concentrations to a level less than the LC_{50} for bluegill in a short time after the spill.

Effect of Flow Regimes

The effect of reservoir flow regimes, interflow and overflow, on the persistence of the toxic contaminant in the late stage of the spill was quantified to examine the hypothesis that an interflow tend to reduce the degradation of MITC and an overflow enhance it. An overflow regime was created by changing the river water temperatures from 18-24 °C to 30 °C while all other conditions were kept unchanged. The spatial distributions of a conservative tracer (top) and MITC (bottom) concentrations for the interflow and the overflow regimes are displayed in Figure 12, showing concentration contours were 10 days after the peak concentration passed the inflow boundary.

In the interflow situation, the plume resided within the thermocline zone. The plume spread out in the longitudinal direction at 6-10 m deep below the water surface while the head of contaminant plume reached up to 15 km from the upstream boundary. The peak chemical concentrations diluted to 350-450 µg/l by flow mixing effect only, which is indicated in the tracer concentrations. The combined effects of dilution and physico-chemical reactions resulted in more reduction of MITC concentrations to 130-200 µg/l. In the overflow case, the plume stayed near the surface of the reservoir and the contaminant head reached only up to 10 km from the upstream boundary. The peak concentration of tracer was about 350-450 µg/l, indicating that the level of dilution due to flow mixing in the overflow situation is similar to that in the interflow situation. However, the overflow toxic plume moved more slowly in the reservoir and experienced greater chemical loss (kinetic degradation) than the interflow. This is because the surface transport of the contaminant provided a suitable environment for great portion of MITC to be evaporated into the air. The level of contaminant concentrations was less than 60 µg/l in most part of the reservoir. These

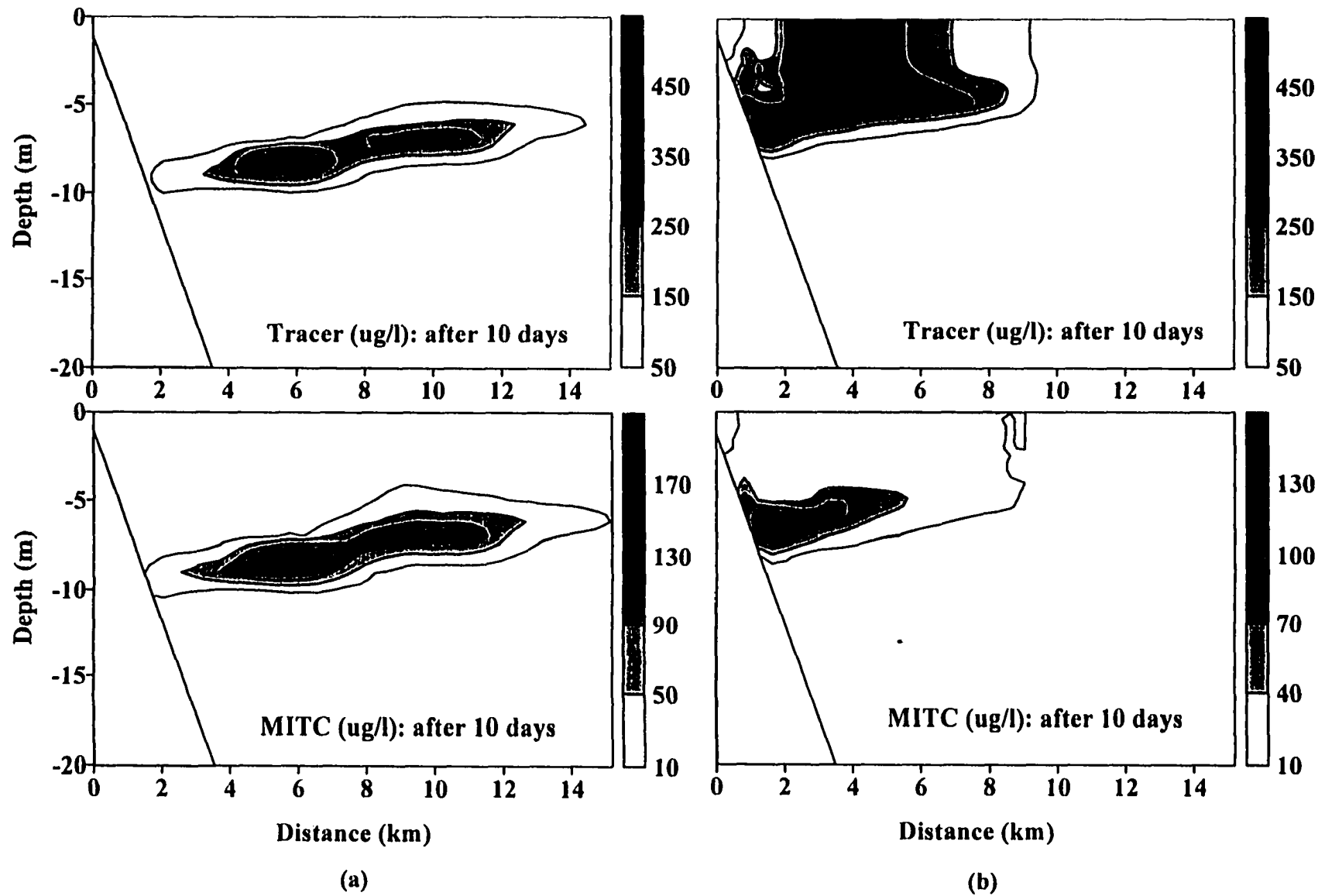
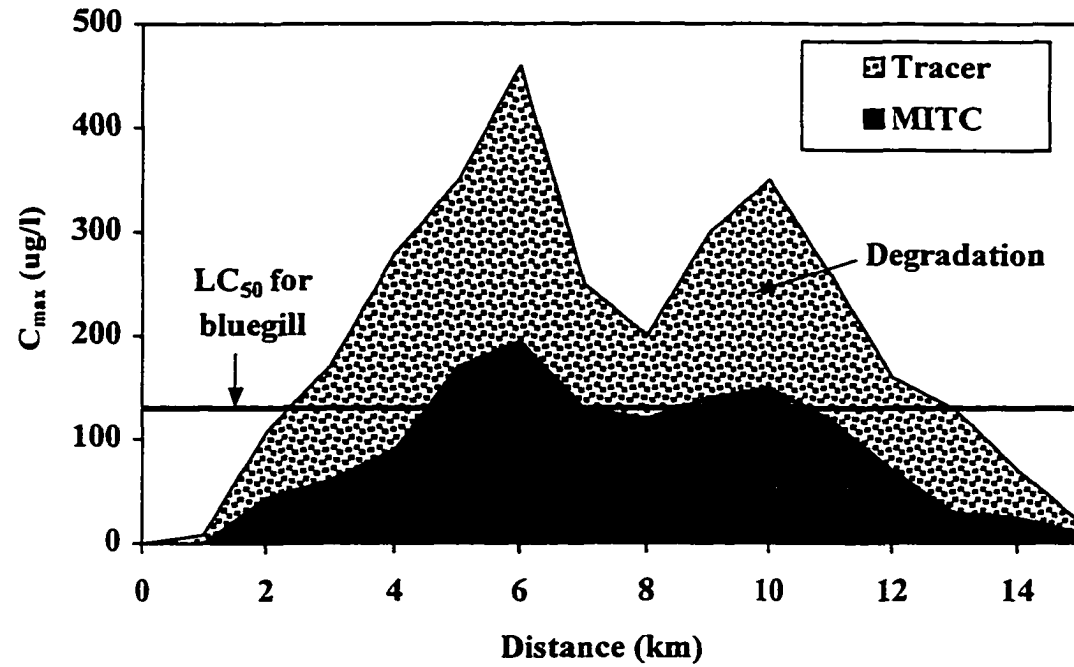


Figure 12. The spatial distributions of tracer (top) and MITC (bottom) concentrations in (a) the interflow regime and (b) the overflow regime after 10 days (7/26/91) in the Shasta Reservoir.

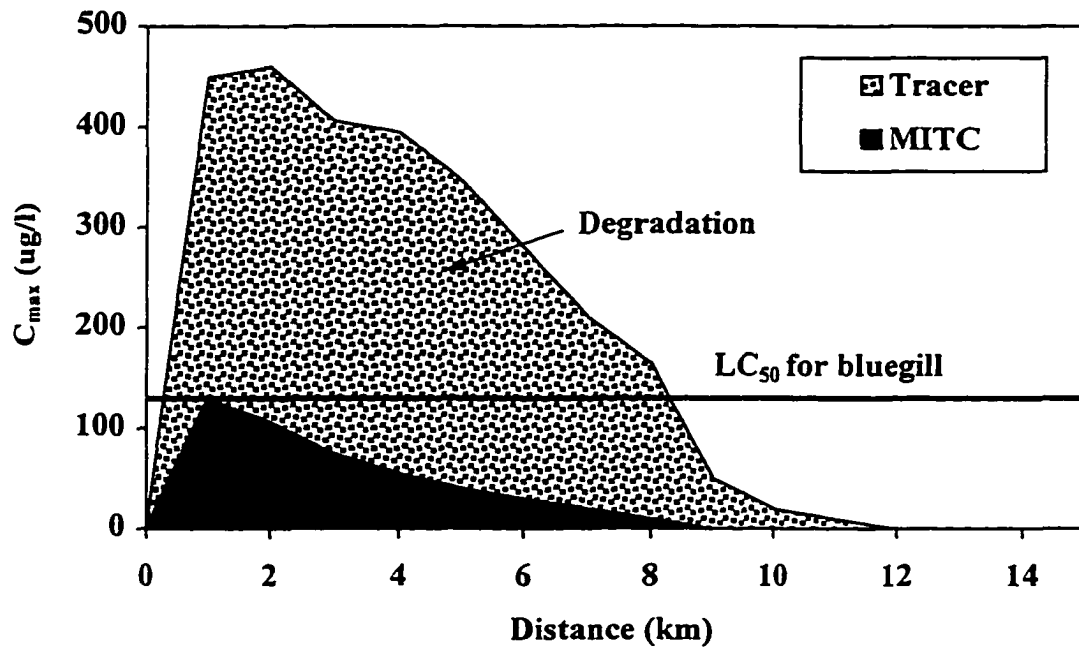
characteristics of an overflow regime may be considered as the positive aspects with respect to water quality management as drinking water intake and downstream discharge structures are generally located near the dam. The high level of chemical concentrations ($> 100 \mu\text{g/l}$) was only located in a small area of the reservoir. An artificial mixing device can be practically used in that area to accelerate the degradation processes of the slowly moving contaminant plume.

Figure 13 shows the maximum tracer and MITC concentrations versus longitudinal distance for the interflow and the overflow situations. The concentration difference between tracer and MITC represents the amount of MITC degradation that occurred due to chemical reactions. It is clearly shown that the effectiveness of physico-chemical reaction processes is greater in the overflow than in the interflow. The peak concentrations reduced to $460 \mu\text{g/l}$ by flow dilution effect only in both flow regimes. In the interflow, the physico-chemical reactions led to more reduction of the MITC concentrations, but the peak concentration ($195 \mu\text{g/l}$) was still greater than the LC_{50} for bluegill ($130 \mu\text{g/l}$). Great amount of MITC degraded by chemical reactions within the upper part of the reservoir (2-4 km from the upstream boundary) in the overflow. The peak concentration was $107 \mu\text{g/l}$ which is less than the LC_{50} for bluegill.

The effects of reservoir flow regime on the fate and transport of MITC are summarized in Table 3. The reduction of the toxic contaminant was mainly achieved by flow dilution (i.e., I_D was greater than 95%) due to the transport and mixing processes in the early stage of the spill, but the effectiveness of chemical reactions (E_R) increased with time as the turbulent mixing diminished. After 10 days, the E_R values reached up to 57.6% and 76.7% for the interflow and overflow, respectively, indicating that the reduction of MITC concentrations primarily accomplished by physico-chemical reaction processes. Therefore, the persistence of the reservoir is dependent upon the effectiveness of chemical reactions in this stage. The persistence (or residence time) of the contaminant may be shorter if the inflow formed an overflow in the reservoir during the spill. An overflow may be the flow regime desirable for managing and remediation of a volatile toxic chemical spill in a reservoir during a short term. The results also suggest that the efficiency of the artificial mixing device, which was installed



(a)



(b)

Figure 13. The longitudinal profiles of maximum tracer and MITC concentrations in the (a) interflow and (b) overflow regimes after 10 days.

Table 3. Effects of reservoir flow regime on the fate and transport of the toxic contaminant, MITC, in the late stage of the spill.

Parameters	Flow regime	
	Interflow	Overflow
Propagation length (km)	15.0	10.0
Tracer concentrations ($\mu\text{g/l}$):		
Peak	460.0	460.0
Spatial average	210.0	220.0
MITC concentrations ($\mu\text{g/l}$):		
Peak	195.0	107.0
Spatial average	90.0	31.0
Reaction Index, I_R (%)	0.76	1.10
Effectiveness of reactions, E_R (%)	57.6	76.7

I_R = Reaction index, $I_R = 100 \times (C_{\text{tracer}} - C_{\text{mitc}}) / (C_o - C_{\text{mitc}})$

E_R = Effectiveness of chemical reactions at time t, $E_R = 100 \times (C_{\text{tracer,t}} - C_{\text{mitc,t}}) / C_{\text{tracer,t}}$

in the interflow region (about 2.6 km downstream from Doney Creek), might be maximized if it was installed within 0.8 km downstream from the upstream boundary. This is because that an overflow would be created if the colder river water is mixed with the warmer ambient surface water before the plume plunged.

Case Study

A hypothetical case was investigated to examine the effects of reservoir flow regimes (interflow and overflow) on the propagation length, dilution, physico-chemical reactions, and spatial distribution of the toxic chemical in other situations through numerical experiments. A reservoir was assumed to be stratified in the vertical direction with a uniform water temperature of 26 °C in the epilimnion (0-5 m from the surface of reservoir) and 10 °C in hypolimnion zones (10-30 m), respectively. A linear decline of water temperature was assumed in the thermocline zone (5-10 m). The total length of 10 km reservoir reach was discretized into a single branch finite-difference grid consisting of 20 longitudinal segments with 0.5 km in length and 30 vertical layers with 0.5-1.0 m in thickness. The slope and half-angle of the reservoir were assumed 0.17° and 3°, respectively.

Total six different cases were generated using the combinations of two flow regimes, interflow and overflow, and three inflow conditions (Table 4). Three different inflow conditions were characterized using Richardson number (Ri), the ratio of buoyancy force to inertia force, at the upstream boundary:

$$Ri = \frac{1}{U_o^2} \frac{\rho_a - \rho_m}{\rho_a} gh_o \quad (10)$$

where U_o is the flow velocity at the inflow boundary, ρ_m is the river water density, ρ_a is the ambient water density, g is the acceleration of gravity, and h_o is the inflow water depth. A Ri number greater than 1 indicates that the buoyancy force is relatively greater than the inertia force. A negative Ri number indicates negative buoyancy (downward force). The flow conditions for high, medium, and low Ri numbers were created by changing the inflow flow rate. The wind speed and air temperature were set for 2 m/sec and 26 °C to minimize the

Table 4. Reservoir flow regimes and inflow conditions used in the hypothetical case study.

Case	Regime	T_{in} (°C)	ρ_{in} (kg/m ³)	Q_o (m ³ /sec)	U_o (m/sec)	Ri	Dominant force
1	Interflow	20	998.207	20	0.2857	-0.17	Inertia
2	Overflow	31	995.327	20	0.2857	0.17	Inertia
3	Interflow	20	998.207	5	0.0714	-2.82	Buoyancy
4	Overflow	31	995.327	5	0.0714	2.82	Buoyancy
5	Interflow	20	998.207	1	0.0143	-68.3	Buoyancy
6	Overflow	31	995.327	1	0.0143	68.3	Buoyancy

T_{in} = Inflow water temperature.

ρ_{in} = Inflow water density corresponding to T_{in} .

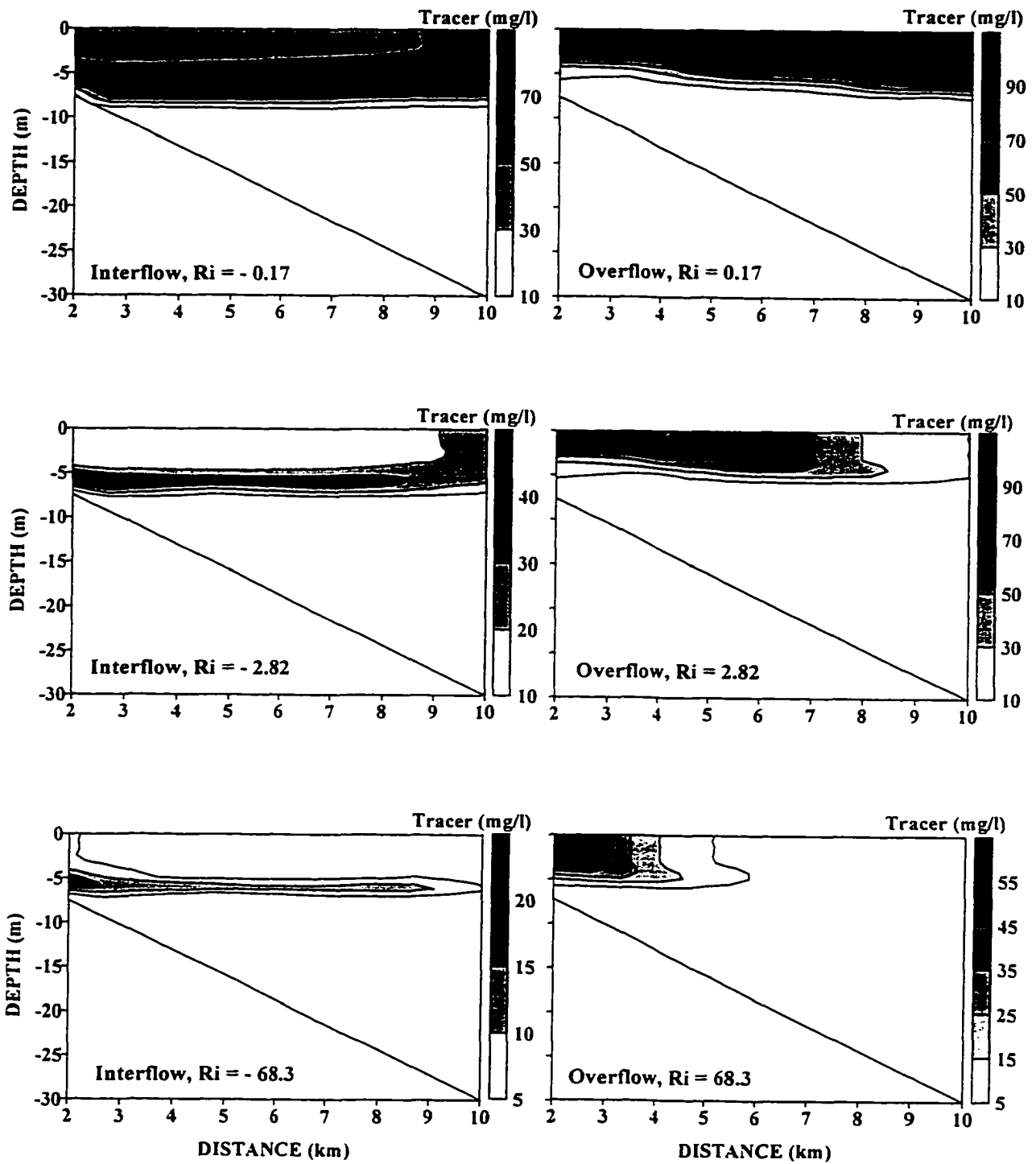
Q_o = Inflow flow rate.

Ri = Richardson number calculated using equation (10) with $\rho_a = 996.787 \text{ kg/m}^3$. The negative sign denotes negative buoyancy force because $\Delta\rho = \rho_a - \rho_{in} < 0$.

weather effect. A constant flow rate and MITC concentration ($C_o = 100$ mg/l) (steady-state) were specified at the upstream boundary for all cases.

Figures 14 and 15 show the spatial distributions of tracer and MITC concentrations, respectively, after 20 days for different flow regimes and Richardson numbers. Comparisons of the concentration contours between the interflow and overflow indicate that the transport and physico-chemical decay processes of MITC are significantly affected by the flow regimes. The contaminant plume in the interflow experienced greater initial dilution due to a greater turbulent mixing in the plunge and underflow regions. However, after the initial mixing, the plume moved along the reservoir thermocline layer with insignificant concentration changes. In the overflow, although the initial mixing was relatively smaller than interflow, the chemical concentrations dropped significantly with distance. A distinct longitudinal stratification of MITC concentrations is observed due to the effective chemical decay processes through physico-chemical reactions such as volatilization and hydrolysis in the overflow. Based on the equivalent plume head concentrations, a greater plume length is observed in the interflow than in the overflow for $Ri = 2.82$ and 68.3 . The length difference increased as the Ri number increases.

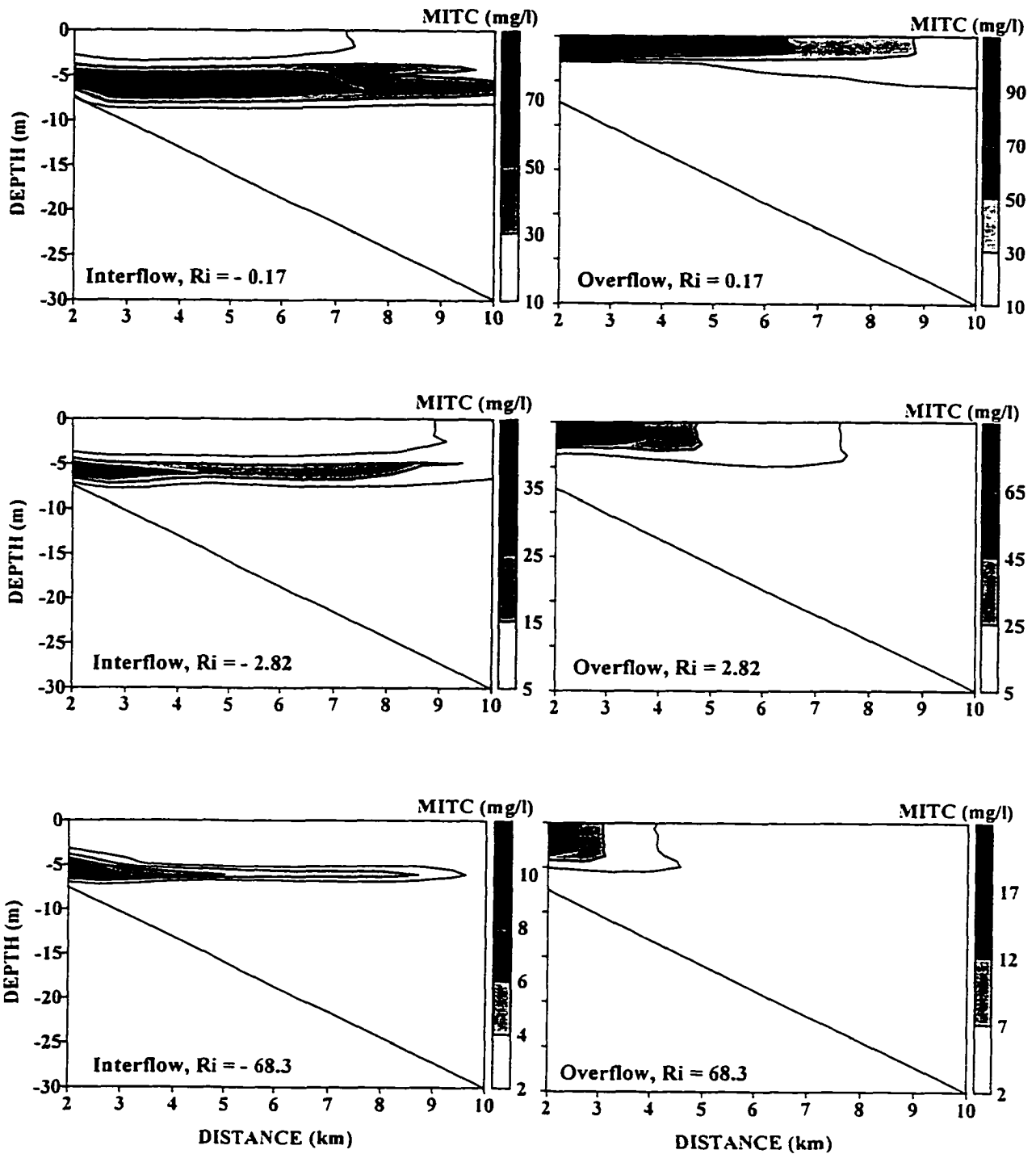
The maximum tracer and MITC concentrations versus reservoir longitudinal distance are presented in Figure 16. The slope of a tracer line indicates the rate of dilution, while that of MITC indicates the rate of chemical degradation due to both mixing and decay processes. Although a greater initial mixing was obvious in the interflow for all flow conditions, the degradation rate of contaminant was always greater in the overflow than in the interflow due to the more effective decay processes in the overflow. A great amount of chemical decay by kinetic processes, which is seen from the vertical difference between the tracer and MITC concentrations, occurred at the downstream part of the reservoir for low Ri number, and at the middle and upstream of the reservoir for medium and high Ri numbers, respectively. For the low Ri number (Fig 16a), which represents an inertia force dominant flow, the dilution rates were small in both flow regimes as indicated by the slopes of the tracer concentrations. As the inertia force decreased (Ri increased), the rate of chemical reduction increased in the overflow regime because of the reduced flow velocity (Table 4) that resulted in more time for



(a)

(b)

Figure 14. The spatial distributions of tracer concentrations in a hypothetical reservoir after 20 days in the (a) interflow and (b) overflow for different values of Richardson number.



(a)

(b)

Figure 15. The spatial distributions of MITC concentrations in a hypothetical reservoir after 20 days in the (a) interflow and (b) overflow for different values of Richardson number.

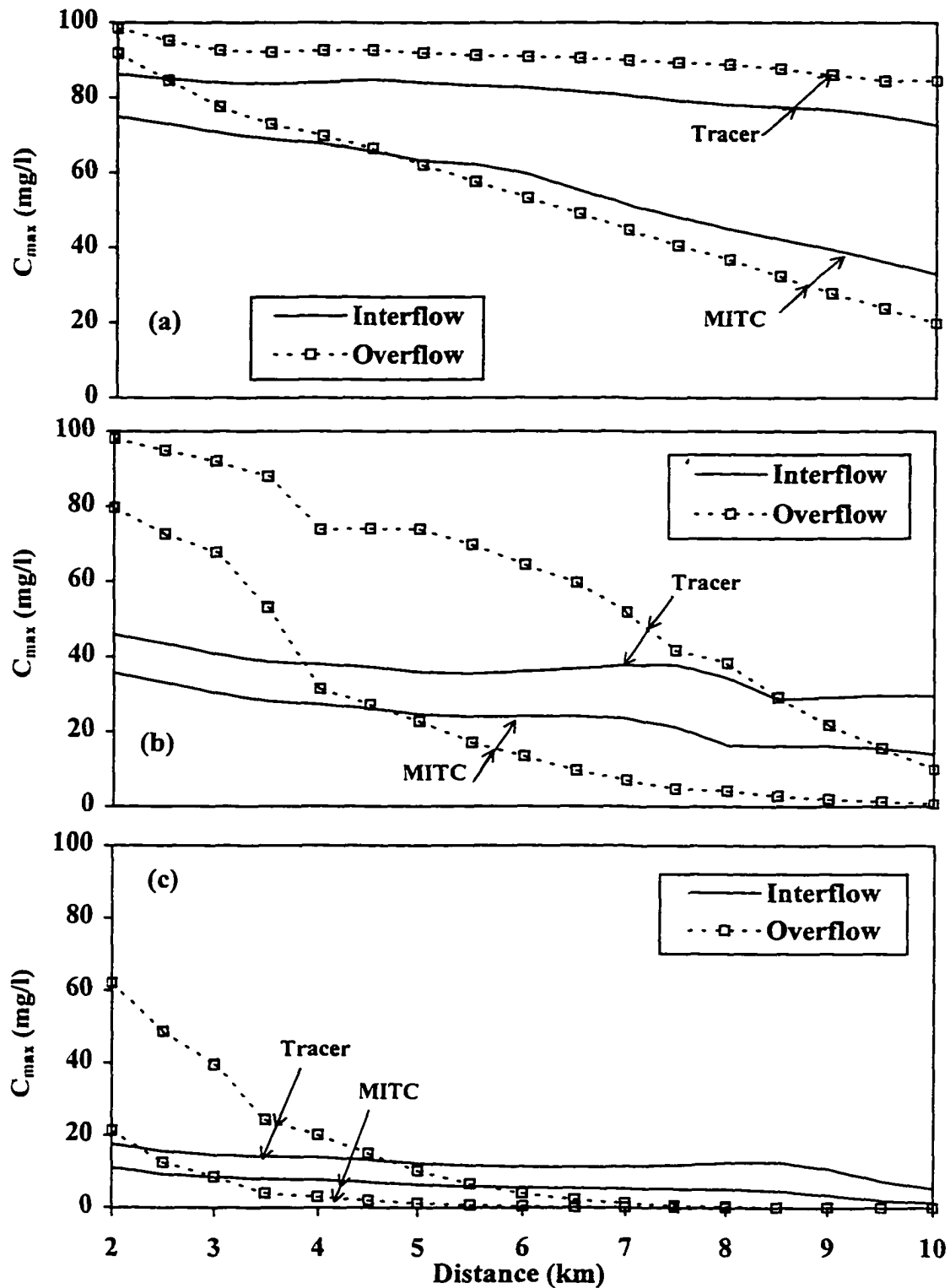


Figure 16. Maximum concentrations of tracer and MITC versus distance for (a) low Ri (0.17), (b) medium Ri (2.82), and (c) high Ri (68.3).

mixing and reactions, but no significant changes are observed in the interflow. This is primarily due to the strong stratification of the reservoir that interfered with the diffusive transport of the contaminant in the vertical direction in the interflow.

Conclusions

A two-dimensional reservoir toxic submodel was developed and incorporated into a laterally integrated hydrodynamics and transport model. The model is capable of simulating the fate and transport of various toxic contaminants, including sorption and desorption, photolysis, hydrolysis, oxidation, biotransformation, volatilization, diffusive exchanges between the bottom sediment and water column, and sediment transport and deposition in a reservoir. The model was applied to the Shasta Reservoir, California to investigate the effect of various flow regimes on the fate and transport of a volatile toxic compound (MITC) that was spilled into the reservoir. Predicted flow velocities, water temperature, and chemical concentrations clearly identified various reservoir flow regimes: plunge flow, underflow, and interflow that created during the spill period.

The effectiveness of physico-chemical reaction processes for total reduction of MITC concentrations was determined for different time in various flow regimes. It was shown that in the underflow and interflow regimes the kinetic degradation processes of MITC were slow, and that resulted in a long persistence of the chemical during the spill. The amount of MITC loss by chemical reactions decreased as the plume plunged into deep layers of the reservoir and formed the underflow and interflow primarily due to a reduced volatilization rate in the deep reservoir. The dilution and reaction index values showed that reduction of the chemical concentrations was mainly achieved by flow dilution due to transport and mixing processes in the early stage of the spill. However, the effectiveness of the physico-chemical reaction processes for the chemical reduction increased with time as the turbulent mixing diminished.

Numerical experiments were conducted to investigate the effects of reservoir flow regimes on the fate and transport of the toxic chemical. The results demonstrated that reservoir flow regime can substantially affect the persistence and transport of the volatile toxic contaminant in the late stage of the spill. The dilution levels in the interflow and

overflow regimes were similar, but the plume moved more slowly and experienced greater chemical loss in the overflow. The overflow regime resulted in a reduced toxic contamination level (less persistent), shorter plume length, and longer response time compare to the interflow. These differences may be considered in water quality management as water intake structures and fishery facilities or other recreational activities are mostly located downstream near the dam. Therefore, wherever or whenever possible and practical, an interflow should be avoid and an overflow should be used to lower contamination levels and to leave longer response time after a toxic spill. An overflow can be created intentionally through artificial mixing to minimize contamination after a toxic spill. The model and results obtained in this study can be used to assist in spill control, field sampling and contamination remediation, and reservoir management including closure of water intakes.

References

- Ambrose, R. B. et al. 1987. WASP4, A General Water Quality Model for Toxic and Conventional Pollutants, EPA-600/3-87-039, US Environmental Protection Agency, Athens, GA.
- Ambrose, R. B., T. A. Wool, J. L. Martin, J. P. Connolly, and R. W. Schanz. 1993. WASP5.x, a Hydrodynamic and Water Quality Model - model theory, user's manual, and programmer's guide. US Environmental Protection Agency, Athens, GA.
- Bath, A. J., and T. D. Timm. 1994. Hydrodynamic simulation of water quality in reservoirs of South Africa. *Commission Internationale Des Grands Barrages*. Q.69 R. 39:625-633.
- Bierman, V. J. Jr., 1994. Partitioning of organic chemicals in sediments: Estimation of interstitial concentrations using organism body burdens. pp153-175, J. V. DePinto, W. Lick, and J. F. Paul, eds. *Transport and Transformation of Contaminants Near the Sediment-Water Interface*, Lewis Publishers, Ann Arbor, USA.
- Capel, P. D., W. Giger, P. Reichert, O. Wanner. 1988. Accidental input of pesticides into the Rhine River. *Environ. Sci. Technol.* 22(9): 992-997.
- Carmack, E. C. and C. R. J. Gary, 1982, Patterns of circulation and nutrient supply in a medium residence-time reservoir, Kootenay Lake, British Columbia. *Can. Wat. Res. J.* 7:51-69.
- Chatterjee, P. 1991. California suffers its worst chemical spill., *New Scientist* 10 Aug. p12.
-

- Chung, S. W. 1996. Simulation and analysis of density flows and contaminant transport in a stratified reservoir. M.S. Thesis, Dept. of Civil and Construction Engineering , Iowa State Univ., Ames, Iowa.
- Chung, S. W., and R. Gu. 1998. Two-dimensional Simulations of Contaminant Currents in a Stratified Reservoir. *J. Hydr. Engrg.*, ASCE., 124(7):704-711.
- Churchill, M. A., 1947. Effects of density currents on Raw Water Quality. *J. of American Water Works Association*, 39(4):357-360.
- Cole, T. M., and E. M. Buchak. 1994. CE-QUAL-W2: A two-dimensional, laterally averaged, hydrodynamic and water quality model, version 2.0 user manual. Army Engineer Waterways Experiment Station, Vicksburg, Miss.
- Di Toro, D. M. 1985. A particle interaction model of reversible organic chemical sorption. *Chemosphere*.14(10):1503-1538.
- Di Toro, D. M., D. J. O'Connor, R. V. Thomann, and J. P. St. John. 1981. Analysis of Fate of Chemicals in Receiving Waters, Phase 1. *Chemical Manufact. Assoc.*, Washington, D.C.
- Draper, W. M. and D. E. Wakeham. 1993. Rate constants for metam-sodium cleavage and photodecomposition in water. *J. Agric. Food Chem.* 41:1129-1133.
- Gloss, S. P., D. E. Kidd, and L. M. Mayer. 1980. Advective control of nutrient dynamics in the epilimnion of a large reservoir. *Limnol. Oceanogr.* 24:219-228.
- Goolsby, D. A., W. A. Battaglin, J. D. Fallon, D. S. Aga, D. W. Kolpin, and E. M. Thurman. 1993. Persistence of herbicides in selected reservoirs in the Midwestern United States: Some preliminary results. *Selected Papers on Agricultural Chemicals in Water Resources of the Midcontinental United States*. US Geological Survey. Denver, CO.
- Gordon, J. A. 1980. An evaluation of the LARM two-dimensional model for water quality management purposes. In Proceedings of the Symposium on Surface-Water Impoundment, ASCE, H. G. Stefan, ed., Minneapolis, Minnesota, June 2-5, 1980, Vol. 1, pp. 518-527.
- Gu, R., S. C. McCutcheon, and P. Wang. 1996. Modeling reservoir density underflow and interflow from a chemical spill. *Water Resources Research*, 32(3):695-705.
- Hallberg, G. R. 1996. Water quality and watersheds: an Iowa perspective. In Proceedings of the Agriculture and Environment -Building Local Partnerships-. Iowa State University, Ames, IA.
-

- Kennedy, R. H. and W. W. Walker, 1990. Reservoir nutrient dynamics. pp.109-131, In K. W. Thornton, B. L. Kimmel, and F. E. Payne eds. *Reservoir Limnology: Ecological Perspectives*, John Wiley & Sons, Inc, USA.
- Kim, B. R., J. M. Higgins, and D. J. Bruggink, 1983. Reservoir circulation pattern and water quality. *J. of Environ. Engrg.*, ASCE, 109(6):1284-1294.
- Leonard, B. P. 1979. A stable and accurate convective modeling procedure based on quadratic upstream interpolation. *Computer Methods in Applied Mechanics and Engineering*, 23:59-98.
- Lyman, W. J., W. F. Reehl, and D. H. Rosenblatt. 1982. *Handbook of chemical property estimation methods*, McGraw-Hill, New York.
- Mackay, D. 1982. Volatilization of organic pollutants from water. EPA/600/3-82/019, Athens, GA.
- Martin, D. B., and R. D. Arneson. 1978. Comparative limnology of a deep-discharge reservoir and a surface discharge lake on the Madison River, Montana. *Freshwater Biol.* 8:33-42.
- Martin, J. L. 1988. Application of two-dimensional water quality model. *J. of Environ. Engrg.*, 114(2): 317-336.
- O'Connor, D. J. 1983. Wind effects on gas-liquid transfer coefficients. *J. of Environ. Engrg.* 109(9): 731-752.
- Riley, M. J., and H. G. Stefan, 1987. *Dynamic Lake Water Quality Simulation Model MINLAKE*. Report 263, St. Anthony Falls Hydraulic Laboratory, University of Minnesota, Minneapolis, MN.
- Rosario, A., J. Remoy, V. Soliman, J. Dhaliwal, J. Dhoot, and K. Perera. 1994. Monitoring for selected degradation products following a spill of VAPAM into the Sacramento River. *J. Environ. Qual.*, 23:279-286.
- Schnoor, J. L. 1996. *Environmental Modeling: Fate and transport of pollutants in water, air, and soil.*, John Wiley & Sons, New York, USA.
- Schnoor, J. L., D. J. Mossman, V. A. Borzilov, M. A. Novitsky, O. I. Voszhenniov, and A. K. Gerasimenko. 1992. Mathematical model for chemical spills and distributed source runoff to large rivers. In *Fate of Pesticides and Chemicals in the Enviroment*, J. L. Schnoor ed., John Wiley & Sons, Inc., 347-370.

- Schnoor, J. L., C. Sato, D. McKechnie, and D. Sahoo. 1987. Processes, coefficients, and models for simulating toxic organics and heavy metals in surface waters. EPA/600/3-87/015, Athens, GA.
- Thomann, R. V. and J. A. Mueller. 1987. Principles of surface water quality modeling and control. Harper & Row, New York.
- Tomlin, C. 1994. The Pesticide Manual. Tenth Edition, The British Crop Protection Council, UK.
- Thurman, E. M., D. A. Goolsby, M. T. Meyer and D. W. Kolpin. 1991. Herbicides in surface waters of the Midwestern United States: The effect of spring flush. *Environ. Sci. Technol.* 25:1794-1796.
- U.S. Army Corps of Engineers, Hydrologic Engineering Center. 1985. Water Quality for River-Reservoir Systems (WQRRS), User's Manual. CPD-8, Davis, Calif.
- U.S. Army Corps of Engineers, Hydrologic Engineering Center. 1986. HEC-5 Simulation of Flood Control and Conservation Systems, Appendix on Water Quality Analysis. Davis, Calif.
- Wang, P. F., T. Mill, J. L. Martin, and T. A. Wool. 1997. Fate and transport of metham spill in Sacramento River. *J. of Environ. Engrg.* 123(7):704-712.
- Whitman, R. G. 1923. A preliminary experimental confirmation of the two-film theory of gas absorption. *Chem. Metallurg. Eng.* 29:146-148.
- Worthing, C. R. 1987. The Pesticide Manual. 8th ed., The British Crop Protection Council, UK.
- Zepp, R. G. and D. M. Cline. 1977. Rates of direct photolysis in aquatic environment. *Eviron. Sci. and Techn.*, 11(4):359-366.

Notation

The following symbols are used in this paper:

- ϕ bed sediment porosity;
- λ_{\max} the wave length of the maximum light absorption;
- μ_{\max} maximum specific growth rate;
- Φ_{NPS} lateral nonpoint source mass flow rate per unit volume;

γ_{om}	rate multiplier for organic matter;
Δz	finite difference grid cell thickness
C_a	vapor phase concentration;
C_b	sediment concentration in the stationary bed sediment;
C_B	bacterial concentration;
C_d	dissolved chemical concentration;
C_{dt}	detritus concentration;
C_{mitc}	maximum MITC concentration;
C_o	peak concentration at inflow boundary;
C_p	particulate adsorbed chemical concentration;
C_s	sediment concentration in water column;
C_{ss}	suspended solids concentration;
C_t	total chemical concentration;
C_{tracer}	maximum tracer concentration;
D	radiation distribution function;
D_o	radiation distribution function near water surface;
D_z	vertical diffusion coefficient;
E_R	the effectiveness of chemical reactions for the total concentration reduction;
f_d	the fraction of the total chemical concentration that is dissolved;
f_p	the fraction of the total chemical concentration that is particulate;
H	Henry's constant;
I'	light intensity at which K_{do} was measured;
I_o	the average daily amount of incoming solar radiation at the water surface;
K	partition coefficient;
K_a	acid catalyzed hydrolysis rate;
K_b	base catalyzed hydrolysis rate;
K_B	biotransformation rate;
K_{do}	direct near surface photolysis rate;
K_{dt}	detritus decay rate;

K_e	extinction coefficient;
K_r	diffusive exchange rate between water column and pore water of the bed;
K_g	gas film coefficient;
K_H	hydrolysis rate;
k_l	volatilization rate;
K_l	liquid film coefficient;
K_n	neutral hydrolysis rate;
K_o	oxidation rate;
K_p	overall photolysis rate;
K_s	organic bed sediment decay rate;
K_x	half-saturation constant;
M	molecular weight of a chemical;
q_b	the lateral mass flow rate of sediments in reservoir bed per unit volume;
q_l	the lateral mass flow rate of sediments in water column per unit volume;
R_T	total MITC reduction rate;
u_b	longitudinal bed load velocity;
v_d	deposition velocity of sorbed chemical in the air; and
v_s	the net settling velocity of sorbed chemical in water column;
v_{ss}	the net settling velocity of suspended solids;
w_b	vertical bed load velocity; and
y_B	bacterial yield coefficient;

CHAPTER 3. ESTIMATING TIME-VARIABLE KINETIC TRANSFORMATION RATE OF ATRAZINE IN A RESERVOIR

A paper to be submitted to the Journal of Environmental Engineering

Se-Woong Chung and Ruochuan Gu

Abstract

The persistence of atrazine, one of the most applied herbicides in corn cropping areas, in an aquatic environment is dependent upon environmental conditions, i.e., temperature, sunlight, and microorganism. As these conditions are changing seasonally, accurate determination of time-variable degradation rate is important in the prediction of the fate and transport of the chemical in surface water. A mass balance model was constructed to estimate time-variable kinetic transformation rate (or half-life) of atrazine in the Des Moines River and the Saylorville Reservoir. The half-life varied monthly from 2 to 58 days depending upon the environmental conditions. Simulated atrazine concentrations were compared with field data to validate the estimated half-life, which agreed reasonably well with the trends of observed values. A significant inverse relationship was obtained between the half-life and the hours of sunlight, showing the effectiveness of photodegradation. Estimated annual atrazine budget showed that reservoir outflows and kinetic transformations control most of atrazine loadings from the farm land into the reservoir. A case study, however, revealed that an 86% increase in atrazine uses could alter the reservoir water quality. A high level of concentrations occurred in the month of May and persisted for the rest of the year. The half-life values obtained for the study area can be used as an initial approximation of atrazine degradation rate in water quality modeling for other sites with similar environmental conditions.

Introduction

A frequent detection of herbicides in source and drinking waters is one of the major water quality issues for the aquatic ecosystem and human health in Iowa and the Midwestern United States (Thurman et al. 1991; Goolsby and Battaglin 1993; Pereira and Hostettler

1993). Atrazine [2-chloro-4-ethylamino-6-isopropylamino-1,3,5-triazine] (Figure 1), a heterocyclic nitrogen compound, is one of the most extensively used herbicides for weed control in the corn cropping area in the Midwest Corn Belt. Atrazine can reach surface water system through various pathways: surface runoff, seepage flow, artificial drain flow, aerial drift during application and re-deposition in waters upon volatilization, and precipitation. Thus it has been found in surface water, groundwater, and even rainfall for three decades since its first use in 1959 (Richard et al. 1987; Nations and Hallberg 1992; Hallberg 1996; Hatfield et al. 1996). The United States Environmental Protection Agency (USEPA) ranks atrazine as a class C (possible) carcinogen and established the maximum contamination level (MCL) of 3.0 $\mu\text{g/l}$ for drinking water, which is the limiting concentration at which adverse health effects would not be expected to occur for an adult from 70 years exposure (Richard et al 1995).

Although extensive field monitoring studies of surface waters have detected atrazine concentrations that exceed the MCL between the late spring and midsummer in these agricultural area (Goolsby et al. 1991; Thurman et al. 1991; Thurman et al. 1992; Goolsby and Battaglin 1993), only limited field studies have been conducted to understand the fate of atrazine in surface water because they are costly and technically difficult (Kolpin and Kalkhoff 1993). A mathematical model can be economically and practically applied to investigate the fate and transport processes of atrazine in a watershed and a waterbody and to assess the environmental impacts of various alternative upstream watershed management strategies on the quality of surface waters. However, it is important to accurately estimate the degradation rate or half-life ($t_{0.5}$) of atrazine for applying the model and investigating its persistence in a specific aquatic system because the behavior of atrazine is quite different under different environmental conditions.

In general, the $t_{0.5}$ of atrazine is known to be 60 days in soils, but in aquatic environments it has shown to be in a wide range from 0.33 days to more than 1 year depending on the site specific conditions, such as temperature, sunlight, and microorganism concentrations (Table 1). The $t_{0.5}$ value of atrazine in surface water is relatively shorter than those measured in soils ($t_{0.5}$ = 10-100 days) because the contribution of abiotic processes such

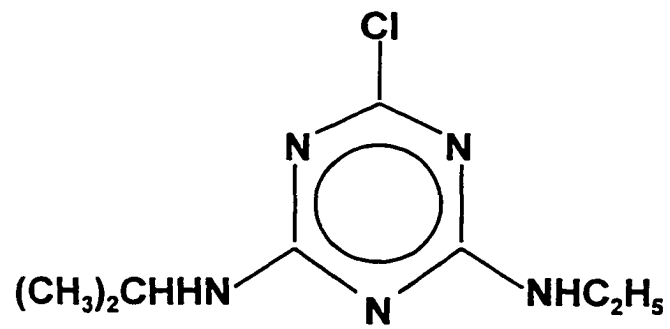
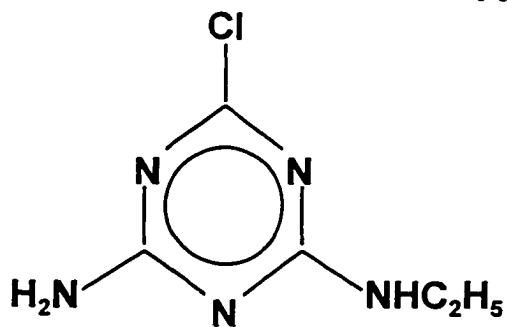
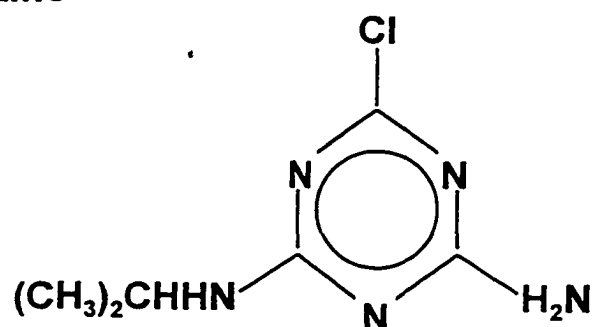
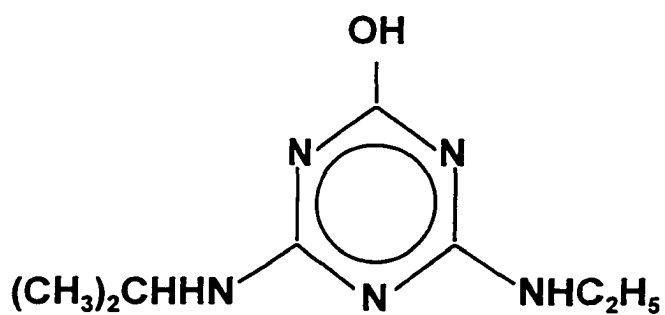
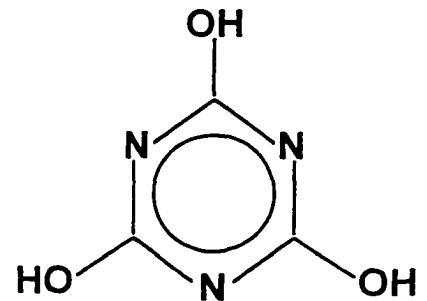
**Atrazine****Deisopropylated
Atrazine****Deethylated
Atrazine****Hydroxyatrazine****Cyanuric Acid****Figure 1. Atrazine and its degradation products**

Table 1. Atrazine half-life values documented in the previous studies.

Reference	Half-life (days)	Environment
Goldberg et al. (1991)	1.6 - 13.3	Cedar River, IA
Kolpin and Kalkhoff (1993)	1.5 - 7.0	Roberts Creek, IA
Schottler and Eisenreich (1997)	> 365	Great Lakes
Torrents et al. (1997)	0.33 ^a - 7.2 ^b	Laboratory
Portnoy (1989)	10 - 100	Soil
Paterson and Schnoor (1992)	16	Soil
Kanwar et al. (1993)	53 - 78	Soil
Tomlin (1994)	35 - 50	Soil
	105 - 200	Groundwater

^aNitrate-mediated indirect photolysis

^bDirect photolysis

as photolysis and hydrolysis is stronger and more effective for atrazine degradation in surface water environment, while biotic processes such as biotransformations are dominant in soil environment. Atrazine can be transformed into numerous different degradation products by either biotic or abiotic processes in the nature. The biotic transformation products include desethylatrazine [4-Amino-2-chloro-6-isopropylamino-s-triazine] and deisopropylatrazine [2-Amino-4-chloro-6-ethylamino-s-triazine] (Figure 1), while abiotic transformation products include hydroxyatrazine [2-Hydroxy-4-ethylamino-6-isopropylamino-s-triazine] and cyanuric acid [2,4,6-Trihydroxy-s-triazine] which is the end product of atrazine by photolysis (Figure 1). To water quality managers, the exposure level of atrazine is particularly interesting rather than other degradation products because it is known to have much higher chronic toxicity than its degradation products (Pugh 1994).

Previous studies concluded that atrazine in surface waters is degraded primarily by photolysis. Goldberg et al. (1991) and Pelizzetti et al. (1990) found that atrazine in surface water samples is rapidly degraded by photolysis with the $t_{0.5}$ values in the range between 1.6 days and 13.3 days from their laboratory studies. Kolpin and Kalkhoff (1993) investigated the major degradation processes of atrazine at Roberts Creek in northeastern Iowa. Atrazine concentrations decreased by about 25-60% as it traveled along the 11.2-km reach of the stream. They concluded from a limited field data that abiotic processes are the primary atrazine degradation pathways in the stream environment because the concentrations of the two biotic degradation products, desethylatrazine and deisopropylatrazine, were unchanging or decreasing downstream. They also demonstrated a significant inverse relationship between the number of sunlight hours and the $t_{0.5}$ of atrazine. A seasonally varied atrazine $t_{0.5}$ was obtained with the minimum of 1.5 days and maximum of 7.1 days occurring during July and October, respectively. The mechanistic of direct and indirect (or sensitized) photolysis of atrazine in aqueous solutions was investigated more in depth by Torrents et al. (1997). Their laboratory study showed that atrazine degrades more rapidly in the presence of nitrate nitrogen ($\text{NO}_3\text{-N}$) because nitrate generates hydroxyl radicals in water in the presence of sunlight. The hydroxyl radicals then cause to transform atrazine by dealkylation and alkyl oxidation (indirect photolysis). However, in the presence of dissolved organic carbon (DOC),

the direct photolysis may be more dominant because DOC efficiently scavenge hydroxyl radicals but does not compete with atrazine for sunlight (Torrents et al. 1997). In summary, the previous studies suggested with one consent that sunlight is an important driving force to degrade atrazine level by either direct or indirect photolysis in surface water.

The objectives of this study are to estimate time-variable kinetic transformation rates of atrazine using a mass balance model in the Saylorville Reservoir, Iowa (Figure 2) and investigate environmental factors that influencing the effectiveness of biotic and abiotic degradation processes of atrazine at the study site. The mass balance model was constructed using the field data collected earlier by Baumann et al. (1979) and Leung (1979) based on the assumptions of a well-mixed reservoir condition. Boundary input conditions were prepared on a monthly basis because only limited field data are available. The time-variable atrazine kinetic transformation rates were estimated by solving the mass balance model in conjunction with an optimal parameter estimation tool. The relations of the half-life values to the environmental parameters such as number of sunlight hours, water temperature, and nitrate concentration were examined to determine the significance of these parameters on the effectiveness of biotic and abiotic degradation processes in the reservoir. A case study was attempted to project monthly contamination levels of atrazine in response to increased atrazine uses in the watershed by applying the model and estimated half-life values to the reservoir.

Description of Study Site

The Saylorville Reservoir was impounded in April, 1977 and is located on the upper Des Moines River basin, Iowa (Figure 2). The reservoir was built primarily for the purposes of flood control, low flow augmentation for water quality control, and recreational activities (US Army Corps of Engineers 1983). At full flood control pool, elevation 271.3 m, the reservoir extends 86.9 km above Saylorville dam and occupies about 67.6 km². At conservation pool, the reservoir water surface elevation is about 254.8 m and occupies 24.1 km². The mean and maximum depths of the reservoir are 4.3 m and 13.8 m, respectively at the conservation level. The reservoir water surface elevations were fluctuated between 253.8

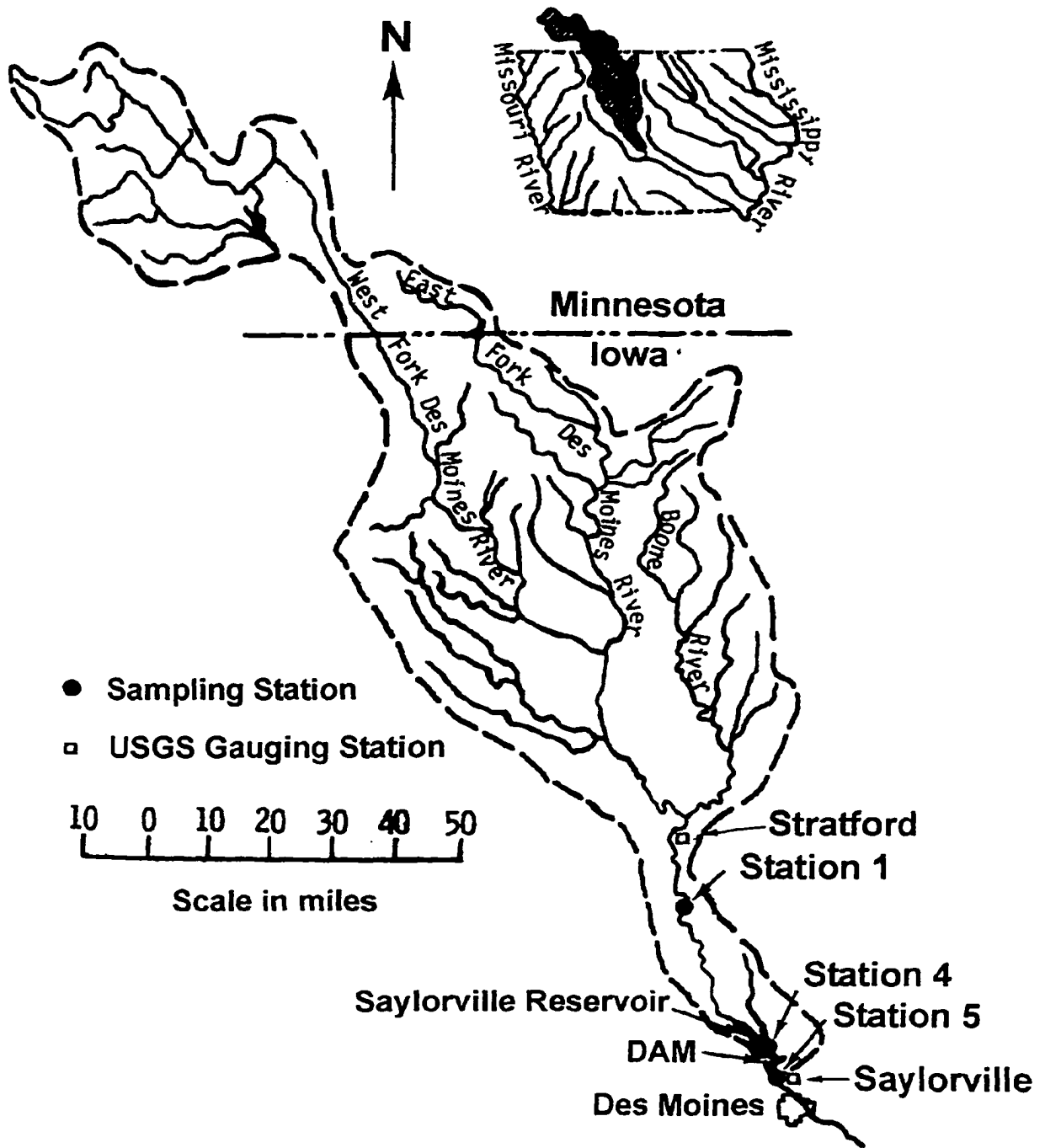


Figure 2. Map of study site and the location of sampling stations.

m (capacity 88.4 million m³) and 255.1 m (capacity 118.5 million m³) during the study period, from January, 1978 through December, 1978. Approximately 79% of the upstream watershed was cropland, 6% was permanent pasture, 5% was forest, and 7% was urban at the time of study period (Iowa Department of Environmental Quality 1976). Corn and soybeans are two major crops in the area. The annual precipitation during the study period was 797 mm which is slightly less than the normal annual precipitation of 813 mm in Iowa.

The observed data used in this study were collected weekly or biweekly at three sampling stations, denoted as Stations 1, 4, and 5 (Leung 1979). These stations are part of total 8 sampling stations installed in the Des Moines River by the Engineering Research Institute of Iowa State University to monitor the long-term impacts of Saylorville and Red Rock reservoirs on water quality and quantity (Baumann et al 1979; Lutz and Cavender 1997). Table 2 describes the location and drainage area for each sampling station. Samples were collected from three depths (subsurface, mid-depth, and bottom) of the reservoir at Station 4. Although the historical water quality monitoring data showed a distinct thermal and chemical stratifications during the summer months in the reservoir (Lutz and Cavender 1997), very weak stratifications were occurred during the study period, which allowed the use of well-mixed reservoir condition assumption. Atrazine levels in the reservoir water ranged from 0 to 1,356 ng/l during the sampling period, from September, 1977 through November, 1978, with an overall mean of 223 ng/l. Peak concentrations were observed in the late spring and early summer resulting from several short-term storm events following the application of atrazine in the agricultural fields of the study area.

Table 2. Description of sampling stations.

Station	Distance from Dam (km)	Drainage area (km ²)
1	71.8 upstream	14,539
4	0.3 upstream	15,081
5	3.0 downstream	15,128

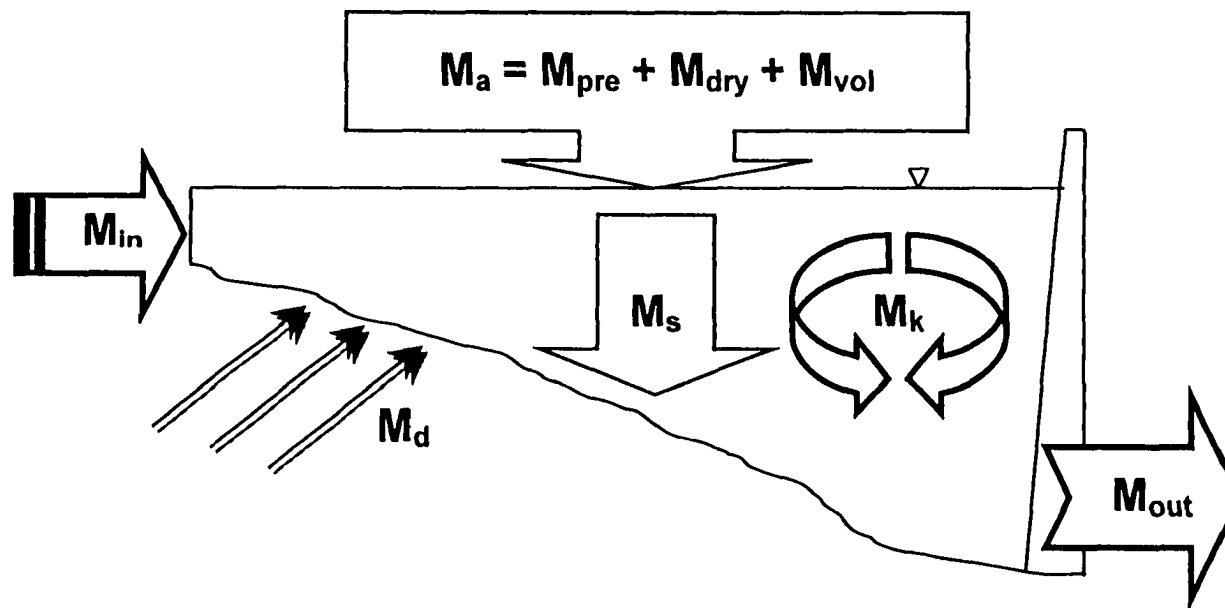
Method

Governing Equation

The reservoir waterbody from inflow boundary (Station 1) to the Saylorville Dam was assumed to be a completely-mixed system (Figures 2 and 3). Longitudinal non-homogeneity and stratification in vertical directions of the reservoir was assumed negligible. The governing equation for the conservation of atrazine mass was constructed by identifying mass loss and gain components. A similar approach to the input-output model for a well-mixed reactor has been used by Schottler and Eisenreich (1997) for the Great Lakes. Mass inputs into the system include the upstream loading from above watershed (M_{in}), direct loading through runoff and drainage flows (M_d), and atmospheric loading (M_a) by wet (M_{pre}), dry (M_{dry}) and gaseous deposition (M_{vol}). Mass outputs out of the system include atrazine mass losses via reservoir outflow (M_{out}), kinetic transformations by photolysis, hydrolysis, and biotransformation (M_k), and adsorption/settlement (M_s). By taking all components into account, the governing equation is expressed as following:

$$\frac{dM_i}{dt} = Q_{in,i} C_{in,i} + A_p A_D s_i \left(\prod_{i=1}^4 f_i \right) + p_i W A_s + C_{a,i} A_s f v_d - k_l A_s (C_{w,i} - C_{a,i} (1-f) / H) - Q_{out,i} C_{out,i} - k_s C_s C_{ss} V_i - k_t C_{w,i} V_i \quad (1)$$

where subscript i denotes any month of the year; M_i is total mass in the reservoir water column in month i (kg); Q_{in} is the upstream inflow (m^3/s); C_{in} is the atrazine concentration in the inflow ($\mu g/l$); A_p is the annual atrazine application rate in the watershed ($kg/km^2/yr.$); A_D is the drainage area (km^2); s_i is fraction of annual load via runoff and seepage flows occurring in month i ; f_1 is fraction of corn and soybean cropping area to the total drainage area; f_2 is fraction of corn cropping area to corn and soybean cropping area; f_3 is fraction of atrazine applied area to corn cropping area; f_4 is fraction of atrazine which is delivered into the river to the A_p ; p_i is fraction of annual load via precipitation occurring in month i ; W is the annual deposition rate via precipitation ($\mu g / m^2/yr.$); A_s is the surface area of reservoir (km^2); C_a is the atrazine concentration in the air (ng/m^3); f is the fraction of air concentration sorbed on



- M_{in} : Mass input due to upstream loading;
- M_a : Mass input via precipitation (M_{pre}), dry deposition (M_{dry}), and volatilization (M_{vol});
- M_d : Mass input through surface runoff, seepage flow, and drainage flow;
- M_s : Mass output by adsorption and settlement;
- M_k : Mass output due to biotic and abiotic degradation processes; and
- M_{out} : Mass output via reservoir outflow.

Figure 3. Schematic description of the mass balance model for atrazine in the Saylorville Reservoir, Iowa.

particles; v_d is the dry deposition velocity (cm/s); k_l is the overall volatilization transfer rate (m/day); C_w is the atrazine concentration in the reservoir water column ($\mu\text{g/l}$); H is the Henry's law constant ($\text{atm}\cdot\text{m}^3/\text{mol}$); Q_{out} is the outflow (m^3/s); C_{out} is the atrazine concentration in the outflow ($\mu\text{g/l}$); k_s is the sedimentation rate constant (/month); C_s is the sorbed concentration on particles ($\mu\text{g}/\text{kg}$); C_{ss} is the suspended solids concentration in the reservoir (mg/l); V_i is the total volume of reservoir in month i (m^3); and k_i is the kinetic transformation rate including photolysis, hydrolysis, and biotransformation in month i (/month).

Solution Method

The governing equation was solved iteratively to minimize sum of the root mean square errors (RMSE) between observed and simulated atrazine concentrations using the optimal parameter estimation tool, SOLVER, in the Microsoft Excel program. The objective function and constraints used to solve the governing equation are:

$$\begin{aligned}
 \text{Objective function:} & \quad \text{Min} \sum_{i=1}^n \sqrt{(C_{sim,i} - C_{obs,i})^2} / n \\
 \text{Constraints:} & \quad k_i \geq 1.0 \times 10^{-6}, \quad I = 1, 2, 3, \dots, n \\
 & \quad C_{sim,i} \geq 0.0 \quad (2)
 \end{aligned}$$

where n is the number of month; C_{sim} and C_{obs} are simulated and observed monthly mean atrazine concentrations in the reservoir in month i , respectively. C_{sim} was obtained dividing the total mass of atrazine present in the reservoir during any month by the volume of reservoir water. The k_i values were iteratively changed until the simulated atrazine concentrations fit measured values with minimum RMSE. The initial mass of atrazine presented in the waterbody ($M_0 = 3.7 \text{ kg}$) was obtained multiplying the atrazine concentration in the water column ($C = 40.7 \text{ ng/l}$) and the volume of reservoir ($V = 90.9 \times 10^6 \text{ m}^3$) measured on December 27, 1977 in the reservoir. The atrazine mass in the waterbody for next time was repeatedly computed by solving the equation (1) using a forward difference method until the objective function and constraints were satisfied.

Input Data and Parameters Estimation

Model inputs were provided on a monthly basis. Most of input data were obtained from field monitoring. Some input data and model parameters were estimated from physico-chemical properties of atrazine, hydrologic characteristics of the watershed, and literature survey for this site. The major parameters and monthly input data used in this study are presented in Tables 3 and 4, respectively. The atrazine concentrations measured at Station 1 were used to estimate the mass loading (M_{in}) from the whole watershed above that point. The flow data at Station 1 were estimated from the data collected at the US Geological Survey (USGS) gauging station near Stratford, which is located about 28 km upstream from Station 1 (USGS 1978). The flows gauged at Stratford station were multiplied by the ratio of drainage area between the two points. The flows and atrazine concentrations measured at Station 5 were used to estimate mass output via reservoir water discharge (M_{out}).

Annual total amount of direct mass input through runoff and drainage flows was calculated based on the amount of atrazine applied in the watershed and the percentage of total atrazine that is delivered to the waterbody. Typically 1.6-3.4 kg/ha of atrazine is applied to corn cropland in Iowa (Paterson and Schnoor 1992; Rice 1996). A value of $A_p=2.7$ kg/ha, which is slightly greater than the mean value, was chosen because the historical data showed that total atrazine use in the United States was peak (48 million kg) around 1979-1980 (Schottler and Eisenreich 1997). The s_i value was used as a weighting factor for representing an intensive atrazine loading patterns during late spring and summer at the study site. It was estimated using the flow and concentration data collected at Station 1 (Table 3) because the trend of instream water quality is directly associated with the pattern of NPS loading in this area. The s_i for any month was obtained dividing the amount of mass loaded in that month by the annual total load at Station 1, which represents atrazine loading pattern of the entire watershed. The fraction values, $f_1 = 0.71$, $f_2 = 0.61$, and $f_3 = 0.55$ were obtained from the survey data for this site (Naylor 1975; Leung 1979). The percentage of applied atrazine which is delivered into surface waters (f_i) may vary depending upon tillage practices, the amount, intensity, and timing of rainfall after application of atrazine in the agricultural land. Previous studies have reported that approximately 0.5-5% of the atrazine applied to the Iowa

Table 3. Input parameters used for estimating time-variable kinetic transformation rate of atrazine in the Saylorville Reservoir.

Parameter	Unit	Value	Reference
A_p	$\text{kg}(\text{ha})^{-1}(\text{yr})^{-1}$	2.7	Paterson and Schnoor (1992) Rice (1996) Schottler and Eisenreich (1997)
f_1		0.71	Naylor (1975), Leung (1979)
f_2		0.61	Naylor (1975), Leung (1979)
f_3		0.55	Naylor (1975), Leung (1979)
f_4	%	0.5-2.0	Harmon and Duncan (1978) Johnson and Baker (1982) Wilson (1987), Rice (1996)
W	$\mu\text{g}(\text{m})^{-2}$	75	Goolsby et al. (1993)
v_d	$\text{cm}(\text{sec})^{-1}$	0.2	Schottler and Eisenreich (1997)
k_1	$\text{m}(\text{month})^{-1}$	1.69×10^{-3}	Estimated using two-film theory
f_{oc}		0.02	Estimated using measured data
k_s	$(\text{month})^{-1}$	1.0	Estimated

Table 4. Monthly input data used for mass balance model at the study site.

Month	Q_{in} m ³ /sec	Q_{out} m ³ /sec	C_{in} μg/m ³	C_{out} μg/m ³	C_a ng/m ³	C_{ss} g/m ³	V ×10 ⁶ m ³	s_i	p_i
1	8.88	10.95	29.0	29.3	0.0	6.0	89.9	0.002	0.014
2	5.58	5.90	20.5	11.5	0.0	24.0	89.3	0.001	0.024
3	51.79	52.69	25.0	15.0	0.0	144.0	89.1	0.011	0.151
4	75.15	95.41	46.5	56.8	0.5	796.0	94.3	0.028	0.140
5	53.15	60.81	638.2	299.0	0.6	93.0	91.5	0.282	0.170
6	77.87	78.59	490.5	687.0	1.0	196.0	94.4	0.307	0.171
7	111.70	120.88	285.7	363.0	0.1	256.0	98.0	0.266	0.203
8	26.56	30.86	189.3	188.8	0.0	173.0	92.4	0.042	0.030
9	57.59	64.76	115.3	149.8	0.0	283.0	99.4	0.053	0.038
10	20.96	24.61	27.0	86.7	0.0	555.0	104.5	0.005	0.000
11	11.35	17.18	23.0	49.5	0.0	27.0	102.4	0.002	0.053
12	7.33	18.74	23.0	49.5	0.0	11.0	95.5	0.001	0.006

Q_{in} = Upstream inflow.

Q_{out} = Outflow.

C_{in} = Atrazine concentration in the inflow.

C_{out} = Atrazine concentration in the outflow.

C_a = Atrazine concentration in the air.

C_{ss} = Suspended solids concentration in the water column.

V = Volume of the reservoir storage in month i.

s_i = Fraction of direct annual load occurring in month i.

p_i = Fraction of annual precipitation load occurring in month i.

farm fields can be delivered into surface waters by runoff and drainage flows (Harmon and Duncan 1978; Wilson 1987; Rice 1996). Johnson and Baker (1982) suggested that average annual herbicides losses from Iowa agricultural fields to streams are 0.2% for the least persistent herbicide to 1.6% for the most persistent one. As no field monitoring data are available at the study site, a deterministic estimation of f_4 value is difficult. Thus three different f_4 values, i.e., 0.5%, 1.0%, and 2.0%, were used based upon the previous studies for the estimation of atrazine half-life.

The annual atmospheric atrazine mass inputs into the reservoir were estimated to complete the mass budget although the amounts are small at the study site. Atrazine loading via precipitation was allowed to vary by monthly using the weighting factor p_i . The p_i values for each month (Table 4) were estimated using the data collected at Walnut Creek watershed, which is located nearby the study site (Hatfield et al. 1996). Goolsby et al. (1993) estimated that the annual atrazine precipitation loading is 50-100 $\mu\text{g}/\text{m}^2$ in this site from field monitoring data. An average value of 75 $\mu\text{g}/\text{m}^2$ was used for the annual atrazine precipitation loading (W). Atrazine dry deposition is proportional to the dry deposition velocity and particulate atrazine concentration in the air. The deposition velocity of 0.2 cm/s and $f = 0.85$, which were used in the Great Lakes study by Schottler and Eisenreich (1997), were used in the model. The monthly atrazine air concentrations that measured in other similar Midwestern agricultural watersheds were used for this study (Schottler and Eisenreich 1997). This is a rough estimation, but it was assumed not to affect model results significantly because the atmospheric mass exchanges of atrazine are very small for the study site. The overall atrazine volatilization transfer rate (k_1) was calculated using a modified two-film model (Thomann and Mueller 1987). Using the properties of atrazine shown in Table 5 and the flow conditions at the study site, $k_1 = 1.69 \times 10^{-3}$ m/month was obtained.

Mass sink by adsorption and sedimentation was estimated using physical property of atrazine (Octanol-water partition coefficient, $\log(K_{ow}) = 2.5$), reservoir sediment property (organic carbon fraction, $f_{oc} = 0.02$), and a net sedimentation rate constant ($k_s = 1.0$ /month). The k_s value was estimated by assuming that all sorbed atrazine in any month settles down to

Table 5. Physical and chemical properties of atrazine.

Properties	Unit	Values
Molecular weight	g(mol) ⁻¹	215.7
Solubility (at 20 °C in water)	mg(l) ⁻¹	33
Vapor pressure at 20 °C	atm.	4×10 ⁻¹⁰
Henry's constant	atm-m ³ (mol) ⁻¹	3×10 ⁻⁹
Log K _{ow} at 25 °C	-	2.5
Specific gravity at 20 °C	g(cm) ⁻³	1.187

the bottom of the reservoir within that month. The amount of atrazine mass that lost from the water column by adsorption to suspended solids was estimated with a linear partitioning relationship:

$$C_s = 0.617 f_{oc} K_{ow} C_w \quad (3)$$

The mass sinks by kinetic transformations were subjected to include the amount of atrazine mass that degraded by photolysis, hydrolysis, and biotransformation, but it may include any other processes such as plant and fish uptakes if they are considerable. The kinetic transformation processes can be expressed as either pseudo-first-order reactions or second-order-reactions. The reaction rates of these processes for atrazine in a surface water system depend both on the physico-chemical properties of atrazine and the properties of the aquatic environments (i.e., water depth, temperature, pH, intensity and spectrum of solar radiation, wind speed, and microbial concentration). In this study, a bulk first-order reaction rate that collectively includes biotic and abiotic degradation processes was used to determine the mass output by transformation processes because it is extremely difficult to determine

each kinetic transformation rate using the limited data. The monthly bulk transformation rates were treated as unknown values and determined by the optimal parameter estimation process explained previously.

Results and Discussion

Half-life of Atrazine

The optimal solutions for the monthly atrazine kinetic transformation rates (k) were found after 35 iterations with a small error, i.e., RMSE = 3.8. The half-life ($t_{0.5}$) value, the time required for the transformation of one-half of atrazine to its degradation products, was obtained from the calculated k values with the assumption of first-order kinetics:

$$\frac{dC}{dt} = -kC \quad (4)$$

Using the solution of (4), $C = C_0 e^{-kt}$ where C_0 is initial concentration, the first-order kinetic transformation rate k value can be converted into $t_{0.5}$ value using the following relationship.

$$t_{0.5} = \ln 2 / k \quad (5)$$

Table 6 shows the estimated atrazine half-life values for each month of the year. Observed mean daily hours of sunlight (T_s) and monthly mean water temperature (T_w) at Station 1 for each month are also presented in the Table. The persistence of atrazine in the waterbody, as determined using the atrazine half-life value, varied seasonally. It was maximum during the winter months and minimum during the spring and summer months. The long persistence or half-life of atrazine during the winter months are mainly due to the extremely lower level of atrazine concentrations, less hours of sunlight, and lower water temperature during these periods, which weaken the effectiveness of photolysis and biodegradation. The half-life varied from 2 to 58 days with respect to the monthly environmental conditions of the reservoir. The variations of half-life agreed well with those found at Roberts Creek, Iowa by Kolpin and Kalkhoff (1993) where the atrazine half-life

Table 6. Estimated atrazine half-life values (days) for each month.

Month	T_s (hrs)	T_w (°C)	f_d			Mean (days)
			0.005	0.01	0.02	
1	9.56	0.7	34.0	24.0	16.0	24.7
2	10.61	0.4	30.0	22.0	14.0	22.0
3	11.94	2.4	7.0	4.0	2.0	4.4
4	13.34	9.1	11.0	7.0	4.0	7.3
5	14.53	14.0	6.0	3.0	2.0	3.7
6	15.14	20.5	11.0	7.0	4.0	7.3
7	14.85	23.8	11.0	5.0	2.0	6.0
8	13.81	24.2	10.0	7.0	5.0	7.3
9	12.48	19.9	21.0	10.0	5.0	12.0
10	11.09	11.6	40.0	35.0	24.0	33.0
11	9.87	4.8	44.0	36.0	28.0	36.0
12	9.22	1.2	58.0	47.0	35.0	46.7

T_s = The number of daily hours of sunrise to sunset.

T_w = Water temperature measured at sampling station 1.

varied from 1.5 to 7.1 days during the period of April-October. Relatively larger atrazine $t_{0.5}$ values were obtained in the Saylorville Reservoir due, in part, to the larger drainage area and deeper depth of flow. In general, atrazine degrades exponentially with time in surface water, thus the small creek that received a high level of atrazine concentrations via the surface runoff from adjacent agricultural fields might have experienced more rapid degradation. However, relatively longer half-life may occur at the outlet of a watershed such as near a reservoir due to low concentrations and deep flow conditions that reduce the effectiveness of abiotic degradation processes. In addition, in a larger watershed, hydrologic conditions may be more non-homogeneous, including rainfall distribution, intensity, and tributaries, which can lead to a greater variations of $t_{0.5}$.

It is shown that the atrazine $t_{0.5}$ values were sensitive to the f_4 values. A greater f_4 value, indicating a greater amount of atrazine being delivered into the reservoir, resulted in shorter half-life to satisfy the conservation of mass equation. Therefore, a careful estimation of f_4 value for a watershed is required through field monitoring study. For the fate modeling of atrazine, the average of the estimated $t_{0.5}$ values from three different f_4 values can be used for each month.

Simulated monthly atrazine concentrations are compared with the field data measured at Station 4 in the reservoir to validate the estimated atrazine half-life (Figure 4). The observed data in the Figure are the mean of atrazine concentrations that measured at three different depths of the reservoir, surface, middle, and bottom. The simulated values represent the well-mixed atrazine concentrations in the reservoir that obtained when the optimal first-order atrazine transformation rates were obtained. The simulated concentrations follow the trend of observed atrazine concentrations well, which validates the estimated time-variable transformation rates of atrazine in the reservoir. Some discrepancies were obvious in mid-May, the period of peak concentrations. The explanation is that the simple mass balance model was not intended to catch the peak atrazine concentrations resulting from short-duration storm events following intensive applications of atrazine.

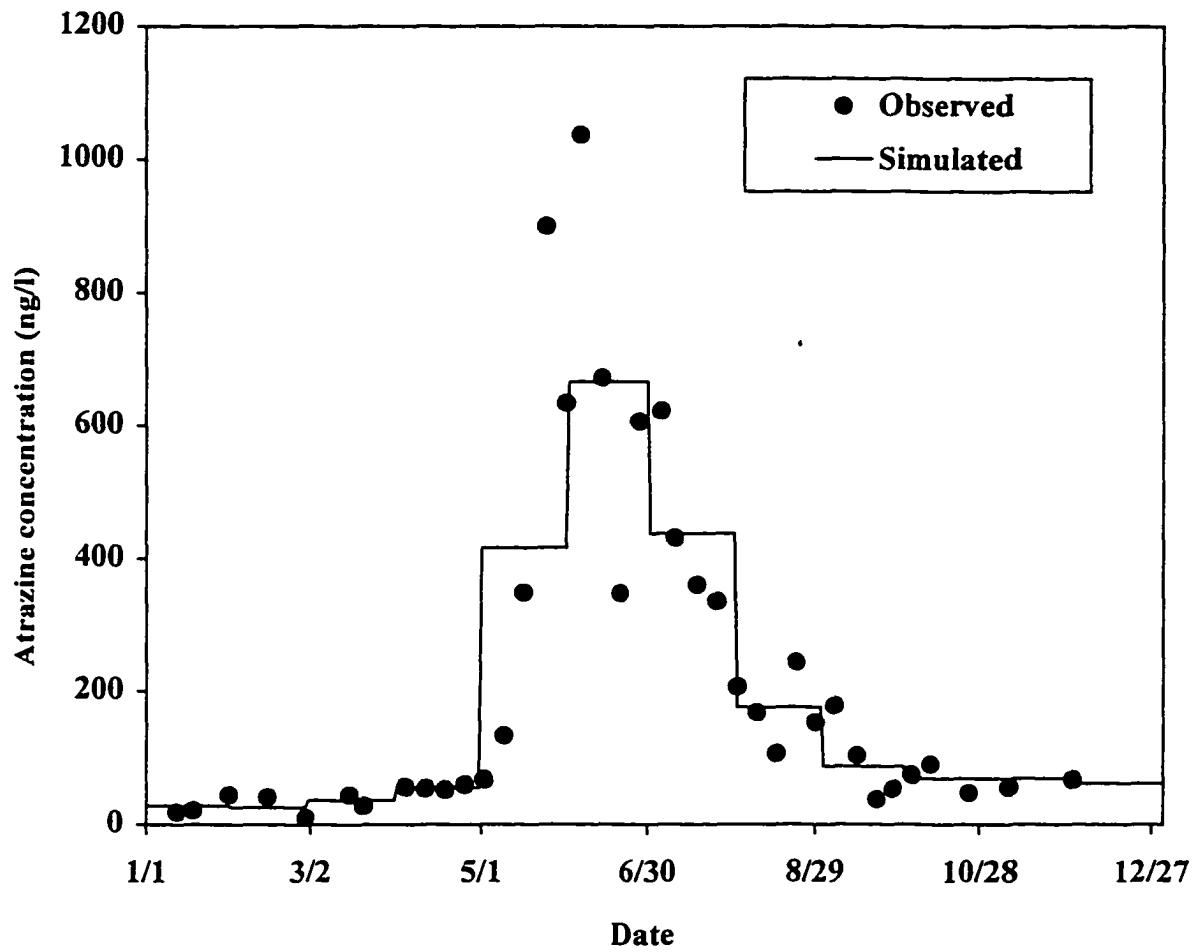
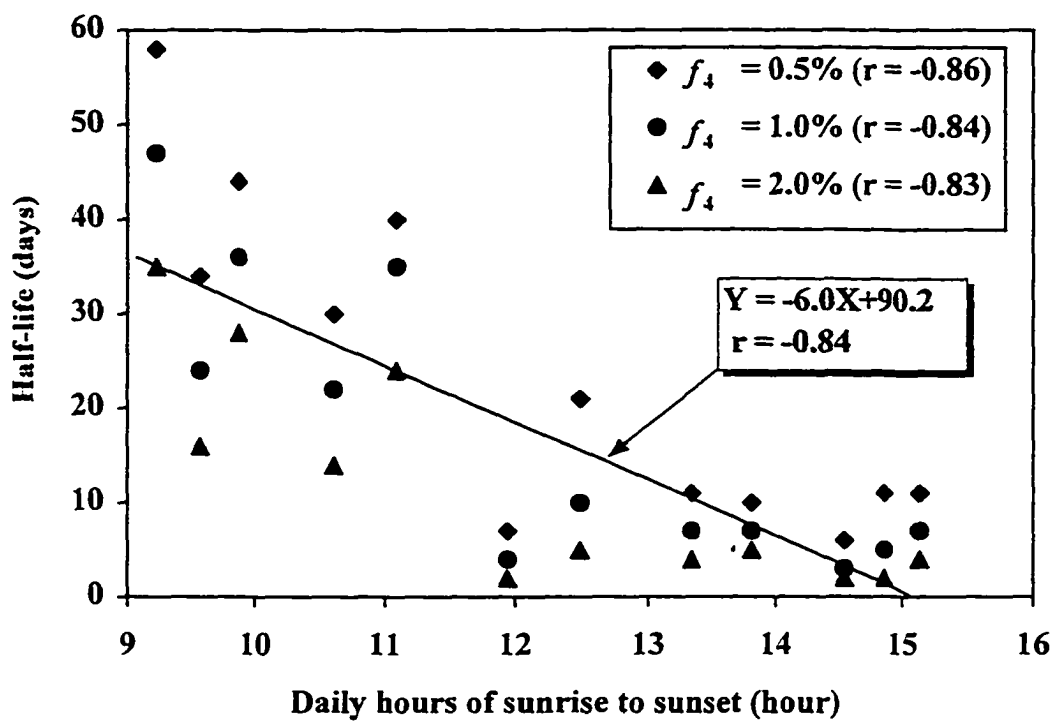


Figure 4. Comparison of model results with observed atrazine concentrations.

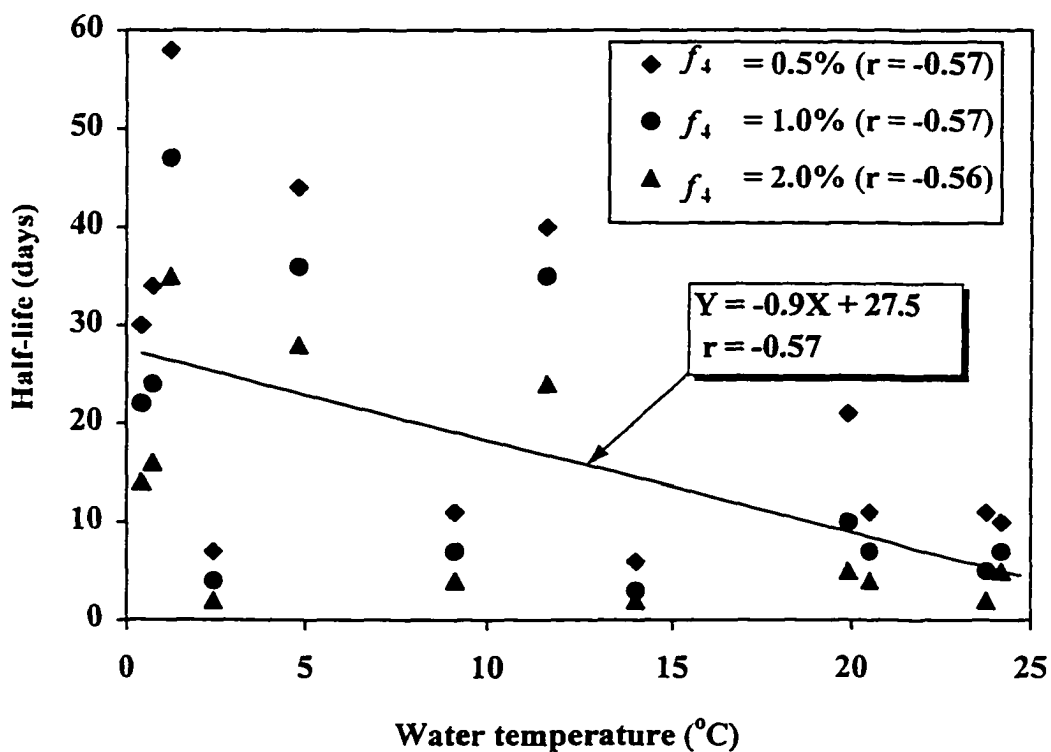
Atrazine Degradation Processes

It is difficult to describe the degradation processes of atrazine in a surface waterbody without sufficient measurements of various degradation products along a reach of the waterbody. Water temperature and the number of daily hours of sunlight (T_s) were used as indirect indicators for determining the significance of biotransformation and photodegradation processes in a previous field study (Kolpin and Kalkhoff 1993). The relationships between these environmental parameters and the half-life values may assist in examining the significance of biotic and abiotic degradation processes of atrazine in the reservoir.

Figures 5a and 5b show the estimated atrazine half-life values and the observed daily hours of sunlight and water temperature (Table 6), respectively. A significant inverse relation with the correlation coefficient $r = (-0.83) \sim (-0.86)$ exists between the half-life and the daily hours of sunlight. A linear regression equation, $Y = -6.0X + 90.2$ where X and Y denote the number of daily hours of sunlight in any month and atrazine half-life during that month, was obtained from all data points with $r = -0.84$. The equation suggests that the half-life of atrazine without sunlight in the waterbody may be about 90.2 days, in which atrazine is mainly degraded by biotic processes. The results support the findings in previous studies (Pelizzetti et al. 1990; Goldberg et al. 1991; Kolpin and Kalkhoff 1993; Torrents et al. 1997) that the amount of sunlight is an important factor for driving photodegradation processes of atrazine in surface water. Previous laboratory studies (Goldberg et al. 1991; Torrents et al. 1997) showed that the degradation rate of atrazine increased with increasing nitrate nitrogen concentrations in surface water by indirect (i.e., nitrate mediated) photolysis. In this study, however, it was found that insignificant relationship ($r < 0.1$) exists between the half-life and the nitrate nitrogen concentrations. This may imply that the direct photolysis may be the major atrazine photodegradation mechanism rather than indirect photolysis at the study site. The results are consistent with the findings of Torrents et al. (1997) that in the presence of dissolved organic carbon (DOC), the direct photolysis can be more dominant because DOC efficiently scavenge hydroxyl radicals but does not compete with atrazine for sunlight.



(a)



(b)

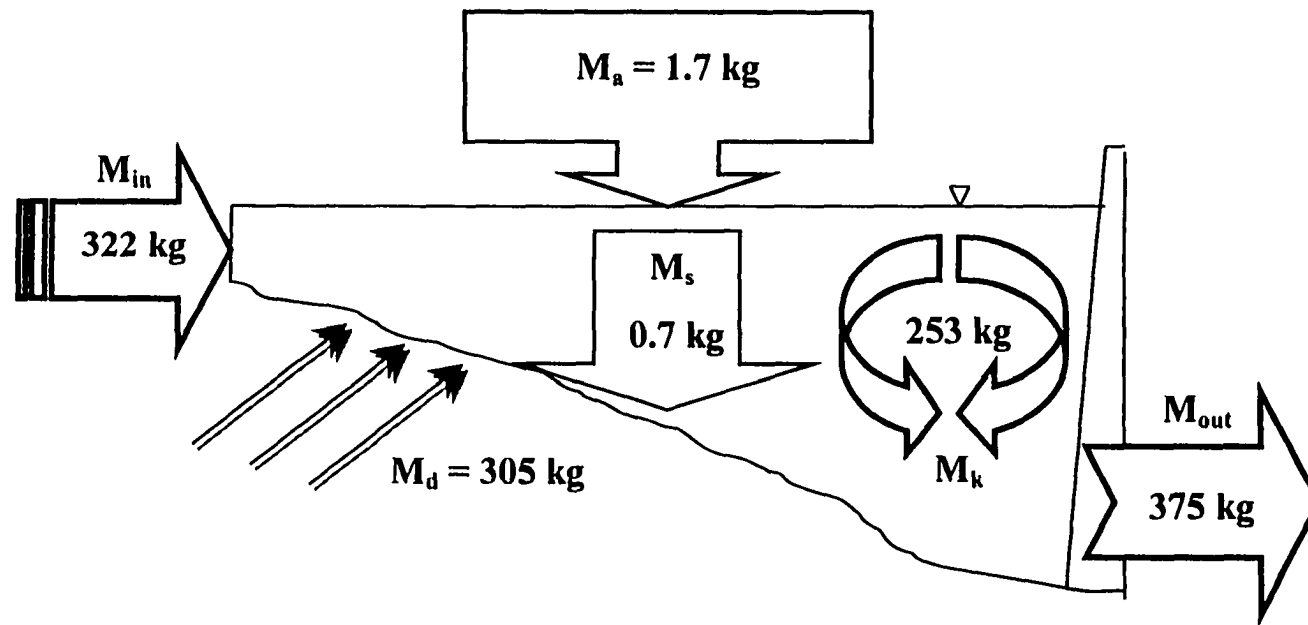
Figure 5. Relations of time-variable atrazine half-life to (a) the daily hours of sunlight and (b) water temperature.

A moderate inverse correlation with $r = (-0.57) \sim (-0.60)$ was obtained for the half-life values and the water temperatures. This indicates that the effectiveness of biotic degradation process on the atrazine degradation tends to decrease as water temperature decreases. The result is consistent with the previous findings by Schottler and Eisenreich (1997). These relationships can be used to describe the importance of biotic and abiotic degradation processes depending upon the environmental conditions. An intensive field monitoring study, however, is required to measure the various degradation products of atrazine in order to describe and quantify the individual degradation process.

Atrazine Mass Budget

The annual mass budget of atrazine in the Saylorville Reservoir was analyzed to determine the relative importance of various source and sink terms in the waterbody. Figure 6 shows the annual amount of various sources and sinks of atrazine into and out of the reservoir. The total amount of atrazine present in the reservoir water column slightly increased from the initial mass of atrazine in the reservoir $M_o = 3.7$ kg in December 1977 to the simulated closing mass $M_f = 4.9$ kg in December 1978. This implies that the reservoir regulates the loaded atrazine adequately on the annual basis. The small net accumulation of atrazine, at least in parts, attributed to the severe drought occurred in the previous year and the increasing trend of atrazine use at that time. The mean daily discharges for the Des-Moines River at Stratford in water years 1977 and 1978 were $7.3 \text{ m}^3/\text{s}$ and $43.1 \text{ m}^3/\text{s}$ (USGS 1977 and 1978), respectively, indicating the hydrologic situations of the study period. Therefore, the atrazine residue that remained in the watershed during the drought year may be flushed into the reservoir in the following year.

Approximately 322 kg of atrazine entered the reservoir via the inflows, 305 kg via direct runoff and drainage flows, and 1.7 kg through atmospheric depositions during the study period. This indicates that major sources of atrazine enter the reservoir by way of the upstream inflows and distributed nonpoint source loading, which contribute more than 99% of total inputs. The atrazine loadings through precipitation, dry deposition, and gaseous exchange were found to be negligible at the study site.



M_0 : Estimated initial atrazine mass in the reservoir = 3.7 kg
 M_f : Simulated final atrazine mass in the reservoir = 4.9 kg

Figure 6. Estimated annual atrazine mass budget in the Saylorville Reservoir, Iowa.

About 374.5 kg of atrazine was lost from the reservoir through downstream discharges, 253 kg by the kinetic transformations such as photolysis, hydrolysis, and biotransformations, and 0.65 kg by adsorption and settlement. This means that approximately 60% and 40% of atrazine that loaded into the reservoir from the farm land were controlled by outflows and kinetic transformations, respectively. The amount of atrazine loss due to adsorption and settlement is insignificant (Thomann and Mueller 1987) as expressed by the following relationship and shown in Figure 7.

$$f_d = \left(1 + \frac{2f_{oc}K_{ow}C_{ss}}{1 + C_{ss}f_{oc}K_{ow}/1.4}\right)^{-1} \quad (6)$$

The fraction of dissolved form of atrazine is a function of physical property of atrazine K_{ow} (Table 5), suspended solids concentrations (C_{ss}), and organic carbon fraction (f_{oc}) in the reservoir. The suspended solids concentrations varied from 5 to 1480 mg/l during the study period. Under this condition, if f_{oc} is less than 0.1, more than 97% of atrazine remains in the dissolved form in the water column of the reservoir. During the study period, the organic carbon concentrations were in the range of 3 to 27 mg/l and f_{oc} was less than 0.02 in the reservoir (Baumann et al 1979).

Case Study

The atrazine contamination levels in the upper Des Moines River and Saylorville Reservoir were found below the MCL for drinking water during the study period. However, they would exceed MCL if the amount of atrazine use in the upstream watershed increased. The amount of atrazine use in the agricultural fields depends on the cropping system, tillage practices, and land area of corn cropping fields. For examples, the acreage of corn cropping fields and continuous corn rotations will possibly increase if the corn production produces more revenue than soybean production in the future. An increasing trend of no tillage agriculture in the Midwestern United States is another potential factor for the increase of atrazine use because more herbicides are used under no tillage system to control weeds. Therefore, a case study was attempted using the mass balance model and the estimated

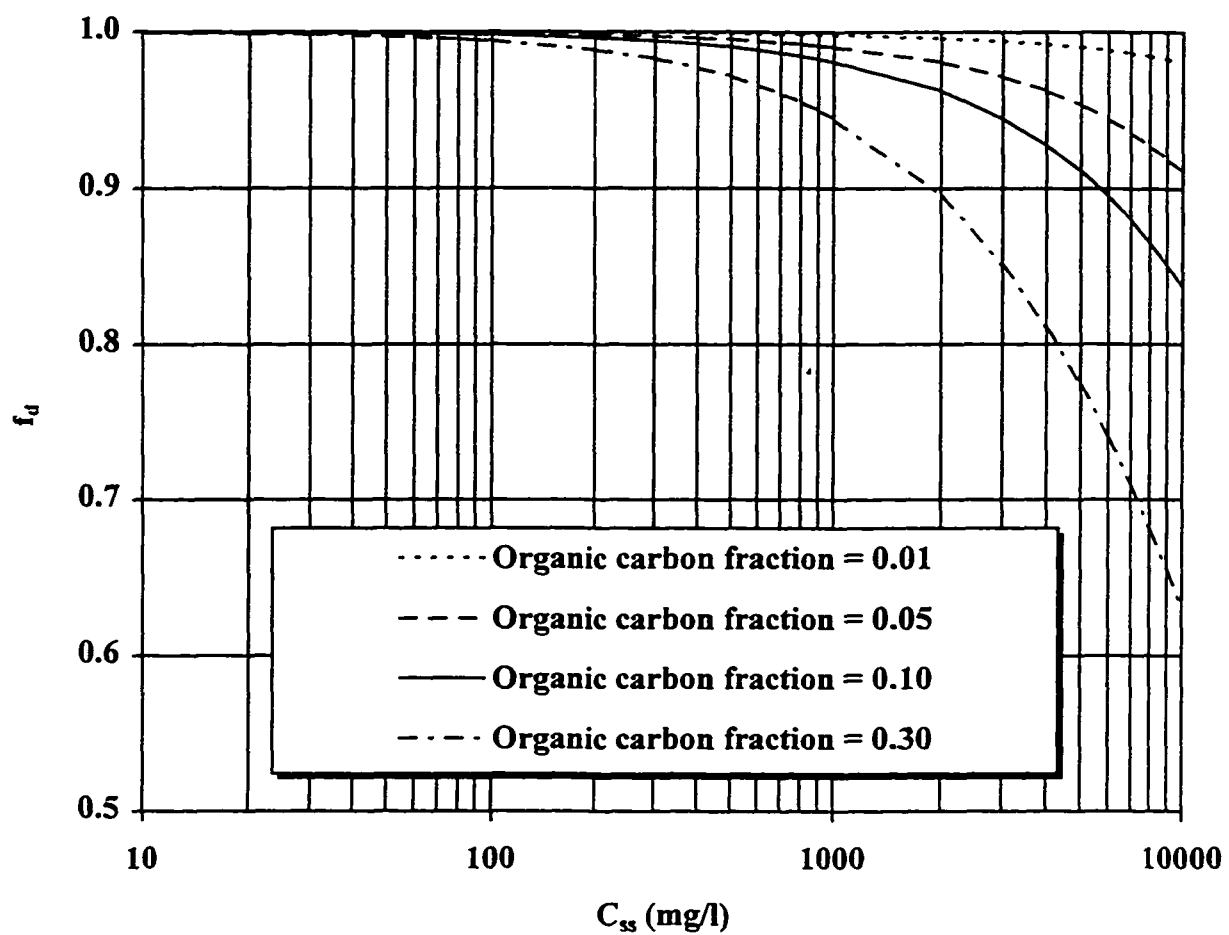


Figure 7. The fraction of dissolved atrazine to total concentrations as a function of sediments concentrations and organic carbon fraction in water.

atrazine half-life values to examine the change in the contamination levels of atrazine in the reservoir in response to a potential increase in atrazine uses.

In Table 7 three different scenarios considered in this study are listed. Case 1 is the baseline conditions for which the agricultural management system and the amount of atrazine use were assumed corresponding to that in 1978. For Case 2, the fraction of corn and soybean cropping area (f_1) and the fraction of atrazine applied area in the watershed (f_3) were assumed to increase by 14% and 5% from baseline, respectively. This is an 52% increase in atrazine use compare to the baseline. For Case 3, the fraction of corn cropping area in the corn and soybean cropping area (f_2) and the fraction of atrazine applied area in the watershed (f_3) were assumed to increase by 4% and 5% from Case 2. This is equivalent to 86% increase in atrazine use compare to the baseline. These scenarios represent the hypothetical situations in which the increase in uses of atrazine is a results of increases in crop land area, corn cropping area percentage, and atrazine applied area in the watershed.

Table 7. Scenarios for different atrazine uses in the upstream watershed of the Saylorville Reservoir, IA.

Case	A_p (kg/ha)	f_1	f_2	f_3	f_4
1	2.70	0.71	0.61	0.55	0.01
2	2.70	0.85	0.61	0.70	0.01
3	2.70	0.85	0.65	0.80	0.01

Figure 8 shows the reservoir water quality in response to the increased atrazine uses. The level of atrazine concentrations reached up to 2,600 ng/l in the month of May under Case 2, but dropped quickly to the level of less than 1,000 ng/l in the following months. The atrazine contamination level, however, exceeded the MCL in the month of May under Case 3, and it remained over the rest of the year with the high level of atrazine concentrations greater than 2,000 ng/l. This indicates that an 86% increase in atrazine uses in the upper Des Moines River watershed could alter the status of reservoir water quality. The reservoir loses

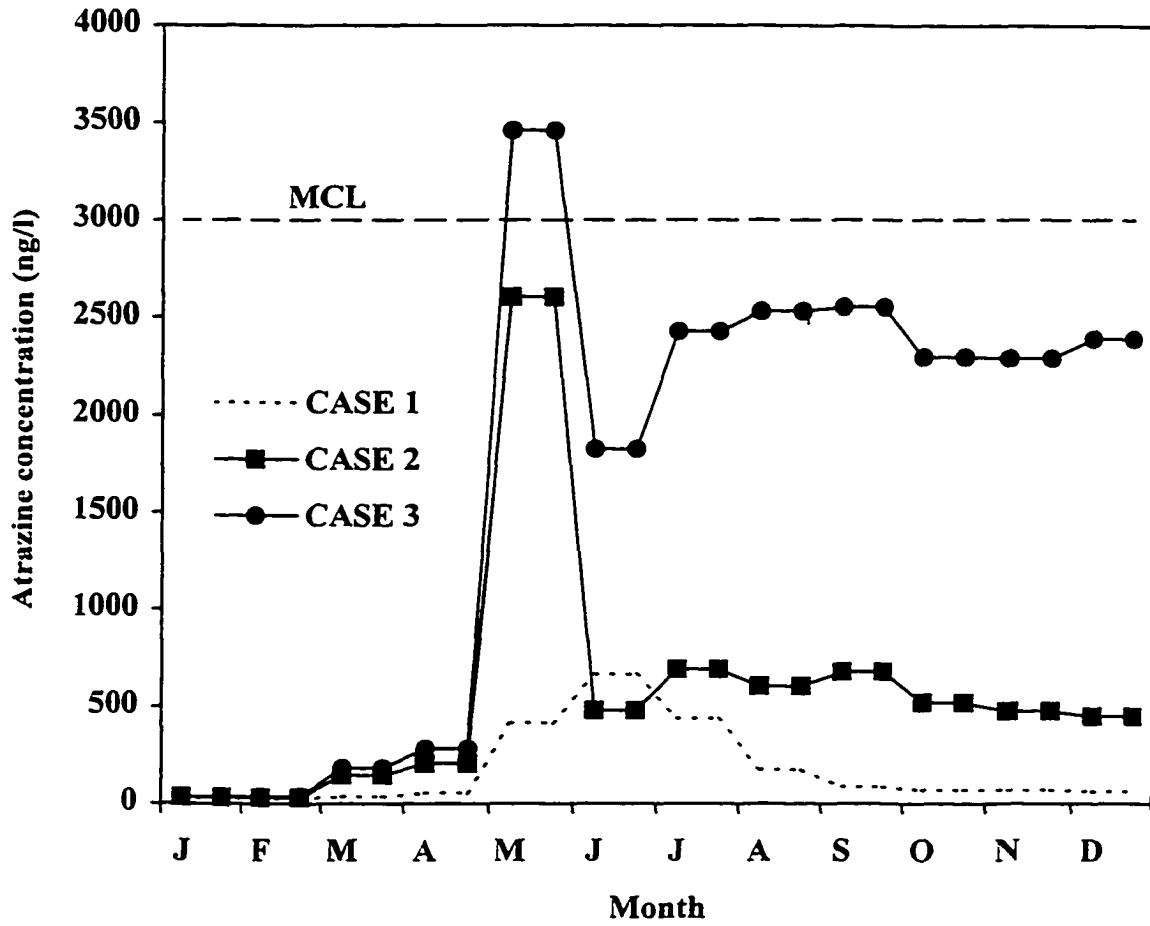


Figure 8. Saylorville reservoir water quality response to changes in atrazine use.

its regulation function to mitigate atrazine concentrations in the reservoir by equilibrating the mass inputs with the losses via outflow discharges and kinetic transformations after the month of May in Case 3. It is because the contaminant loading rate exceeds the self-purification capacity (degradation rate) of the reservoir through biotic and abiotic degradation processes. Although Case 3 may not occur in the future at the study site, it is an important finding for the agricultural decision and policy makers because the long persistence of highly elevated atrazine concentrations in a reservoir is harmful for aquatic ecosystem and safe water supply. The results provide a potential worst scenario in the future and can be used as a rough guideline for the control of atrazine use in the Midwest Corn Belt area.

Conclusions

A mass balance model for atrazine was constructed for the Saylorville Reservoir, Iowa and applied to estimate the time-variable transformation rate or half-life using field data collected earlier. The atrazine half-life varied monthly from 2 to 58 days depending upon the environmental conditions such as water temperature and daily hours of sunlight. A significant inverse relation was obtained between the half-life and the daily hours of sunlight, showing the significance of photodegradation at the study site. The results of this study support the findings in previous studies that photodegradation is an effective process for degrading atrazine level and that sunlight is an important factor to degrade atrazine in surface water. The effect of nitrate concentration on the half-life of atrazine was insignificant possibly due to the high level of dissolved organic carbon in the waterbody. This suggests that the direct photolysis is a dominant atrazine degradation process rather than nitrate-mediated indirect photolysis at the study site. The estimated annual mass budget of atrazine showed that the major sources of atrazine come from the upstream inflow loading and direct loading via runoff and drainage flows. A great portion of atrazine transported into the reservoir waterbody from the farm land was mainly controlled by outflows and kinetic transformations. However, a case study showed that a hypothetical 86% increase in atrazine uses in the upper Des Moines River basin would alter the pattern of reservoir water quality

response because the loading rate was greater than the self-purification capacity of the reservoir.

Additional field studies are needed to measure the levels of various degradation products to describe major degradation processes of atrazine. A well-mixed reservoir condition assumption used in this study may not be valid for a deep reservoir where stratification occurs because the fate of atrazine can be affected by various flow regimes that are associated seasonal reservoir stratification patterns. The rate of atrazine degradation can be reduced under an interflow regime during a strong summer stratification period as it is difficult for sunlight to reach the deep intruding depth. In this case, more comprehensive reservoir toxic model is required to predict the persistence of atrazine and capture the occurrence of peak concentrations with temporal and spatial distributions under various flow regimes, which requires the estimated transformation rate or half-life in this study.

References

- Baumann, E. R., C. A. Beckert, M. K. Butler, D. M. Soballe. 1979. Water quality studies-EWQOS sampling Red Rock and Saylorville Reservoirs Des Moines River, Iowa. Engineering Research Institute, Iowa State University, Ames, Iowa.
- Goolsby, D. A., E. M. Thurman and D. W. Kolpin. 1991. Herbicides in streams: Midwestern United States. Irrigation and Drainage Proceedings, July 22-26, Honolulu, HI.
- Goolsby, D. A. and W. A. Battaglin. 1993. Occurrence, distribution, and transport of agricultural chemicals in surface waters of the Midwestern United States. *Selected Papers on Agricultural Chemicals in Water Resources of the Midcontinental United States*. U.S. Geological Survey. Denver, CO.
- Goolsby, D. A., E. M. Thurman, M. L. Pomes, M. Meyer, and W. A. Battaglin. 1993. Occurrence, deposition, and long range transport of herbicides in precipitation in the Midwestern and Northeastern United States. *Selected Papers on Agricultural Chemicals in Water Resources of the Midcontinental United States*. U.S. Geological Survey. Denver, CO.
- Goldberg, M. C., K. M. Cunningham, P. J. Squillace. 1991. Photolytic degradation of atrazine in the Cedar River, Iowa, and its tributaries. In U.S. Geol. Survey Toxic Substances Hydrology Program-Proceedings of the Technical Meeting, Mallard, G. E. and D. A. Aronson Eds., Monterey, CA, March 11-15.

- Hallberg, G. R. 1996. Water quality and watersheds: an Iowa perspective. Proceedings of the Agriculture and Environment -Building Local Partnerships-. Iowa State University, Ames, IA.
- Harmon, L., and E. R. Duncan. 1978. A technical assessment of nonpoint pollution in Iowa. Iowa State University, Ames, Iowa.
- Iowa Department of Environmental Quality. 1976. Water quality management plan. Des Moines River Basin. Iowa Dept. Environ. Qual., Des Moines, Iowa.
- Johnson, H. P. and J. L. Baker. 1982. Field-to-stream transport of agricultural chemicals and sediment in an Iowa watershed. *EPA-600/3-83-032*. U.S. Environmental Protection Agency, Athens, Georgia.
- Kanwar, R. S., D. L. Karlen, T. S. Colvin, W. S. Simpkins, and V. J. McFadden. 1993. Evaluation of Tillage and Crop Rotation Effects on Groundwater Quality--Nashua Project. Leopold Grant No. 90-41, Iowa State University, National Soil Tilth laboratory, Ames, Iowa.
- Kolpin, D. W. and S. J. Kalkhoff. 1993. Atrazine degradation in a small stream in Iowa, *Environ. Sci. Technol.*, 27(1):134-139.
- Leung, Siu-Yin. 1979. The effect of impounding a river on the pesticide concentration in warmwater fish. Ph.D. dissertation. Iowa State University, Ames, IA.
- Lutz, D. S. and A. Cavendar. 1997. Water Quality Studies--Red Rock and Saylorville Reservoirs Des Moines River, Iowa. Iowa State University, Ames, IA.
- Naylor, L. M. 1975. A statistical study of the variations in Des Moines River water quality. Ph.D. dissertation, Iowa State University, Ames, IA.
- Nations, B. K. and G. R. Hallberg. 1992. Pesticides in Iowa precipitation. *J. Environ. Qual.* 21:486-492.
- Hatfield, J. L., C. K. Wesley, J. H. Prueger, and R. L. Pfeiffer. 1996. Herbicide and nitrate distribution in central Iowa rainfall. *J. Environ. Qual.* 25:259-264.
- Paterson, K. G. and J. L. Schnoor. 1992. Fate of alachlor and atrazine in a riparian zone field site. *Water Environ. Res.*, 63(3):274-283.
- Pereira, W. E., and F. D. Hostettler. 1993. Nonpoint source contamination of the Mississippi River and its tributaries by herbicides. *Environ. Sci. Technol.* 27:1542-1552.
-

- Pelizzetti, E., V. Maurino, C. Minero, V. Carlin, E. Pramauro, O. Zerbinati and M. L. Tosato. 1990. Photocatalytic degradation of atrazine and other *s*-triazine herbicides. *Environ. Sci. Technol.*, 24:1559-1565.
- Pugh, K. C. 1994. Toxicity and physical properties of atrazine and its degradation products; A literature survey. Waste Management and Remediation Environmental Research Center, Muscle Shoals, Alabama.
- Rice, P. J. 1996. The persistence, degradation, and mobility of metolachlor in soil and the fate of metolachlor and atrazine in surface water, surface water/sediment, and surface water/aquatic plant systems. Ph.D. dissertation, Iowa State University, Ames, IA.
- Richards, R. P., J. W. Kramer, D. B. Baker, and K. A. Krieger. 1987. Pesticides in rainwater in the northeastern United States. *Nature*. 327:129-131.
- Richards, R. P., D. B. Baker, B. R. Christensen, and D. P. Tierney. 1995. Atrazine Exposures through drinking water: Exposure assessments for Ohio, Illinois, and Iowa. *Environ. Sci. Technol.* 29:406-412.
- Schottler, S. P. and S. J. Eisenreich. 1997. Mass balance model to quantify atrazine sources, transformation rates, and trends in the Great Lakes. *Environ. Sci. Technol.* 31:2616-2625.
- Thomann, R. V. and J. A. Mueller. 1987. Principles of surface water quality modeling and control. HarperColinsPublishers Inc., New York, NY.
- Thurman, E. M., D. A. Goolsby, M. T. Meyer, M. S. Mills, M. L. Pones and D. W. Kolpin. 1992. A reconnaissance study of herbicides and their metabolites in surface water of the Midwestern United States using immunoassay and gas chromatography/mass spectrometry. *Environ. Sci. Technol.* 26:2440-2447.
- Thurman, E. M., D. A. Goolsby, M. T. Meyer and D. W. Kolpin. 1991. Herbicides in surface waters of the Midwestern United States: The effect of spring flush. *Environ. Sci. Technol.* 25:1794-1796.
- Torrents, A., B. G. Anderson, S. Bilbouljian, W. E. Johnson, and C. J. Hapeman. 1997. Atrazine photolysis: Mechanistic investigations of direct and nitrate-mediated hydroxy radical processes and the influence of dissolved organic carbon from the Chesapeake Bay. *Environ. Sci. Technol.* 31:1476-1482.
- U.S. Army Corps of Engineers, Rock Island District. 1983. Upper Mississippi River Basin Des Moines River, Iowa and Minnesota Master Reservoir Regulation Manual.

U.S. Geological Survey. 1977. Water Resources Data for Iowa

U.S. Geological Survey. 1978. Water Resources Data for Iowa

Wilson, L. J., 1987, Iowa groundwater protection strategy, Environ. Protection Comm., Iowa Dep. Nat. Resour., Des Moines, Iowa.

Notation

The following symbols are used in this paper:

A_D	=	drainage area (km^2);
A_p	=	annual atrazine application rate in a watershed ($\text{kg}/\text{km}^2/\text{yr.}$);
A_s	=	the surface area of reservoir (km^2);
C_a	=	mean concentration of atrazine in the air (ng/m^3);
C_{in}	=	mean concentration in the inflow ($\mu\text{g}/\text{l}$);
C_{out}	=	mean atrazine concentration in the outflow ($\mu\text{g}/\text{l}$);
C_s	=	the sorbed atrazine concentration on particles ($\mu\text{g}/\text{kg}$);
$C_{obs,i}$	=	observed atrazine concentration in a reservoir water in month i ($\mu\text{g}/\text{l}$);
$C_{sim,i}$	=	simulated atrazine concentration in a reservoir water in month i ($\mu\text{g}/\text{l}$);
C_{SS}	=	the mean suspended solids concentration in the reservoir (mg/l);
C_w	=	the observed mean atrazine water concentration ($\mu\text{g}/\text{l}$);
f	=	fraction of air concentration sorbed on particles;
f_1	=	fraction of corn and soybean cropping area to the drainage area;
f_2	=	fraction of corn cropping area to f_1 ;
f_3	=	fraction of atrazine applied area to f_2 ;
f_4	=	fraction of A_p , which is delivered to surface water;
f_{oc}	=	fraction of organic carbon;
H	=	Henry's law constant ($\text{atm}\cdot\text{m}^3/\text{mol}$);
k	=	the kinetic transformation rate of atrazine (/month);
k_l	=	overall volatilization transfer rate (m/day);
K_{ow}	=	octanol-water partition coefficient;

k_s	=	the sedimentation rate constant (/month);
M_a	=	atmospheric atrazine mass loading (kg);
MCL	=	the maximum contamination level ($\mu\text{g/l}$);
M_d	=	direct atrazine mass loading via runoff and drainage flow (kg);
M_{dry}	=	atrazine mass loading by dry deposition (kg);
M_i	=	the total mass of atrazine in a reservoir water column in month i (kg);
M_{in}	=	upstream atrazine mass loading (kg);
M_k	=	atrazine mass output by kinetic transformations (kg);
M_{out}	=	atrazine mass output via downstream discharge (kg);
M_{pre}	=	atrazine mass loading via precipitation (kg);
M_s	=	atrazine mass output by adsorption and settlement (kg);
M_{vol}	=	atrazine gaseous mass transfer via air-water exchange (kg);
n	=	the number of months;
p_i	=	fraction of annual precipitation load occurring in month i ;
Q_{in}	=	upstream inflow (m^3/s);
Q_{out}	=	outflow (m^3/s);
r	=	correlation coefficient;
s_i	=	fraction of direct annual load occurring in month i ;
$t_{0.5}$	=	half-life of atrazine (days);
T_s	=	mean daily hours of sunlight (hours);
V	=	total volume of reservoir (m^3);
v_d	=	dry deposition velocity (cm/s); and
W	=	annual atrazine deposition rate via precipitation ($\mu\text{g}/\text{m}^2/\text{yr.}$).

CHAPTER 4. PREDICTION OF THE FATE AND TRANSPORT OF ATRAZINE WITH A 2D RESERVOIR TOXIC MODEL

A paper to be submitted to the Journal of Environmental Engineering

Se-Woong Chung and Ruochuan Gu

Abstract

A frequent detection of high level herbicide concentrations in the reservoirs of the Midwestern United States during late spring and summer is a great concern because of its adverse impacts on a safe water supply and aquatic ecosystem. Thus, the reservoir operators need timely information about the contamination levels, persistence, and temporal and spatial distributions of these chemicals in a reservoir for an adequate water quality management in the area. A two-dimensional reservoir toxic model was applied to the Saylorville Reservoir, Iowa for simulating the fate and transport processes of atrazine, the most commonly used herbicide for preemergent weed control in the corn cropping area, in the reservoir. Simulated reservoir flow velocities, water temperatures, and atrazine concentrations were used to investigate the seasonal transport processes and persistence of atrazine. The model accurately simulated the temporal variations of observed atrazine concentrations and captured the peak concentrations occurred during late spring by using a time-variable kinetic transformation rate. Comparisons of model results with field data indicated that the use of site-specific temporal transformation rates of atrazine improves the model accuracy. The methodology employed in this study can be used to model commonly detected herbicides such as atrazine, alachlor, cyanazine, and metolachlor in other reservoirs located in agricultural areas.

Introduction

Atrazine [2-chloro-4-ethylamino-6-isopropylamino-1,3,5-triazine] is the most commonly used herbicide in the spring for preemergent weed control in the corn cropping area in Iowa and the Midwestern United States. Although the intensive use of atrazine has dramatically improved corn production efficiency in this area since its first use in 1959, the

public concerns about its potential adverse impacts on aquatic ecosystem and human health has also been grown because it has been detected with a significant level in surface water, ground water, drinking waters, and even in precipitation around a year (Thurman et al. 1991; Nations and Hallberg 1992; Goolsby and Battaglin 1993; Pereira and Hostettler 1993; Hallberg 1996; Hatfield et al. 1996). Approximately 3.4 million kg of atrazine is applied to the agricultural fields of Iowa annually (Goolsby et al. 1991; Paterson and Schnoor 1992; Kolpin and Kalkhoff 1993) with a typical application rate of 1.6-3.4 kg/ha (Paterson and Schnoor 1992; Rice 1996). Because of its potential chronic harmful impact on human health, the United States Environmental Protection Agency (USEPA) ranked atrazine as a class C (possible) carcinogen and established the maximum contamination level (MCL) of 3.0 $\mu\text{g/l}$ for drinking water (Richard et al 1995).

In general, significant amount of atrazine is flushed into surface waters from agricultural lands during late spring and early summer by several storm events following application of atrazine in the agricultural fields. Approximately 0.5-5 percent of field-applied atrazine is delivered into rivers and reservoirs carried by surface runoff and subsurface drainage flows (Harmon and Duncan 1978; Johnson and Baker 1982; Wilson 1987; Rice 1996). During the period of peak loading, atrazine is known to occur in streams and reservoirs at exposure levels ranging from 0.3 to 3 $\mu\text{g/l}$ with peak concentrations more than 100 $\mu\text{g/l}$ in surface runoff from agricultural fields adjacent to bodies of water during times of application (Thurman et al. 1991; Goolsby et al. 1993). This can substantially affect a downstream reservoir because the reservoir collects and stores the storm runoff that contains high concentrations of atrazine for a certain period (i.e., residence time). Goolsby et al. (1993) reported that atrazine is the most frequently detected chemical with highest concentrations in 76 Midwestern reservoirs from their field monitoring study of herbicides. They indicated that a relatively long-term residence time of reservoir water containing high concentrations of atrazine is problematic not only for the reservoir water quality but also for downstream water quality because elevated concentrations can persist for much longer periods of time in the downstream due to the effect of reservoir storage.

A long-term exposure of elevated atrazine concentrations in raw waters is concerned not only due to environmental issues but also due to economic perspectives. Atrazine is not easily removed from drinking water by conventional water treatment processes, thus tap water concentrations are similar to raw water concentrations unless a high-level of treatment process such as carbon filtration is employed (Hallberg 1996). Therefore, a reservoir operator needs timely information about the occurrences, exposure levels, and persistence of peak concentrations, and the temporal and spatial distributions of atrazine during the concerned period for an adequate water quality management. A mathematical model can be economically and efficiently used to provide timely answers for these questions. In particular, the mathematical model is a unique and valuable tool to assess the environmental impact of a different upstream watershed management strategy on the quality of reservoir water. Agricultural policy makers and decision makers can rely on the model to assess the environmental consequences of alternative policies.

The transport and transformation processes of atrazine in a reservoir are complicated and highly influenced by seasonal reservoir circulation patterns as well as its physico-chemical properties. Therefore, a mathematical model should be able to accurately simulate both the reservoir hydrodynamics and chemical reaction kinetics to capture the real distributions of atrazine in a reservoir. A laterally integrated two-dimensional (2D) hydrodynamics and transport model, CE-QUAL-W2 (Cole and Buchak 1994), has been widely used for the modeling of temperature and conventional constituents (i.e., dissolved oxygen and nutrient) in many reservoirs (Gordon 1980, Kim et. al 1983, Martin 1988, Bath and Timm 1994). However, use of the model for the fate and transport of toxic chemicals such as herbicides and insecticides has been limited because it is not capable of modeling toxic substances. Chung and Gu (1998) applied the model to simulate and analyze the transport of contaminated density currents in the Shasta Reservoir using the 1991 chemical spill data. The model accurately predicted the field measurements of water temperature and field observations of plume intruding depth and thickness. Although the study was only limited to the simulation of transport and mixing processes of a spilled toxic chemical in the reservoir, it laid a basis for the development of a toxic submodel.

The objective of this study is to investigate the fate and transport of atrazine in the Saylorville Reservoir, Iowa (Figure 1) by predicting the temporal and spatial (longitudinal and vertical) distributions of atrazine concentrations using a 2D reservoir toxic model. In particular, the model was applied to capture the occurrence and persistence of peak concentrations that observed during late spring and early summer. Four steps were taken: (1) incorporating a toxic modeling component into the 2D reservoir hydrodynamics and water quality model, (2) establishing various input data for the toxic model, (3) applying the model to simulate the unsteady longitudinal and vertical distributions of atrazine, and (4) analyzing the fate and transport of atrazine using the observed and simulated flow velocities, water temperatures, and concentrations. The site-specific and time-variable atrazine kinetic transformation rates (or half-life) used in this study are a function of environmental conditions, i.e., sunlight, temperature, and microorganisms (Chung and Gu 1998). A sensitivity analysis was conducted to identify the potential model error associated with the use of the parameter (half-life). The model was validated against field data collected earlier including water temperatures and atrazine concentrations.

Method

Description of the Model

The 2D reservoir toxic simulation model was designed to describe unsteady vertical and longitudinal distributions of toxic chemicals in water column and bed sediments in response to various boundary loads: upstream, tributary, distributed, and atmospheric (Chung and Gu 1998). The model was developed using the finite-difference solution of a laterally integrated equations of hydrodynamics and mass transport (Cole and Buchak 1994): (1) horizontal momentum; (2) mass transport; (3) free water surface elevation; (4) hydrostatic pressure; (5) continuity; and (6) an equation of state for density. The state variables include water surface elevation, pressure, density, horizontal and vertical velocities, and chemical concentration. The independent variables are longitudinal distance, vertical flow depth, and time. The governing equations for the transport and fate of atrazine in a reservoir were obtained by

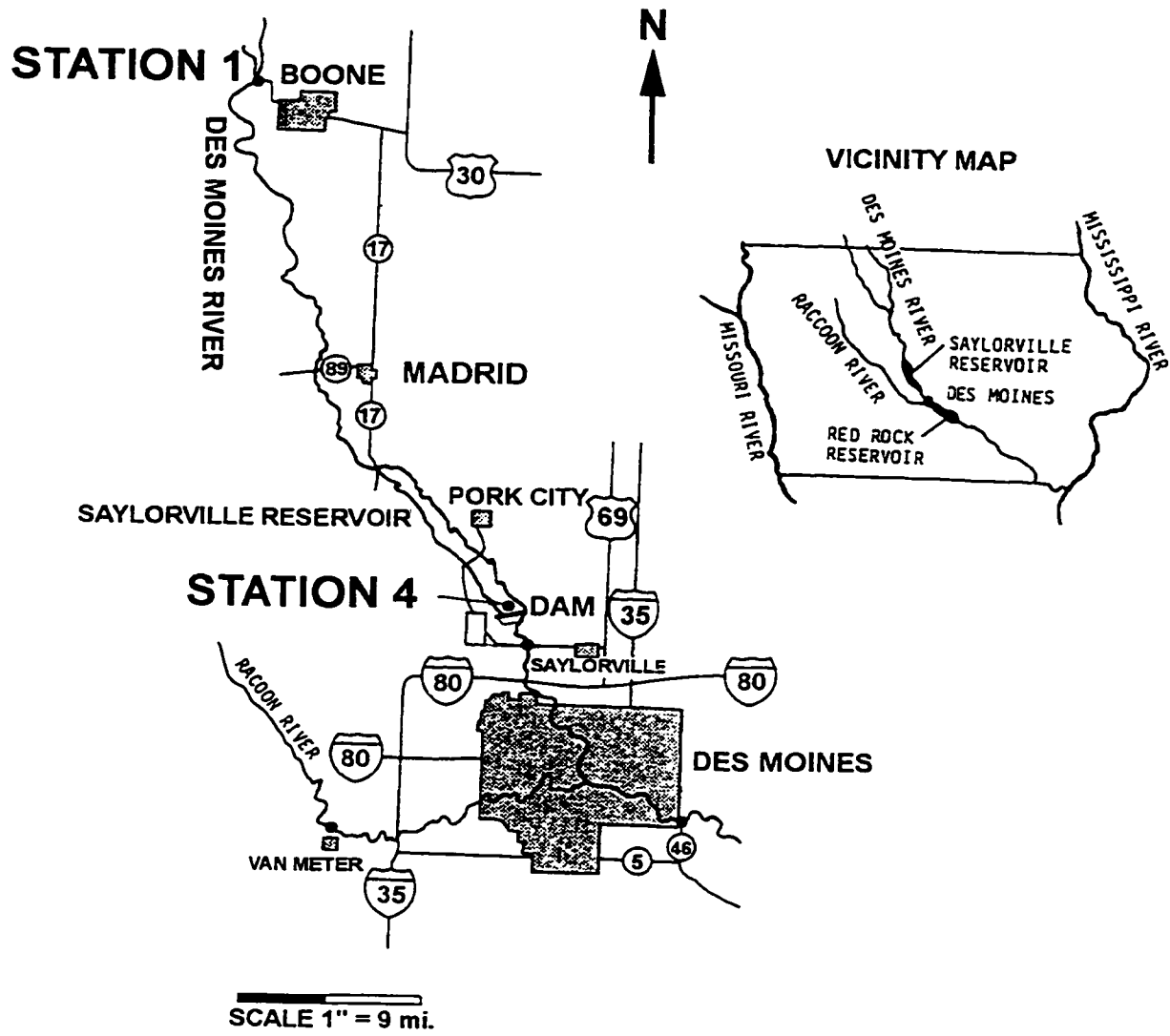


Figure 1. Map of the Saylorville Reservoir, vicinity area, and sampling Stations.

considering mass conservation. The governing equations for total atrazine concentration in the water column ($C_{t,w}$) and in bed sediments ($C_{t,b}$) were expressed as:

$$\begin{aligned} & \frac{\partial(BC_{t,w})}{B\partial t} + \frac{\partial(UBC_{t,w})}{B\partial x} + \frac{\partial(WBC_{t,w})}{B\partial z} - \frac{\partial}{B\partial x}(BD_x \frac{\partial C_{t,w}}{\partial x}) - \frac{\partial}{B\partial z}(BD_z \frac{\partial C_{t,w}}{\partial z}) \\ & = \frac{K_f}{y}(f_{d,b}C_{t,b} / \phi - f_{d,w}C_{t,w}) - K_d f_{d,w}C_{t,w} + \frac{k_l}{z}\{(C_a / H) - f_{d,w}C_{t,w}\} \\ & - \frac{v_s}{z}f_{p,w}C_{t,w} + \Phi_{NPS} \end{aligned} \quad (1)$$

$$\frac{\partial(BC_{t,b})}{B\partial t} = -\frac{K_f}{y}(f_{d,b}C_{t,b} / \phi - f_{d,w}C_{t,w}) - K_d f_{d,b}C_{t,b} + \frac{v_s}{z}f_{p,w}C_{t,w} \quad (2)$$

where subscripts t, d and p denote the total, dissolved, and particulate phases of atrazine, respectively; subscripts a, w and b denote air, water, and bed, respectively; f_d and f_p are the fractions of dissolved and particulate chemicals to the total chemical; t is time (sec); x is longitudinal Cartesian coordinate (positive to the right); B is waterbody width (m); U and W are longitudinal and vertical flow velocities (m/sec); D_x and D_z are longitudinal and vertical constituent dispersion coefficients (m^2/sec); K_r is diffusive exchange rate between water column and pore water of the bed (cm/sec); ϕ is the porosity of the bed sediment; K_d is the sum of first-order kinetic transformation rates for atrazine photolysis, hydrolysis, and biotransformation (/sec); H is Henry's law constant (atm/mole/ m^3); C_a is vapor phase concentration (g/m^3); Φ_{NPS} is nonpoint source (NPS) mass flow rate per unit volume via runoff and drainage flows ($g/m^3/sec$); v_s is the net settling velocity of sorbed chemical (m/sec); z is the depth of water from water surface (m); and y is the vertical distance from reservoir bottom (m). The chemical considered is expected to be in dissolved and particulate forms and vary in longitudinal and vertical directions of the water column and the bed sediments.

The first term of right hand side (RHS) in (1) is the diffusive exchange of dissolved atrazine between sediment and water column. The second term is the degradation of

dissolved atrazine form due to photolysis, hydrolysis, and microbial decay. The model can compute the various degradation processes either separately by providing individual kinetic reaction rates or collectively by providing a lumped transformation rate or half-life value. A time-variable half-life value can be specified in the model input. The third term is the air-water exchange of atrazine due to volatilization. The fourth term is the net settling of atrazine in the particulate phase. The model uses a net settling velocity as inputs for sediments, which does not explicitly account for particle type, grain size, density, viscosity, and turbulence. The last term is the external nonpoint source loading that can be estimated either by a simple mass balance model or a complicated NPS model. The second term of RHS in (2) is the degradation of dissolved form in bed sediment due to hydrolysis and microbial decay.

The governing equations were solved using finite difference method to the laterally integrated hydrodynamics, mass transport, and transformation equations. The free water surface elevation and momentum equations were solved simultaneously based on an implicit finite-difference scheme, which allows the use of reasonable time scale for field application over entire stratification cycles (Martin 1988; Cole and Buchak 1994). The transport processes of atrazine and sediment were solved using an explicit numerical scheme, QUICKEST finite difference scheme, which was used for temperature simulation in CE-QUAL-W2 model (Cole and Buchak 1994). Vertical turbulent transfer of atrazine and sediments was determined from the vertical shear of horizontal velocity and a density gradient dependent Richardson number function. The physical, chemical, and biological transfer and transformation processes of a toxic chemical were computed in the toxic submodel. The toxic submodel was created and linked into the hydrodynamics and transport model using the FORTRAN Powerstation (Chung and Gu 1998). The source and sink terms of atrazine (physical transfer and degradation processes) may be computed less frequently than hydrodynamics. The physical and chemical properties of a toxicant and kinetic reaction rates need to be provided through an independent input file.

Kinetic Processes of Atrazine

Atrazine can be transformed into numerous different degradation products by either biotic or abiotic transformation processes. Biotic transformation of atrazine is generally

accomplished by biotransformation and results in N-dealkylation of the atrazine structure to initially produce either desethylatrazine [4-Amino-2-chloro-6-isopropylamino-s-triazine] or deisopropylatrazine [2-Amino-4-chloro-6-ethylamino-s-triazine]. Abiotic transformation processes such as photolysis and hydrolysis can transform atrazine into hydroxyatrazine [2-Hydroxy-4-ethylamino-6-isopropylamino-s-triazine], and eventually into cyanuric acid [2,4,6-Trihydroxy-s-triazine] that is the end product of atrazine by photolysis (Pugh 1994).

The reaction rates of these transformation processes for atrazine in a natural water system depend both on the physico-chemical properties of atrazine and the conditions of the aquatic environment (i.e., water depth, temperature, pH, intensity and spectrum of solar radiation, wind speed, microorganism concentration, and suspended solids concentration). Individual degradation processes in the reservoir may be considered in the simulations and analysis of the fate of atrazine. But due to the limited measurement data (i.e., no degradation products were measured), a time-variable bulk first-order kinetic transformation rate (K_d) that collectively includes photolysis, hydrolysis, and biotransformation processes was used to compute the degradation of atrazine in the waterbody (Table 1). The time-variable K_d values

Table 1. Time-variable kinetic transformation rate and half-life of atrazine.

Month	1	2	3	4	5	6	7	8	9	10	11	12
K_d	0.03	0.03	0.16	0.10	0.19	0.10	0.12	0.10	0.06	0.02	0.02	0.01
$t_{0.5}$	24.7	22.0	4.4	7.3	3.7	7.3	6.0	7.3	12.0	33.0	36.0	46.7

for the Saylroville Reservoir were obtained in previous study using a mass balance model and field monitoring data (Chung and Gu 1998). The atrazine half-life values varied from 3.7 to 12.0 days during the study period, from March to September, 1978, with minimum and maximum values in the months of May and September, respectively, depending upon the environmental conditions such as sunlight and water temperature.

A partition coefficient (K_p) was used to separate the fractions of dissolved and particulate forms of atrazine to the total atrazine concentration based on the assumption of

linear sorption and desorption kinetics (Thomann and Mueller 1987). The dissolved and particulate concentrations were expressed as

$$C_{d,w} = f_{d,w} C_{t,w} \quad (3)$$

$$C_{p,w} = f_{p,w} C_{t,w} = r C_{ss} = K_p C_{ss} C_{d,w} \quad (4)$$

where $f_{p,w} = \frac{K_p \cdot C_{ss}}{1 + K_p \cdot C_{ss}}$, $f_{d,w} = \frac{1}{1 + K_p \cdot C_{ss}}$, r is the concentration of atrazine expressed on

a dry weight solids basis (mg/kg), and C_{ss} is the suspended solids concentration (kg/m^3).

Thus, the distribution of atrazine concentrations between particulate and dissolved phases was determined dependent upon the partition coefficient and the solids concentrations.

A two-film theory (Whitman 1923; Mackay 1985) was used to compute the gaseous transfer of atrazine from air to water and water to air. The exchange rate was computed as a function of the atrazine concentration gradient between the reservoir water column and the overlying atmosphere and the conductivity across the interface of the two fluids. The conductivity was influenced by both physico-chemical properties of atrazine and environmental conditions at the air-water interface. The overall volatilization transfer coefficient, k_1 , was given as:

$$\frac{1}{k_1} = \frac{1}{K_l} + \frac{1}{K_g H} \quad (5)$$

where K_l is the liquid film coefficient and K_g is the gas film coefficient. The k_1 value was computed as a function of the chemical characteristics (H , K_l and K_g), water velocity, and wind speed in the model. Since the transfer coefficient for the open bodies of water such as reservoir and lake is largely affected by wind, the equation suggested by Mackay (1985) was used to estimate the liquid and gas film transfer coefficients.

Model Application

Study Site

The Saylorville Reservoir is located on the upper Des Moines River basin, Iowa (Figure 1). The reservoir was built primarily for the purposes of flood control, low flow augmentation for water quality control, and recreational activities (US Army Corps of Engineers 1983). At full flood control pool, elevation 271.3 m, the reservoir extends 86.9 km above dam and occupies about 67.6 km². At conservation pool, the reservoir water surface elevation is about 254.8 m and occupies 24.1 km². The mean and maximum depths of the reservoir are 4.3 m and 13.8 m at the conservation level, respectively. Approximately 79% of the upstream watershed was cropland, 6% was permanent pasture, 5% was forest, and 7% was urban at the time of study period (Iowa Department of Environmental Quality 1976). Corn and soybeans are two main crops in the area. The amount of annual precipitation during the study period was 797 mm which is slightly less than the normal annual precipitation of 813 mm in Iowa.

The field monitoring data used in this study were collected weekly or biweekly at two sampling stations, denoted as Stations 1 and 4. These stations are part of 8 sampling stations installed in the Des Moines River basin by the Engineering Research Institute of Iowa State University to monitor the long-term impacts of Saylorville and Red Rock reservoirs on water quality and quantity (Baumann et al 1979; Lutz and Cavender 1997). Station 1 is located near the Boon water plant about 71.8 km upstream from Saylorville Dam and considered as the upstream boundary of the reservoir at conservation pool. Station 4 is located within the reservoir with an upstream drainage area of 15,081 km². Samples were collected from three depths (subsurface, mid-depth, and bottom) at Station 4 in the reservoir. Although the historical water quality monitoring data showed a distinct thermal and chemical stratifications during the summer months in this site (Lutz and Cavender 1997), a weak stratification was observed during the study period. The mean daily inflow at Station 1 and outflow from the dam were 42.5 m³/sec and 48.6 m³/sec and water surface elevation was fluctuated between 253.8 m (capacity 88.4 million m³) and 255.1 m (capacity 118.5 million m³) during the study period, from March to September, 1978. The mean water residence time

(volume/outflow) in the reservoir was 17.7 days with minimum 9.4 days during July and with maximum 34.7 days during August.

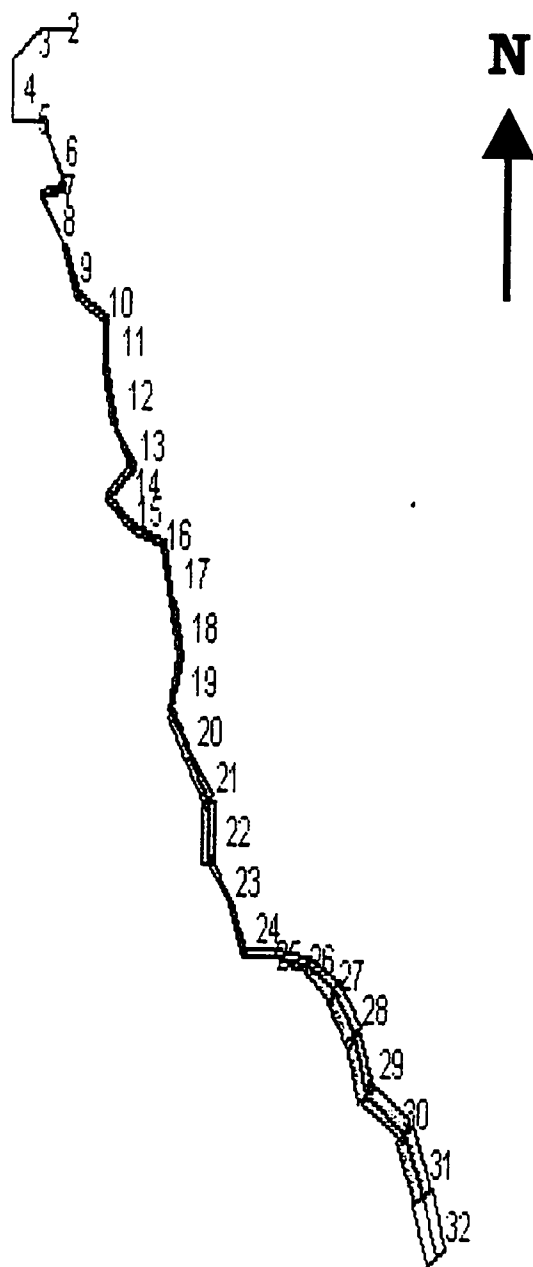
Simulation Domain and Initial Conditions

The reservoir reach from sampling Station 1 to Saylorville Dam was discretized into a single branch finite-difference grid consisting of 31 longitudinal segments with average 2.3 km in length and 28 vertical layers with 0.8 - 1.0 m in thickness (Figure 2). The inflow from the Big Creek lake, which was built mainly for flood control and is located at about 12 km upstream from the Saylorville Dam, was treated as a tributary. The reservoir bathymetry data, i.e., elevation and width of the reservoir cross-section for each segment, were obtained from the United States Geological Survey (USGS) 7.5 minute topographic maps (1:24,000 scale) for this site. The accuracy of bathymetry data was evaluated by comparing the volume-elevation curve generated by the model with the project volume-elevation curve for the reservoir (US Army Corps of Engineers 1983) (Figure 3).

The time frame of model application was from March 1 to September 30, 1978 because the period is corresponding to corn growing season and the months when a significant level of atrazine is detected. A variable timestep was computed in the model to maintain numerical stability using an autostepping algorithm that was embedded in the model. The average time step was 1088 seconds over the simulation period. The initial conditions for water temperature and atrazine concentration in the reservoir were set at 2 °C and 0.01 µg/l for all cells, respectively, based on the field measurement data for February 28, 1978. The ice cover simulation option of CE-QUAL-W2 model (Cole and Buchak 1994) was used when the reservoir is covered by ice in the month of March.

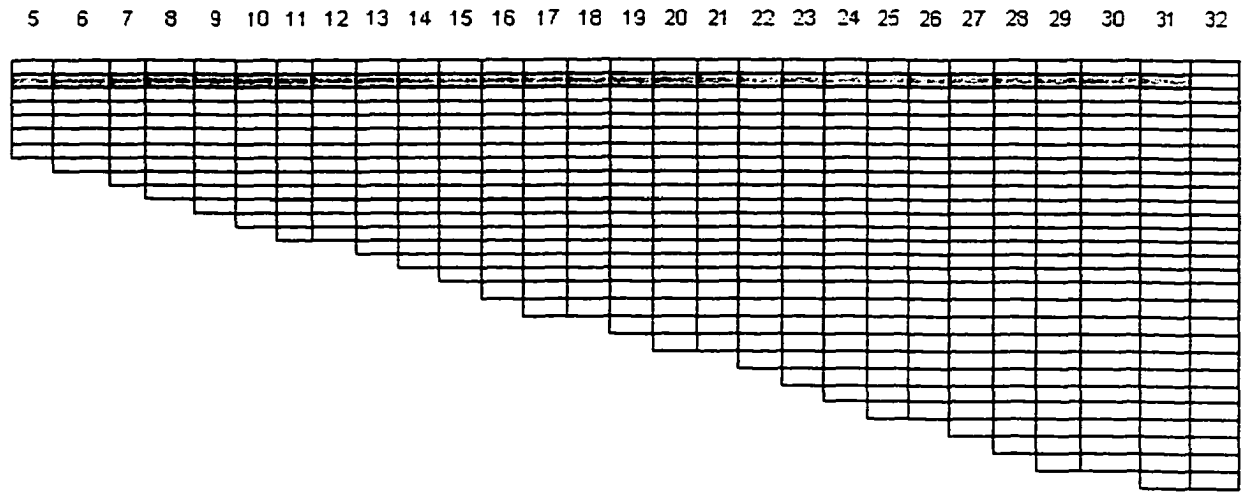
Input Data and Boundary Conditions

Most of input data were obtained from field monitoring. Some parameters were estimated from physico-chemical properties of atrazine, hydrologic characteristics of the watershed, and literature survey for this site. The daily values of precipitation, inflow, outflow, and reservoir water storage during the study period are presented in Figure 4. The atrazine concentrations and water temperatures measured weekly or biweekly at sampling Station 1 were used as the time-variable upstream boundary conditions. The flow data for this



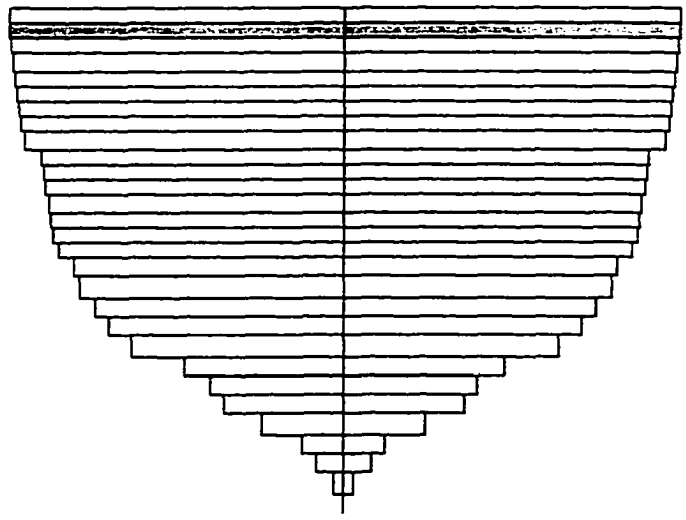
(a) Plan view

Figure 2. The finite difference grid system of the Saylorville Reservoir: (a) plan view



(b) Longitudinal view

32



(c) Cross sectional view for segment 32

Figure 2. (continued) (b) vertical view, and (c) cross sectional view.

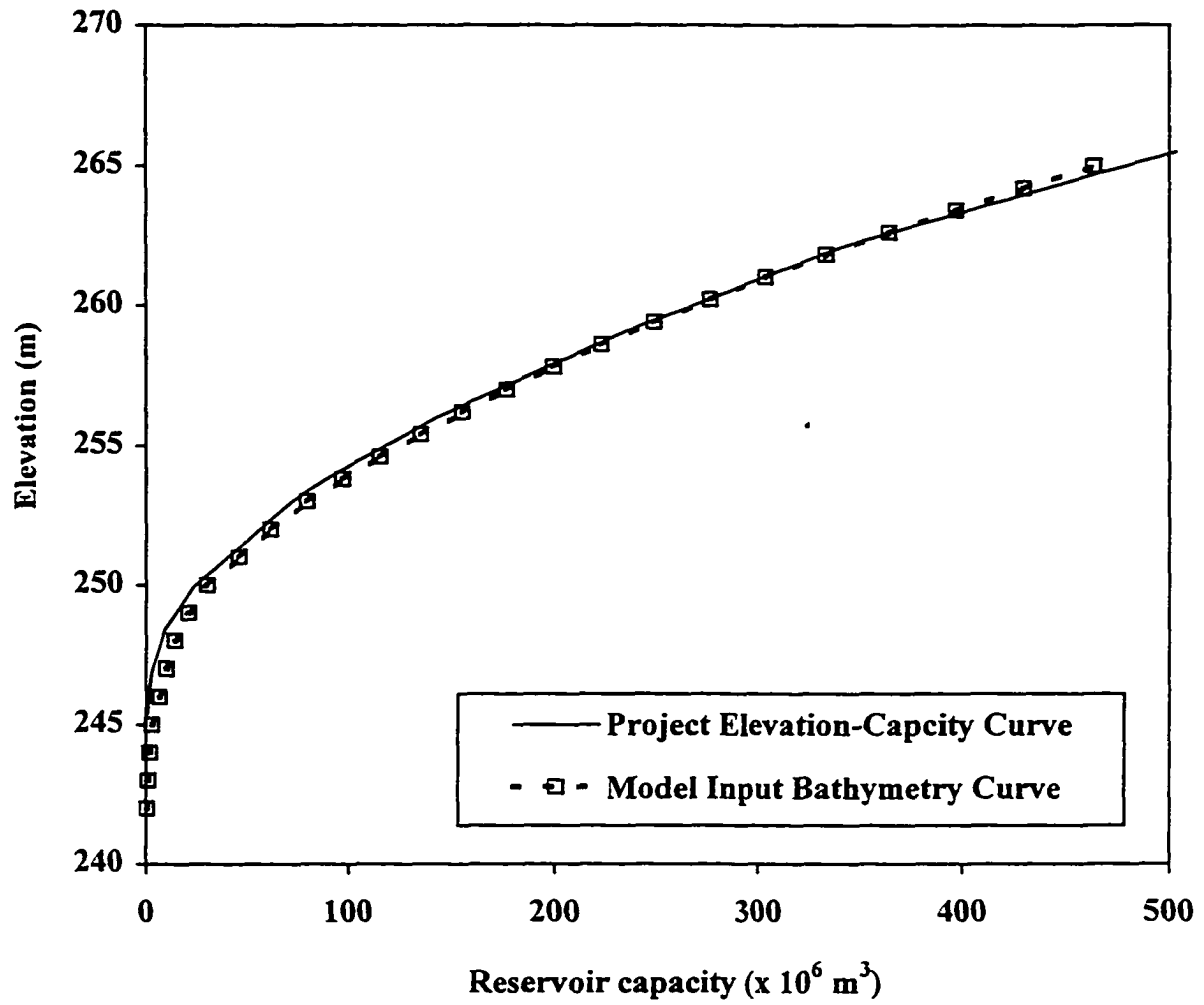


Figure 3. Comparison of elevation-capacity curve obtained from model bathymetry data with project elevation-capacity curve of the Saylorville Reservoir.

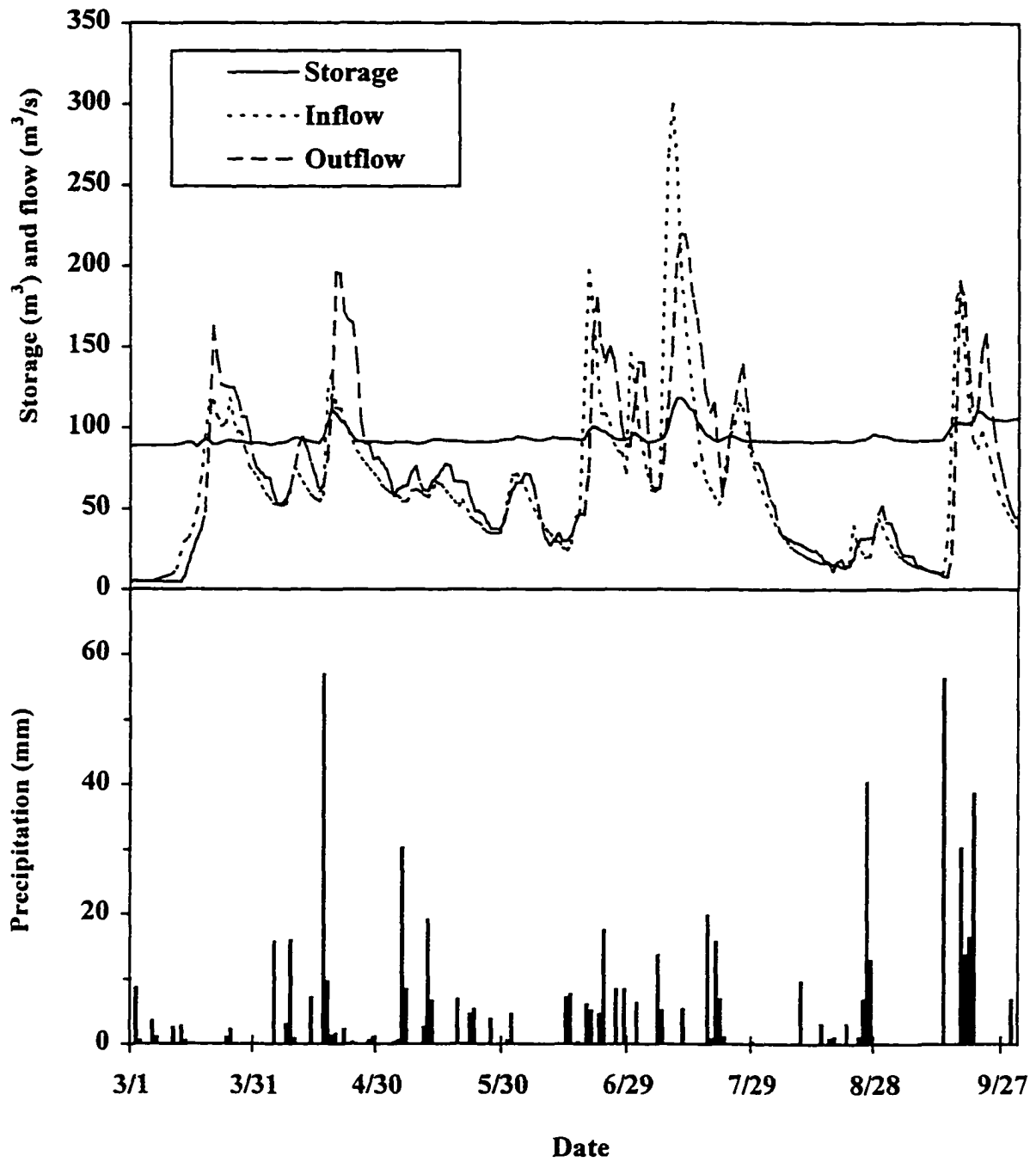


Figure 4. Daily precipitation, inflow, outflow, and storage of the Saylorville Reservoir during the study period.

station were estimated from the daily flow data collected at the USGS gauging station near Stratford, which is located about 28 km upstream of Station 1 (USGS 1978) multiplying by the ratio of drainage area of Station 1 to that of Stratford station. The time-dependent boundary input data were interpolated for each timestep in the model.

Meteorological data were obtained from the Des Moines, Iowa National Oceanic and Atmospheric Administration station, located just downstream of the reservoir. Since nighttime convective mixing is an important physical process affecting reservoir hydrodynamics, daily maximum and minimum temperatures rather than daily average air temperatures were used for the boundary conditions at the water surface. Surface wind speeds were slightly reduced (about 5%) using a sheltering coefficient of 0.95 based on a flat surrounding topography of the reservoir. The daily meteorological data were interpolated for each timestep to compute solar radiation, equilibrium temperatures, and coefficients of heat exchange for use in computing surface heat exchange.

The model requires distributed flows and atrazine concentrations for each time step to compute the nonpoint source mass flow rate (Φ_{NPS}). About ten small creeks collect the distributed atrazine loads from the watersheds via overland flow, surface runoff, and subsurface drainage flows and discharge into the reservoir. In this study, the nonpoint source mass flow rate (Φ_{NPS}) collectively included the contributions of these tributaries and the distributed atrazine loading along the main branch of the reservoir. Unfortunately, no state-of-the-art watershed-scale models are validated for simulating the fate and transport processes of toxic chemicals in the distributed flows (Donigian and Huber 1991; Wurbs 1995). These models also require enormous input data including soil, weather, agricultural management (planting, chemical application, tillage, and harvesting), and the chemical transformation rate in field, surface and subsurface flows, which are difficult to obtain in the watershed, to simulate the time-variable atrazine loading into the reservoir. Thus the NPS atrazine loading rate was estimated based on the amount of atrazine that applied within the watershed, the percentage of total atrazine that is delivered to the waterbody, and a weighting factor that represents the dynamic loading pattern of atrazine at the study site. The detailed estimation process of NPS loading is presented in the previous paper (Chung and Gu 1998).

Approximately 2.7 kg/ha of atrazine was assumed to have been applied in the corn cropping area of surrounding watershed. The fraction values for $f_1 = 0.71$, $f_2 = 0.61$, and $f_3 = 0.55$ were used based on the previous survey data for this site (Naylor 1975; Leung 1979), where f_1 is the fraction of corn and soybean cropping area to the drainage area (542 km²), f_2 is the fraction of corn cropping area to the f_1 , f_3 is the fraction of atrazine applied area to the f_2 . The percentage of applied atrazine which is delivered to surface waters (f_4) was assumed as 0.5% based on the previous studies for the region (Harmon and Duncan 1978; Johnson and Baker 1982; Wilson 1987; Rice 1996).

Figure 5 shows the estimated monthly distributed flow (Q_d), nonpoint source mass loading (M_d) and concentration of atrazine (C_d) during the year of 1978. The monthly amount of direct mass input through distributed flows (M_d) was calculated based on the application rate of atrazine, the fraction values (f_1 , f_2 , and f_3), the percentage of total atrazine that is delivered to the waterbody (f_4), and a monthly weighting factor (s_i) that represents the loading pattern of the study site (Chung and Gu 1998). The atrazine concentrations in the distributed runoff flows were computed dividing the mass (M_d) by the flows (Q_d) that were calculated from the daily flow data measured at the USGS gauging station near Stratford, assuming a linear relationship between the flow and drainage area. The Q_d and C_d values were interpolated in the model for each time step.

The model requires the specification of several model coefficients for hydrodynamics and mass transport. The model coefficients used for this study are listed in Table 2. The longitudinal eddy viscosity and diffusivity were estimated as a function of flow characteristics (i.e., discharge, depth, and roughness) using the equation suggested by Liu (1977). Vertical diffusion coefficients for momentum and constituents that varied in space and time were computed using the time-variable vertical shear of horizontal velocity and a density gradient dependent local Richardson number function. The Chezy coefficient is used in calculating the effects of bottom roughness. The default value provided by the model for most reservoir applications was used in this study because it is not a sensitive parameter to model results. The fraction of solar radiation absorbed in surface layer, β , and light extinction coefficient for pure water, ϵ , were estimated from the secchi depth observed at the study site

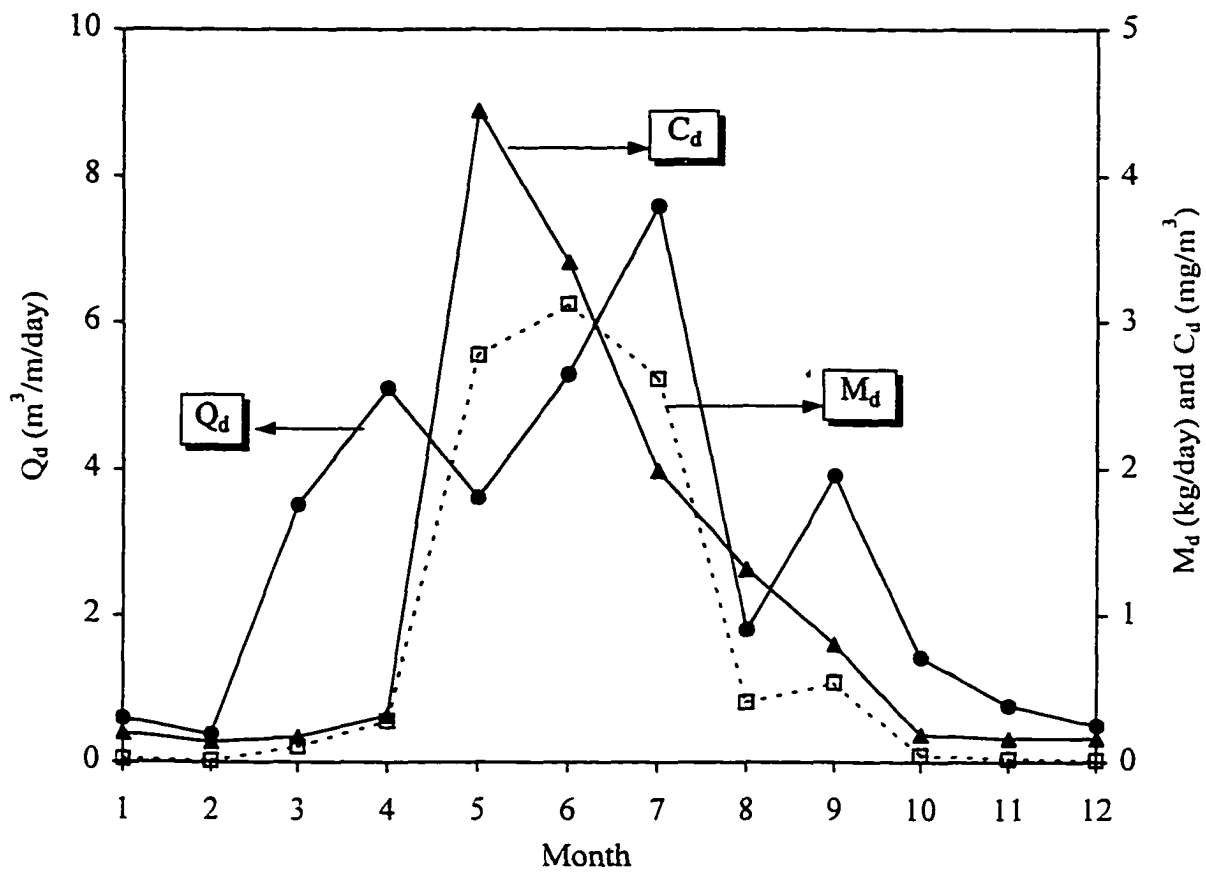


Figure 5. Estimated monthly-distributed flow (Q_d), atrazine mass loading (M_d), and concentration (C_d) in 1978 for the Saylorville Reservoir.

Table 2. Hydrodynamics and transport model coefficients used in the model.

Coefficient	Unit	Value
Longitudinal eddy viscosity, A_x	m^2/sec	225.0
Longitudinal eddy diffusivity, D_x	m^2/sec	225.0
Chezy coefficient	$m^{1/2}/sec$	70.0
Wind sheltering coefficient	-	0.95
Solar radiation absorbed in surface layer, β	-	0.64
Extinction coefficient for pure water, ϵ	/m	1.11

(Cole and Buchak 1994). The secchi depth varied from 0.22 - 1.9 m in the reservoir over the historical sampling period, thus an average value of 1.0 m was used for the estimation of these parameters.

Results and Discussion

Hydrodynamics and Thermal Structure

An accurate simulation of water balance, hydrodynamics, and thermal structure over time is important to the prediction of fate and transport of atrazine in a reservoir. In general, reservoir water level varies with time in response to various boundary flow conditions including inflow, surface runoff, seepage flow, precipitation, outflow, and evaporation. Therefore, the simulated water elevations were compared with the observed values to examine and validate the accuracy of water balance computation of the model in Figure 6. The model results follow the observed water surface variations reasonably well during the entire study period. The estimated distributed flows (Q_d) resulted in a slight error, e.g., the simulated values showed a smooth increase and decrease of water levels in the month of April, while observed values showed a sharp increase during the same period due to short-term runoff events by snow melt and storms, but the accuracy of computed water balance is

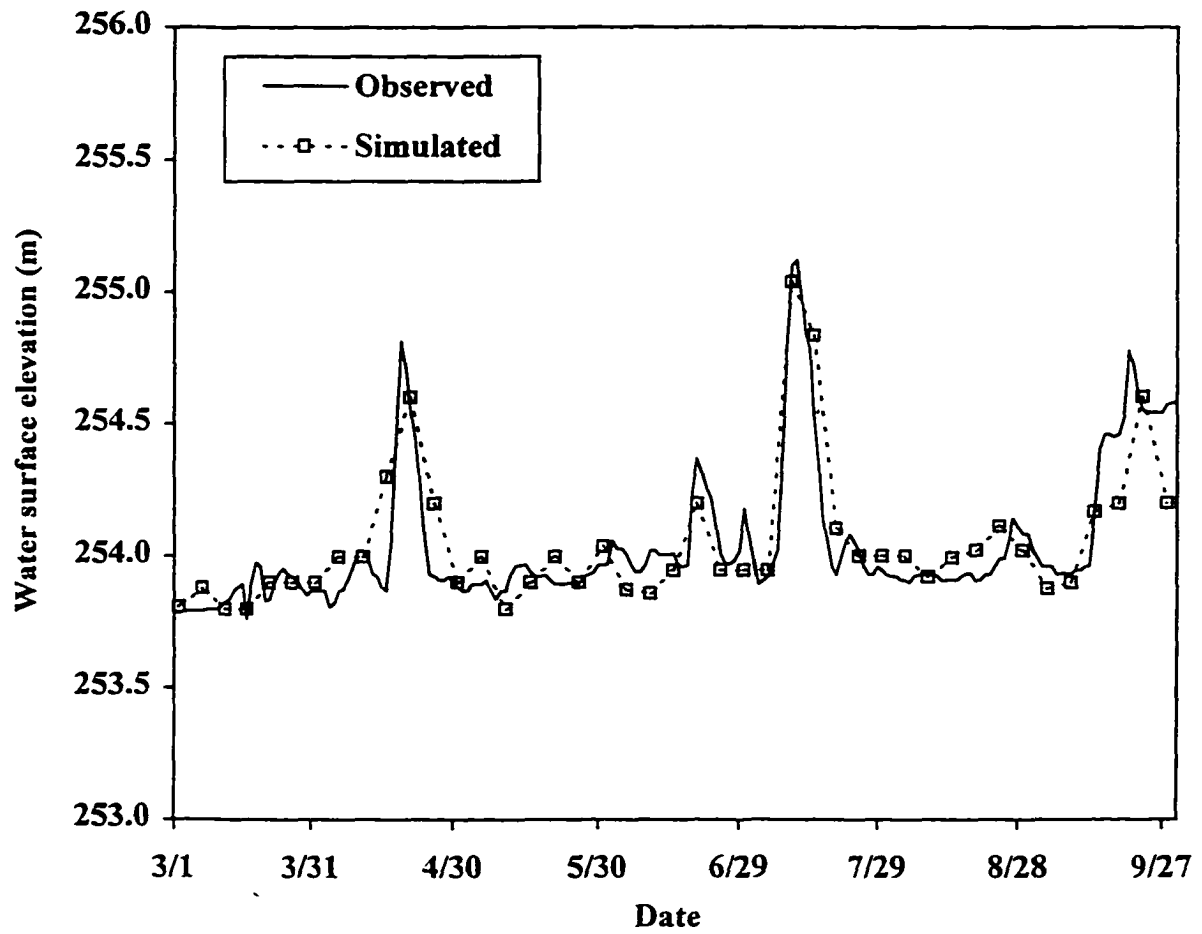


Figure 6. Observed and simulated reservoir water surface elevations.

satisfactory to simulate the fate and transport of atrazine. The water balance simulation can be further improved if a field- or watershed- scale model is applied to compute and provide runoff values from individual storm events.

Figure 7 shows the computed flow velocity vectors for various dates. The velocity fields represent typical seasonal circulation patterns in the reservoir during early spring, late spring, summer, and fall, respectively. It should be noted that only part of the reservoir (about 30 km upstream from the dam) is plotted due to the large spatial variations in flow velocities between upstream and downstream. The direction and magnitude of the vectors represent the resultant of vector product between the longitudinal and vertical velocities. The vector plots should be interpreted carefully because the length of one segment is too long, approximately 2.5 km, to capture the details of velocity fields, i.e., one velocity vector represents the flow characteristic of a 2.5 km \times 1.0 m cell of the reservoir. They were used only to examine the characteristics of seasonal water circulation patterns in the reservoir.

Two different circulation patterns are detected for the four different periods. Similar circulation patterns were obtained for early spring and fall, although the driving forces are different. During the early spring, inflows entered the reservoir as a plug flow about 20 km upstream from the dam and moved toward the dam as forming an overflow in the reservoir because of the temperature difference between the upstream river waters ($T_w = 1^\circ\text{C}$) and the reservoir water ($T_w = 2\text{-}3^\circ\text{C}$). The density of river water was slightly less than that of ambient reservoir water during the period (Figure 8). The flows moved downward near the dam face and formed a reversal flow at the bottom of reservoir, but the reversal flow was captured again at about 15 km upstream from the dam by the inertia force driven by inflow and formed an upward movement. During the fall, however, the river water was slightly colder (Figure 8) than the ambient reservoir water, although the circulation pattern is quite similar to that in spring (Figure 7). This implies that the dominant mixing mechanism for this period was convective overturn as surface waters cooled. The river water temperatures during the late spring and summer were about 1°C and 3°C less than water temperatures in reservoir surface, respectively (Figure 8). This resulted in the development of an underflow during that periods. The flow moved straight along the slope of the reservoir and formed an upward

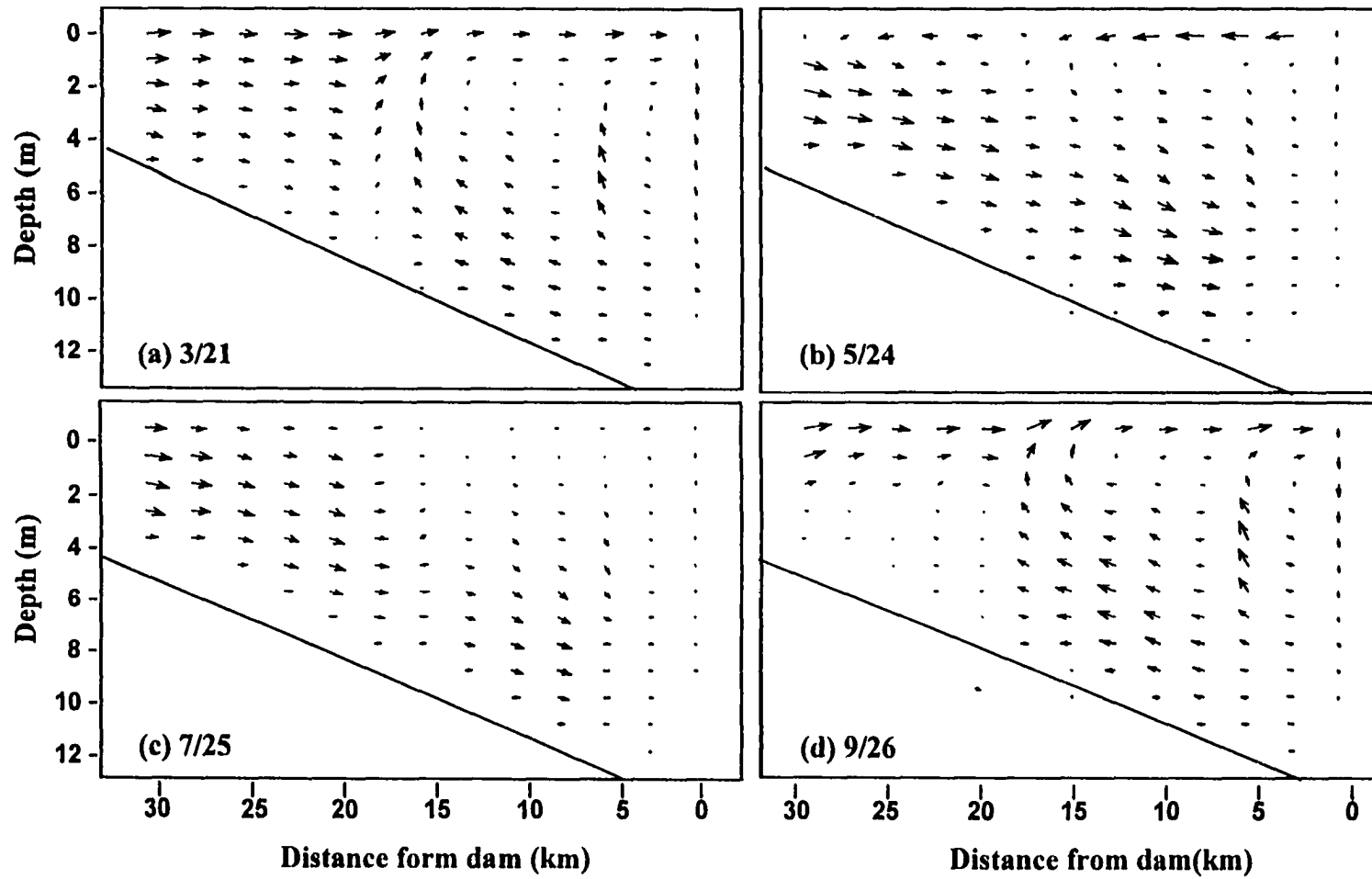


Figure 7. Seasonal reservoir circulation patterns during (a) early spring, (b) late spring, (c) summer, and (d) fall.

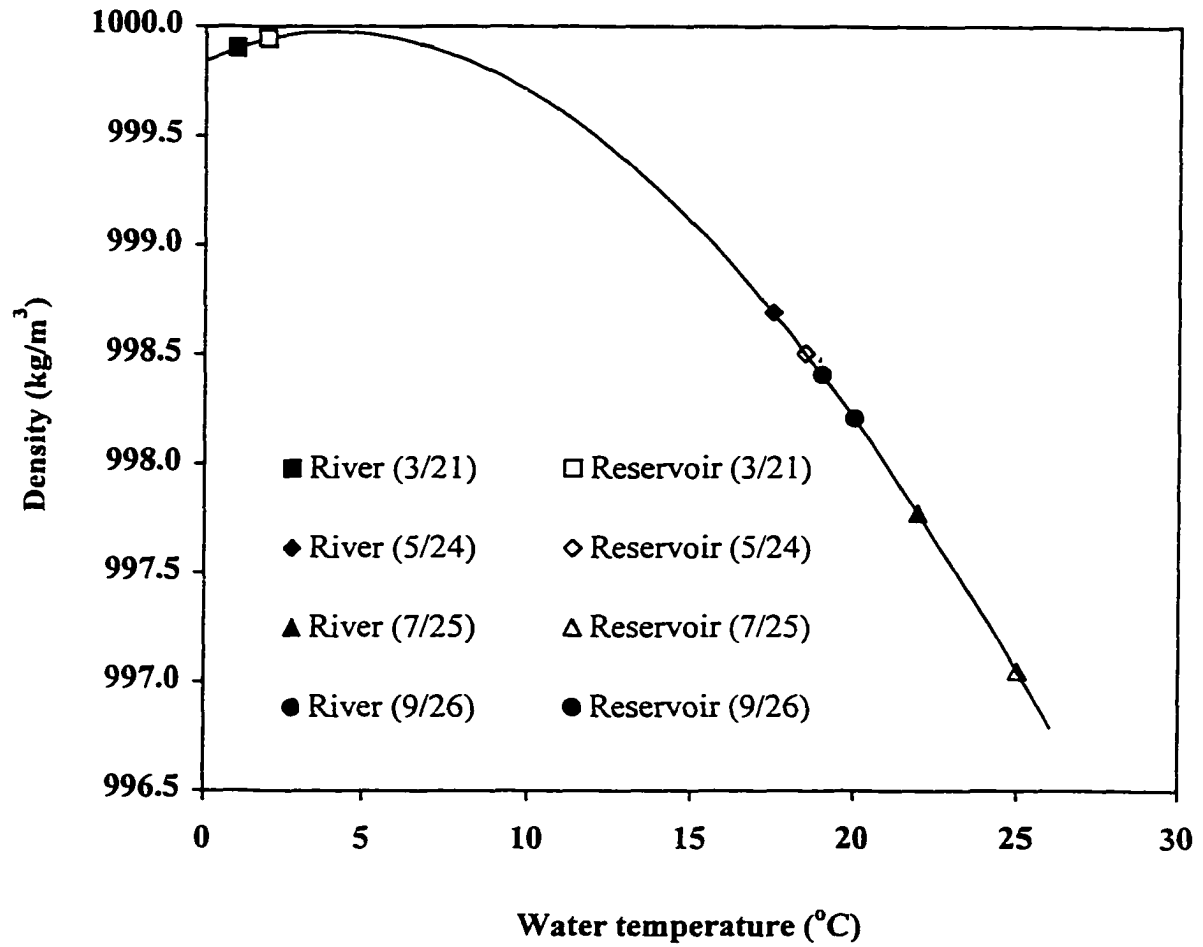


Figure 8. Observed river water and reservoir surface water temperatures on 3/21, 5/24, 7/25, and 9/26.

movement at the dam face. A strong wind speed during the late spring caused to develop a reversal flows near the surface of the reservoir. A weak reservoir mixing is detected near the dam and surface of the reservoir during the summer because of a short circuiting of flows.

Reservoir thermal structure is a particular concern because it can results in water quality differences at various locations in the reservoir. Figure 9 depicts the seasonal reservoir thermal structures using water temperature contours at various times. Simulation results agreed well with the observed values, which measured at surface (S), mid-depth (M), and bottom (B) of the reservoir at about 0.3 km upstream from the dam. The reservoir water temperatures were quite uniform in the vertical direction during the early spring (Figure 9a). The temperature variations in the vertical and longitudinal directions were 0.5 °C and 1.5 °C, respectively. The weak longitudinal stratification resulted from small temperature differences between river and reservoir waters. During the late spring (Figure 9b), vertical stratification was observed in the reservoir. The simulated water temperatures were about 1.5 °C higher at the surface and lower at the bottom of the reservoir compare to the observed values. This might be caused partially by the use of inaccurate model parameters for heat exchanges at water surface and bottom of the reservoir and the underestimation of the mixing effect of storm runoffs that occurred during this periods. During the summer (Figure 9c), the longitudinal and vertical variations of water temperatures were small. Simulated water temperatures near the dam ranging from 24 to 26 °C agreed well with the observed values, 24.5-25 °C. A slightly colder river water appeared in the upper part of the reservoir and pushed the warmer reservoir water, which is well consistent with the unique circulation pattern described in the velocity vector during the same period (Figure 7c). The reservoir thermal structure in the fall is characterized as a well mixed condition in longitudinal and vertical directions (Figure 9d). The simulation results agreed well with observed water temperatures at three depths, except near the bottom of reservoir. In general, simulated water temperatures near the bottom of reservoir were underestimated over the entire simulation periods, which indicates a weak model performance in computing heat exchanges between water and sediments at the bottom of reservoir.

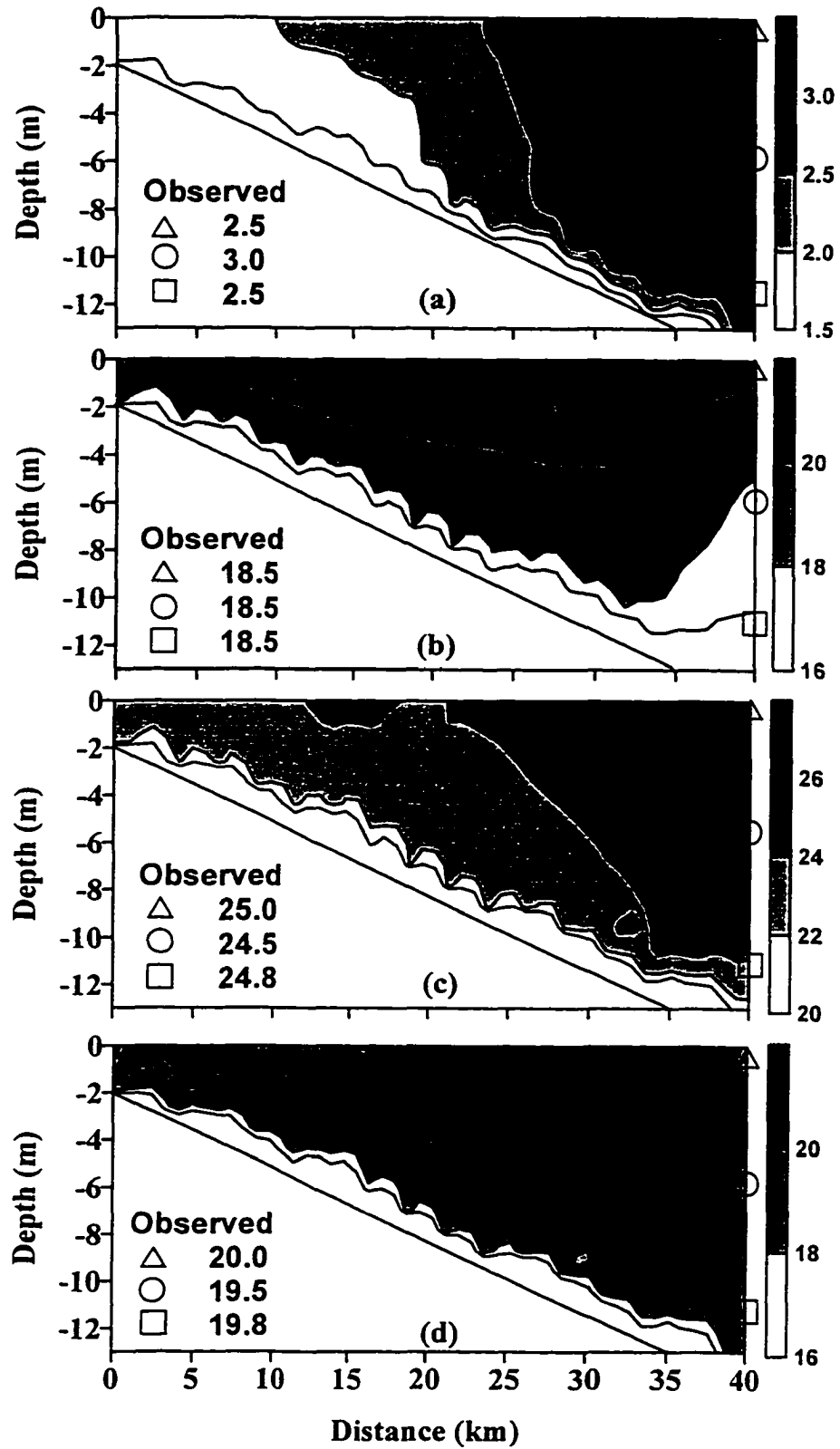


Figure 9. Simulated and observed seasonal thermal structures of the Saylorville Reservoir during (a) early spring, (b) late spring, (c) summer, and (d) fall.

Spatial Distribution of Atrazine

Spatial distributions of toxic contaminants in a reservoir are particularly important to selective raw water intake, spill control, and downstream water quality management. The contamination levels of atrazine in the reservoir for four different seasons are depicted by simulated atrazine concentrations in Figure 10. The observed atrazine concentrations at surface, middle, and bottom of the reservoir are compared in the Figure. Comparisons between the thermal structures and the spatial distributions of atrazine concentrations indicate a strong relationship between them.

In the early spring (Figure 10a), the simulated atrazine concentrations in the reservoir were uniform in the range of 19-21 ng/l and compared well with the observed values at three depths. The well-mixed and low levels of atrazine concentrations during that period are mainly due to the steady state load of atrazine with low concentrations from upstream over the long winter periods of the previous year. The atrazine concentrations in the upstream river waters (Station 1) varied from 10 to 44 ng/l during the winter periods. A weak vertical stratification of atrazine concentrations was observed in the late spring (Figure 10b), which is consistent with the simulated thermal structure of the reservoir during the same period (Figure 9b). Atrazine was distributed in the reservoir with concentrations of 800-1000 ng/l depending on the reservoir water depth. Predicted vertical distributions of atrazine near the dam agreed well with the observed values over the depths except at the bottom of the reservoir.

During the summer, relatively high level of atrazine concentrations was located at the surface of the reservoir near the dam. This was expected from the insignificant mixing in the surface layers of reservoir as depicted in the circulation pattern in Figure 7c and well consistent with the thermal structure for that period (Figure 9c). The successive inflows containing a lower level of atrazine followed by the peak concentrations, intruded into the reservoir below the surface, and flushed out the lower part of reservoir waters that contained elevated atrazine concentrations. The short circuiting of flows led to less dilution and resulted in higher atrazine concentrations near the surface of the reservoir. The distribution of atrazine concentrations during the fall is characterized as a well mixed condition in the vertical

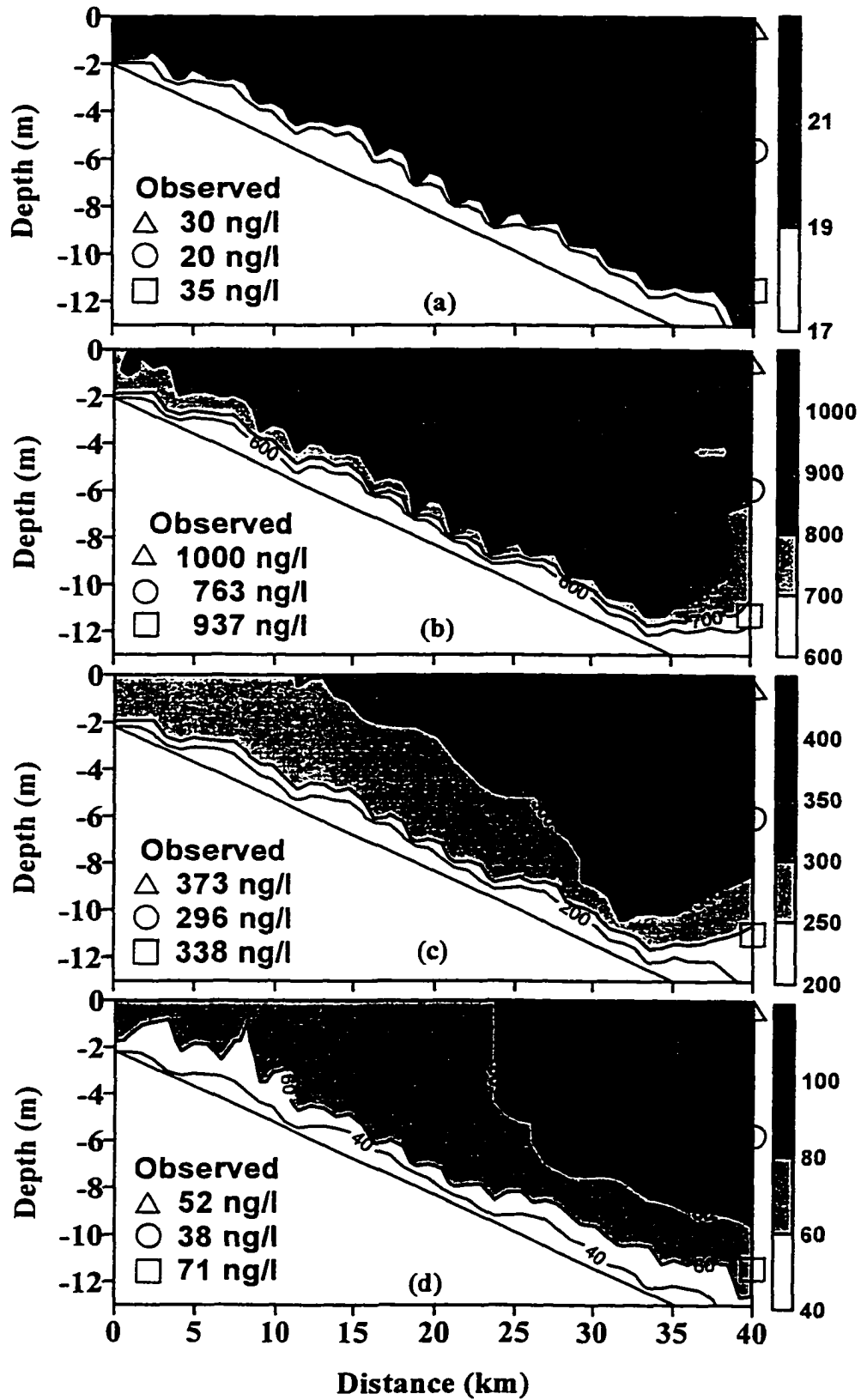


Figure 10. Simulated and observed spatial distributions of atrazine in the Saylorville Reservoir during (a) early spring, (b) late spring, (c) summer, and (d) fall.

direction with low levels of concentrations less than 100 ng/l. The significant vertical mixing induced by convective overturn (Figure 7d) removed the weak vertical stratification of atrazine that occurred during the summer. Although the model overestimated the maximum concentrations at the surface of reservoir, the overall model performance in predicting the spatial distributions of atrazine concentrations in response to seasonal flow behavior is satisfactory.

Temporal Exposure Level of Atrazine

Figure 11 shows the observed and simulated temporal variations of water temperatures and atrazine concentrations at three depths (surface, middle, and bottom) in the reservoir. The simulated results accurately tracked the variations of observed water temperatures over the entire simulation periods. In general, no strong thermal stratification was noticed from both observed and simulated water temperatures, although the model results showed a trend of slightly higher water temperature near the surface than at the bottom of the reservoir during the summer months. The simulated atrazine concentrations are in reasonably good agreement with the measured values at all depths. A weak vertical stratification displayed in the simulated atrazine concentrations during the summer months is directly associated with the thermal structure of the periods. The model successfully captured the peak concentrations occurred at the end of May and in early June in the reservoir. The observed peak atrazine concentrations (greater than 1356 ng/l) at the inflow boundary, Station 1, on 5/16 resulted in the occurrence of peak concentrations in the reservoir after 15 days, and the model captured it reasonably well. The travel time (or response time) of atrazine (15 days) was slightly less than the residence time of flow 17-19 days, which calculated from reservoir volume and flows, indicating that the effect of flow short circuiting on the transport of the contaminant is insignificant in the shallow Saylorville Reservoir.

Time series of the averaged water temperatures and atrazine concentrations over the depth are presented in Figure 12. The r^2 value, which is used as an indicator for the performance of the model in predicting the temporal variations of observed temperatures and concentrations, is 0.97 and 0.84 for water temperature and atrazine concentrations, respectively. The r^2 values implies that the model is reliable in generating the temporal

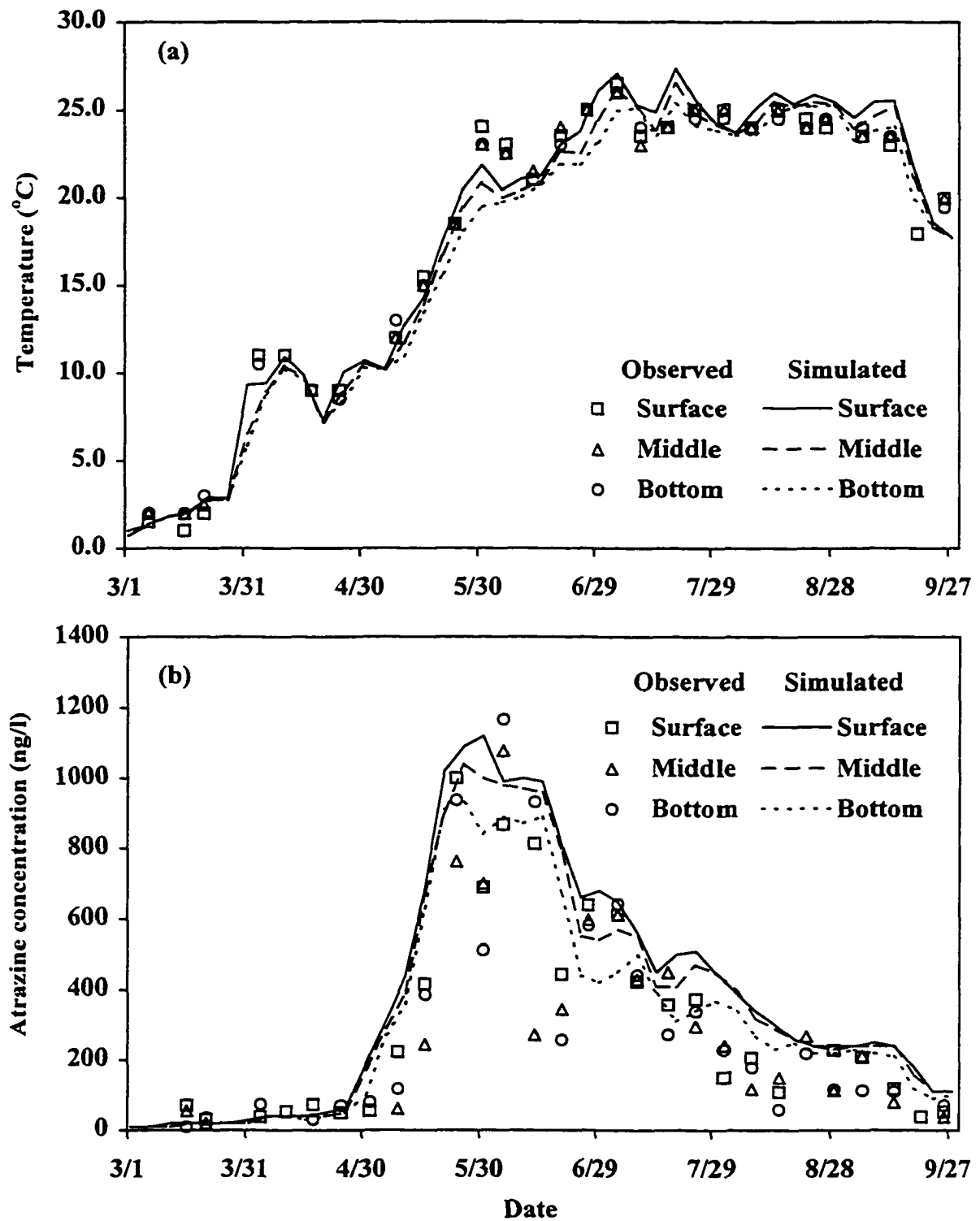


Figure 11. Observed and simulated (a) water temperatures and (b) atrazine concentrations versus time at three depths (surface, middle, and bottom) in the reservoir.

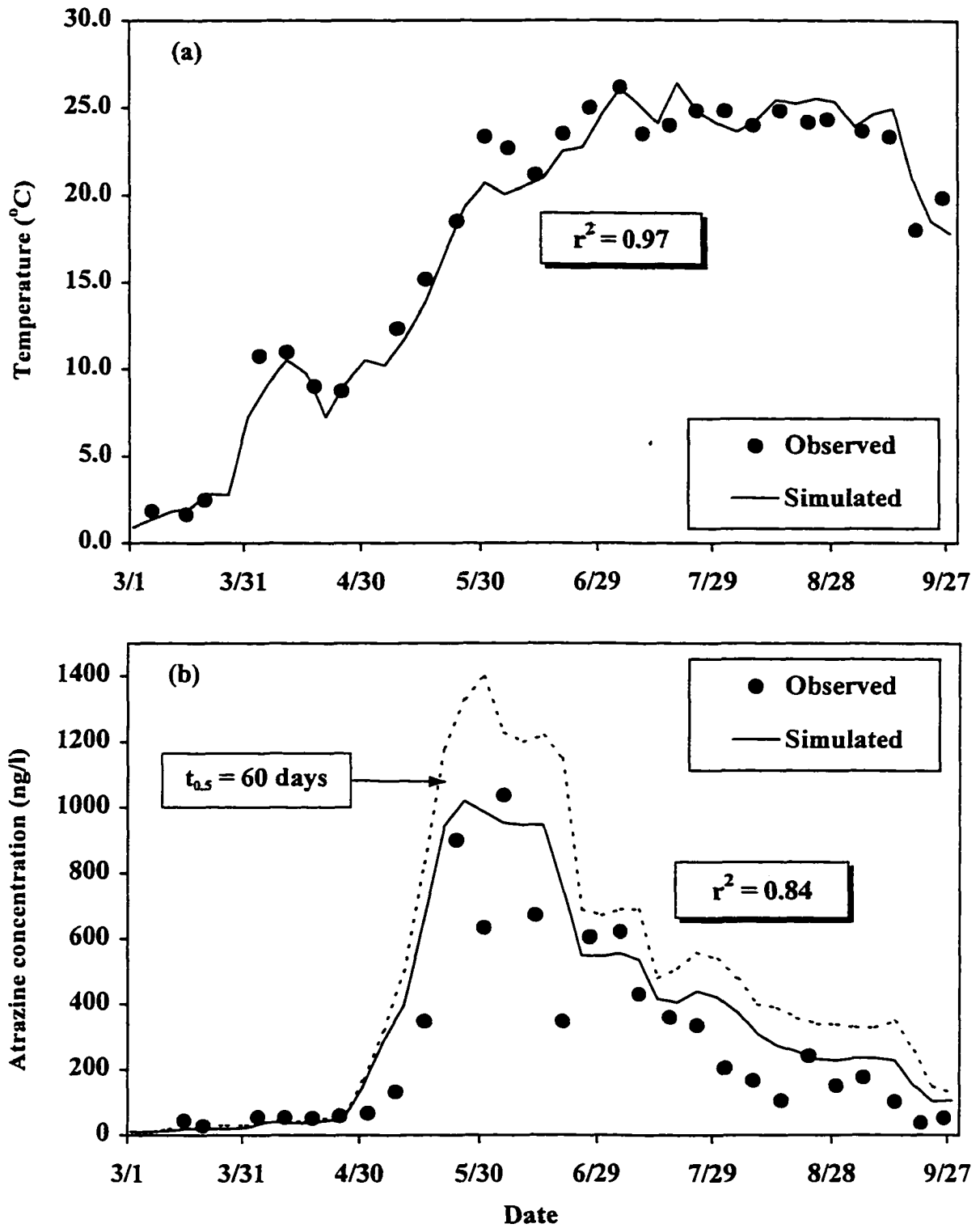


Figure 12. Observed and simulated depth-mean (a) water temperatures and (b) atrazine concentrations versus time in the reservoir.

variations of water temperatures and atrazine contamination levels in the reservoir. The results may be attributed to the accuracy of the estimated model inputs and the time-variable kinetic transformation rates of atrazine obtained in the previous study.

To address the important aspect of a site-specific and time-variable kinetic transformation rate of atrazine for modeling of the contaminant fate in surface water, the model results obtained with a constant half-life value, 60 days that is generally known for atrazine half-life, are also presented in Figure 12b for comparison. Overestimation of atrazine concentration associated with the assumption of steady atrazine persistence (half-life 60 days) became significant after April and maximized at the time of peak concentrations in early June. The simulated peak atrazine concentration was about 1400 ng/l at the end of May with the constant half-life, which is about 40% overestimation compare to the observed value and the simulated value with time-variable half-life (1000 ng/l). On the average, the assumption of steady atrazine persistence resulted in about 30% overestimation in the prediction of concentrations for the entire periods. This emphasizes that an accurate estimation of the kinetic transformation rate of atrazine for a specific aquatic environment should be made to obtain good model results. This is because the persistence of a toxic chemical in an aquatic system is quite different under different environmental conditions and during different seasons (i.e., temperature, sunlight, and microorganism) (Gladyshev and Gribovskaya 1994; Chung and Gu 1998).

Conclusions

The fate and transport processes of atrazine in the Saylorville Reservoir, Iowa were investigated using the observed and simulated seasonal flow circulation patterns, thermal structures, and spatial and temporal distributions of atrazine concentrations. The results of 2D reservoir toxic model revealed that the fate and transport of atrazine in the reservoir are strongly related to the seasonal circulation patterns, thermal structures, and environmental conditions of the reservoir as well as its physico-chemical properties. In general, no strong thermal stratification was noticed from both observed and simulated results. The effect of flow short circuiting on the transport of atrazine was notable during summer as less

mixing and corresponding higher concentrations occurred near the surface of the reservoir. The model accurately simulated the temporal variations of observed atrazine concentrations and captured the peak concentrations during the end of May and early June. The use of the site-specific and time-variable kinetic transformation rates of atrazine led to more accurate predictions of atrazine concentrations. The assumption of steady or constant atrazine transformation rate over the entire periods resulted in a 40% overestimation in predicting peak concentrations. Therefore, it is recommended that an accurate estimation of atrazine transformation rates in a specific aquatic environment or during a season should be performed before model application because the persistence of a toxic chemical is substantially affected by environmental conditions such as temperature, sunlight, and microbial concentrations during different seasons.

The Saylorville Reservoir and the watershed are typical in the Midwest of United States where tons of herbicides are applied in upstream watersheds farm lands for an intensive crop production. Therefore, the results presented here can provide a useful guide for reservoir water quality modeling and herbicides control in other reservoirs in the region or other agricultural areas. The methodology and model application processes employed in this study can also be used to investigate the fate of other commonly detected herbicides such as alachlor, cyanazine, and metolachlor. If field monitoring data are not available or sufficient in a reservoir, a watershed model is needed to generate the required input data. Unfortunately, most of the watershed-scale models are rarely validated and need further improvement for the simulation of transport and transformations of toxic substances. These are areas of research and investigation requiring further work to better understand the fate and transport processes of agricultural chemicals along the entire pathway of pollutants in overland flow, surface runoff, groundwater, and stream flow.

References

- Baumann, E. R., C. A. Beckert, M. K. Butler, D. M. Soballe. 1979. Water quality studies-EWQOS sampling Red Rock and Saylorville Reservoirs Des Moines River, Iowa. Engineering Research Institute, Iowa State University, Ames, Iowa.

- Bath, A. J., and T. D. Timm. 1994. Hydrodynamic simulation of water quality in reservoirs of South Africa. *Commission Internationale Des Grands Barrages*, Q.69 R. 39, 625-633.
- Chung, S. W., and R. Gu. 1998. Two-dimensional simulations of contaminant currents in a stratified reservoir. *J. Hydr. Engrg.*, ASCE, 124(7):704-711.
- Chung, S. W., and R. Gu. 1998. Two-dimensional modeling of the fate and transport of toxic substance in a reservoir.
- Chung, S. W., and R. Gu. 1998. Estimating time-variable kinetic transformation rate of atrazine in a reservoir.
- Cole, T. M., and E. M. Buchak. 1994. CE-QUAL-W2: A two-dimensional, laterally averaged, hydrodynamic and water quality model, version 2.0 user manual. Army Engineer Waterways Experiment Station, Vicksburg, Miss.
- Donigian, Jr. A. S., and W. C. Huber. 1991. Modeling of nonpoint source water quality in urban and non-urban areas. EPA/600/3-91/039. U.S. Environmental Protection Agency, Athens, GA.
- Gladyshev, M. I., and I. V. Gribovskaya. 1994. Phenol biodegradation in the Yenisei River and the Krasnoyarsk Reservoir, Russia. *Hydrologic, Chemical, and Biological Processes of Transformations and Transport of Contaminants in Aquatic Environments*. Ed. Norman, E. P., J. A. Rod, and V. T. Vladimir. IAHS Publication No. 219. pp217-221.
- Goolsby, D. A., E. M. Thurman and D. W. Kolpin. 1991. Herbicides in streams: Midwestern United States. *Irrigation and Drainage Proceedings 1991*, July 22-26, 1991 Honolulu, HI, pp17-23.
- Goolsby, D. A. and W. A. Battaglin. 1993. Occurrence, distribution, and transport of agricultural chemicals in surface waters of the Midwestern United States. *Selected Papers on Agricultural Chemicals in Water Resources of the Midcontinental United States*. U.S. Geological Survey. Denver, CO.
- Goolsby, D. A., W. A. Battaglin, J. D. Fallon, D. S. Aga, D. W. Kolpin, and E. M. Thurman. 1993. Persistence of herbicides in selected reservoirs in the Midwestern United States: Some preliminary results. *Selected Papers on Agricultural Chemicals in Water Resources of the Midcontinental United States*. U.S. Geological Survey. Denver, CO.
- Goolsby, D. A., E. M. Thurman, M. L. Pomes, M. Meyer, and W. A. Battaglin. 1993. Occurrence, deposition, and long range transport of herbicides in precipitation in the Midwestern and Northeastern United States. *Selected Papers on Agricultural Chemicals*
-

- in Water Resources of the Midcontinental United States*. U.S. Geological Survey. Denver, CO.
- Gordon, J. A. 1980. An evaluation of the LARM two-dimensional model for water quality management purposes. In Proceedings of the Symposium on Surface-Water Impoundment, ASCE, H. G. Stefan, ed., Minneapolis, Minnesota, June 2-5, 1980, Vol. 1, pp. 518-527.
- Hatfield, J. L., C. K. Wesley, J. H. Prueger, and R. L. Pfeiffer. 1996. Herbicide and nitrate distribution in central Iowa rainfall. *J. Environ. Qual.* 25:259-264.
- Hallberg, G. R. 1996. Water quality and watersheds: an Iowa perspective. In Proceedings of the Agriculture and Environment -Building Local Partnerships-. Iowa State University, Ames, IA.
- Harmon, L. and E. R. Duncan. 1978. A technical assessment of nonpoint pollution in Iowa. Iowa State University, Ames, Iowa.
- Iowa Department of Environmental Quality. 1976. Water quality management plan. Des Moines River Basin. Iowa Dept. Environ. Qual., Des Moines, Iowa.
- Johnson, H. P. and J. L. Baker. 1982. Field-to-stream transport of agricultural chemicals and sediment in an Iowa watershed. EPA-600/3-83-032. U.S. Environmental Protection Agency, Athens, Georgia.
- Kim, B. R., J. M. Higgins, and D. J. Bruggink. 1983. Reservoir circulation pattern and water quality. *J. of Environ. Engrg.*, ASCE, 109(6):1284-1294.
- Kolpin, D. W. and S. J. Kalkhoff. 1993. Atrazine degradation in a small stream in Iowa. *Environ. Sci. Technol.*, 27(1):134-139.
- Leung, Siu-Yin. 1979. The effect of impounding a river on the pesticide concentration in warmwater fish. Ph.D. dissertation. Iowa State University, Ames, IA.
- Liu, H. 1977. Predicting dispersion coefficient of streams. *J. of Envir. Engrg.*, ASCE, 103 EE1:59-69.
- Lutz, D. S. and A. Cavendar. 1997. Water Quality Studies--Red Rock and Saylorville Reservoirs Des Moines River, Iowa. Iowa State University, Ames, IA.
- Mackay, D. 1982. Volatilization of organic pollutants from water. EPA/600/3-82/019, Athens, GA.
-

- Martin, J. L. 1988. Application of two-dimensional water quality model., *J. of Envir. Engrg.*, ASCE, 114(2), 317-336.
- Nations, B. K. and G. R. Hallberg. 1992. Pesticides in Iowa precipitation. *J. Environ. Qual.* 21:486-492.
- Naylor, L. M. 1975. A statistical study of the variations in Des Moines River water quality. Ph.D. dissertation, Iowa State University, Ames, IA.
- Paterson, K. G. and J. L. Schnoor. 1992. Fate of alachlor and atrazine in a riparian zone field site. *Water Environ. Res.*, 63(3):274-283.
- Pereira, W. E., and F. D. Hostettler. 1993. Nonpoint source contamination of the Mississippi River and its tributaries by herbicides. *Environ. Sci. Technol.*, 27:1542-1552.
- Pugh, K. C. 1994. Toxicity and physical properties of atrazine and its degradation products; A literature survey. Waste Management and Remediation Environmental Research Center, Muscle Shoals, Alabama.
- Rice, P. J. 1996. The persistence, degradation, and mobility of metolachlor in soil and the fate of metolachlor and atrazine in surface water, surface water/sediment, and surface water/aquatic plant systems. Ph.D. dissertation, Iowa State University, Ames, IA.
- Richards, R. P., D. B. Baker, B. R. Christensen, and D. P. Tierney. 1995. Atrazine Exposures through drinking water: Exposure assessments for Ohio, Illinois, and Iowa. *Environ. Sci. Technol.* 29:406-412.
- Thomann, R. V. and J. A. Mueller. 1987. Principles of surface water quality modeling and control. HarperColinsPublishers Inc., New York, NY.
- Thurman, E. M., D. A. Goolsby, M. T. Meyer and D. W. Kolpin. 1991. Herbicides in surface waters of the Midwestern United States: The effect of spring flush. *Environ. Sci. Technol.* 25:1794-1796.
- U.S. Army Corps of Engineers, Rock Island District. 1983. Upper Mississippi River Basin Des Moines River, Iowa and Minnesota Master Reservoir Regulation Manual.
- U.S. Geological Survey. 1978. Water Resources Data for Iowa
- Wilson, L. J. 1987 Iowa groundwater protection strategy, Environ. Protection Comm., Iowa Dep. Nat. Resour., Des Moines, Iowa.
-

Whitman, R. G. 1923. A preliminary experimental confirmation of the two-film theory of gas absorption. *Chem. Metallurg. Eng.* 29:146-148.

Wurbs, R. A. 1995. Water management models: A guide to software. Prentice Hall, Inc. Englewood Cliffs, NJ.

Notations

The following symbols are used in this paper:

- β = the fraction of solar radiation absorbed in surface layer;
- ε = the light extinction coefficient for pure water;
- ϕ = the porosity of the bed sediment;
- Φ_{NPS} = the mass flow rate per unit volume via runoff and drainage flow ($\text{g}/\text{m}^3/\text{sec}$);
- A_x = longitudinal eddy viscosity (m^2/s);
- B = waterbody width (m);
- C_a = the vapor phase concentration of atrazine (g/m^3);
- C_d = the concentration of atrazine in the distributed load (mg/m^3);
- $C_{p,w}$ = the particulate concentration of atrazine in the water column (g/m^3);
- C_{SS} = the suspended solids concentration (kg/m^3);
- $C_{t,b}$ = the total concentration of atrazine in the bed sediment (g/m^3);
- $C_{t,w}$ = the total concentration of atrazine in the water column (g/m^3);
- D_x = longitudinal eddy diffusivity (m^2/s);
- D_z = vertical eddy diffusivity (m^2/s);
- f_1 = fraction of corn and soybean cropping area in the drainage area;
- f_2 = fraction of corn cropping area in f_1 ;
- f_3 = fraction of atrazine applied area in f_2 ;
- f_4 = fraction of A_p which delivered to surface water;
- f_d = fraction of dissolved form of chemical to total chemical;
- f_p = fraction of particulate form of chemical to total chemical;
- H = Henry's law constant ($\text{atm}\cdot\text{m}^3/\text{mol}$);
- K_d = the first-order transformation rate of atrazine;

K_f	=	diffusive exchange rate between water and pore water of the bed (m/day);
K_g	=	the gas film coefficient;
k_l	=	overall volatilization transfer rate (m/day);
K_l	=	the liquid film coefficient;
K_p	=	the partition coefficient of atrazine (l/kg);
MCL	=	the maximum contamination level ($\mu\text{g/l}$);
M_d	=	direct atrazine mass loading via surface runoff and seepage flows (kg/day);
Q_d	=	estimated distributed runoff and seepage flows (m^3/day);
r	=	the concentration of atrazine expressed on a dry weight solids basis (mg/kg);
s_i	=	fraction of direct annual mass load occurring in month i ;
t	=	time;
T_w	=	the water temperature ($^{\circ}\text{C}$);
U	=	longitudinal flow velocities (m/sec);
v_s	=	the net settling velocity of sorbed chemical (m/sec);
W	=	vertical flow velocities (m/sec);
x	=	longitudinal Cartesian coordinate (positive to the right);
y	=	the depth of water from reservoir bottom (m).; and
z	=	the depth of water from water surface (m).

CHAPTER 5. VALIDATION OF EPIC FOR TWO WATERSHEDS IN SOUTHWEST IOWA

A paper submitted to the Journal of Environmental Quality

S. W. Chung, P. W. Gassman, L. A. Kramer, J. R. Williams, and R. Gu

Abstract

The Erosion Productivity Impact Calculator (EPIC) model was evaluated using long-term data collected for two Southwest Iowa watersheds in the Deep Loess Soil Region, which have been cropped in continuous corn (*Zea Mays L.*) under two different tillage systems (conventional tillage versus ridge-till). The annual hydrologic balance was calibrated for both watersheds during 1988-94 by adjusting the runoff curve numbers and residue effects on soil evaporation. Model validation was performed for 1976-87, using various statistical tests. The errors between the 12-year predicted and observed means or medians were less than 10% for nearly all of the hydrologic and environmental indicators, with the major exception of a nearly 44% over prediction of the N surface runoff loss for Watershed 2. The predicted N leaching rates, N losses in surface runoff, and sediment loss for the two watersheds clearly showed that EPIC was able to simulate the long-term impacts of tillage and residue cover on these processes. However, results also revealed weaknesses in the model's ability to replicate year-to-year variability, with r^2 values generally below 50% and relatively weak goodness-of-fit statistics for some processes. This was due in part to simulating the watersheds in a homogeneous manner, which ignored complexities such as slope variation. Overall, EPIC was able to replicate the long-term relative differences between the two tillage systems and that the model is a useful tool for simulating different tillage systems in the region.

Introduction

Agricultural decision makers are encountering increasingly complex challenges in ensuring a stable and cost-efficient food supply. These challenges are multi-faceted, often requiring that management and policy alternatives be considered both for potential economic

and environmental impacts. For instance, an agricultural policy change that results in crop production shifts can also trigger questions concerning the corresponding water quality and soil erosion effects. Field and monitoring studies provide essential data and critical answers for many of these types of questions. However, field studies are prohibitively costly to perform across all possible landscape, weather, management, and cropping system combinations, especially for large agricultural regions. Also, monitoring of water quality, soil erosion, and/or other environmental indicators only captures baseline conditions, and will not provide projections of future impacts that result from current policy decisions.

For these reasons, increasing applications of integrated modeling systems are being made that provide economic and environmental outcomes in response to alternative management systems and/or agricultural policies. Integrated modeling systems range from farm-level (Foltz et al. 1993; Taylor et al. 1992; Wossink et al. 1992), to watershed (Bouzaher et al. 1990; Lakshminarayan et al. 1991), and ultimately to regional (Bernardo et al. 1993; Bouzaher et al. 1995; Lakshminarayan et al. 1996) applications. In each of these systems, functions and/or models are incorporated to predict environmental indicators for different combinations of landscape, soil, management, and climate conditions.

The Erosion Productivity Impact Calculator (EPIC) model (Williams 1990; Williams 1995) has been adapted within several integrated modeling systems, because of its flexibility in handling a wide array of crop rotations, management systems, and environmental conditions. Originally, EPIC was designed to simulate the impacts of erosion on soil productivity (Williams et al. 1984). Current versions of EPIC can also produce indicators such as nutrient loss from fertilizer and animal manure applications (Edwards et al. 1994; Phillips et al. 1993), climate change impacts on crop yield and soil erosion (Favis-Mortlock 1991; Stockle et al. 1992; Williams et al. 1996), losses from field applications of pesticides (Williams et al. 1992), and soil carbon sequestration as a function of cropping and management systems (Mitchell et al. 1998).

The flexibility of EPIC has led to its adoption within the Resource and Agricultural Policy System (RAPS), an integrated modeling system designed to project shifts in production practices (crop rotations, tillage levels, and conservation practices) and evaluate

the resulting environmental impacts, in response to agricultural policies implemented for the North Central United States (Babcock et al. 1997). The focus of the EPIC applications within RAPS is to provide nitrogen loss and soil erosion (both wind and water) indicators in response to variations in crop rotation, tillage, soil, fertilizer applications, and environmental conditions. Although EPIC has proven to be a robust tool within RAPS, there is an ongoing need to test the model with as much site-specific data as possible, to further improve its prediction capabilities. To date, limited validation studies of EPIC with field data have been performed in the RAPS study region; thus, testing of EPIC with site-specific data has been incorporated as a component within RAPS.

The goal of this study is to test EPIC version 5300 (EPIC5300) using long-term data sets collected by the U.S. Department of Agriculture – Agricultural Research Service (USDA-ARS) at two field-sized watersheds denoted as Watersheds 2 and 3 located in southwestern Iowa (Kramer et al. 1989; Kramer and Hjelmfelt 1989; Kramer et al. 1990). These watersheds are representative of the 2.2 million ha Deep Loess Soil Major Land Resource Area (MLRA 107) that covers much of western Iowa and northwestern Missouri. Water balance, sediment, and nutrient loss data have been collected from both watersheds, which have been cropped with continuous corn (*Zea Mays L.*) and managed with contrasting tillage systems (conventional versus ridge tillage) for at least two decades.

The effect of conservation tillage systems relative to conventional tillage systems on water balance, nutrient transport, soil loss, and crop yield can range from slight to substantial (Singh and Kanwar 1995; Phillips et. al 1980; Christensen and Norris 1983; Steiner 1989). At Treynor, Kramer et. al (1989) reported reduced surface runoff, increased seepage flow, and increased leached nitrogen for the Watershed 3 ridge-till system relative to the conventional tillage system used for Watershed 2. Kramer and Hjelmfelt (1989) also found that the ridge-till system greatly reduced soil erosion during storms of high erosion potential compared to the conventional tillage system.

The objectives of this research are to confirm that EPIC5300 can replicate the impacts of the two different tillage systems by: (1) calibrating the model using observed water balance data for the period 1988-94; and (2) validating the simulated water balance, nutrient

loss, and crop yields using measured data for 1976 through 1987. Estimates of soil erosion are also reported; however, these could not be compared directly with measured data. Summary statistics and graphical comparisons are the primary tools used to assess model validity; parametric and nonparametric statistical tests are also used within the validation step.

Materials and Methods

Watershed Description

Watersheds 2 and 3 cover 34.4 and 43.3 ha over rolling topography defined by gently sloping ridges, steep side slopes, and alluvial valleys with incised channels that normally end at an active gully head, typical of the deep loess soil in MLRA 107 (Kramer et al. 1990). Slopes usually range from 2-4 % on the ridges and valleys and 12-16 % on the side slopes. An average slope of about 8.4 % was estimated for both watersheds, using first-order soil survey maps. The major soil types are well-drained Typic Hapludolls, Typic Udorthents, and Cumulic Hapludolls (Marshall-Monona-Ida and Napier series), classified as fine-silty, mixed, mesics. The surface soils consist of silt loam and silty clay loam textures that are very erosion prone, requiring suitable conservation practices to prevent serious gully and sheet-rill erosion.

The regional geology is characterized by a thick layer of loess overlying glacial till, that together overlay bedrock. The loess thickness ranges from 3 m in the valleys to 27 m on the ridges. Seepage flow continuously discharges into the valley gully channels from a saturated zone located at the loess-till interface, due to the much greater permeability of the loess. Stream flow at each watershed outlet, consisting of the perennial seepage flow and surface runoff during storm events, was continuously recorded with instrumented broad crested V-notch weirs. Precipitation was measured with three Universal recording rain gauges placed on each of the watershed boundaries.

Watershed 2, cropped with continuous corn, has been consistently managed with conventional tillage on the approximate contour from 1964 through the study period. The conventional tillage system consisted of moldboard plowing or heavy tandem disking around

mid-April to incorporate corn stalk residues, followed by shallower tandem disking or field cultivation about two weeks later to complete seedbed preparation. One or two cultivations were performed during the growing season for weed control. An average annual equivalent mineral nitrogen (N) application rate of 185 kg/ha was applied to Watershed 2 during 1976-94, the period used for the simulation study.

Watershed 3 was originally managed as bromegrass pasture from 1964 to 1971 and was converted in 1972 to a continuous corn ridge-till plant system consisting of an early May planting with a 4-row Buffalo till planter in the corn residue on the approximate contour. One or two cultivations with a 4-row Buffalo cultivator were performed to control weeds and to construct ridges along the corn rows. The average annual N application rate at Watershed 3 was 169 kg/ha during 1976-94 (1972-75 data were assumed to represent a land use transition and were considered nonrepresentative of the ridge-till system). The average Watershed 3 residue coverage was estimated to be about 60%.

Simulation Methodology and Input Data

The EPIC model can be subdivided into nine separate components (Williams 1990) defined as weather, hydrology, erosion, nutrients, soil temperature, plant growth, plant environment control, tillage, and budgets (Williams 1990). It is a field-scale model, designed to simulate drainage areas of up to 100 ha (Williams et al. 1996) that are characterized by homogeneous weather, soil, landscape, crop rotation, and management system parameters. It operates on a continuous basis using a daily time step and can perform long-term simulations of hundreds of years. More detailed discussions of EPIC are given in Williams (1990) and Williams (1995).

The average slope of 8.4% was assumed for both watersheds, to satisfy the requirement of homogeneity. The dominant soil type, Monona, was also assumed representative of both watersheds for the EPIC simulations. Up to 20 soil layer parameters can be input into EPIC; required values include layer depth, bulk density, wilting point, field capacity, percentage sand, percentage silt, pH, and percentage organic carbon. Table 1 lists the layer data for the 1.8 m Monona soil profile. This data was primarily obtained from the USDA (USDA. 1991. Primary characterization data, project 81P 92, Pottawattamie County-Treynor Exp. Station.

Table 1. Properties by layer for the Monona soil.

Property	Soil layer								
	1	2	3	4	5	6	7	8	9
Depth (m)	.01	0.05	0.20	0.35	0.50	0.85	1.10	1.55	1.80
BD (Mg/m ³)	1.08 ^a (0.87) ^b	1.08 (0.87)	1.25	1.38	1.26	1.28	1.35	1.41	1.44
WP ^c (m ³ /m ³)	0.13	0.13	0.13	0.13	0.12	0.12	0.11	0.11	0.12
FC ^d (m ³ /m ³)	0.25	0.25	0.25	0.26	0.26	0.26	0.28	0.27	0.28
Sand (%)	4.3	4.3	4.1	3.7	5.1	5.4	6.1	6.3	6.4
Silt (%)	68.7	68.7	68.3	68.9	70.2	70.3	73.0	71.4	73.5
Soil pH	5.5	5.5	5.5	7.3	7.4	7.6	8.0	8.0	8.0
Org. C (%)	1.97	1.97	1.21	0.68	0.38	0.30	0.24	0.17	0.16

^aBulk density for Watershed 2 under conventional tillage system.

^bA Bulk density for Watershed 3 under ridge tillage system.

^cWilting point.

^dField capacity.

U.S. Dept. Agric., Soil Conser. Ser., National Soil Survey Lab., Lincoln, NE). Bulk density inputs for the upper 20 cm are mean values measured by Kramer and Grossman (1992) during the spring season between 1979 and 1991 (no measurements were made in 1988-89). The surface layer pH values (top 20 cm) were based on measurements made in Watersheds 2 and 3 in 1989 and 1995 (Kramer 1995, USDA-ARS, National Soil Tilth Laboratory, Deep Loess Research Station, Council Bluffs, Iowa). These low pH values resulted from little or no liming inputs over several years. The pH values for the remainder of the profile were obtained from Monona soil data included in the EPIC soil database (Mitchell et al. 1996).

EPIC is driven by observed and/or simulated daily climatic inputs that include total precipitation, maximum and minimum air temperature, total solar radiation, average relative humidity, and average wind speed. Measured precipitation and temperature values were input for the 19-year simulation period. The remaining climatic inputs were generated using monthly weather statistics for Oakland, Iowa, located approximately 25 km northeast of the watersheds, the nearest climatic station available in the EPIC weather generator parameter database. The average annual precipitation levels were 824 and 802 mm at Watersheds 2 and 3 during 1976-94, reflecting the variability in rainfall patterns and amounts that occur within the 3 km distance between the two watersheds.

Simulation of tillage, planting, fertilizer, and harvest passes were performed on the dates recorded for each year. A single date was assumed for operations that spanned several days. The simulated amounts and forms of N fertilizer were varied annually according to records for both watersheds. Total amounts of N applied ranged from 166 to 237 kg/ha and 160 to 190 kg/ha for Watersheds 2 and 3 during the 1976-87 validation period (N applications were also simulated during the calibration period). For Watershed 2, 90% of the applied N was simulated as anhydrous ammonia injected 20 cm deep and the remaining portion was surface-applied. The majority of N used on Watershed 3 was assumed surface-applied; simulation of anhydrous ammonia was also performed for a portion of the total N application during 1976-78. Tillage passes simulated in EPIC directly affect soil bulk density and residue cover levels. Reduced tillage will result in higher amounts of simulated residue cover and thus lower erosion losses. However, the impact of tillage on the

hydrologic balance has to be indirectly simulated by adjusting curve numbers. Simulation of constructed ridges for Watershed 3 was not feasible in EPIC and thus a no-till planter was assumed representative of the Buffalo till planter.

Calibration Process

The EPIC calibration process focused primarily on the infiltration and runoff partition at the soil surface and the effects of soil residue on the soil evaporation portion of evapotranspiration (ET). The 1988-94 time frame was chosen as the calibration period because it included the driest (just over 400 mm in 1988) and wettest (over 1300 mm in 1993) years in the entire 19-year precipitation record, allowing the remaining 12-year period (1976-87) to be used for validation. Calibration of nutrient and sediment losses, and crop yield, were not performed because (1) data were not available for some of these indicators over all of the calibration period, and (2) these indicators are a direct function of the hydrologic balance.

Comparisons between EPIC output and measured seepage flows was difficult, because leaching was only simulated to a 1.8 m depth in EPIC. An approximate comparison approach was used, in which the combined EPIC leaching and lateral subsurface flow output were assumed to be equal to the measured seepage flows in the gully channels. However, correlation analyses performed for 1976-94 between the measured annual precipitation and seepage flows showed r^2 values of 0.15 and 0.50 for Watersheds 2 and 3. This indicates that a lag-time greater than one year exists before much of the infiltrated precipitation discharges from the gullies, especially for Watershed 2. Thus, comparing measured seepage flows with EPIC predictions has limited meaning on an annual basis.

The USDA Soil Conservation Service (SCS) runoff curve number method (Mockus 1972) is used to partition precipitation between infiltration and runoff volume in EPIC, with modifications incorporated for slope and soil profile water distribution effects as described by Williams (1995). The effect of frozen soil on surface runoff is also simulated. Standard runoff curve numbers (CN2) have been tabulated for different hydrologic soil-cover complexes and antecedent moisture condition 2 (average moisture conditions for the preceding five day period) as given in Mockus (1969). These CN2 values represent

conventional tillage practices and need to be reduced to reflect the impacts of conservation tillage (Rawls et al. 1980; Rawls and Richardson 1983). Thus, a key calibration step for the EPIC simulations was the adjustment of the curve number for Watershed 3 to reflect the effects of surface residue and ridges, as described in the calibration results section.

Adjustment of residue impacts on the soil evaporation portion of ET was also performed in the calibration phase. "Measured ET" was inferred for both watersheds by using an annual water balance equation in which ET was set equal to precipitation minus surface runoff and seepage flow, assuming steady state soil water storage changes ($dS/dt=0$) from year to year. Field measurements of surface runoff and seepage flow over 1976-94 indicated that less ET occurred from Watershed 3 relative to Watershed 2, implying that the greater residue cover on Watershed 3 led to more infiltration and seepage flow, and conversely less ET. Phillips et al. (1980) reported a similar response for a four-year study in central Kentucky, where ET rates under conventionally-tilled continuous corn averaged 85 mm per year (20%) more than that for no-tilled continuous corn.

EPIC computes soil water evaporation and plant transpiration separately by an approach similar to that of Ritchie (1972). The depth distributed estimate of soil water evaporation may be reduced according to the following equation if soil water is limited in a layer

$$SEV_l^* = SEV_l \exp\left(\frac{parm(12)(SW_l - FC_l)}{FC_l - WP_l}\right), \quad SW_l < FC_l \quad (1)$$

$$SEV_l^* = SEV_l, \quad SW_l \geq FC_l \quad (2)$$

where SEV_l is the potential soil evaporation for layer l (mm), SEV^* is the adjusted soil water evaporation (mm), SW is the soil water content for layer l (mm), FC is the field capacity (mm), and WP is the wilting point (mm). $Parm(12)$ is a parameter that governs the rate of soil evaporation from upper 0.2 m of soil as a function of residue cover. The effect of the Watershed 3 residue cover on soil water evaporation was simulated by adjusting $parm(12)$, as discussed in the calibration results section.

A final calibration step was the selection of the minimum C factor values for simulating water erosion with the Universal Soil Loss Equation (USLE) option (Wischmeier and Smith 1978) in EPIC. The C-factor measures the combined crop and residue cover effects upon soil erosion for a given management system, relative to the corresponding soil loss that would occur for the same landscape under conditions of clean-tilled continuous fallow (Wischmeier and Smith 1978). For this study, the appropriate C-factors of 0.2 for Watershed 2 and 0.023 for Watershed 3 were chosen on the basis of model documentation and guideline of Natural Resources and Conservation Service (NRCS 1990) rather than actual calibration.

Slope lengths of 81.4 and 79.4 m were simulated for Watersheds 2 and 3, which were derived from topographic maps for a previous set of USLE calculations (USDA-ARS, unpublished data, Deep Loess Research Station, Treynor, Iowa). These slope lengths represent the cropped portions of the watersheds that include the upland ridges and sideslope areas. The EPIC USLE simulations provided estimates of sediment loss to the bottom of these slopes, using the assumed average gradient of 8.4% for each watershed. These USLE estimates could not be directly compared with the measured soil erosion levels at the gully headcuts, because sediment movement from the steeper sideslopes to the gully headcuts must be estimated by applying sediment delivery theory. However, the USLE estimates do provide an indication of the model's ability to replicate tillage and residue impacts on erosion.

Model Evaluation Methods

Summary statistics and goodness-of-fit measures were selected to evaluate the model performance, following suggestions given by Loague and Green (1991) and Zacharias et al. (1996) for normally and non-normally distributed parameters. The summary statistics for the normally distributed variables include long-term means, standard deviations, the percentage error (E), and the coefficient of determination (r^2). The median and median absolute deviation (MAD) were used for the non-normally distributed variables instead of the mean and standard deviation. The MAD is expressed as:

$$MAD = 1.4826 \times \text{median} \{|x_i - x_m|: i = 1, 2, \dots, n\} \quad (3)$$

where x_i is the i^{th} observation, x_m is the sample median, and n is the sample size. These summary statistics, along with graphical illustrations, were the primary means of comparison between model output and field measurements.

Goodness-of-fit measures were used to further assess the difference between the predicted and observed values (residual errors analysis). Statistical tests were performed with SAS (SAS Inst. Inc. 1989) to assess whether the measured data (annual totals over 1976-94) were normally or non-normally distributed and thus determine the appropriate statistical measures (Table 2). All the hydrologic variables were identified as being normally distributed at a significance level of $\alpha = 0.1$. However, the tests indicated that nitrate losses via leaching and runoff, soil erosion, and crop yield were distributed in a non-normal fashion.

Goodness-of-fit tests selected for evaluating the normally distributed indicators include the normalized root mean square error (RMSE), modeling efficiency (EF), and coefficient of residual mass (CRM):

$$RMSE = \left[\sum_{i=1}^n (P_i - O_i)^2 / n \right]^{0.5} \cdot \frac{100}{O_m} \quad (4)$$

$$EF = \left(\sum_{i=1}^n (O_i - O_m)^2 - \sum_{i=1}^n (P_i - O_i)^2 \right) / \sum_{i=1}^n (O_i - O_m)^2 \quad (5)$$

$$CRM = \left(\sum_{i=1}^n O_i - \sum_{i=1}^n P_i \right) / \sum_{i=1}^n O_i \quad (6)$$

where O_i and P_i are the observed and predicted values at each comparison point i , n is the number of observed and predicted values that are being compared, and O_m is the mean or median of the observed values. In contrast, the normalized median absolute error (MdAE) and robust modeling efficiency (REF) are used to evaluate the goodness-of-fit of the non-normally distributed variables:

$$MdAE = \text{median} \{ |O_i - P_i| : i = 1, 2, \dots, n \} \times \left(\frac{100}{O_m} \right) \quad (7)$$

Table 2. Results of the univariate normality test for the observed annual hydrologic and environmental state variables.

State Variables	n ^a	P-value		Averaged	Normality ^b
		Watershed 2	Watershed 3	P-value	
Precipitation	19	0.9772	0.9521	0.9647	Normal
Surface runoff	19	0.3298	0.0431	0.1865	Normal
Seepage flow	19	0.0286	0.2146	0.1216	Normal
ET	19	0.7676	0.1975	0.4826	Normal
NO ₃ -N leaching	15	0.0056	0.1025	0.0541	non-normal
NO ₃ -N runoff	15	0.0001	0.0001	0.0001	non-normal
Soil erosion	17	0.0001	0.0001	0.0001	non-normal
Crop yield	19	0.0001	0.0001	0.0001	non-normal

^an is the number of years.

^bA normality test was used to test the null hypothesis H_0 : Normal distribution, vs. the alternative hypothesis H_A : Non-normal distribution with level of significance, $\alpha=0.1$.

$$REF = median\left[\frac{median\{|O_i - O_m|:i = 1,2,\dots,n\} - median\{|O_i - P_i|:i = 1,2,\dots,n\}}{median\{|O_i - O_m|:i = 1,2,\dots,n\}}\right] \quad (8)$$

The RMSE and MdAE are basically the overall difference in the sum of squares normalized to the number of observations. The desired value is zero for the RMSE, MdAE, and CRM, and one for the EF and REF. Negative values can result for the EF, CRM, and REF measures. Negative values for the CRM indicate model overprediction while positive CRM values point to a trend in underpredicting the observed data. Negative EF and REF values suggest that it is better to use the observed mean than the model predictions.

Explicit standards for model evaluation using these statistics are not established, partly because the judgment of model results is highly dependent on the purpose of the model application. Clouse and Heatwole (1996) further state that “no guidelines for rating model performance based on these statistics have been established, therefore they are primarily useful in assessing which modeling scenarios are predicted better than other scenarios”. They simply evaluated the goodness-of-fit statistics in terms of how close they were to the optimum values. A similar approach was used by Penell et al. (1990) who compared output from several pesticide leaching models. However, Ramanarayan et al. (1997) took a different approach by setting definitive criterion for several statistics including 0.5 for r .

For this study, the following criteria were set to assess if the model results were satisfactory: RMSE and MdAE < 50%, EF and REF > 0.3, and $-0.2 < CRM < +0.2$. Standards of < 20% for E and > 0.5 for r^2 were also set, which have optimum values of zero and one. These standards provide a useful guideline to indicate when the model predictions are deviating greatly from the observed values.

Results and Discussion

Model Calibration

To simulate the differences between these two tillage systems, the CN2 and parm(12) values were calibrated in EPIC using annual surface runoff, seepage flow, and ET levels

observed from 1988 to 1994. The CN2 and parm (12) values were adjusted until the percentage error between the observed and simulated average values were less than 5 %. Table 3 shows the calibrated parameter values for the CN2 and parm (12). The calibration process for Watershed 2 resulted in a CN2 value of 74, a slight reduction from the standard value of 75 (Mockus 1969). The Watershed 2 calibration also resulted in a parm(12) value of 4.0, a slight increase over the EPIC default value of 2.5.

The Watershed 3 calibration resulted in a curve number of 61, which is a reduction of about 19% from the standard value of 75. Rawls et al. (1980) analyzed surface runoff data from small watershed and plot areas managed under different tillage systems, to determine appropriate CN2 adjustments for different residue coverage levels. They showed a maximum CN2 reduction of 10% would occur for conservation tillage systems leaving greater than 60% residue cover. Rawls (Rawls, W.J. 1997. Personal communication, U.S. Dep. Agric., Agric. Res. Ser., Beltsville, MD) confirmed that an even greater CN2 reduction could be expected with ridge tillage, due to the “mini-terracing” effects of the ridges. A parm(12) value of 14 was selected based on the Watershed 3 ET calibration, reflecting the effect of greater residue cover on ET.

Table 3. Model parameters for conventional and ridge till systems in Treynor, IA.

Parameters	Watershed 2 (CT) ^a	Watershed 3 (RT) ^b
CN2	74	61
Parm (12)	4.0	14

^aConventional tillage system.

^bRidge tillage system.

Table 4 shows the summary statistics of observed and simulated hydrologic variables after calibration. The percentage errors between the simulated and observed average surface runoff, seepage flow, and ET levels were all less than 5%. The majority of the variability between years was also captured by EPIC (average $r^2 = 0.75$). However, the weak r^2 for the

Table 4. Observed and simulated annual hydrologic variable summary statistics for the 1988-1994 calibration period.

Watershed	Variables	<u>Observed</u>		<u>Simulated</u>		E ^a	r ²
		Mean	Std. Dev.	Mean	Std. Dev		
		mm					
2	Surface runoff	51.7	66.9	53.2	40.3	+2.8	0.92
	Seepage flow	155.2	123.1	148.9	200.5	-4.2	0.42
	ET	583.1	200.9	581.2	39.8	-0.3	0.76
3	Surface runoff	32.5	48.8	32.0	31.4	-1.7	0.83
	Seepage flow	210.3	125.5	214.0	213.9	+1.8	0.74
	ET	541.3	159.4	538.1	36.1	-0.6	0.83

^aPercent error = (simulated-observed)/observed × 100.

Watershed 2 seepage flow underscores the problem of comparing EPIC output with the measured seepage flow, due to the previously discussed lag-time issue. This comparison difficulty is further confirmed by the much greater seepage flow standard deviations predicted by EPIC, as compared to the observed values. The large discrepancy between the simulated and observed ET standard deviations indicate that the steady state assumption for soil water storage is valid over the long-term but does not hold on an annual basis. Apparently, excess soil moisture is stored in the unsaturated and saturated zones below the root zone during wetter periods and then discharged during drier periods, which violates the assumption of $dS/dt = 0$ on an annual basis.

Model Validation

The calibrated model was validated against a second set of observed data for 1976-87 that included annual surface runoff, seepage flow, ET, nitrate-nitrogen (NO₃-N) losses via leaching and runoff, soil erosion, and crop yield. Short- and long-term predictions for each indicator were validated by comparing both annual and 12-year average estimates with field data.

Water balance

The summary statistics of observed and simulated 12-year average hydrologic variables are compared in Table 5. The statistics indicate that predicted mean surface runoff, seepage flow, and ET are in good agreement with observed values for both watersheds. The percent error of each estimated indicator is within 5% of the corresponding observed level, except

Table 5. Observed and simulated annual hydrologic variable summary statistics for the 1976-1987 validation period.

Watershed	Variables	Observed		Simulated		E ^a	r ²
		Mean	Std. Dev.	Mean	Std. Dev.		
		----- mm -----					
2	Surface runoff	74.4	39.3	76.0	39.3	+2.1	0.62
	Seepage flow	141.6	57.4	155.7	82.8	+10.0	0.37
	ET	627.6	144.9	612.0	35.4	-2.5	0.69
3	Surface runoff	40.0	23.7	40.1	21.7	+0.2	0.59
	Seepage flow	218.8	82.2	211.7	93.1	-3.2	0.48
	ET	553.7	100.2	560.9	35.9	+1.3	0.44

^aPercent error = (simulated-observed)/observed × 100.

for the Watershed 2 mean seepage flow. Data analysis of Watershed 2 has revealed that the seepage flow component of the overall runoff has increased during the later part of the study period, for unexplained reasons. Thus, a calibration performed for 1988-94 can be expected to result in overprediction of the seepage flow in earlier years. The large difference between the simulated and observed ET standard deviation values again reveals the weakness of the steady state soil water storage assumption. The r² values are generally satisfactory, with the weakest explanatory power for the Watershed 2 seepage flow and Watershed 3 ET levels.

Annual time series of observed precipitation, runoff, and seepage flow, and simulated surface runoff and seepage flows are plotted in Figures 1.a. and 1.b. In most years, EPIC

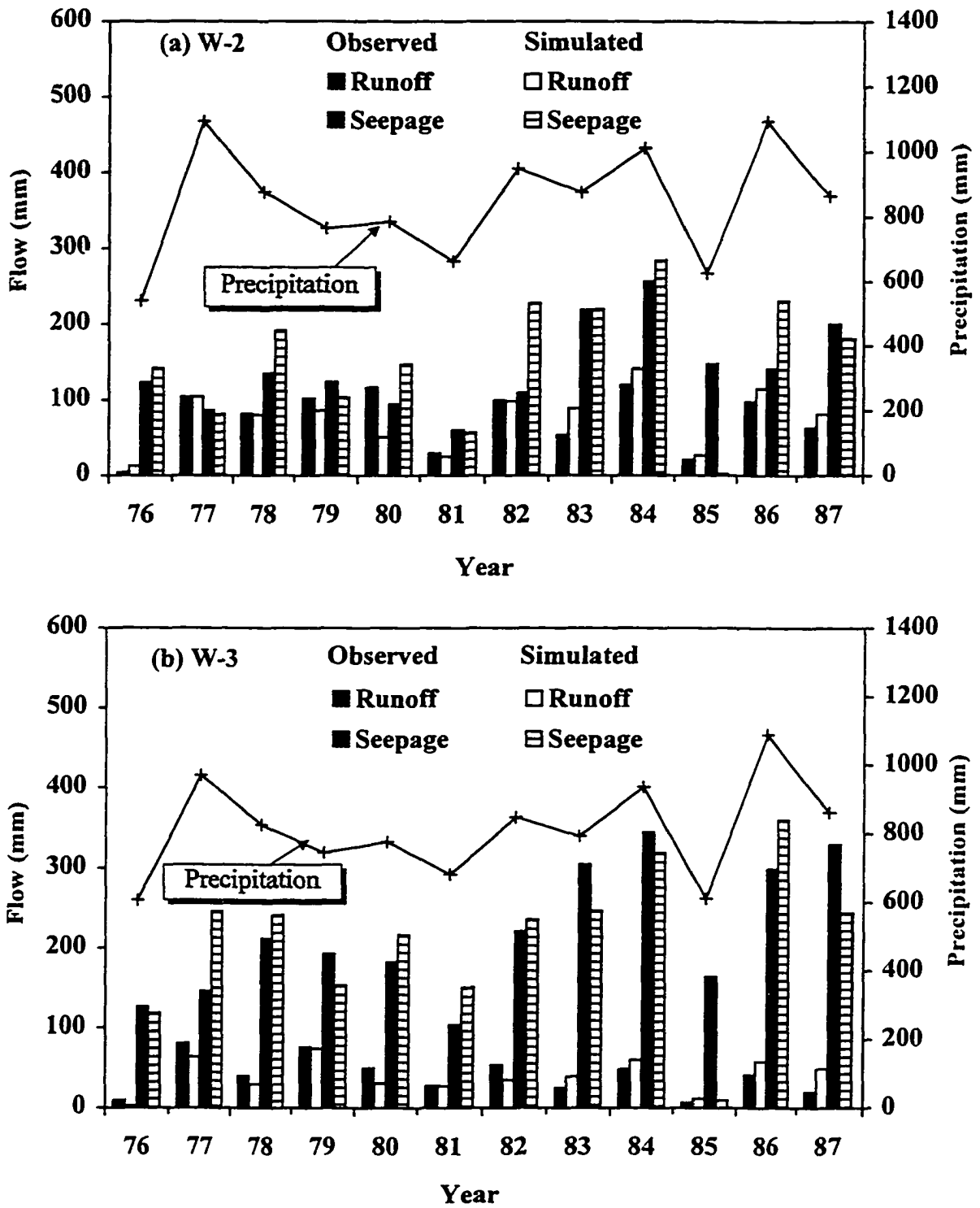


Figure 1. Annual precipitation, observed and simulated surface runoff and seepage flows for (a) Watershed 2 and (b) Watershed 3 during the validation period.

reliably tracked the annual level of observed surface runoff for both watersheds. The model's ability to track seepage flow was not as consistent, especially for Watershed 2. This conforms to expectations because water movement was not simulated through the deeper loess to the gully discharge points. The seepage flow comparisons reveal trends of overprediction during wetter years and underprediction during the driest years. This may be due in part to the simple storage routing technique used in EPIC to simulate percolation and lateral subsurface flow, that does not allow for more complex water movement such as the effect of matric potential on the upward movement of soil water (Warner et al. 1995). However, it is also clearly a function of the inability to simulate the water flow throughout the complete system, thus missing dynamics such as water storage during wetter periods that is subsequently discharged during drier years.

The goodness-of-fit measures for the predicted hydrologic outputs are summarized in Table 6. Based on the previously established criterion, the goodness-of-fit statistics are all satisfactory except the EF seepage flow of 0.26 for Watershed 3, which was slightly below

Table 6. Parametric model evaluation statistics for the simulated hydrologic variables over the 1976-1987 validation period.

State Variables	<u>Watershed 2</u>			<u>Watershed 3</u>		
	RMSE ^a (0.0) ^d	EF ^b (1.0)	CRM ^c (0.0)	RMSE (0.0)	EF (1.0)	CRM (0.0)
Surface runoff	32.5	0.59	-0.02	34.5	0.56	0.00
Seepage flow	46.0	0.40	-0.10	30.9	<u>0.26</u> ^e	0.03
ET	18.3	0.32	0.04	14.0	0.35	0.00

^aNormalized root mean square error (%).

^bModeling efficiency.

^cCoefficient of residual mass.

^dOptimal value.

^eUnderlined value is outside of target criteria.

the cutoff of 0.3. The negative CRM value of -0.1 for the Watershed 2 seepage flow indicates that the model tended to slightly overpredict this variable. Otherwise, little systematic model over- or underprediction occurred.

Nitrogen, soil losses, and crop yield

Observed and simulated 12-year median, MAD, E, and r^2 values are listed in Table 7 by watershed for the N loss and crop yield indicators. Median and MAD values are also shown for the soil erosion estimates, but % error and r^2 calculations were not performed because the soil erosion estimates could not be compared with the measured data. The predicted 12-year medians are in close agreement with the measured values for the N loss and

Table 7. Observed and simulated annual environmental variables summary statistics for the 1976-1987 validation period.

Watershed	Variables	Observed		Simulated		E ^a	r ²
		Median	MAD	Median	MAD		
2	NO ₃ -N runoff (kg/ha)	1.6	0.8	2.3	1.2	+43.8	0.42
	Leached NO ₃ -N (kg/ha)	8.0	5.9	7.3	6.8	-8.8	0.35
	Soil erosion (Mg/ha)	11.7 ^b	15.3 ^b	58.8 ^c	37.8 ^c	- ^d	-
	Crop yield (Mg/ha)	7.4	2.1	7.7	0.5	+4.1	0.30
3	NO ₃ -N runoff (kg/ha)	2.7	1.8	2.7	1.4	0.0	0.36
	Leached NO ₃ -N (kg/ha)	32.2	25.3	33.7	36.8	+4.7	0.69
	Soil erosion (Mg/ha)	1.1 ^b	1.4 ^b	3.6 ^c	1.5 ^c	-	-
	Crop yield (Mg/ha)	7.9	0.5	7.8	0.8	-1.3	0.29

^aPercent error = (simulated-observed)/observed \times 100.

^bObserved soil erosion measured at headcut.

^cSimulated soil erosion at the source of watershed.

^dNot feasible for direct comparison.

crop yield variables. However, the Watershed 2 surface runoff N loss was overpredicted by about 44%. The r^2 values are generally weak; only the predicted Watershed 3 N leaching indicators explain greater than 50% of the annual variability.

Median erosion rates of 58.8 and 3.6 Mg/ha were predicted for Watersheds 2 and 3 (Table 7), which clearly reflect the effect of the different tillage systems used for each watershed. As expected, these simulated erosion rates were higher than those measured at the headcuts, due to the sediment deposition that would occur across the grassed waterways between the bottom of the slopes and the gullies. Based on these median estimates, approximately 20 to 30 % of the predicted sediment loss would actually be transported to the gully headcuts. Confirmation of these predicted losses are not possible, for reasons previously stated.

The calibrated model accurately captured the effects of ridge tillage, predicting less soil erosion and greater N leaching for Watershed 3 relative to Watershed 2. However, the median predicted crop yields were essentially identical rather than reflecting the 0.5 t/ha difference harvested over the period. Yields harvested from the USDA Watersheds 1 and 4 are similar to those measured for Watershed 3. However, a greater coefficient of variation has been observed for the Watershed 2 yields for unexplained reasons. Thus it is possible that specific soil or other conditions exist in Watershed 2 that affect crop yields but were not accounted for in our parameterization of EPIC.

Graphical time series comparisons between the predicted and measured annual levels of N loss in leaching and surface runoff are shown in Figures 2 and 3. The model's ability to capture the N leaching trends (Figure 2) was mixed for both watersheds, in part due to the issues of the water movement lag-time previously discussed. It is clearly shown from the Figures that greater N leaching occurred at Watershed 3 under no-till treatment compare to Watershed 2 for the same year. The large deviations between observed and simulated N leaching were seen in 1982 and 1986 at both Watersheds, which mainly occurred due to the trends of model errors for seepage flows that detected during wetter years and driest years. The predicted surface runoff N losses for Watershed 2 followed the observed annual variations reasonably well, although general overprediction is obvious. Less consistent

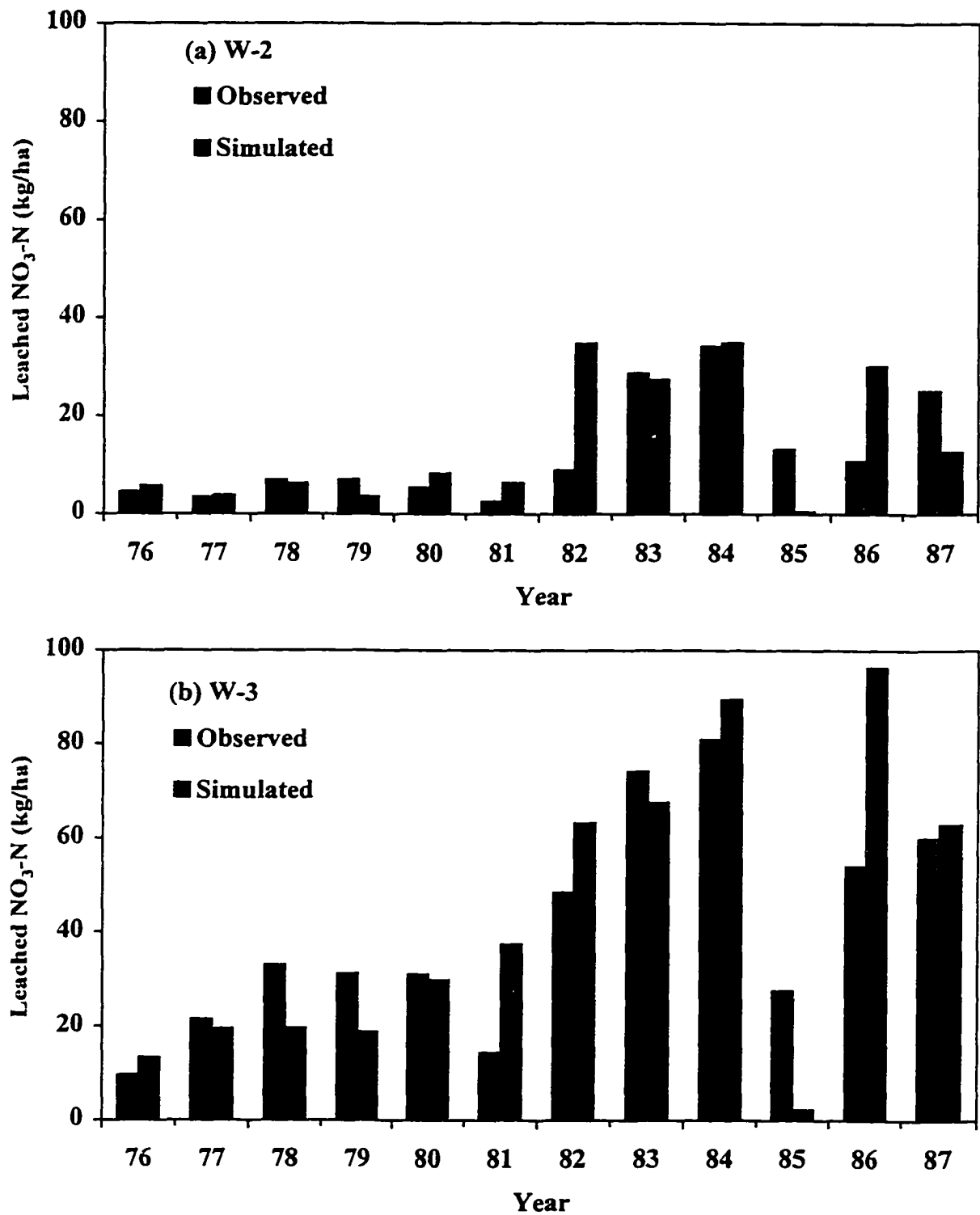


Figure 2. Observed and simulated annual leached $\text{NO}_3\text{-N}$ for (a) Watersheds 2 and (b) Watershed 3 during the validation period.

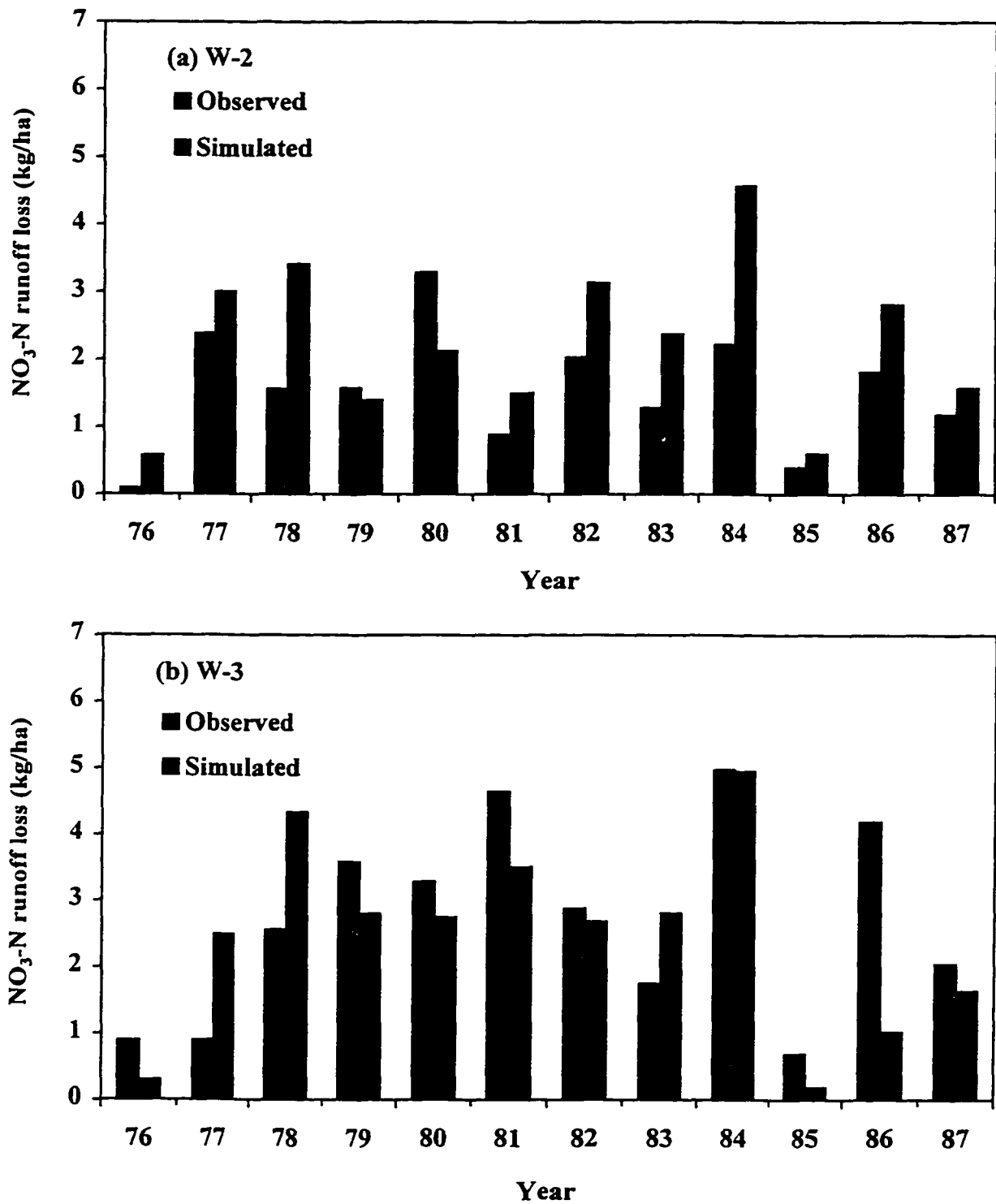


Figure 3. Observed and simulated annual $\text{NO}_3\text{-N}$ runoff loss for (a) Watershed 2 and (b) Watershed 3 during the validation period.

tracking by EPIC is shown for the Watershed 3 surface runoff N losses, particularly at the start and finish of the simulation period.

The time series plots of crop yields in Figure 4 clearly shows that EPIC missed the measured yield variability for both watersheds. Kiniry et al. (1995), Touré et al. (1994), and Moulin and Beckie (1993) also found similar results with EPIC; i.e., generally good agreement between long-term and predicted yields but inaccurate reflection of year-to-year yield variability.

Goodness-of-fit statistics are listed in Table 8 for the N loss and Crop yield indicators. The majority of the statistics satisfy the pre-established criterion, with the main exceptions being N loss in surface runoff for Watershed 2. The negative value of REF for the Watershed 2 N surface runoff indicates that the model-predicted N runoff amounts are worse than simply using the measured median values.

Table 8. Non-parametric model evaluation statistics for the simulated environmental variables for the 1976-87 validation period.

State Variables	<u>Watershed 2</u>		<u>Watershed 3</u>	
	MdAE ^a (0.0) ^c	REF ^b (1.0)	MdAE (0.0)	REF (1.0)
NO ₃ -N runoff	<u>52.07</u> ^d	<u>-0.50</u> ^d	25.32	0.44
NO ₃ -N leaching	39.45	<u>0.21</u> ^d	32.69	0.38
Crop yield	15.65	0.38	8.18	0.32

^aNormalized median absolute error.

^bRobust modeling efficiency.

^cOptimum value.

^dUnderlined values are outside of target criteria.

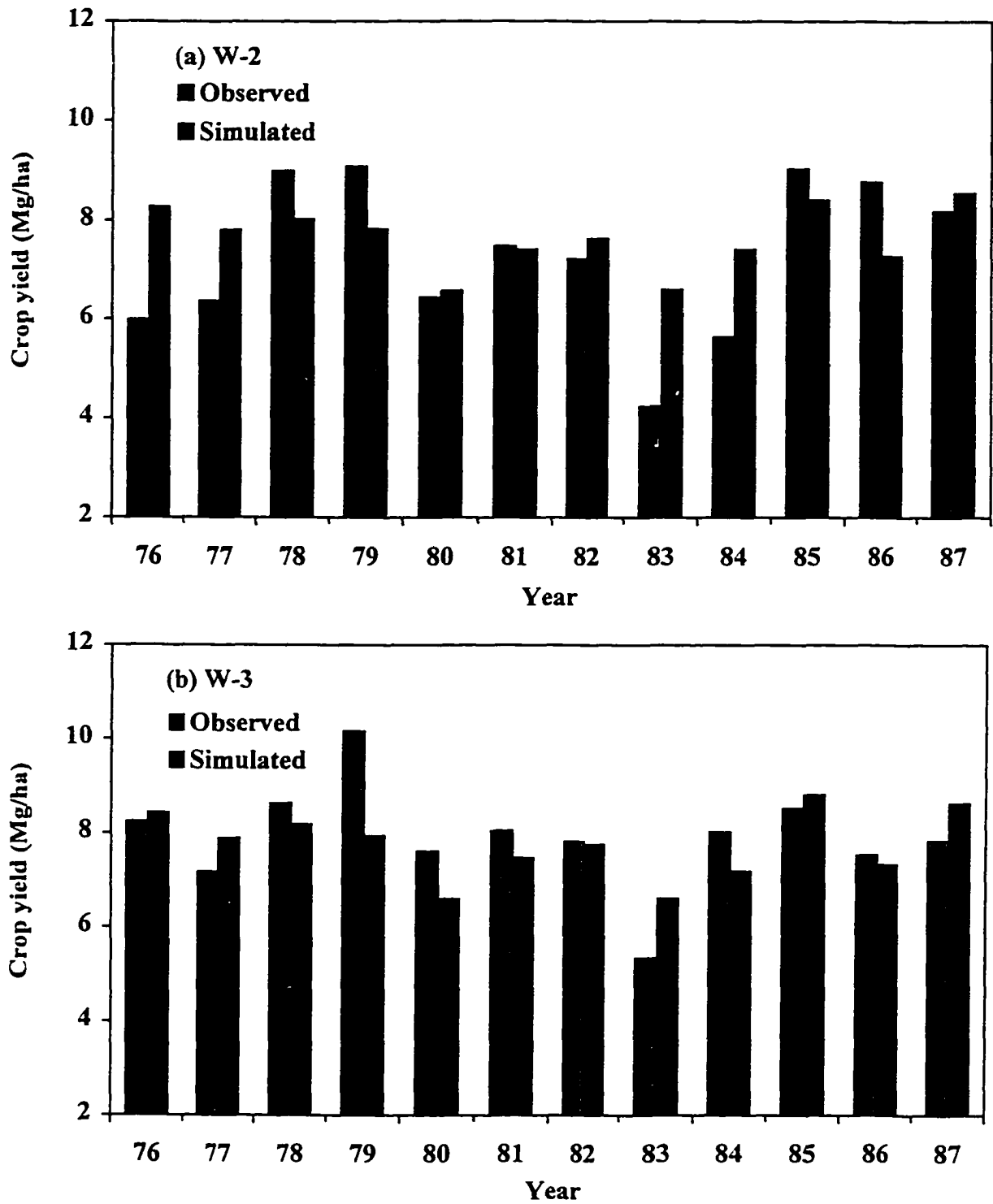


Figure 4. Observed and simulated annual crop yield for (a) Watersheds 2 and (b) Watershed 3 during the validation period.

Summary and Conclusions

Calibration of the hydrologic balance in EPIC was performed for 1988-94 for both Watersheds 2 and 3 at the USDA Deep Loess Research Station near Treynor, Iowa. The calibration process relied on adjusting the runoff curve number (CN2) for Watershed 3, to adequately reflect the impacts of ridge tillage. Recent versions of EPIC incorporate an alternative method of partitioning precipitation between surface runoff and precipitation, based on the theory originally proposed by Green and Ampt (1911), that might provide a more physically-based method for estimating surface runoff. EPIC could also be potentially enhanced by including the ability to more directly simulate ridge tillage in the model, rather than relying on the more empirical CN2 approach used here. Nevertheless, the CN2 adjustment procedure resulted in a successful calibration of the model.

The calibrated model captured the long-term trends (means, medians, and percent errors) for the hydrologic and environmental indicators during the 1976-87 validation period. The large differences observed in soil erosion and nutrient leaching between the two watersheds were clearly reflected in the model output. Overprediction of N loss in surface runoff by more than 40% for Watershed 2 was the weakest model response. However, the corresponding estimated surface N runoff loss was greater for Watershed 3, mirroring the general observed trends between the two watersheds. Overall, the output shows that EPIC was able to replicate the long-term relative differences between the two tillage systems, which is the major emphasis in applying the model within many integrated systems including RAPS. The results also strengthen the application of EPIC within the Loess Hills region (MLRA 107), which the watersheds represent.

The r^2 and goodness-of-fit statistics, and graphical comparisons, revealed that EPIC was weaker at capturing the inter-annual variation that was observed for both watersheds. This was likely due in part to simulating the watershed in a homogeneous manner, which ignored landscape slope complexities and lag-time in discharge of seepage flow. Despite this fact, it seems clear that EPIC will miss much of the inherent variability in crop yields and other indicators, based on the results reported here, by Touré et al. (1994), and others. Thus

the model should be used cautiously for risk and other analyses that require reliance on simulated variability, especially on an event basis.

The results presented here confirm earlier studies by Rawls et al. (1980) and Rawls and Richardson (1983) that standard tabulated CN2 values (Mockus 1969) should be reduced to represent the impacts of residue cover on the partition of precipitation between surface runoff and infiltration. The large reduction (19%) required for this study is likely an extreme; reductions of 10% or less should be adequate for the majority of conservation tillage systems as determined previously by Rawls et al. (1980). The results also underscore the importance of ongoing model testing, for guidance in the selection of the most suitable input parameters to depict different management systems.

Acknowledgments

Journal Paper No. J-17835 of the Iowa Agriculture and Home Economics Experiment Station, Ames, Iowa. This research was partially funded by the U.S. Environmental Protection Agency. The views expressed in this paper are not necessarily those of the U.S. Environmental Protection Agency.

References

- Babcock, B.A., J. Wu, T. Campbell, P.W. Gassman, P.D. Mitchell, T. Otake, M. Siemers, and T.M. Hurley. 1997. RAPS 1997: Agriculture and environmental outlook. Cent. for Agric. and Rural Dev., Iowa State Univ., Ames, IA.
- Bernardo, D.J., H.P. Mapp, G.J. Sabbagh, S. Geleta, K.B. Watkins, R.L. Elliot, and J.F. Stone. 1993. Economic and environmental impacts of water quality protection policies 2. application to the Central High Plains. *Water Resour. Res.* 29(9):3081-3091.
- Bouzaher, A., J.B. Braden, and G.V. Johnson. 1990. A dynamic programming approach to a class of nonpoint source pollution control problems. *Manage. Sci.* 36(1):1-15.
- Bouzaher, A., J.F. Shogren, P.W. Gassman, D.J. Holtkamp, and A.P. Manale. 1995. Use of a linked biophysical and economic modeling system to evaluate risk-benefit tradeoffs of corn herbicide use in the Midwest. p. 369-381. *In* M.L. Leng et al. (ed.) *Agrochemical Environmental Fate: State of the Art*. CRC Press, Boca Raton, FL.

- Christensen, L. A., and P. E. Norris. 1983. A comparison of tillage systems for reducing soil erosion and water pollution. Agricultural Economic Report Number 499, U.S. Dep. Agric., Econ. Res. Ser., Washington, D.C.
- Clouse, R.W. and C.D. Heatwole. 1996. Evaluation of GLEAMS considering parameter uncertainty. ASAE paper No. 96-2023, St. Joseph, MI.
- Edwards, D.R., V.W. Benson, J.R. Williams, T.C. Daniel, J. Lemunyon, and R.G. Gilbert. 1994. Use of the EPIC model to predict runoff transport of surface-applied inorganic fertilizer and poultry manure constituents. *Trans. ASAE* 37(2):403-409
- Favis-Mortlock, D.T., R. Evans, J. Boardman, and T.M. Harris. 1991. Climate change, winter wheat yield and soil erosion on the English South Downs. *Agric. Syst.* 37:415-433.
- Foltz, J.C., J.G. Lee, and M.A. Martin. 1993. Farm-level economic and environmental impacts of eastern corn belt cropping systems. *J. Prod. Agric.* 6(2):290-296.
- Green, W.H. and G. Ampt. 1911. Studies of soil physics part I: the flow of air and water through soils. *J. Agrc. Sci.* 4:1-24.
- Kiniry, J.R., D.J. Major, R.C. Izaurralde, J.R. Williams, P.W. Gassman, M. Morrison, R. Bergentine, and R.P. Zentner. 1995. EPIC model parameters for cereal, oilseed, and forage crops in the northern Great Plains region. *Can. J. Plant Sci.* 75:679-688.
- Kramer, L. A. and A. T. Hjelmfelt. 1989. Watershed erosion from ridge-till and conventional-till corn. ASAE Paper No. 89-2511, St. Joseph, MI.
- Kramer, L. A., A. T. Hjelmfelt and E. E. Alberts. 1989. Watershed runoff and nitrogen loss from ridge-till and conventional-till corn. ASAE Paper No. 89-2502, St. Joseph, MI.
- Kramer, L. A., E. E. Alberts, A. T. Hjelmfelt, and M. R. Gebhardt. 1990. Effect of soil conservation systems on groundwater nitrate levels from three corn-cropped watersheds in southwest Iowa. p. 175-189. *In* J. Lehr (ed.) Proceedings of the 1990 Cluster of Conferences, Kansas City, MO. 20-21 Feb. 1990. Nat. Ground Water Assoc., Westerville, OH.
- Kramer, L.A. and R.B. Grossman. 1992. Tillage effects on near surface soil bulk density. ASAE Paper No. 92-2131, St. Joseph, MI.
- Lakshminarayan, P.G., J.D. Atwood, S.R. Johnson, and V.A. Sposito. 1991. Compromise solution for economic-environmental decisions in agriculture. *J. of Environ. Manage.* 33:51-64.

- Lakshminarayan, P.G., P.W. Gassman, A. Bouzaher, and R.C. Izaurralde. 1996. A metamodeling approach to evaluate agricultural policy impact on soil degradation in Western Canada. *Can. J. Agr. Econ.* 44:277-294.
- Loague, Keith and Green, R. E. 1991. Statistical and graphical methods for evaluating solute transport models: overview and application. *J. of Cont. Hydr.* 7:51-73
- Mitchell, G., R.H. Griggs, V. Benson, and J. Williams. 1996. EPIC user's guide (draft) version 5300: the EPIC model environmental policy integrated climate (formerly erosion productivity impact calculator). The Tex. Agric. Exper. Station, Blackland Res. Cent., Temple, TX.
- Mitchell, P.D., P.G. Lakshminarayan, B.A. Babcock, and T. Otake. 1998. The impact of soil conservation policies on carbon sequestration in agricultural soils of Central U.S. p. 125-142. *In* R. Lal et al. (ed.) *Management of Carbon Sequestration in Soil*. CRC Press, Boca Raton, FL.
- Mockus, V. 1969. Hydrologic soil-cover complexes. p. 10.1-10.24. *In* SCS National Engineering Handbook, Section 4, Hydrology. U.S. Dep. Agric., Soil Conser. Ser., Washington, D.C.
- Mockus, V. 1972. Estimation of direct runoff from storm rainfall. p. 9.1-9.11. *In* SCS National Engineering Handbook, Section 4, Hydrology. U.S. Dep. Agric., Soil Conser. Ser., Washington, D.C.
- Moulin, A.P. and H.J. Beckie. 1993. Evaluation of the CERES and EPIC models for predicting spring wheat grain yield over time. *Can. J. Plant Sci.* 73:713-719.
- NRCS. 1990. Predicting rainfall erosion losses: Universal Soil Loss Equation. Iowa Field Office Tech. Guide, Section I-C-1. U.S. Dep. Agric., Nat. Resour. Conser. Ser., Des Moines, IA.
- Pennell, K.D., A.G. Hornsby, R.E. Jessup, and P.S.C. Rao. 1990. Evaluation of five simulation models for predicting aldicarb and bromide leaching under field conditions. *Water Resour. Res.* 26(11):2679-2693.
- Phillips, D.L., P.D. Hardin, V.W. Benson, and J.V. Baglio. 1993. Nonpoint source pollution impacts of alternative agricultural management practices in Illinois: a simulation study. *J. Soil and Water Conser.* 48(5):449-457.
- Phillips, R. E., Blevins, R. L., Thomas, G. W., Frye, W. W., and Phillips, S. H. 1980. No-tillage agriculture. *Sci.* 208:1108-1113.

- Ramanarayanan, T.S., J.R. Williams, W.A. Dugas, L.M. Hauck, and A.M.S. McFarland. 1997. Using APEX to identify alternative practices for animal waste management. ASAE Paper No. 97-2209, St. Joseph, MI.
- Rawls, W. J., C. A. Onstad and H. H. Richardson. 1980. Residue and tillage effects on SCS runoff curve numbers. *Trans. ASAE* 23:357-361.
- Rawls, W. J. and H. H. Richardson. 1983. Runoff curve number for conservation tillage. *J. Soil and Water Conser.* 38:494-496.
- Ritchie, J.T. 1972. A model for predicting evaporation from a row crop with incomplete cover. *Water Resour. Res.* 17(1):182-190.
- SAS Inst. Inc. 1989. SAS/STAT user's guide, version 6, fourth edition, volume 1. SAS Inst. Inc., Cary, NC.
- Singh, P. and R. S. Kanwar. 1995. Modification of RZWQM for simulating subsurface drainage by adding a tile flow component. *Trans. ASAE* 38(2):489-498.
- Steiner, J. L. 1989. Tillage and surface residue effects on evaporation from soils. *J. Soil Sci. Soc. Am.* 53:911-916.
- Stockle, C.O., P.T. Dyke, J.R. Williams, C.A. Jones, N.J. Rosenberg. 1992. A method for estimating the direct and climatic effects of rising atmospheric carbon dioxide on growth and yield of crops: part II - sensitivity analysis at three sites in the Midwestern USA. *Agric. Syst.* 38:239-256.
- Taylor, M.L., R.M. Adams, and S.F. Miller. 1992. Farm-level response to agricultural effluent control strategies: the case of the Willamette Valley. *J. Agric. Resour. Econ.* 17(1):173-185.
- Touré A., D.J. Major, and C.W. Lindwall. 1994. Comparison of five wheat simulation models in southern Alberta. *Can. J. Plant Sci.* 75:61-68.
- Warner, G.S., J.D. Stake and K. Guillard. 1995. Validation of EPIC for soil nitrate prediction in a shallow New England soil. p. 148-153. *In* C.D. Heatwole (ed.) *Water Quality Modeling, Proceedings of the International Symposium, Orlando, FL. 2-5 April, 1995.* ASAE, St. Joseph, MI.
- Williams, J., M. Nearing, A. Nicks, E. Skidmore, C. Valentin, K. King, and R. Savabi. 1996. Using soil erosion models for global change studies. *J. Soil and Water Cons.* 51(5):381-385.

- Williams, J.R. 1990. The erosion productivity impact calculator (EPIC) model: a case history. *Philos. Trans. R. Soc. London* 329:421-428.
- Williams, J.R. 1995. The EPIC Model. In: *Computer Models of Watershed Hydrology* (Ed.: V.P. Singh). Water Resources Publications, Highlands Ranch, CO.
- Williams, J.R., C.A. Jones, and P.T. Dyke. 1984. A modeling approach to determining the relationship between erosion and soil productivity. *Trans. ASAE* 27(1):129-144.
- Williams, J.R., C.W. Richardson, and R.H. Griggs. 1992. The weather factor: incorporating weather variance into computer simulation. *Weed Technol.* 6:731-735.
- Wischmeier, W.H. and D.D. Smith. 1978. Predicting rainfall erosion losses – a guide to conservation planning. *Agriculture Handbook No. 537*, U.S. Dep. Agric., Washington, D.C.
- Wossink, G.A.A., T.J. De Koeijer, J.A. Renkema. 1992. Environmental policy assessment: a farm economics approach. *Agric. Syst.* 39:421-438.
- Zacharias, S., C. D. Heatwole and C. W. Coakley. 1996. Robust quantitative techniques for validating pesticide transport models. *Trans. ASAE* 39(1):47-54.
-

CHAPTER 6. USE OF EPIC FOR ASSESSING THE ENVIRONMENTAL IMPACT OF ALTERNATIVE AGRICULTURAL MANAGEMENT SYSTEMS

A paper to be submitted to the Transactions of the ASAE

S. W. Chung, P. W. Gassman, R. Gu, and R. S. Kanwar

Abstract

Agricultural policy makers are requiring enhanced analytical tools to assess the environmental and economic impacts of alternative agricultural management strategies, to ensure that reliable policies are implemented. One tool that has been widely used for over a decade within agricultural policy analyses is the Erosion Productivity Impact Calculator (EPIC) model. EPIC has been tested and validated under a range of conditions; however, there is an ongoing need to further test the model to improve its prediction capabilities. In this study, EPIC was tested using 3 years of data collected from a field site near Nashua, Iowa. The model's performance and reliability was evaluated by assessing its ability to replicate the effects of various tillage and crop rotation systems on subsurface flow, nitrogen loss, and crop yield. Predicted monthly drain flows and leached nitrogen agreed well with observed values and were statistically acceptable for nearly all of the simulated management systems. However, there were consistent errors in the EPIC daily predictions, such as underpredicting peak flows and nitrogen losses during storm events. The results of paired t-tests clearly showed that EPIC can replicate the effects of various agricultural management alternatives on downward nitrogen movement at the study site. But EPIC showed a limited capability to reproduce tillage and crop rotation effects on crop yield, similar to results found in several previous studies. Further testing is needed to refine and improve the model's performance under conditions similar to those that exist at the Nashua site.

Introduction

Agricultural activities are affecting soil and water environments via a complicated matrix of hydrologic, geological, meteorological, and agronomic processes. A great number of experimental studies have provided essential data and important answers towards

understanding these processes, but they are prohibitively costly to perform across all possible landscape, weather, management, and cropping system combinations. Therefore, mathematical simulation models such as HSPF (Johanson et al. 1984), SWRRB (Williams et al. 1985), GLEAMS (Leonard et al. 1987), AGNPS (Young et al. 1987), SWAT (Arnold et al. 1993) have been developed to interpret these processes and predict the environmental outcomes of alternative agricultural management and cropping systems. These mathematical models are playing increasingly important roles within the context of integrated modeling systems, which are designed to provide policy makers with both economic and environmental outcomes of proposed agricultural policies.

One of the most widely used simulation models for agricultural policy analysis is the Erosion Productivity Impact Calculator (EPIC) model, originally developed by the United States Department of Agriculture (Williams 1990; Williams 1995). EPIC has been applied for studies ranging from farm-level to multiple states, such as the 1985 Resources Conservation Act analysis. The model was originally designed to simulate the impacts of erosion upon soil productivity. However, current versions of EPIC have incorporated many advanced functions related to water quality and global climate/ CO_2 change, which has resulted in the model being renamed to Environmental Policy Integrated Climate (Williams et al. 1996). Environmental indicators that can be output from EPIC include the transport and fate of nutrients from fertilizer and manure applications on eroded sediment, in runoff, and in leached water, pesticide leaching and runoff, the impact of atmospheric carbon levels on crop yield, sequestration of carbon in soil, and erosion losses due to water and wind.

The EPIC model has been adopted within the Resources and Agricultural Policy System (RAPS), an integrated modeling system designed to evaluate the economic and environmental impacts of agricultural policies for the North Central U.S. (Babcock et al. 1997). The main use of EPIC within RAPS is to provide nitrogen loss, soil erosion, and crop production indicators in response to variations in tillage treatment and crop rotation. Therefore, an important aspect that may limit the use of the model in the RAPS is whether EPIC can realistically replicate the impact of different agricultural management systems on the environment. Although EPIC has been tested and validated for several specific sites, there

is further need to test the model under a wider range of conditions that occur within the RAPS study region.

The purpose of this study is to examine the performance and reliability of the EPIC model in simulating subsurface drain flow, nitrogen loss, and crop yield in response to various tillage and crop rotation systems. A total of six management systems were simulated in this study, that included combinations of three different tillage systems, (moldboard plow, chisel plow, and no-till) and two crop rotation systems (continuous corn and soybean-corn). Daily field data were used to test and judge the model performance including tile drain flow and leached nitrate nitrogen ($\text{NO}_3\text{-N}$) collected during 1990 - 1992 (Kanwar et al., 1993).

Materials and Methods

Field Description

The study site is located at Iowa State University's Northeast Research Center, Nashua, IA. Field experiments have been conducted at this site since the early 1980s to evaluate the effects of tillage and crop rotation systems on the quantity and quality of groundwater (Kanwar et al., 1993). The site has 36 0.4-ha experimental plots with different tillage and crop rotation systems. The subsurface tile drainage systems were installed in 1979 in the middle of each plot about 1.2 meters deep at a spacing of 28.5 meters to improve the subsoil drainage. Twelve combinations of four different tillage treatments, moldboard plow (MB), chisel plow (CP), ridge-tillage (RT) and no-tillage (NT), and three crop rotations, continuous corn (CCR), corn-soybean (CSR), and soybean-corn (SCR), were studied across the 36 plots. Each tillage and crop rotation combination was replicated three times for each of the 12 different management cases.

In the present study, EPIC was tested with data collected from plots managed with MB, CP, and NT in combination with CCR and SCR. The 3-year field monitoring study revealed that these different tillage and cropping systems definitely affected the quantity of subsurface tile drain flow and the corresponding $\text{NO}_3\text{-N}$ loss (Kanwar et al., 1993). On average, greater tile drainage flows were observed under NT compared to MB, and from CCR relative to SCR. The $\text{NO}_3\text{-N}$ concentrations in tile water were greater under the MB

treatment than the conservation tillage systems (CP and NT). But the total $\text{NO}_3\text{-N}$ losses (kg/ha) through the tile drains were much greater from the NT and CP systems compared to MB, because of greater drainage flows. The EPIC predicted annual, monthly, and daily values were compared with observed values using various statistics and graphical displays to evaluate the model performance in replicating these tillage and crop rotation effects.

Input Data

The soil at this site is predominantly a Kenyon silty-clay loam soil with 3 to 4 % organic matter, which was assumed representative of all plots for the EPIC simulations. A soil profile depth of 1.2 m was assumed, that was divided into 6 soil layers. The average slope of 3.5% was obtained from the EPIC soil database and input for each simulation. Up to 20 physical and chemical soil properties for each soil layer can be input into EPIC. The main soil properties obtained from the EPIC soil database and Singh and Kanwar (1995) are shown in Table 1.

EPIC requires daily climatic input data including precipitation, maximum and minimum air temperatures, solar radiation, average relative humidity, and average wind speed. Field measurements at the study site were available for all of these climatic inputs except wind speed and part of the precipitation record: January, February, and December for 1990 - 1992. The omitted daily precipitation and wind speed data were generated by the EPIC model using monthly weather statistics for Osage, Iowa, which is the nearest climatic station available in the EPIC weather generator database. The Penman-Monteith evapotranspiration method was used to estimate the potential evaporation. Daily values of soil water evaporation and plant transpiration were then computed as a function of potential evaporation and leaf area index in the model (William 1995).

The EPIC management component requires information about different operations such as planting, fertilizer applications, tillage, and harvesting. Operation dates, fertilizer amounts, and other pertinent management information were obtained from Kanwar et al. (1993). Equivalent mineral nitrogen (N) application rates of 200 kg-N/ha to corn within CCR and 168 kg-N/ha to corn within SCR were simulated; nitrogen applications were not simulated for soybean.

Table 1. Soil properties used in the simulations for Nashua site, Iowa.

Soil property	Soil layer number					
	1	2	3	4	5	6
Lower boundary (m)	0.01	0.41	0.50	0.69	0.89	1.20
Bulk Density (Mg/m ³)	1.32	1.32	1.55	1.60	1.65	1.70
Wilting point (m ³ /m ³)	0.14	0.14	0.15	0.15	0.15	0.15
Field capacity (m ³ /m ³)	0.30	0.30	0.26	0.28	0.28	0.26
Sand content (%)	38	41	42	43	44	44
Silt content (%)	42	34	32	30	28	31
pH	6.5	6.5	6.2	6.2	6.2	6.2
Organic carbon (%)	2.0	2.0	0.6	0.4	0.3	0.2
Coarse fragment content (%)	1.4	1.4	7.6	7.6	7.6	7.6

Simulation Methodology

EPIC directly simulates tillage practice effects by incorporating nutrients and crop residues below the soil surface, changes in the soil bulk density, and conversion of standing residue to flat residue. The impact of tillage on surface runoff has to be indirectly accounted for, by adjusting the runoff curve numbers to reflect crop residue amounts as discussed below.

The USDA Soil Conservation Service (SCS) curve number method (Mockus 1969) was used to partition precipitation between surface runoff volume and infiltration. Conservation tillage effects were taken into account by adjusting the runoff curve number values for antecedent moisture condition 2 (CN2), the average moisture conditions for the preceding five day period. These CN2 values represent conventional tillage and have to be reduced to reflect the impacts of conservation tillage (Rawls et al 1980; Rawls and Richardson 1983; Chung et al. 1998). The crop residue left on the surface was used as the independent variable to estimate the percent reduction of CN2 for the chisel plow and no-till treatments. The residue levels were obtained from Singh and Kanwar (1995), who estimated them from crop yield and percent cover using the residue amount estimation technique of Wischmeier and Smith (1978). A CN2 value of 81 was chosen for MB, reflecting row crops with straight row and hydrologic soil group B (Mockus 1969). This curve number value was reduced about 6% for CP (CN2 = 76) and 11% for NT (CN2 = 72), based on the estimated amounts of surface crop residues.

Nitrogen transport and transformation processes simulated in EPIC include runoff of $\text{NO}_3\text{-N}$, organic-N transport by sediment, $\text{NO}_3\text{-N}$ leaching, upward $\text{NO}_3\text{-N}$ movement by soil water evaporation, denitrification, immobilization, mineralization, crop uptake, volatilization of NH_3 , and fixation (Williams 1995). All of these processes were taken into account for both the CCR and SCR systems where appropriate (leguminous N-fixation was only simulated for soybean within the SCR system). N-fixation occurs when nitrogen gas (N_2) is transformed into a chemical compound that can be used by a crop. Fixation of nitrogen in cropland is predominantly accomplished by specialized microorganisms and the interaction between such microorganisms and plants. The EPIC N-fixation subroutine was developed to simulate

annual legumes in which fixation is sensitive to early nodule development, nodule senescence late in growth, soil water in the top 30 cm, and soil mineral N in the root zone (Lawn and Burn, 1974; Patterson and Larue, 1983; Bouniols et al., 1991; Williams 1995). An empirical parameter, PARM (7), can be adjusted to take into account the sensitivity of these environmental factors on N-fixation. In this study, PARM (7) was set to 1.0 for soybean to fully account for these environmental factors.

The daily N-fixation was computed as a fraction of daily plant N uptake for soybean using the following relationship:

$$WFX_i = FXR_i \cdot UN_i, \quad WFX \leq 6.0 \quad (1)$$

where WFX is the amount of N-fixation in kg/ha/day, FXR is the fraction of uptake for day i , and UN is the daily plant N uptake rate in kg/ha/day. The FXR value was estimated as a function of plant growth stage, soil water content, and soil NO_3 -N amount. The soil water content factor reduces N-fixation when the water content at the top 30 cm is less than 85% of field capacity. The amount of NO_3 -N in the root zone reduces N-fixation when it is greater than 100 kg/ha /m and prohibits N-fixation when it is greater than 300 kg/ha/m.

Drain Flow Routing for Daily Comparisons

EPIC operates on a daily time step and is driven by daily climatic inputs. However, daily comparisons are difficult because the predicted drainage flows are the flows which move downward below the root zone, while the field data were measured at the outlet of the tile line. Therefore, flow routing from the bottom of root zone to the outlet of tile line is required to indirectly compare the EPIC predicted daily drainage flows and nitrogen losses with the observed values.

The tile line was assumed to act as a storage reservoir that leads a lagged and damped peak flow at the outlet during storm events. A continuity equation was used to rout the drainage flows. The continuity equation for the inflow I , outflow O , and the rate of storage change S , in the tile line was formulated as following:

$$\frac{dS}{dt} = I - O \quad (2)$$

where the difference between the drainage inflow from the bottom of the root zone and outflow out of the tile line outlet is equal to the rate of water volume change stored within the system. Equation (2) was approximated using the forward finite-difference method:

$$\frac{S^{i+1} - S^i}{\Delta t} = \frac{1}{2}(I^i + I^{i+1}) - \frac{1}{2}(O^i + O^{i+1}) \quad (3)$$

where Δt is the routing time interval and the superscripts i and $i+1$ denote the variables at the beginning and ending of the routing interval. By rearranging the known and unknown terms, equation (3) was expressed as:

$$I^i + I^{i+1} + \frac{2S^i}{\Delta t} - O^i = O^{i+1} + \frac{2S^{i+1}}{\Delta t} \quad (4)$$

The storage term in (4) can be expressed as a function of outflow $S = kO$, where k is the travel time of drainage flow, provided that the water level in the tile line is horizontal to ensure removal of dynamic effects (Chow et al. 1988). By substituting the S terms into (3), the flow at the end of tile line (O^{i+1}) was computed using the following solution:

$$O^{i+1} = \left(\frac{\Delta t}{\Delta t + 2k}\right)(I^i + I^{i+1}) + \left(\frac{-\Delta t + 2k}{\Delta t + 2k}\right)O^i \quad (5)$$

This solution was used to route the EPIC generated daily subsurface drain flows (I^i and I^{i+1}) from the bottom of the root zone to tile line outlet by assuming that the initial condition for $O^{i=0}$ is equal to zero.

Model Evaluation Methods

Statistical analyses were conducted using the SAS software system (SAS Inst. Inc. 1989) to compare the observed and simulated values and their monthly and daily variations, and to evaluate EPIC's reliability in replicating the effects of various tillage and cropping systems. The statistics used for comparing the observed and simulated values, and their

variations, include percent error (E), modeling efficiency (EF), r-square (r^2), and a paired t-test between observed and simulated values. The paired t-test was also conducted to evaluate reliability of EPIC in replicating the effects of various tillage and cropping systems. The formulas of these statistics are:

$$E = \frac{(P_i - O_i)}{O_i} \times 100 \quad (6)$$

$$EF = \left[\sum_{i=1}^n (O_i - O_m)^2 - \sum_{i=1}^n (P_i - O_i)^2 \right] / \sum_{i=1}^n (O_i - O_m)^2 \quad (7)$$

$$r^2 = \left[\frac{n \left(\sum_{i=1}^n O_i P_i \right) - \left(\sum_{i=1}^n O_i \right) \left(\sum_{i=1}^n P_i \right)}{\left(n \sum_{i=1}^n O_i^2 - \left(\sum_{i=1}^n O_i \right)^2 \right) \left(n \sum_{i=1}^n P_i^2 - \left(\sum_{i=1}^n P_i \right)^2 \right)} \right]^2 \quad (8)$$

where O_i and P_i are the observed and predicted values at each comparison point i , n is the number of observed and predicted values that are being compared, and O_m is the mean of the observed values.

The E value was mainly used to assess the error associated with the long-term (annual) performance of the EPIC model. The EF describes the proportion of the variance, of the observed values over time, accounted for by the EPIC model, where the variance is relative to the mean value of the observed data (Nash and Sutcliffe, 1970; Martin et al. 1993). The EF can vary from 1 to negative infinity; an EF value of 1 indicates that the model predictions are exactly the same as the observed values. If EF is equal to or less than 0, it means that the observed mean value is as good an overall predictor as the model (or a better predictor of observed values than the model). The r^2 value indicates how accurately the model tracks the variation of observed values. The r^2 value can range from 0 to 1, where r^2 value of 1 indicates that the model can completely explain the variations of the observed indicators. The main difference between the EF and the r^2 value is that the latter can not interpret the model performance in replicating individual observed values, while the EF can.

The null hypothesis (H_0) of the paired t-test between the observed and simulated monthly values was $\mu_d = \mu_o - \mu_s = 0$, in which μ_d is the difference between the mean values of the observed (μ_o) and simulated (μ_s) indicators. The alternative hypothesis (H_A) was $\mu_d \neq 0$. Thus, the acceptance of the null hypothesis indicates that the EPIC predicted mean value is statistically same as the observed one. The H_0 was rejected when the significance value level (P-value) was less than half of a specific level of significance ($\alpha/2$). The level of significance $\alpha = 0.05$ (or 95% confidence level) was used in this study. The null hypothesis (H_0) for the paired t-test among different management systems was $\mu_d = \mu_A - \mu_B = 0$, in which μ_d is the difference between the mean values of management alternatives A (μ_A) and B (μ_B). The alternative hypothesis (H_A) is $\mu_d = \mu_A - \mu_B > 0$. Therefore, rejection of the null hypothesis means that management A results in greater nitrogen leaching losses (or whatever environmental indicator is of interest) than management B. The H_0 was rejected when the P-value was less than the level of significance ($\alpha = 0.05$).

Explicit standards for evaluating model performance with statistics such as the EF and r^2 are not well-established, because the judgment of model results is highly dependent on the purpose of the model application. For this study, the criteria set by Chung et al. (1998) were used to judge if the model results were satisfactory; i.e., $EF > 0.3$ and $r^2 > 0.5$.

Results and Discussion

Subsurface Drain Flow

For the comparisons of model results with observed data, it was assumed that the measurements at the tile line outlets were identical to the EPIC predicted subsurface flows that move downward below the root zone (1.2 m in this study). This is a reasonable assumption for the monthly and annual comparisons because the experimental plots (0.4 ha) and the tile line spacings (28.5 m) are small enough to carry the entire flow from the bottom of root zone to the tile line outlet within several days. Thus the effects of the tile line such as lagging and damping of peak flows were ignored. The daily values are, however, indirectly compared considering these effects using the simple flow routing technique.

Table 2 shows the observed and simulated annual subsurface drain flows for the different tillage and crop rotation systems. The E values (Table 2) indicate the percent errors between the observed and simulated annual mean values of subsurface drain flow. Although several large deviations were seen between the simulated and observed values for drainage flow for the 1991 NT, 1992 CP, and 1992 NT systems, the overall model performance was satisfactory under CCR. The simulated 3-year average drain flows for all tillage systems were especially consistent with the observed values, with $E < 10\%$. However, larger deviations resulted for all simulated tillage treatments under the SCR system, with E values greater than 10% for the predicted drainage flows under CP and NT. In 1991 and 1992, the observed data indicates that the SCR tillage effects on drainage flow were not significant, but the model results showed the same tillage effects as observed in the CCR system. The results suggest that the subsurface flow mechanisms and pathways are different for SCR relative to CCR, and that these were not accurately simulated by the model.

Time series comparisons between the observed and simulated monthly subsurface drain flows are shown in Figure 1. The EPIC predicted values followed the observed trends reasonably well under all management systems, although several deviations were detected during the peak time periods. The EPIC model considerably overpredicted the peak flows in July 1990 and April through June of 1992, but underpredicted during April through May of 1991. Overall, the EPIC model responded well to the precipitation patterns of the study area; i.e., frequent heavy rainfall events during the late spring and summer.

The EPIC predicted daily drain flows for 1990 NT under CCR were compared with daily observed values (Figure 2), in order to further assess the model performance. This case was selected because of the small deviations between observed and simulated total annual drainage flow and nitrogen loss. A satisfactory r^2 value (0.63) was obtained between observed and simulated daily drain flows, indicating that the daily variations in the observed drainage flows were reasonably explained by the model. However, the EPIC predicted values contained abundant errors and missed peak drainage flows at several points. The model errors may be due in part to the daily time step and the lack of a preferential flow component in the model. Preferential flow can occur through macropores during heavy storm events resulting

Table 2. Observed and simulated annual total subsurface drain flows (mm).

Rotation	Year	Precipitation (mm)	<u>Observed</u>			<u>Simulated</u>		
			MB ^a	CP ^b	NT ^c	MB	CP	NT
CCR ^d	1990	1235.3	89.8	183.0	274.5	105.8	183.9	280.3
	1991	994.6	180.8	271.2	329.2	182.8	228.1	262.7
	1992	826.1	98.5	115.8	132.2	113.1	164.7	205.7
	Mean	1018.7	123.0	190.0	245.3	133.9	192.2	249.6
	E ^f					(8.9)	(1.2)	(1.7)
SCR ^e	1990	1235.3	106.7	156.8	169.3	125.6	234.3	233.9
	1991	994.6	265.3	317.9	284.9	152.3	201.4	198.7
	1992	826.1	71.8	61.7	43.8	129.0	181.1	161.6
	Mean	1018.7	147.9	178.8	166.0	135.6	205.6	198.1
	E					(-8.3)	(14.9)	(19.3)

^aMoldboard plow.

^bChisel plow.

^cNo-till.

^dContinuous corn rotation.

^eCorn and soybean rotation.

^fPercent error = (simulated-observed)/observed × 100.

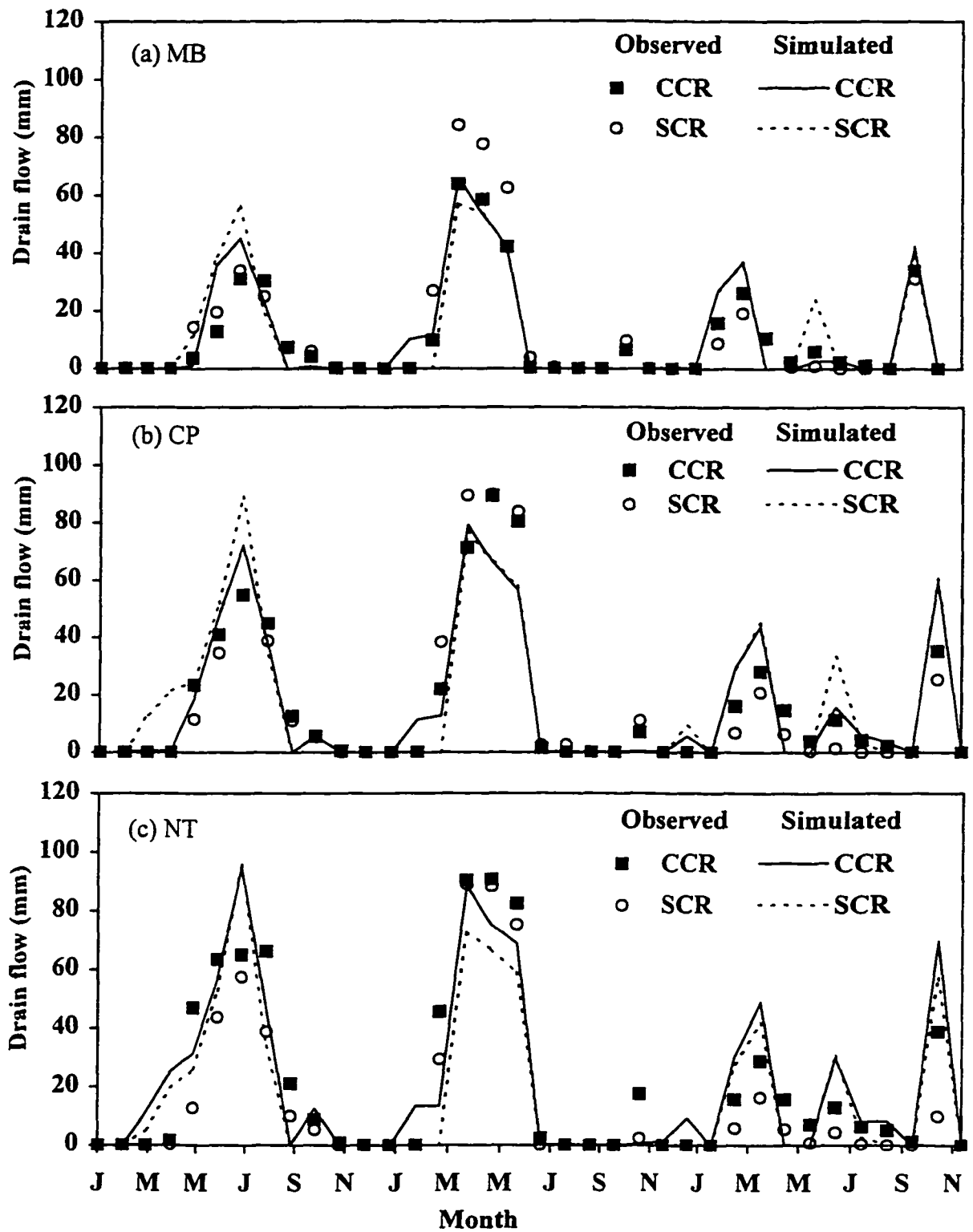


Figure 1. Observed and simulated monthly subsurface drain flows under (a) moldboard, (b) chisel plow, and (c) no-till systems for 1990-1992 at Nashua, Iowa.

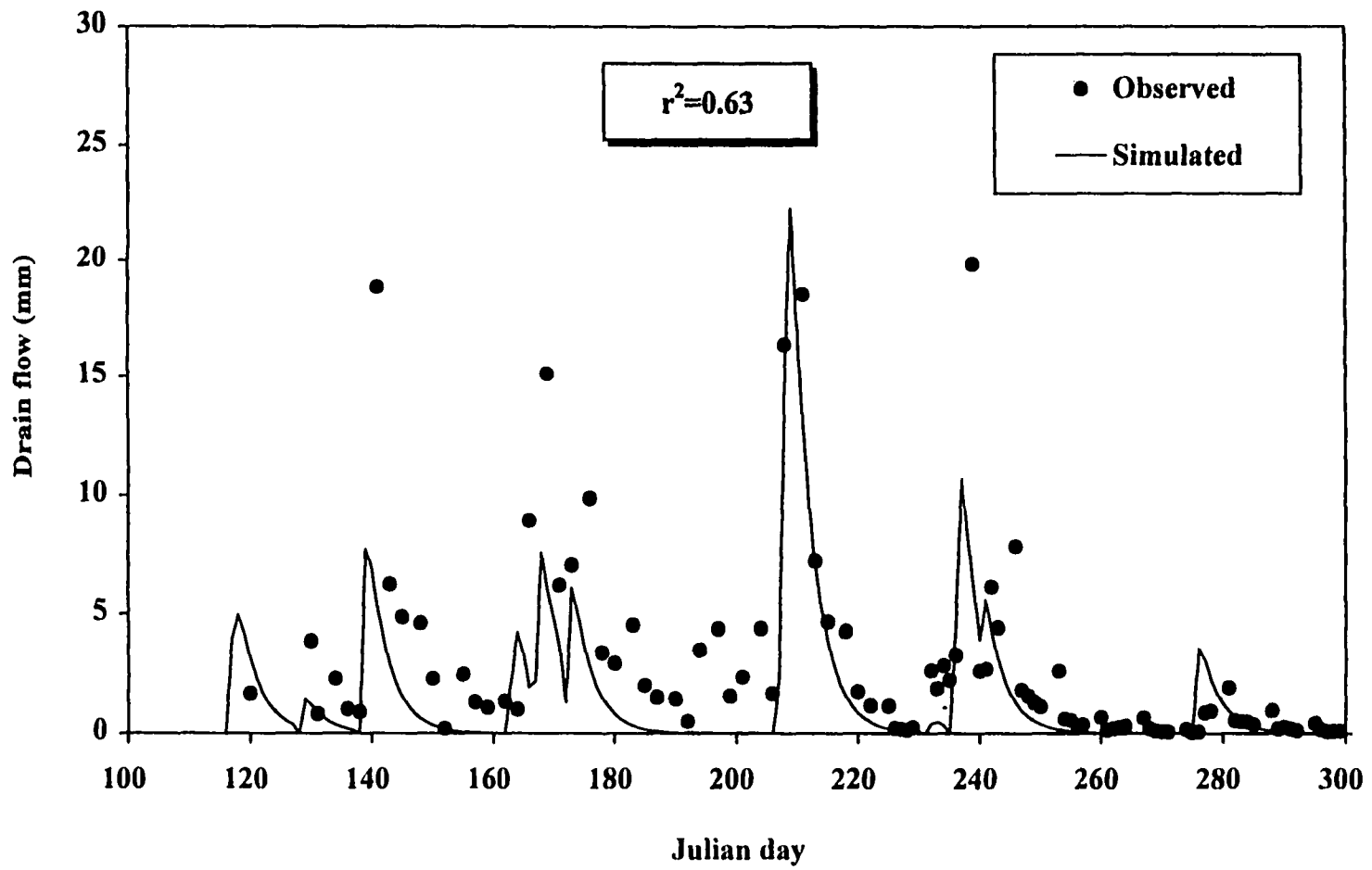


Figure 2. Observed and simulated daily subsurface drain flows under no-till and continuous corn rotation for 1990 at Nashua, Iowa.

in quick movement of flow and nutrients from the soil surface to the bottom of root zone (Kanwar et al 1993; Singh and Kanwar, 1995), a process that can not be simulated in EPIC.

Nitrogen Loss

Observed and simulated total annual nitrogen losses via drainage flow under the various tillage and crop rotation systems are listed in Table 3. The model performance varied greatly between the different simulated management systems. Except for the first year, the deviations between the observed and predicted values were significant for all tillage plots under CCR. However, the predicted CP and NT values showed much higher nitrogen losses relative to MB, consistent with the observed values. The model considerably over estimated the nitrogen losses under all tillage treatments in 1992. In that year, EPIC predicted greater nitrogen losses under CP and NT treatments than under MB, although the measured data showed little difference among treatments. For SCR, the model predicted the annual leached nitrogen more accurately than the previously discussed drainage flow. In general, the predicted 3-years average nitrogen losses under all management systems were within roughly 5 percent of the corresponding measured values, except when NT was simulated in combination with SCR (Table 3). This indicates that EPIC is able to replicate the long-term water and nitrate leaching trends for these systems.

Figure 3 shows the time series comparisons between the observed and simulated monthly values of leached nitrogen. As expected from the drain flow comparisons, the predicted values followed the observed trends reasonably well although several deviations were obvious during the peak leaching periods across all management alternatives. A great amount of leached nitrogen was lost in 1990 due to the high precipitation that occurred following two consecutive years of drought (1988 and 1989), which was captured by the model. The nitrogen that accumulated within the soil profile during the drought years was washed out via the abundant subsurface drainage flows during the heavy storm events in 1990. EPIC considerably overpredicted the nitrogen losses during the early spring (March and April) of 1992 at all tillage plots under the CCR, and in 1990 NT under SCR. This implies that the fate and transport of nitrogen in this site may be more complicated than the theory used in the model.

Table 3. Observed and simulated annual total leached nitrogen (kg/ha).

Rotation	Year	Precipitation (mm)	Observed			Simulated		
			MB ^a	CP ^b	NT ^c	MB	CP	NT
CCR ^d	1990	1235.3	58.1	100.0	107.2	57.6	101.6	106.7
	1991	994.6	62.7	76.0	61.7	50.9	56.4	43.3
	1992	826.1	16.6	17.0	14.9	27.1	36.6	34.9
	Mean	1018.7	45.8	64.3	61.2	45.2	64.9	61.6
	E					(-1.3) ^f	(0.8)	(0.6)
SCR ^e	1990	1235.3	41.1	50.8	31.7	36.3	57.1	58.5
	1991	994.6	41.0	46.0	31.9	51.6	43.5	41.1
	1992	826.1	10.2	7.3	4.4	10.0	6.5	5.0
	Mean	1018.7	30.7	34.7	22.7	32.5	35.7	34.9
	E					(5.5)	(2.8)	(58.3)

^aMoldboard plow.

^bChisel plow.

^cNo-till.

^dContinuous corn rotation.

^eCorn and soybean rotation.

^fPercent error = (simulated-observed)/observed × 100.

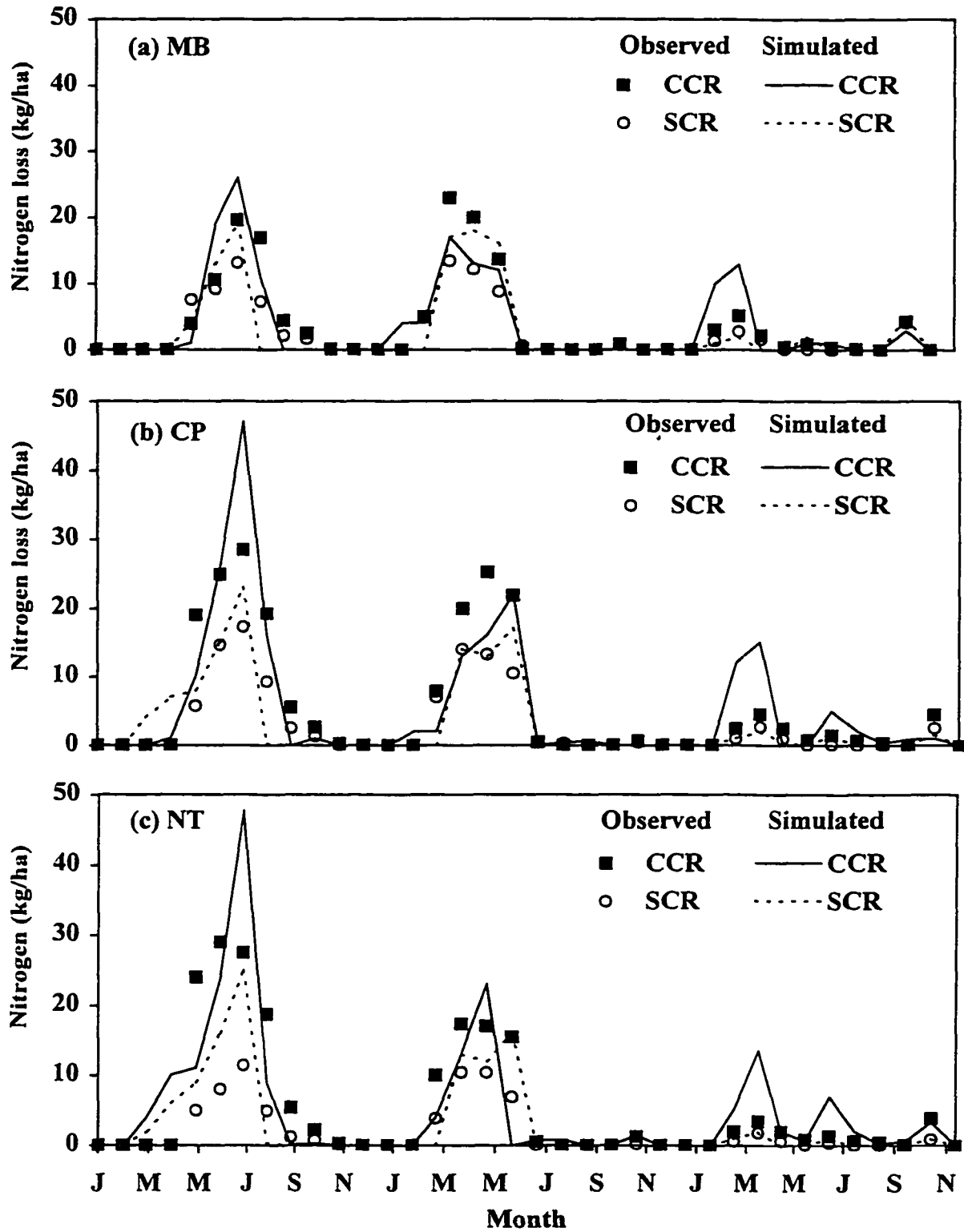


Figure 3. Observed and simulated monthly leached $\text{NO}_3\text{-N}$ under (a) moldboard, (b) chisel plow, and (c) no-till systems for 1990-1992 at Nashua, Iowa.

During and after the two consecutive wet years of 1990 and 1991, an anoxic condition may have developed within the soil profile due to a high soil water content. If so, it is possible that some of the remaining nitrogen denitrified via consumption by heterotrophic bacteria. If this scenario is correct, it appears that the empirical equation used in EPIC for simulating denitrification failed to capture this process. Whether this occurred or not, it is clear that the overprediction of nitrogen losses during this period are directly associated with the overpredicted drainage flows.

The predicted daily values of nitrogen loss for 1990 NT under CCR are compared with the observed values in Figure 4. A relatively weaker r^2 (0.51) was predicted for the leached nitrogen compared to the subsurface drain flows. As detected for the daily drain flow comparisons, the model was not capable of capturing the peak nitrogen losses for several storm events. This again indicates that nitrogen may have moved preferentially through the root zone during heavy storm events. The trends of both observed and simulated daily leached nitrogen values (Figure 4) are consistent with the corresponding subsurface drain flows (Figure 2), confirming that the fate and transport of nitrogen is strongly correlated with water flow.

Statistical Analyses

Results of the EF, r^2 , and P-value evaluations are presented in Table 4. The statistics are based on 36 observations of monthly simulation output ($n=36$). Strong modeling efficiencies are shown in Table 4 for every combination of cropping system, management, and drainage flow or leached nitrogen, except for nitrogen leached under no-till. Overall, more than 60 and 50 percent of the variances in the observed monthly drain flows and leached nitrogen were accounted for by the EPIC model, relative to the mean value of observed data. The negative EF value for the leached nitrogen under no-tilled SCR indicates that the observed mean value is a better predictor of observed values than the model. The r^2 values for the subsurface drain flows and leached nitrogen were satisfactory under all combinations of tillage and cropping systems. The r^2 values ranged from 0.67 to 0.89 for the tile drain flows and 0.60 to 0.83 for the leached nitrogen. The slightly lower nitrogen loss r^2 values can likely be attributed to errors in simulating complicated nitrogen transformation processes such as immobilization,

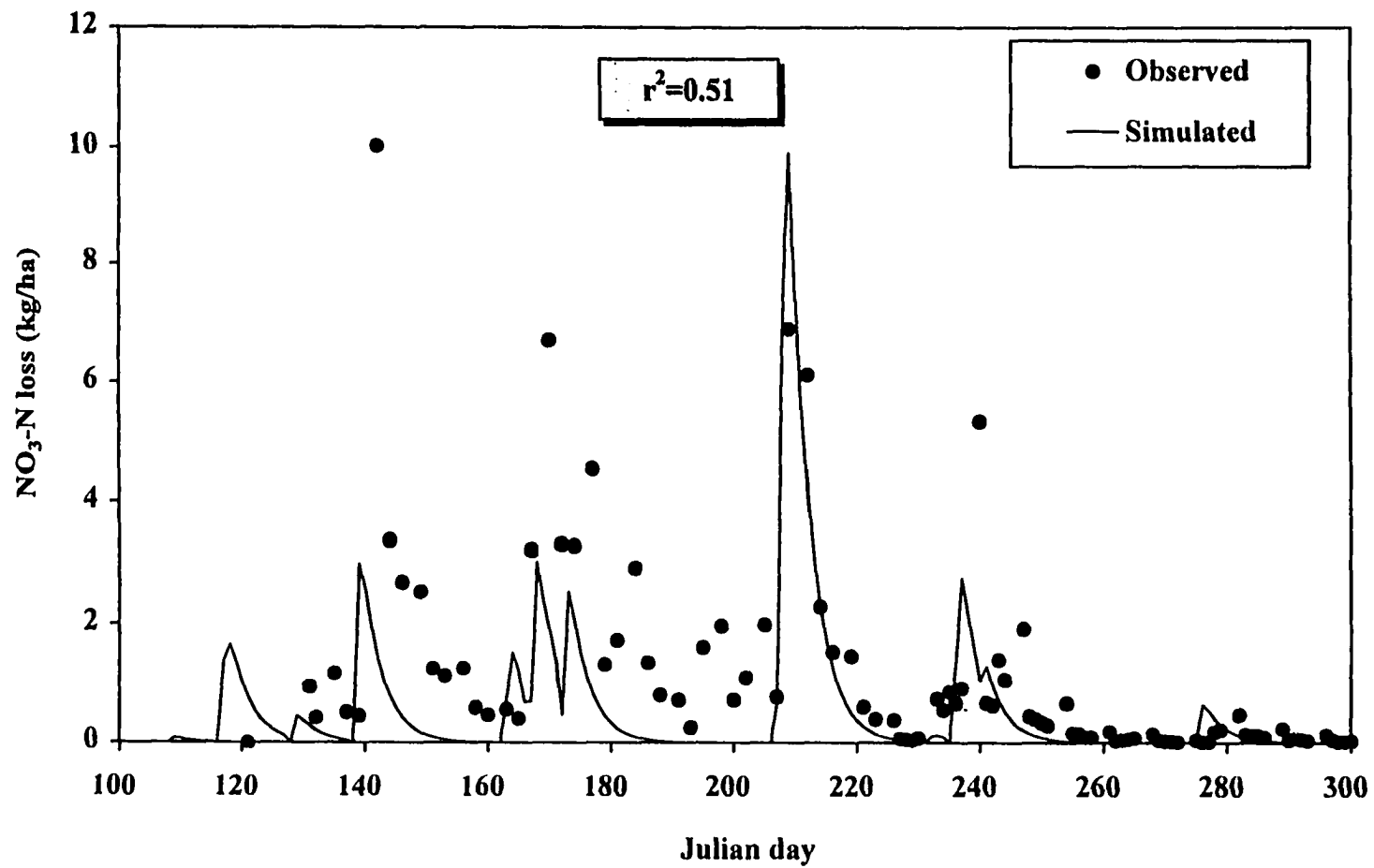


Figure 4. Observed and simulated daily NO₃-N losses under no-till and continuous corn rotation for 1990 at Nashua, Iowa.

Table 4. The statistics used to evaluate the performance of EPIC model.

Rotation	Tillage	Drain flow			Leached nitrogen		
		EF	r ²	P-value ^f	EF	r ²	P-value
	MB ^a	0.85	0.89	0.404	0.73	0.75	0.607
CCR ^d	CP ^b	0.84	0.85	0.909	0.69	0.75	0.403
	NT ^c	0.76	0.78	0.880	0.49	0.60	0.296
	MB	0.70	0.70	0.933	0.58	0.83	0.751
SCR ^e	CP	0.63	0.67	0.959	0.67	0.77	0.824
	NT	0.64	0.69	0.975	<u>-0.08^g</u>	0.80	<u>0.008</u>

^aMoldboard plow.

^bChisel plow.

^cNo-till.

^dContinuous corn rotation.

^eCorn and soybean rotation.

^fH₀: the population mean of observed values is identical to that of predicted values; H₀ is rejected if P-value is less than the level of significance ($\alpha/2 = 0.025$).

^gUnderlined value is outside of target criteria.

nitrification, denitrification, and fixation. The EPIC model simulates these processes using empirical equations developed on the basis of field experiments; however, it is difficult to assess modeling error of these processes due to the insufficient field measurements. The paired t-test (p-values) results indicate that the simulated drain flows and leached nitrogen agree well with observed values. Thus the null hypothesis, that the population mean of observed values is identical to that of the predicted values, was accepted for all management alternatives at significance level of $\alpha = 0.05$, except SCR managed in tandem with NT.

In summary, the EPIC estimates were statistically acceptable for all management systems, except for nitrogen leaching EF and p-values computed for SCR managed with no-till. This resulted from considerable overprediction of nitrate leaching during the period of May - July 1990. However, the predicted nitrogen losses followed observed trends well as evidenced by the r^2 value given in Table 4.

EPIC Reliability for Tillage Effects

Table 5 shows the results of paired t-tests (p-values) that were performed to assess the reliability of EPIC to replicate the effects of various tillage treatments on the subsurface drain flow and leached nitrogen. The null hypothesis, that the population mean of an indicator under tillage A is equal to the corresponding value for tillage B, was rejected if the p-value is less than the level of significance ($\alpha = 0.05$).

A p-value less than 0.05 resulted for CP and NT relative to MB when cropped with CCR and between CP and MB used in tandem with SCR, for both the observed and simulated drainage flows. This means that greater tile drain flows occurred in the field for these conservation tillage and cropping system combinations as compared to MB, and that the EPIC model replicated these tillage effects. However, the model failed to replicate the observed tillage effect on the drainage flows between NT and MB under SCR.

The null hypothesis that equivalent N leaching would occur for CP versus MB was rejected for CCR but accepted for SCR for both the measured and simulated leached nitrogen results. Thus EPIC correctly predicted that nitrogen leaching losses increased due to CP, relative to MB, under CCR but not under SCR. Both the observed and simulated nitrogen loss results accepted the null hypothesis that equivalent N leaching would occur under NT

Table 5. The results of t-test used to assess the model reliability for tillage effects.

Variable	Rotation	Null hypothesis	Observed ^c	Simulated ^c	Comparison ^d
Drain flow	CCR ^a	$\mu_d = \mu_{CP} - \mu_{MB} = 0$	0.0011	0.0001	O
		$\mu_d = \mu_{NT} - \mu_{MB} = 0$	0.0002	0.0000	O
	SCR ^b	$\mu_d = \mu_{CP} - \mu_{MB} = 0$	0.0116	0.0001	O
		$\mu_d = \mu_{NT} - \mu_{MB} = 0$	0.1283	0.0006	X
N loss	CCR	$\mu_d = \mu_{CP} - \mu_{MB} = 0$	0.0121	0.0155	O
		$\mu_d = \mu_{NT} - \mu_{MB} = 0$	0.0597	0.0668	O
	SCR	$\mu_d = \mu_{CP} - \mu_{MB} = 0$	0.0737	0.1965	O
		$\mu_d = \mu_{MB} - \mu_{NT} = 0$	0.0001	0.3002	X

^aContinuous corn rotation

^bCorn and soybean rotation

^cP-value; $H_0: \mu_A - \mu_B = 0$, which means the population mean of an indicator under management alternative A is equivalent to that under management alternative B; H_A is $\mu_A - \mu_B > 0$; H_0 is rejected if P-value is less than the level of significance ($\alpha = 0.05$).

^dIf the t-test results are same between observation and simulation, mark O, otherwise X.

and MB for CCR. This same comparison was rejected under SCR measured conditions but accepted by EPIC. These results indicate that tillage effects on nitrogen loss vary according to cropping system, and that EPIC captured these effects except for the SCR NT and MB conditions. As a whole, the EPIC model adequately replicated the impacts of various tillage systems on the drainage flows and nitrogen losses.

The crop yield comparisons in Figure 5 reveal that EPIC failed to capture the observed yield variability due to tillage effects in 1990 and 1991 CCR and 1991 SCR. Although it is difficult to judge the model reliability using only a 3-year data set, the model seems to have a limited capability to reproduce the effects of different tillage treatments on crop yield. Chung et al. (1998) also found that EPIC's yield estimates were not sensitive to tillage for two watersheds in southwest Iowa. In general, EPIC yield estimates are consistent with long-term measured means, but fail to reflect year-to-year yield variability (Martin et al. 1993; Moulin and Beckie 1993; Kiniry et al. 1995).

EPIC Reliability for Crop Rotation Effects

Paired t-test results used to assess the model reliability for crop rotation effects are presented in Table 6. The null hypothesis, that the population mean of an indicator under CCR is equal to the mean under SCR, is rejected if the p-value is less than the level of significance ($\alpha = 0.05$).

The p-values showed good agreement between the observed and simulated results except for the MB drainage flows. The observed drain flows indicated that greater drainage flows occurred due to SCR relative to CCR, but identical values were predicted by the EPIC. For CP, both the observed and simulated results indicate no difference between SCR and CCR for drain flows, but greater nitrogen loss occurred under CCR than SCR. This is because of greater application rate of nitrogen within CCR. The simulated and measured outcomes across all three tillage treatments rejected the null hypothesis for nitrogen loss, indicating that greater nitrogen losses would result from CCR relative to SCR.

The yield comparisons (Figure 5) between the CCR and the SCR systems in 1991 reveal that EPIC was not able to reproduce the crop rotation effect on corn yields at this site. The model predicted a uniform crop yield regardless of cropping system, but the measured

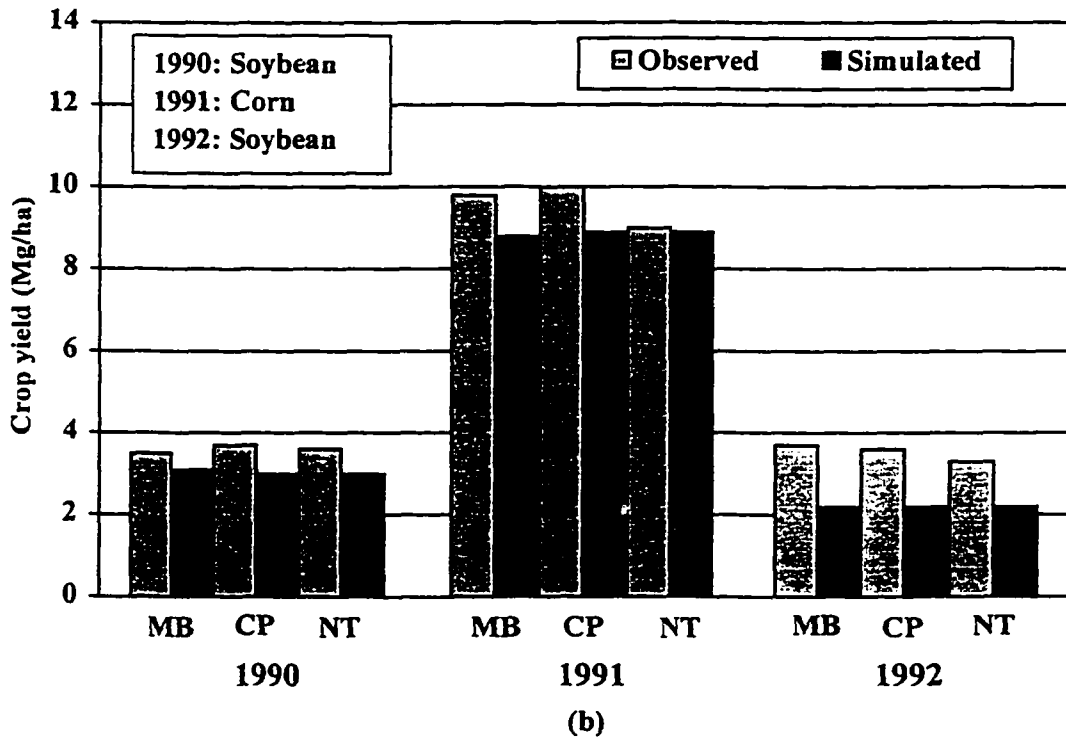
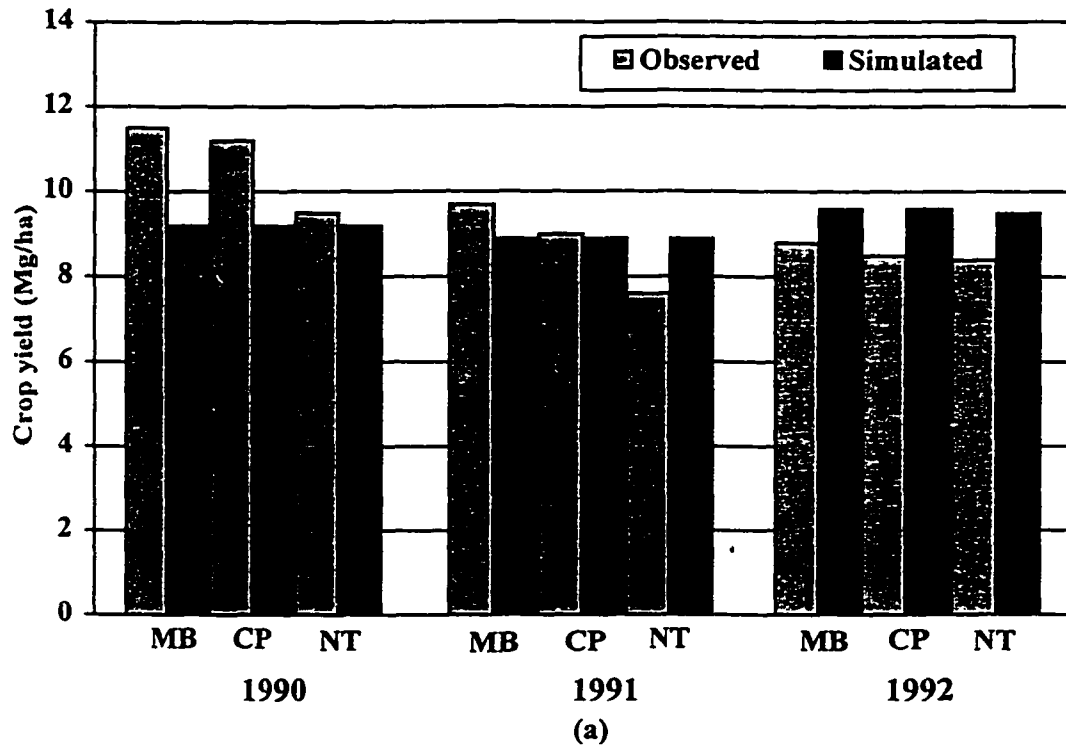


Figure 5. Observed and simulated crop yields under (a) continuous corn and (b) soybean-corn rotation systems for 1990-1992 at Nashua, Iowa.

Table 6. The results of t-test used to assess the model reliability for crop rotation effects.

Variable	Tillage	Null hypothesis	Observed ^d	Simulated ^d	Comparison ^e
Drain flow	MB ^a	$\mu_d = \mu_{SCR} - \mu_{CCR} = 0$	0.0418	0.4376	X
	CP ^b	$\mu_d = \mu_{CCR} - \mu_{SCR} = 0$	0.1790	0.1639	O
	NT ^c	$\mu_d = \mu_{CCR} - \mu_{SCR} = 0$	0.0000	0.0000	O
N loss	MB	$\mu_d = \mu_{CCR} - \mu_{SCR} = 0$	0.0061	0.0433	O
	CP	$\mu_d = \mu_{CCR} - \mu_{SCR} = 0$	0.0006	0.0084	O
	NT	$\mu_d = \mu_{CCR} - \mu_{SCR} = 0$	0.0008	0.0115	O

^aMoldboard plow

^bChisel plow

^cNo-till

^dP-value; $H_0: \mu_A - \mu_B = 0$, which means the population mean of an indicator under cropping system A is equal to that under B; $H_A: \mu_A - \mu_B > 0$; H_0 is rejected if P-value is less than the level of significance ($\alpha = 0.05$).

^eIf the t-test results are same between observation and simulation, mark O, otherwise X.

yields show that SCR corn yields exceeded CCR yields by almost 1 Mg/ha in 1991 for the conservation tillage systems.

Summary and Conclusions

The EPIC was evaluated to test its ability to replicate measured tile drain flow and associated nitrate losses for six alternative management systems over three years for data collected at research plots near Nashua, Iowa. The alternative management systems consisted of combinations of three tillage treatments (MB, CP, and NT) and two crop rotations (CCR and SCR)..

The statistical tests and graphical displays of the observed and simulated indicators revealed that the drain flows and leached nitrogen predicted by EPIC on an annual and monthly basis were acceptable for all management systems, except for the estimated nitrogen loss under SCR managed with no-till. In general, the EF and r^2 values for the drainage flows and leached nitrogen were satisfactory under all combinations of tillage and cropping systems. The r^2 values ranged 0.67-0.89 for the drain flows and 0.60-0.83 for the leached nitrogen. However, the predicted daily values contained abundant errors and missed peak drainage flows and nitrogen losses during several storm events. Moderately satisfactory r^2 values resulted from comparisons of observed and simulated daily values. The daily time step and the lack of a preferential flow component were discussed as possible source of errors.

The paired t-test results among various tillage and crop rotation systems clearly showed that the EPIC model was able to replicate the effects of variation in agricultural management on the amount of subsurface drain flow and nitrogen loss at this site. The paired t-test results for the tillage and crop rotation effects showed that the observed and simulated results were in agreement for 11 out of 14 total tests. However, the EPIC model showed a limited capability to replicate the impact of different tillage treatments and crop rotation systems on crop yield. The EPIC predicted crop yields were not sensitive to the different agricultural management systems, in contrast to what has been observed at the site.

Overall, EPIC proved sensitive to variations in tillage and cropping practices, producing satisfactory estimates of drainage flow and nitrate losses for the majority of

simulated management systems. The results presented here confirm that EPIC can be used to estimate nitrate losses in response to different management systems in integrated modeling frameworks such as RAPS, especially for establishing long-term trends for nitrate leaching losses. However, clear discrepancies occurred between some model estimates and corresponding measured values, such as peak losses for specific storm events and tile drainage flow and nitrate losses that occurred under no-tilled SCR. Two potential sources of these errors in EPIC include: (1) the lack of a preferential flow component, and (2) nitrogen transformation routines that may not adequately reflect all of the processes that occur in the field. Further testing and refinement of EPIC is required, both at Nashua (with 1993-96 measured data) and for other soil, landscape, and climate combinations, to improve the model capability to replicate management system impacts.

References

- Arnold, J. G., P. M. Allen, and G. Bernhardt. 1993. A comprehensive surface-groundwater flow model. *J. Hydrol.* 142:47-69.
- Babcock, B.A., J. Wu, T. Campbell, P.W. Gassman, P.D. Mitchell, T. Otake, M. Siemers, T.M. Hurley. 1997. RAPS 1997: Agriculture and the environmental quality. Center for Agricultural and Rural Development, Iowa State University, Ames, Iowa.
- Bouniols, A., M. Cabelguenne, C. A. Jones, A. Chalamet, J. L. Charpentreau, and J. R. Marty. 1991. Simulation of soybean nitrogen nutrition for a silty clay soil in southern France. *Field Crops Res.*, 26:19-34.
- Chow, V. T., D. R. Maidment, L. W. Mays. 1988. Applied hydrology. McGraw-Hill, Inc. New York.
- Chung, S. W., P. W. Gassman, L. A. Kramer, J. R. Williams, and R. Gu. 1998. Validation of EPIC for two watersheds in southwest Iowa. Submitted to the *J. Envr. Qual.*
- Johansen, N. B., J. L. Imhoff, J. L. Kittle, and A. S. Donigian, 1984. Hydrologic Simulation Program-Fortran (HSPF): User's Manual. EPA-600/3-84-066, U.S. EPA, Athens, Georgia.
- Kanwar, R. S., D. L. Karlen, T. S. Colvin, W. S. Simpkins, and V. J. McFadden. 1993. Evaluation of Tillage and Crop Rotation Effects on Groundwater Quality--Nashua Project.

- Leopold Grant No. 90-41, Iowa State University, National Soil Tilth laboratory, Ames, Iowa.
- Kiniry, J. R., D. J. Major, R. C. Izaurralde, J. R. Williams, P. W. Gassman, M. Morrison, R. Bergentine, and R. P. Zentner. 1995. EPIC model parameters for cereal, oilseed, and forage crops in the northern Great Plains region. *Can. J. Plant Sci.* 75:679-688.
- Lawn, R. J. and W. Brun. 1974. Symbiotic nitrogen fixation in soybeans. I. Effect of photosynthetic source-sink manipulations. *Crop Sci.*, 14:11-16.
- Leonard, R. A., W. G. Knisel, and D. A. Still. 1987. "GLEAMS: Groundwater Loading Effects of Agricultural Management Systems." *Trans. of the ASAE*, 30(5):1403-1418.
- Martin, S. M., M. A. Nearing, R. R. Bruce. 1993. An evaluation of the EPIC model for soybeans grown in southern piedmont soils. *Trans. of the ASAE*, 36(5):1327-1331.
- Mockus, V. 1969. Hydrologic soil-cover complexes. In: *SCS National Engineering Handbook, Section 4, Hydrology*. Soil Conservation Service, United States Department of Agriculture, Washington, D.C.
- Moulin, A. P. and H. J. Beckie. 1993. Evaluation of the CERES and EPIC models for predicting spring wheat grain yield over time. *Can. J. Plant Sci.* 73:713-719.
- Nash, J. E. and J. V. Sutcliffe. 1970. River flow forecasting through conceptual models, Part I, A discussion of principles. *J. Hydr.* 10:282-290.
- Patterson, T. G. and T. A. Larue. 1983. Nitrogen fixation (C_2H_2) by soybeans: cultivars and seasonal effects and comparison of estimates. *Crop Sci.*, 23:488-492.
- Phillips, R. E., R. L. Blevins, G. W. Thomas, W. W. Frye, and S. H. Phillips. 1980. No-tillage agriculture. *Sci.* 208:1108-1113.
- Rawls, W. J. and H. H. Richardson. 1983. Runoff curve number for conservation tillage. *J. Soil and Water Conser.* 38:494-496.
- Rawls, W. J., C. A. Onstad and H. H. Richardson. 1980. Residue and tillage effects on SCS runoff curve numbers. *Trans. ASAE* 23:357-361.
- SAS Inst. Inc. 1989. SAS/STAT user's guide, version 6, fourth edition, vol. 1. Cary, NC.
- Singh, P., and R. S. Kanwar. 1995. Modification of RZWQM for simulating subsurface drainage by adding a tile flow component. *Trans. ASAE* 38(2):489-498.

- Williams, J. R. 1990. The erosion productivity impact calculator (EPIC) model: a case history. *Phil. Trans. R. Soc. Lond.* 329: 421-428.
- Williams, J. R. 1990. The erosion productivity impact calculator (EPIC) model: a case history. *Philos. Trans. R. Soc. London* 329:421-428.
- Williams, J. R., A. D. Nicks, and J. G. Arnold. 1985. Simulator for water resources in rural basins. ASCE, *J. Hydraul. Eng.* 111(6):970-986.
- Williams, J. R., M. A. Nearing, A. D. Nick, E. L. Skidmore, and M. R. Savabi. 1996. Using soil erosion models for global change studies. *J. Soil and Water Conser.* 51:381-385.
- Williams, J.R. 1995. The EPIC Model. In: *Computer Models of Watershed Hydrology* (Ed.: V.P. Singh). Water Resources Publications, Highlands Ranch, Colorado.
- Wischmeier, W. H. and D. D. Smith. 1978. Predicting rainfall erosion losses - A guide to conservation planning. USDA Handbook No. 537. Washington, D. C.
- Young, R. A., C. A. Onstad, D. D. Bosch, and W. P. Anderson. 1987. AGNPS, agricultural non-point-source pollution model. USDA-ARS, Morris, MN, Conserv, Res. Rep. 35.
-

CHAPTER 7. GENERAL CONCLUSIONS

Model Development

A 2D reservoir toxic submodel was developed using finite difference numerical solutions to the laterally integrated hydrodynamics, mass transport, and transformation equations. The model is capable of simulating the fate and transport processes of various toxic contaminants, including advection and diffusion in the longitudinal and vertical directions, sorption and desorption, photolysis, hydrolysis, oxidation, biotransformation, volatilization, diffusive exchanges between the bottom sediment and water column, and sediment transport and deposition in a reservoir. The important feature of the model is that it accounts for the effects of reservoir flow regime on the physico-chemical reaction processes in a stratified reservoir. The model can be used to investigate the fate and transport of commonly used agricultural chemicals such as herbicides, fungicides, and insecticides in reservoirs. It also can be applied to a intended or existing reservoir for establishing a contingent plan to assist in spill control, sampling and remediation, and providing timely information for selective water intakes.

The model was applied to the Shasta Reservoir, California to investigate the effects of reservoir flow regime on the persistence and behavior of a spilled toxic compound, methyl isothiocyanate (MITC). The model was also calibrated and validated using field data for a herbicide, atrazine [2-chloro-4-ethylamino-6-isopropylamino-1,3,5-triazine], collected from the Saylorville Reservoir, Iowa. A mass balance model was constructed in the reservoir to estimate a time-variable kinetic transformation rate or half-life of atrazine. The 2D reservoir toxic model was used to simulate the occurrence, levels, and persistence of peak atrazine concentrations, and their temporal and spatial distributions in the reservoir.

Effects of Flow Regime on the MITC Degradation

The 2D reservoir toxic model showed a good performance in simulating various reservoir flow regimes: plunge flow, underflow, and interflow during the spill period as presented through flow velocities, water temperature, and chemical concentrations. The

results revealed that in the underflow and interflow regimes the kinetic degradation processes of MITC were slow, and that resulted in a long persistence of the chemical during the spill. The amount of MITC loss by chemical reactions decreased as the plume plunged into deep layers of the reservoir and formed the underflow and interflow due to a reduced volatilization rate. The reduction of chemical concentrations was mainly achieved by flow dilution due to transport and mixing processes in the early stage of the spill. However, the importance of the physico-chemical reaction processes increased with time as the turbulent mixing diminished. In the late stage of the spill, the effect of kinetic processes on the persistence of the contaminant became significant and the reduction of contaminant concentrations considerably relied on physico-chemical reactions, i.e., volatilization and hydrolysis.

The results of numerical experiments demonstrated that reservoir flow regime substantially affects the persistence and behavior of the contaminant. That is, the dilution levels in the interflow and overflow regimes were similar, but the plume moved more slowly and experienced greater chemical loss in the overflow. The overflow regime resulted in a reduced toxic contamination level (less persistent), shorter plume length, and longer response time compare to the interflow. These differences may be considered in water quality management as water intake structures and fishery facilities or other recreational activities are mostly located downstream near the dam. Therefore, wherever or whenever possible and practical, an interflow should be avoid and an overflow should be used to lower contamination levels and to leave longer response time after a toxic spill.

The Fate and Transport of Atrazine

The time-variable half-life of atrazine was estimated with a mass balance concept in the Saylorville Reservoir, Iowa. The half-life varied monthly from 2 to 58 days depending upon the environmental conditions, such as temperature, sunlight, and microorganism. A significant inverse relationship was obtained between the half-life and the daily hours of sunlight, showing the significance of photodegradation at the study site. The results support the findings in previous studies (Pelizzetti et al. 1990; Goldberg et al. 1991; Kolpin and Kalkhoff 1993; Torrents et al. 1997) that photolysis is an effective process for degrading

atrazine level and that sunlight is an important factor to degrade atrazine in surface water. The effect of nitrate concentration on the half-life of atrazine was insignificant possibly because the direct photolysis is a dominant atrazine degradation process rather than nitrate-mediated indirect photolysis at the study site. The estimated annual mass budget showed that a great portion of atrazine transported into the reservoir waterbody from the farm land was mainly controlled by outflows and kinetic transformations. However, a case study showed that an 86% increase in atrazine uses in the upper Des Moines River basin would alter the pattern of reservoir water quality response because the loading rate is greater than the self-purification capacity of the reservoir.

The results of 2D toxic model revealed that the fate and transport of atrazine in the reservoir are strongly related to the seasonal circulation patterns, thermal structures, and environmental conditions of the reservoir. In general, no strong thermal stratification was noticed from both observed and simulated results. The effect of short circuiting of flow on the transport of atrazine was notable during summer as less mixing and corresponding higher concentrations occurred near the surface of the reservoir. The model accurately simulated the temporal variations of observed atrazine concentrations and captured the peak concentrations during the late spring. The use of the site-specific and time-variable kinetic transformation rates of atrazine led to more accurate predictions of atrazine concentrations. The assumption of steady atrazine transformation rate over the entire periods resulted in a 40% overestimation in predicting peak concentrations. Therefore, an accurate estimation of atrazine transformation rates in a specific aquatic environment or during a season should be performed before model application because the persistence of a toxic chemical is substantially affected by environmental conditions such as temperature, sunlight, and microbial concentrations during different seasons.

Evaluation of EPIC Model

The EPIC evaluation study supported the earlier findings by Rawls et al. (1980) and Rawls and Richardson (1983) that standard tabulated curve number values (Mockus 1969) should be reduced to represent the impacts of residue cover on the partition of precipitation

between surface runoff and infiltration. In this study, the curve number values for conservation tillage treatments were adequately calibrated to take into account the crop residue effects. The reduction of 10% or less should be adequate for the majority of conservation tillage systems as determined previously by Rawls et al. (1980).

After the EPIC model was calibrated with the Treynor watershed data, the model captured the long-term trends of the hydrologic and environmental indicators during the validation period. The model was capable of replicating the long-term relative differences between the two tillage systems, which is the main emphasis in applying the model within many environmental impact analysis systems. However, results also revealed weaknesses in the model's ability to capture year-to-year variability due in part to simulating the watersheds in a homogeneous manner, which ignored complexities such as slope and soil variations. In the Nashua site, the drain flows and leached nitrogen predicted by EPIC on an annual and monthly basis were acceptable for all management systems, except for the estimated nitrogen loss under SCR managed with no-till. In general, the EF and r^2 values for the drainage flows and leached nitrogen were satisfactory under all combinations of tillage and cropping systems. However, the predicted daily values contained abundant errors and missed peak drainage flows and nitrogen losses during several storm events. The paired t-test results among various tillage and crop rotation systems clearly showed that the EPIC model was able to replicate the effects of variation in agricultural management on the amount of subsurface drain flow and nitrogen loss at Nashua site. But, the model showed a limited capability to replicate the impact of different tillage and crop rotation systems on crop yield at both sites, i.e., the EPIC predicted crop yields were not sensitive to the different management systems, in contrast to what has been observed at the sites.

Overall, EPIC proved sensitive to variations in tillage and cropping practices, producing satisfactory estimates of drainage flow, nitrate loss, and soil loss for the majority of simulated management systems. The results confirmed that EPIC can be used to estimate nitrate losses in response to different management systems in integrated modeling frameworks such as RAPS, especially for establishing long-term trends for nitrate leaching losses. However, clear discrepancies occurred between some model estimates and

corresponding measured values, such as peak losses for specific storm events and tile drainage flow and nitrate losses that occurred under no-tilled SCR. Two potential sources of these errors in EPIC include: (1) the lack of a preferential flow component, and (2) nitrogen transformation routines that may not adequately reflect all of the processes that occur in the field.

Contribution

This study enhanced the analytical capabilities of the reservoir water quality model (CE-QUAL-W2) and the understanding toward the fate and transport of toxic chemicals in a reservoir through model development and applications. The originality of this study is that it is the first research to investigate the effects of reservoir flow regime on the persistence and behavior of toxic contaminants in a stratified reservoir. The study also improved the understanding about the fate of atrazine and the environmental factors that affecting the persistence of the chemical in the surface water system. The EPIC validation studies presented the capabilities and limitations of the model as a tool for agricultural policy analysis and provided a practical guidance in the selection of the most suitable input parameters to depict different management systems.

Future Research

For future studies, more testing and validation efforts are required for the 2D reservoir toxic model to make the model more reliable. Field monitoring studies need to be conducted simultaneously to provide sufficient data and accurate model parameters such as kinetic transformation rate. Parameter and model uncertainties are areas of research and investigation requiring further work to better understand the limits of simulation. Ultimately, the model needs to be linked to a watershed model based on the concept of integrated modeling system (Srinivasan and Engel 1994; Srinivasan and Arnold 1994; Tim and Jolly 1994; Arnold et al. 1998) to assess trends in reservoir water quality to changing watershed management system. Limited studies have been attempted to link the instream water quality models to watershed models for simulating both hydrology and water quality on a river basin scale (Summer et al.

1990; Ramanarayanan et al. 1998). Unfortunately, most of nonpoint source simulation models are rarely validated and need further improvement for the simulation of transport and transformations of pesticides and toxic substances.

Since the intent of EPIC model in RAPS system is to apply the model over a wide range situations encountered in the study region, further testing and refinement of EPIC is required, both at Nashua (with 1993-96 measured data) and for other soil, landscape, and climate combinations, to improve EPIC's capability to replicate management system impacts (Gassman et al. 1998). The incorporation of preferential flow modeling component into the EPIC model may resolve the model weakness in predicting peak flows and chemical losses during heavy storm events.

References

- J. G. Arnold, R. Srinivasan, R. S. Muttiah, and J. R. Williams. 1998. Large area hydrologic modeling and assessment-Part I: Model development. 1998. *J. of the American Water Res. Assoc.* 34(1):73-89.
- Gassman, P. W., J. Wu, P. D. Mitchell, B. A. Babcock, T. M. Hurley, and S. W. Chung. 1998. Impact of U.S. agricultural policy on regional nitrogen losses. In Proceeding of 3rd International Conference on Diffuse Pollution (Poster Papers), 31 Aug.-4 Sept., Edinburg, Scotland. International Association of Water Quality, London, England. pp. 115-122.
- Goldberg, M. C., K. M. Cunningham, P. J. Squillace. 1991. Photolytic degradation of atrazine in the Cedar River, Iowa, and its tributaries. In U.S. Geol. Survey Toxic Substances Hydrology Program-Proceedings of the Technical Meeting, Mallard, G. E. and D. A. Aronson Eds., Monterey, CA, March 11-15.
- Kolpin, D. W. and S. J. Kalkhoff. 1993. Atrazine degradation in a small stream in Iowa. *Environ. Sci. Technol.*, 27(1):134-139.
- Mockus, V. 1969. Hydrologic soil-cover complexes. In: *SCS National Engineering Handbook, Section 4, Hydrology*. Soil Conservation Service, United States Department of Agriculture, Washington, D.C.
- Pelizzetti, E., V. Maurino, C. Minero, V. Carlin, E. Pramauro, O. Zerbinati and M. L. Tosato. 1990. Photocatalytic degradation of atrazine and other s-triazine herbicides. *Environ. Sci. Technol.*, 24:1559-1565.

- Ramanarayanan, T. S., R. Srinivasan, and J. G. Arnold. 1998. Modeling Wister Lake watershed using a GIS-linked basin-scale hydrologic/water quality model. Unpublished paper.
- Rawls, W. J., C. A. Onstad and H. H. Richardson. 1980. Residue and tillage effects on SCS runoff curve numbers. *Trans. ASAE* 23:357-361.
- Rawls, W. J. and H. H. Richardson. 1983. Runoff curve number for conservation tillage. *J. Soil and Water Conser.* 38:494-496.
- Srinivasan R., and B. A. Engel. 1994. A spatial decision support system for assessing agricultural nonpoint source pollution. *Water Resources Bulletin*, 30(3):441-452.
- Srinivasan R., and J. G. Arnold. 1994. Integration of a basin-scale water quality model with GIS. *Water Resources Bulletin*, 30(3):453-462.
- Summer, R. M., C. V. Alonso, and R. A. Young. 1990. Modeling linked watershed and lake processes for water quality management decisions. *J. Environ. Qual.* 19:421-427.
- Tim, U. S., and R. Jolly. 1994. Evaluating agricultural nonpoint-source pollution using integrated geographic information systems and hydrologic/water quality model. *J. Environ. Qual.* 23:25-35.
- Torrents, A., B. G. Anderson, S. Bilbouljian, W. E. Johnson, and C. J. Hapeman. 1997. Atrazine photolysis: Mechanistic investigations of direct and nitrate-mediated hydroxy radical processes and the influence of dissolved organic carbon from the Chesapeake Bay. *Environ. Sci. Technol.* 31:1476-1482.
-

APPENDIX. SOURCE PROGRAM OF THE 2D RESERVOIR TOXIC SUBMODEL

RETOX_2D.FOR: A Laterally Integrated 2D Reservoir Toxic Submodel
for the Fate and Transport of Toxic Substances
by Se-Woong Chung
Iowa State University

\$message: 'Compiling RETOX_2D.FOR'

```

SUBROUTINE RETOX_2D
**** Include inc files
  INCLUDE 'w2.inc'
**** Variables declaration
  REAL KOW, KAW, KE, KH, KP, KO, KV, KD, KD2
  REAL GKTOP, LFKR, LHLR, MOLWT, NUX, LKOW
  REAL KHN, KHA, KHB, KDPG, IO, IG
  REAL KBW1, KBW2, KBS1, KBS2
  REAL JDAY
  INTEGER NHL
  CHARACTER*20 NAME
  DOUBLE PRECISION DIFW, DIFFA
  DIMENSION DIFSS(KMC,IMC), BLOSS(KMC,IMC), HYDSS(KMC,IMC),
1          PHOSS(KMC,IMC), OXISS(KMC,IMC), VOLSS(KMC,IMC),
2          SETSS(KMC,IMC)
  DIMENSION BLOSSB(KMC,IMC), DIFSSB(KMC,IMC), SETSSB(KMC,IMC)
  DIMENSION FRCDW(KMC,IMC), FRCPW(KMC,IMC), FRCDB(KMC,IMC),
1          FRCPB(KMC,IMC)
  DIMENSION CCTB(KMC,IMC)
  DIMENSION PCW(KMC,IMC), PCB(KMC,IMC)
**** Common block declaration
  COMMON /GLOBLC/ JB,JC,IU,ID,KT,ELKT,DLT,KB(IMP),KTI(IMP)
  COMMON /H_LIFE/ NHL, HLDATE(12), HLLIFE(12)
  COMMON /SCRNC1/ JDAY, DLTS, ILOC, KLOC, MINDLT, JDMIN,
1          IMIN, KMIN, DLTAV, NIT, NV, YEAR,
2          ELTMJD
  COMMON /KIN_SS/ DIFSS, BLOSS, HYDSS, PHOSS, OXISS, VOLSS
  COMMON /SED_SS/ SETSS, SETSSB
  COMMON /TEMPC/ T1(KMP,IMP), T2(KMP,IMP)
  COMMON /TVDMTC/ TAIR, TDEW, CLOUD, PHI, ET, CSHE,
1          SRO, LAT, LONG
  COMMON /SETLC2/ SSETL, DSETL, ASETL, FESETL
  COMMON /SEDCOM/ TWSEDC(KMP,IMP), ABSEDC(KMP,IMP), TBSEDM(KMP,IMP),
1          BSEDC(KMP,IMP), POROS(KMP,IMP)
  COMMON /TOXICC/ CCTW(KMC,IMC), CCPW(KMC,IMC), CCDW(KMC,IMC),
1          CCPB(KMC,IMC), CCDB(KMC,IMC), CCTBSS(KMC,IMC)
  COMMON /FRCTON/ FRCDW, FRCPW, FRCDB, FRCPB
  COMMON /PHYTC2/ BETA, EXH2O, EXINOR, EXORG
  COMMON /GLBLCC/ PALT, ALGDET, O2LIM, WIND, WSCDP, WSC(NDP)
  COMMON /HYDRCL/ U(KMP,IMP), W(KMP,IMP), AZ(KMP,IMP),
1          RHO(KMP,IMP), NDLT(KMP,IMP)
  COMMON /GEOMHC/ EL(KMP), H(KMP), HKT1(IMP),

```

```

1          HKT2 (IMP)
COMMON /TOXCON/ CCTB
COMMON /GEOMBC/ B (KMP,IMP),      BKT (IMP),      BH (KMP,IMP),
1          BHKT1 (IMP), BHKT2 (IMP),  BHRKT1 (IMP), DLX (IMP)
COMMON /GEOMSD/ SAREA (KMP,IMP), SVOL (KMP,IMP), DELTAH (KMP,IMP)
COMMON /GEN_OPON/ GKTOP, LFKR, LHLR
COMMON /KR_OPTON/ HYDRO, PHOTO, OXIDO, BIODO, VOLAO, DIFEO, EXTRA
COMMON /HALFLIFE/ HLHYD, HLPHO, HLOXI, HLBIO, HLVOL
COMMON /CHEMICAL/ NAME, MOLWT, SOLUB, VPRE, LKOW, FOC
COMMON /SORPTION/ PARTW, PARTB, NUX
COMMON /HYDROLYS/ KHN, KHA, KHB, EAN, EAH, EAQH, TREFH
COMMON /PHOTOLYS/ KDPG, IO, IG
COMMON /OXIDATIN/ PKOX, TREFO, EOX
COMMON /BIOD_WAT/ KBW1, KBW2, PBACW, Q10W
COMMON /BIOD_BED/ KBS1, KBS2, PBACS, Q10S
COMMON /VOLATILI/ HENRY, CAIR

```

```
*****
```

```
Define and calculate constants
```

```
*****
```

```
C Universal gas constant (cal/deg-mol)
```

```
R=1.9872
```

```
C Molecular diffusivity for chemical (m2/sec) @ 25 degrees C
```

```
C in the water:
```

```
DIFFW=2.2E-09/(MOLWT**0.6666)
```

```
C in the air:
```

```
DIFFA=1.9E-04/(MOLWT**0.6666)
```

```
C Octanol-water partition coefficient
```

```
KOW = 10.00**LKOW
```

```
*****
```

```
Initialize variables
```

```
*****
```

```
DO I=IU, ID
```

```
DO K=KT, KB (I)
```

```
DIFSS (K, I) = 0.0
```

```
BIOSS (K, I) = 0.0
```

```
HYDSS (K, I) = 0.0
```

```
PHOSS (K, I) = 0.0
```

```
OXISS (K, I) = 0.0
```

```
VOLSS (K, I) = 0.0
```

```
SETSS (K, I) = 0.0
```

```
BIOSSB (K, I) = 0.0
```

```
DIFSSB (K, I) = 0.0
```

```
SETSSB (K, I) = 0.0
```

```
END DO
```

```
END DO
```

```
*****
```

```
Determine solids-water partition coefficient of the chemical in the
water column and bed sediments
```

```
*****
```

```
C in water column
```

```
PART = 0.617*FOC*KOW
```

```
DO I=IU, ID
```

```

DO K=KT,KB(I)
  IF (PARTW .EQ. 0.0) THEN
    PCW(K,I) = PART
  ELSE IF (PARTW .GT. 0.0) THEN
    PCW(K,I) = PARTW
  ELSE
    PCW(K,I) = 2.0*FOC*KOW/(1.0+TWSEDC(K,I)*FOC*KOW/1.0E6/NUX)
  END IF
END DO
END DO
C in the bed sediment
DO I=IU, ID
  DO K=KT,KB(I)
    IF(PARTB .EQ. 0.0) THEN
      PCB(K,I) = PART
    ELSE IF (PARTB .GT. 0.0) THEN
      PCB(K,I) = PARTB
    ELSE
      PCB(K,I) = 2.0*FOC*KOW/(1.0+BSEDC(K,I)*FOC*KOW/1.0E3/NUX)
    END IF
  END DO
END DO
END DO

```

```

*****
Determine the fraction constant of dissolved and sorbed chemical
*****

```

```

DO I=IU, ID
  DO K=KT,KB(I)
    FRCDW(K,I) = 1.0/(1.0+PCW(K,I)*TWSEDC(K,I)/1.0E6)
    FRCPW(K,I) = 1.0 - FRCDW(K,I)
    FRCDB(K,I) = 1.0/(1.0+PCB(K,I)*BSEDC(K,I)/1.0E3)
    FRCPB(K,I) = 1.0 - FRCDB(K,I)
  END DO
END DO

```

```

C Compute air-water partition coefficient of the chemical
KAW = HENRY/(8.206E-05*(TAIR+273.15))

```

```

*****
Calculate the physical, chemical, and biological reaction processes
*****

```

```

C Option 1: No kinetics
IF(GKTOP .EQ. 0) THEN
  DO I=IU, ID
    DO K=KT,KB(I)
      CCTWSS(K,I) = 0.0
      CCTBSS(K,I) = 0.0
    END DO
  END DO
  GOTO 9999
END IF

```

```

C Options 2: Lumped first-order kinetics and half-life
C Options 3: Time-variable first-order kinetics and half-life
IF(GKTOP .GE. 1) THEN
  IF (GKTOP .EQ. 2) THEN

```

```

LFKR = 0.693/LHLR
LFKR = LFKR/86400.
DO I=IU, ID
  DO K=KT, KB(I)
    CCTWSS(K, I) = -LFKR*CCTW(K, I)
  END DO
END DO
ELSE IF (GKTOP .EQ. 3) THEN
  DO I = 1, NHL
    IF (I .LT. NHL) THEN
      IF (JDAY.GE.HLDATE(I) .AND. JDAY.LT.HLDATE(I+1)) THEN
        LHLR = HLIFE(I)
      END IF
    ELSE IF (I .EQ. NHL) THEN
      LHLR = HLIFE(NHL)
    END IF
  END DO
  LFKR = 0.693/LHLR
  LFKR = LFKR/86400.
  DO I=IU, ID
    DO K=KT, KB(I)
      CCTWSS(K, I) = -LFKR*CCTW(K, I)
    END DO
  END DO
END IF
GOTO 9999
END IF

```

C Option 4: Input half-life for each kinetic reactions

```

IF (GKTOP .EQ. -2) THEN
C --- hydrolysis ---
  IF (HLHYD .NE. 0) THEN
    KH = 0.693/HLHYD/86400
    DO I=IU, ID
      DO K=KT, KB(I)
        HYDSS(K, I) = KH*FRCDW(K, I) *CCTW(K, I)
      END DO
    END DO
  END IF
C --- photolysis ---
  IF (HLPHO .NE. 0) THEN
    KP = 0.693/HLPHO/86400.
    DO I=IU, ID
      DO K=KT, KB(I)
        PHOSS(K, I) = KP*FRCDW(K, I) *CCTW(K, I)
      END DO
    END DO
  END IF
C --- oxidation ---
  IF (HLOXI .NE. 0) THEN
    KO = 0.693/(HLOXI*86400.)
    DO I=IU, ID
      DO K=KT, KB(I)
        OXISS(K, I) = KO*FRCDW(K, I) *CCTW(K, I)
      END DO
    END DO
  END IF

```

```

      END DO
    END IF
  C --- biodegradation ---
    IF (HLBIO .NE. 0) THEN
      HLBIO = 0.693/(HLBIO*86400.)
      DO I=IU, ID
        DO K=KT, KB(I)
          BIOSS(K, I) = HLBIO*FRCDW(K, I) *CCTW(K, I)
          BIOSSB(K, I) = HLBIO*FRCDB(K, I) *CCTB(K, I)
        END DO
      END DO
    END IF
  C --- volatilization ---
    IF (HLVOL .NE. 0) THEN
      KV = 0.693/(HLVOL*86400.)
      DEPTH = 0.0
      DO I=IU, ID
        DEPTH= HKT1(I)/2.0
        VOLSS(KT, I) = KV/DEPTH*(FRCDW(KT, I) *CCTW(KT, I) -CAIR/KAW)
        DO K=KT+1, KB(I)
          DEPTH=DEPTH+H(K)/2.0
          VOLSS(K, I) = KV/DEPTH*(FRCDW(K, I) *CCTW(K, I) -CAIR/KAW)
        END DO
      END DO
    END IF
  C Sum up the kinetic source and sink terms
    DO I=IU, ID
      DO K=KT, KB(I)
        CCTWSS(K, I) = -(BIOSS(K, I) +HYDSS(K, I) +PHOSS(K, I) +
1          OXISS(K, I)) -VOLSS(K, I)
      END DO
    END DO
    GOTO 9999
  END IF

  C Option 5: Estimate kinetic rates for each reaction
  IF (GKTOP .EQ. -1) THEN

  C (1) Biodegradation
    IF (BIODO .NE. 0) THEN
      IF (BIODO .EQ. 1) THEN
  C ---- pseudo-1st-order reaction
        DO I=IU, ID
          DO K=KT, KB(I)
            RKBW=KBW1*Q10W**((T1(K, I)-20.)/10)/86400.
            BIOSS(K, I) =RKBW*FRCDW(K, I) *CCTW(K, I)
            RKBS=KBS1*Q10S**((T1(K, I)-20.)/10)/86400.
            BIOSSB(K, I) =RKBS*FRCDB(K, I) *CCTB(K, I)
          END DO
        END DO
      ELSE
  C ---- 2nd-order-reaction
        DO I=IU, ID
          DO K=KT, KB(I)
            RKBW=KEW2*Q10W**((T1(K, I)-20.)/10) *PBACW/86400.

```

```

        BIOS (K, I) = RKBW * FRCDW (K, I) * CCTW (K, I)
        RKBS = KBS2 * Q10S ** ((T1 (K, I) - 20.) / 10) * PBACS / 86400.
        BIOSB (K, I) = RKBS * FRCDB (K, I) * CCTB (K, I)
    END DO
  END DO
END IF
END IF

C   (2) Hydrolysis
    IF (HYDRO .NE. 0) THEN
      IF (HYDRO .GT. 0) THEN
        KH = HYDRO / 86400.
C   ---- 1st-order rate constant
        DO I = IU, ID
          DO K = KT, KB (I)
            HYDSS (K, I) = KH * FRCDW (K, I) * CCTW (K, I)
          END DO
        END DO
      ELSE IF (HYDRO .EQ. -1) THEN
C   ---- 2nd-order rate: estimate using input parameters
        CALL HYDROL
      END IF
    END IF

C   (3) Photolysis
    IF (PHOTO .NE. 0) THEN
      IF (PHOTO .GT. 0) THEN
        PHPTO = PHOTO / 86400.
C   --- 1st-order rate constant
        DO I = IU, ID
          DO K = KT, KB (I)
            PHOSS (K, I) = PHOTO * FRCDW (K, I) * CCTW (K, I)
          END DO
        END DO
      ELSE IF (PHOTO .EQ. -1) THEN
        KDPG = KDPG / 86400.
        DEPTH = 0.0
C   --- Optional: Thomman and Mueller equation
        DO I = IU, ID
          DEPTH = HKT1 (I) / 2.0
          KE = EXH2O + EXINOR * SS (KT, I) + EXORG * (ALGAE (KT, I)
1          + DETRIT (KT, I))
          KP = KDPG * IO / IG * 1.33 * (1 - EXP (-KE * DEPTH)) /
1          (KE * DEPTH)
          PHOSS (KT, I) = KP * FRCDW (KT, I) * CCTW (KT, I)
          DO K = KT + 1, KB (I)
            DEPTH = DEPTH + H (K) / 2.0
            KE = EXH2O + EXINOR * SS (K, I) + EXORG * (ALGAE (K, I)
1            + DETRIT (K, I))
            KP = KDPG * IO / IG * 1.33 * (1 - EXP (-KE * DEPTH)) /
1            (KE * DEPTH)
            PHOSS (K, I) = KP * FRCDW (K, I) * CCTW (K, I)
          END DO
        END DO
      ELSE

```

```

C    --- Beer-Lambert formular: not used currently
      DO I=IU, ID
        DO K=KT, KB(I)
          PHOSS(K, I)=0.0
        END DO
      END DO
    END IF
  END IF

C    (4) Oxidation: Pseudo-first-order reaction
      IF(OXIDO .NE. 0) THEN
        PKOX = PKOX/86400.
        DO I=IU, ID
          DO K=KT, KB(I)
            TEMP = T1(K, I)+273.15
            TREF = TREF0+273.15
            XX = 1000.* (TEMP-TREF) / (R*TEMP*TREF)
            KO = PKOX*EXP (EOX*XX)
            OXISS(K, I) = KO*FRCDW(K, I) *CCTW(K, I)
          END DO
        END DO
      END IF

C    (5) Volatilization
      IF(VOLAO .NE. 0) THEN
C define constants and compute density (g/ml) and viscosity(m^2/s)
        XLAM2 = 4.
        CDRAG = 0.0011
        DENA = 0.001293/ (1.+0.00367*TAIR)
        XNUA = (1.32+0.009*TAIR) *1.E-05
        SCA = XNUA/DIFFA
        IF(VOLAO .GT. 0) THEN
          KV = VOLAO/86400.
C lumped first-order-rate constant: mostly for well-mixed waterbody
          DO I=IU, ID
            DEPTH= HKT1(I)/2.0
            VOLSS(KT, I)=KV/DEPTH* (FRCDW(KT, I) *CCTW(KT, I) -CAIR/KAW)
            DO K=KT+1, KB(I)
              DEPTH=DEPTH+H(K)/2.0
              VOLSS(K, I) = KV/DEPTH* (FRCDW(K, I) *CCTW(K, I) -CAIR/KAW)
            END DO
          END DO
        ELSE IF(VOLAO .EQ. -1) THEN
C    --- use O'Conner's formula to estimate KV
          USTAR = SQRT(CDRAG)*WIND
          DO I=IU, ID
            DEPTH= HKT1(I)/2.0
            DENW = RHO(KT, I)/1000.
            XNUW = (1.14-0.031*(T1(KT, I)-15)+0.00068*
1              (T1(KT, I)-15)**2) *1.E-06
            SCW = XNUW/DIFFW
            XKL = USTAR*SQRT (DENA/DENW) * (0.905/XLAM2) *
1              (1/SCW) **0.666+1.0E-09
            XKG = USTAR* (0.905/XLAM2) * (1/SCA) **0.666+1.E-09
            KV = 1.0/ (1./XKL+1./ (KAW*XKG) )
          END DO
        END IF
      END IF

```

```

VOLSS (KT, I) = KV/DEPTH* (FRCDW (KT, I) *CCTW (KT, I)
1          -CAIR/KAW)
DO K=KT+1,KB (I)
  DEPTH = DEPTH+H (K) /2.0
  DENW = RHO (K, I) /1000.
  XNUW = (1.14-0.031*(T1 (K, I) -15)+0.00068*
1        (T1 (K, I) -15)**2)*1.E-06
  SCW = XNUW/DIFFW
  XKL = USTAR*SQRT (DENA/DENW) * (0.905/XLAM2) *
1        (1/SCW)**0.666+1.0E-09
  XKG = USTAR*(0.905/XLAM2) * (1/SCA)**0.666+1.E-09
  KV = 1.0/(1./XKL+1./ (KAW*XKG))
  VOLSS (K, I) = KV/DEPTH* (FRCDW (K, I) *CCTW (K, I)
1          -CAIR/KAW)
END DO
END DO
ELSE IF (VOLAO .EQ. -2) THEN
C --- use Mackay equation to estimate KV
  USTAR=0.01*WIND*SQRT (6.1+0.63*WIND)
  XKG = USTAR*0.0462*(1/SCA)**0.666+1.E-03
  DO I=IU, ID
    DEPTH= HKT1 (I) /2.0
    DENW = RHO (KT, I) /1000.
    XNUW = (1.14-0.031*(T1 (KT, I) -15)+0.00068*
1        (T1 (KT, I) -15)**2)*1.E-06
    SCW = XNUW/DIFFW
    IF (USTAR .GT. 0.3) XKL=USTAR*0.00341*(1/SCW)**0.5
1        +1.E-06
    IF (USTAR .LE. 0.3) XKL=USTAR**2.2*0.0144*(1/SCW)**
1        0.5+1.E-06
    KV = 1.0/(1./XKL+1./ (KAW*XKG))
    VOLSS (KT, I) = KV/DEPTH* (FRCDW (KT, I) *CCTW (KT, I)
1        -CAIR/KAW)
    DO K=KT+1,KB (I)
      DEPTH=DEPTH+H (K) /2.0
      DENW = RHO (K, I) /1000.
      XNUW = (1.14-0.031*(T1 (K, I) -15)+0.00068*
1        (T1 (K, I) -15)**2)*1.E-06
      SCW = XNUW/DIFFW
      IF (USTAR .GT. 0.3) XKL=USTAR*0.00341*(1/SCW)**0.5
1        +1.E-06
      IF (USTAR .LE. 0.3) XKL=USTAR**2.2*0.0144*(1/SCW)**
1        0.5+1.E-06
      KV = 1.0/(1./XKL+1./ (KAW*XKG))
      VOLSS (K, I) = KV/DEPTH*FRCDW (K, I) *CCTW (K, I)
    END DO
  END DO
END IF
END IF
C (6) Diffusive exchange
IF (DIFEO .NE. 0) THEN
  DO I=IU, ID
    DO K=KT,KB (I)
      KD = 19.0*POROS (K, I) * (1/MOLWT)**0.666*1.0E-02

```

```

          KD = KD/86400.
          KD2= KD*SAREA(K,I)
          DIFSS(K,I)=KD2*(FRCDB(K,I)*CCTB(K,I)/POROS(K,I) -
1              FRCDW(K,I)*CCTW(K,I))/(BH(K,I)*DLX(I))
          DIFSSB(K,I)=KD2*(FRCDB(K,I)*CCTB(K,I)/POROS(K,I) -
1              FRCDW(K,I)*CCTW(K,I))/(SVOL(K,I)*POROS(K,I))
          END DO
        END DO
      END IF

```

C Sum up the kinetic source and sink terms

```

      DO I=IU,ID
        DO K=KT,KB(I)
          CCTWSS(K,I)=DIFSS(K,I) - (BIOSS(K,I)+HYDSS(K,I)+PHOSS(K,I)+
1              OXISS(K,I)) -VOLSS(K,I)
          CCTBSS(K,I)=-BIOSSB(K,I)-DIFSSB(K,I)
        END DO
      END DO
    END IF

```

9999 CONTINUE

```

*****
      Call subroutine SETTTL to compute the souce/sink due to settling
*****
      CALL SETTTL

```

```

*****
      Compute final source and sink terms for water column and bed sediment
*****
      DO I=IU,ID
        DO K=KT,KB(I)
          CCTWSS(K,I)=CCTWSS(K,I)+SETSS(K,I)
          CCTBSS(K,I)=CCTBSS(K,I)+SETSSB(K,I)
        END DO
      END DO
    END

```

```

*****
      HYDROL.FOR: SUBROUTINE for HYDROLYSIS IN WATER COLUMN
*****

```

\$message: 'Compiling HYDROL.FOR'

```

      SUBROUTINE HYDROL
      INCLUDE 'w2.inc'
      REAL KHN, KHA, KHB, NEUH
      COMMON /GLOBLC/ JB, JC, IU, ID, KT, ELKT, DLT, KB (IMP), KTI (IMP)
      COMMON /TEMPC/ T1 (KMP, IMP), T2 (KMP, IMP)
      COMMON /HYDROLYS/ KHN, KHA, KHB, EAN, EAH, EAOH, TREFH
      COMMON /FRCTON/ FRCDW(KMC, IMC), FRCPW(KMC, IMC),
1          FRCDB(KMC, IMC), FRCPB(KMC, IMC)
      COMMON /KIN_SS/ DIFSS(KMC, IMC), BIOSS(KMC, IMC), HYDSS(KMC, IMC),
1          PHOSS(KMC, IMC), OXISS(KMC, IMC), VOLSS(KMC, IMC),
      COMMON /TOXCON/ CCTB(KMC, IMC)
      COMMON /TOXICC/ CCTW(KMC, IMC), CCPW(KMC, IMC), CCDW(KMC, IMC),
1          CCPB(KMC, IMC), CCDB(KMC, IMC), CCTBSS(KMC, IMC)

```

```

R=1.9872
DO I=IU, ID
  DO K=KT, KB(I)
    TEMP = T1(K, I)+273.15
    TREF = TREFH+273.15
    HION = 10**(-PH(K, I))
    OH   = 10**(-14+PH(K, I))
    XX   = 1000.*(TEMP-TREF)/(R*TEMP*TREF)
    ALKH = KHB*EXP(EAOH*XX)
    NEUH = KHN*EXP(EAN*XX)
    ACIH = KHA*EXP(EAH*XX)
    KH   = ALKH*OH + NEUH + ACIH*HION
    HYDSS(K, I) = KH*FRCDW(K, I)*CCTW(K, I)
  END DO
END DO
END

```

```

*****
          SETTL.FOR: SUBROUTINE for settling of particulates
*****

```

```
$message: 'Compiling SETTL.FOR'
```

```

SUBROUTINE SETTL
  INCLUDE 'w2.inc'
  CHARACTER*3 ACC
  DIMENSION SSCW(KMC, IMC), SSCB(KMC, IMC)
  DIMENSION ALGCW(KMC, IMC), ALGCB(KMC, IMC)
  DIMENSION DETCW(KMC, IMC), DETCB(KMC, IMC)
  DOUBLE PRECISION FRW, FRB
  COMMON /GLOBLC/ JB, JC, IU, ID, KT, ELKT, DLT, KB(IMP), KTI(IMP)
  COMMON /SETLC2/ SSETL, DSETL, ASETL, FESETL
  COMMON /GEOMHC/ EL(KMP), H(KMP), HKT1(IMP), HKT2(IMP)
  COMMON /WBFRC/ FRW(KMP, IMP), FRB(KMP, IMP)
  COMMON /TOXICC/ CCTW(KMC, IMC), CCPW(KMC, IMC), CCDW(KMC, IMC),
1  CCPB(KMC, IMC), CCDB(KMC, IMC), CCTBSS(KMC, IMC)
  COMMON /FRCTON/ FRCDW(KMC, IMC), FRCPW(KMC, IMC),
1  FRCDB(KMC, IMC), FRCPB(KMC, IMC)
  COMMON /SED_SS/ SETSS(KMC, IMC), SETSSB(KMC, IMC)
  COMMON /TOXCON/ CCTB(KMC, IMC)
  COMMON /ACONST/ ACC(NCP)

```

```
C Initialize variables
```

```

DO I=IU, ID
  DO K=KT, KB(I)
    SSCW(K, I) = 0.0
    SSCB(K, I) = 0.0
    ALGCW(K, I) = 0.0
    ALGCB(K, I) = 0.0
    DETCW(K, I) = 0.0
    DETCB(K, I) = 0.0
  END DO
END DO

```

```
C Settling of inorganic suspended solid-sorbed toxicant
  IF(ACC(2) .EQ. 'ON') THEN

```

```

DO I=IU, ID
  SSCW(KT, I) = -SSETL*FRCPW(KT, I) *CCTW(KT, I) /HKT2 (I)
  SSCB(KT, I) = -SSCW(KT, I) *FRB(KT, I)
  DO K=KT+1, KB(I)
    SSCW(K, I) = SSETL*(FRCPW(K-1, I) *CCTW(K-1, I) -
1      FRCPW(K, I) *CCTW(K, I)) /H(K)
    SSCB(K, I) = SSETL*FRCPW(K, I) *CCTW(K, I) /H(K) *FRB(K, I)
  END DO
END DO
END IF

C Settling of algae-sorbed toxicant
IF(ACC(7) .EQ. ' ON') THEN
  DO I=IU, ID
    ALGCW(KT, I) = -ASETL*FRCPW(KT, I) *CCTW(KT, I) /HKT2 (I)
    ALGCB(KT, I) = -ALGCW(KT, I) *FRB(KT, I)
    DO K=KT+1, KB(I)
      ALGCW(K, I) = ASETL*(FRCPW(K-1, I) *CCTW(K-1, I) -
1      FRCPW(K, I) *CCTW(K, I)) /H(K)
      ALGCB(K, I) = ASETL*FRCPW(K, I) *CCTW(K, I) /H(K) *FRB(K, I)
    END DO
  END DO
END IF

C Settling of organic particles-sorbed toxicant
IF(ACC(8) .EQ. ' ON') THEN
  DO I=IU, ID
    DETCW(KT, I) = -DSETL*FRCPW(KT, I) *CCTW(KT, I) /HKT2 (I)
    DETCB(KT, I) = -DETCW(KT, I) *FRB(KT, I)
    DO K=KT+1, KB(I)
      DETCW(K, I) = DSETL*(FRCPW(K-1, I) *CCTW(K-1, I) -
1      FRCPW(K, I) *CCTW(K, I)) /H(K)
      DETCB(K, I) = DSETL*FRCPW(K, I) *CCTW(K, I) /H(K) *FRB(K, I)
    END DO
  END DO
END IF

C Compute total source and sink terms due to settling
DO I=IU, ID
  DO K=KT, KB(I)
    SETSS(K, I) =SSCW(K, I) +ALGCW(K, I) +DETCW(K, I)
    SETSSB(K, I) =SSCB(K, I) +ALGCB(K, I) +DETCB(K, I)
  END DO
END DO
END

```

```

*****
          TOXI1.FOR: SUBROUTINE for RETOX_2D.FOR
*****

```

C Read in input data from toxic.npt

\$message: 'Compiling TOXI1.FOR'

```

SUBROUTINE TOXI1
  INTEGER TON, OUT
  INTEGER NHL
  REAL GKTOP, LFKR, LHLR, MOLWT, NUX, LKOW

```

```

REAL KHN, KHA, KHB, KDPG, IO, IG
REAL KBW1, KBW2, KBS1, KBS2
CHARACTER*72 TITLE
CHARACTER*72 OUTFN, TONFN, SEDFN, TOXFN
CHARACTER*20 NAME
PARAMETER (TONFN='toxic.npt')

```

C Statement

```

DIMENSION TITLE(6)
DIMENSION HLDATE(12), HLIFE(12)
COMMON /H_LIFE/ NHL, HLDATE, HLIFE
COMMON /GEN_OPON/ GKTOP, LFKR, LHLR
COMMON /KR_OPTON/ HYDRO, PHOTO, OXIDO, BIODO, VOLAO, DIFEO, EXTRA
COMMON /HALFLIFE/ HLHYD, HLPHO, HLOXI, HLBIO, HLVOL
COMMON /CHEMICAL/ NAME, MOLWT, SOLUB, VPRES, LKOW, FOC
COMMON /SORPTION/ PARTW, PARTB, NUX
COMMON /HYDROLYS/ KHN, KHA, KHB, EAN, EAH, EAOH, TREFH
COMMON /PHOTOLYS/ KDPG, IO, IG
COMMON /OXIDATIN/ PKOX, TREFO, EOX
COMMON /BIOD_WAT/ KBW1, KBW2, PBACW, Q10W
COMMON /BIOD_BED/ KBS1, KBS2, PBACS, Q10S
COMMON /VOLATILI/ HENRY, CAIR
COMMON /BSEDOP/ OP4SI, OP4CI
COMMON /BSEDFN/ SEDFN, TOXFN
DATA TON /30/, OUT /33/
C Open toxic input file
OPEN(TON, FILE=TONFN, STATUS='OLD')
C Read title cards
READ(TON,*)
READ(TON,1000) (TITLE(J), J=1,6)
1000 FORMAT((//8X,A72))
C Read general kinetic options
READ(TON,1010) GKTOP, LFKR, LHLR
1010 FORMAT((//8X,3F8.2))
C Read numbers of half-life, HLDATE and HLIFE
READ(TON,1011) NHL
1011 FORMAT((//8X,I8))
READ(TON,1012) (HLDATE(I), I=1,NHL)
READ(TON,1012) (HLIFE(I), I=1,NHL)
1012 FORMAT((//8X,8F8.0))
READ(TON,1020) HYDRO, PHOTO, OXIDO, BIODO, VOLAO, DIFEO, EXTRA
1020 FORMAT((//8X,7F8.2))
READ(TON,1030) HLHYD, HLPHO, HLOXI, HLBIO, HLVOL
1030 FORMAT((//8X,5F8.2))
READ(TON,1040) NAME, MOLWT, SOLUB, VPRES, LKOW, FOC
1040 FORMAT((//8X, A16,5F8.2))
READ(TON,1050) OP4SI, OP4CI
1050 FORMAT((//8X,2F8.2))
READ(TON,1080) PARTW, PARTB, NUX
1080 FORMAT((//8X,2F8.2, F8.0))
READ(TON,1090) KHN, KHA, KHB, EAN, EAH, EAOH, TREFH
1090 FORMAT((//8X,7F8.2))
READ(TON,1100) KDPG, IO, IG
1100 FORMAT((//8X,F8.2,2F8.0))
READ(TON,1110) PKOX, TREFO, EOX
1110 FORMAT((//8X,3F8.2))

```

```

      READ(TON,1130) KBW1, KBW2, PBACW, Q10W
1130  FORMAT(//8X,2F8.2, F8.0, F8.2)
      READ(TON,1130) KBS1, KBS2, PBACS, Q10S
      READ(TON,1150) HENRY, CAIR
1150  FORMAT(//8X,2F8.0)
      READ(TON,1000) SEDEFN
      READ(TON,1000) TOXFN
      READ(TON,1000) BRSEFN
      READ(TON,1000) OUTFN
***** Convert unit of kinetic rate from /day to /sec
      KHA = KHA/86400.
      KHB = KHB/86400.
      KHN = KHN/86400.
      OPEN(OUT, FILE=OUTFN, STATUS='UNKNOWN')
***** Write the input data to output file(toxi.opt)
      WRITE(OUT,3000) (TITLE(J), J=1,6)
3000  FORMAT(// (1X,A72))
      WRITE(OUT,3010) GKTOP, LFKR, LHLR
3010  FORMAT(/1X,'Global kinetics options =',F8.2,
1      /1X,'Lumped first-order rate =',F8.2,
2      /1X,'Lumped half-life rate =',F8.2)
      WRITE(OUT,3011) NHL
3011  FORMAT(/1X,'Number of half-life =', I8)
      WRITE(OUT,3012) (HLDATE(I), I=1,NHL)
      WRITE(OUT,3012) (HLIFE(I), I=1,NHL)
3012  FORMAT(/ (8X,8F8.2))
      WRITE(OUT,3015)
3015  FORMAT(/1X,'Kinetic rate and option'//,
1      3X,' HYDRO PHOTO OXIDO BIODO VOLAO DIFEO EXTRA')
      WRITE(OUT,3020) HYDRO, PHOTO, OXIDO, BIODO, VOLAO, DIFEO, EXTRA
3020  FORMAT(3X,7F8.2)
      WRITE(OUT,3030) HLHYD, HLPHO, HLOXI, HLBIO, HLVOL
3030  FORMAT(/1X,'Half-life rate for each kinetic reaction',
1      /3X,' HLHYD HLPHO HLOXI HLBIO HLVOL',/3X,5F8.2)
      WRITE(OUT,3040)
3040  FORMAT(/1X,'Chemical Characteristics')
      WRITE(OUT,3045) NAME
3045  FORMAT(3X,'Name of chemical:',A20)
      WRITE(OUT,3046) MOLWT, SOLUB, VPRE, LKOW, FOC
3046  FORMAT(3X,'Molecular weight[g] =',F8.2,2X,'Solubility[mg/L] =',
1      F8.2,/3X,'Vapor Pressure[atm] =',E8.2,2X,'Log KOW
2      =',F8.2,/3X,'Fraction of organic carbon [FOC] =',F8.4)
      WRITE(OUT,3050) OP4SI,OP4CI
3050  FORMAT(/1X,'Initial bed sediment and chemical conditions',
1      /3X,'Bed sediment initial condition[kg/L] =',F8.2,
2      /3X,'Bed chemical initial condition[mg/L] =',F8.2)
      WRITE(OUT,3080) PARTW, PARTB, NUX
3080  FORMAT(/1X,'Partitioning option and data',
1      /3X,'Partitioning in water column :',F8.2,
2      /3X,'Partitioning in bed sediment :',F8.2,
3      /3X,'Sediment effect control factor:',E8.2)
      WRITE(OUT,3090) KHN, KHA, KHB, EAN, EAH, EAOH, TREFH
3090  FORMAT(/1X,'Input Parameters for Hydrolysis'//,
1      8X,'KHN',5X,'KHA',5X,'KHB',5X,'EAN',5X,'EAH',4X,'EAOH',
2      3X,'TREFH',/,3X,7F8.2)

```

```
WRITE(OUT,3100) KDPG, IO, IG
3100 FORMAT(/1X,'Input Parameters for Photolysis',/,
1      7X,'KDPG',6X,'IO',6X,'IG',/,3X,E8.2,2F8.2)
WRITE(OUT,3110) PKOX, TREFO, EOX
3110 FORMAT(/1X,'Input Parameters for Oxidation',/,
1      7X,'PKOX',3X,'TREFO',5X,'EOX',/,3X,3F8.2)
WRITE(OUT,3130) KBW1, KBW2, PBACW, Q10W, KBS1, KBS2, PBACS, Q10S
3130 FORMAT(/1X,'Input Parameters for Biodegradation',/,
1      7X,'KBW1',4X,'KBW2',3X,'PBACW',4X,'Q10W',/,3X,4F8.2,/,
2      7X,'KBS1',4X,'KBS2',3X,'PBACB',4X,'Q10B',/,3X,4F8.2)
WRITE(OUT,3150) HENRY, CAIR
3150 FORMAT(/1X,'Henry law constant[atm/mole/m^3] :',E8.2,/,
1      1X,'Chemical concentration in air [ppb]:',F8.2)

***** CLOSE FILES
CLOSE (TON)
CLOSE (OUT)
END
```

ACKNOWLEDGMENTS

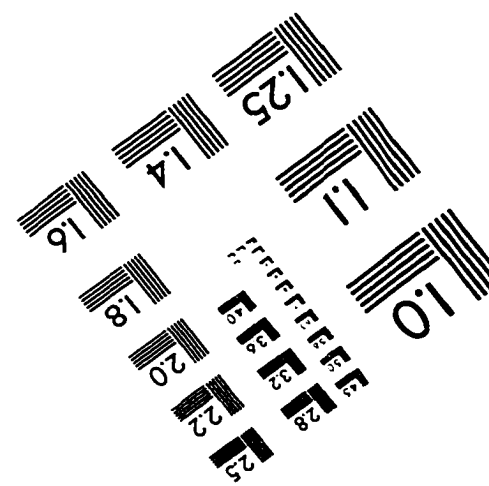
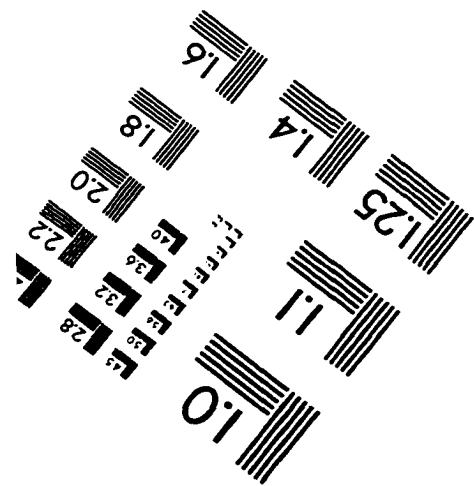
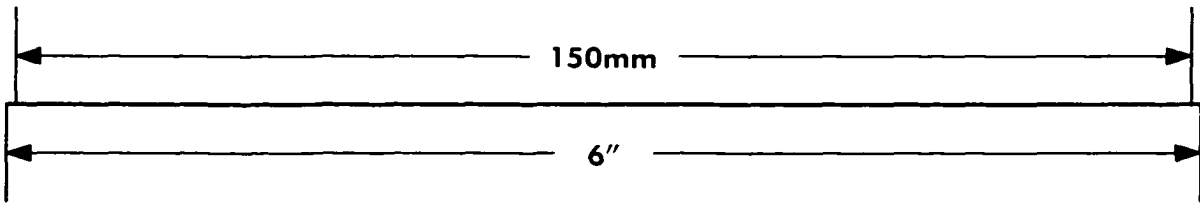
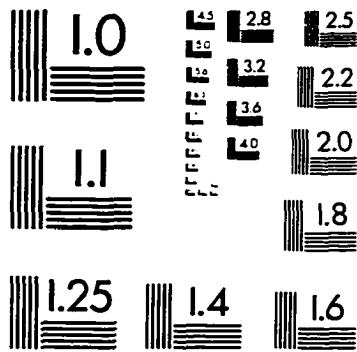
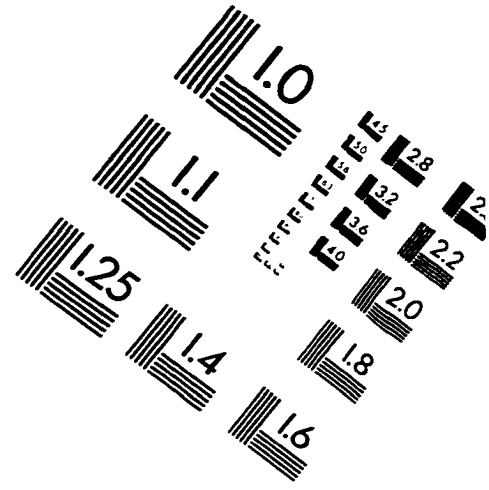
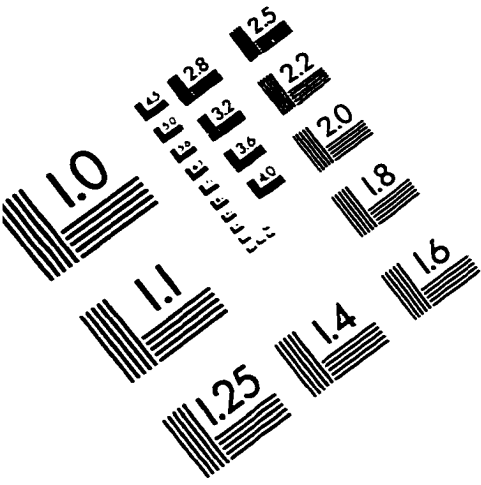
I sincerely appreciate my major professor Dr. Ruochuan Gu for the invaluable advice, guidance, and friendship he provided during the last five years. His engineering knowledge and deep insight make this work more successful. I would like to thank to Drs. Tom Al. Austin, LaDon Jones, Ramesh Kanwar, and Bruce Babcock for their advice and time spent serving on my graduate committee. I also would like to thank Mr. Phil Gassman for his kind cooperation and advice for the EPIC validation study.

Sincere appreciation is extended to Mr. Larry Kramer, Mrs. Donna Lutz, and Dr. Carl Pederson for providing valuable field data for this study, and also to many anonymous people who sampled and analyzed the field data. Special thanks are due to the Center for Agricultural and Rural Development (CARD) for supporting me through the research fund of the US Environmental Protection Agency (Agreement No. CR824165-01-0). I am deeply appreciate to the Korea Water Resources Corporation and the staff for allowing me to continue the Ph.D. study. Many thanks to my fellow Koreans for their encouragement through my graduate studies: Dr. Lim-Seok Kang, Mr. Koo-Youl Chong, Dr. Seon-Hong Kang, Dr. Chulsung Kim, Mr. Youn-Seob Lee, and Mrs. Hyejoung Han Seo.

Special thanks are extended to my mother Ki-Oak Kwon, parents-in-law Kang-Mook Lee and Pu-Ja Oh, my brother and sisters, and brothers-in-law for their love, support, and encouragement along the way. Deepest thanks go to my wife **Young-Ah** for her unchanging love and support that allowed me to finish this work. Thanks as well go to my lovely daughter **He-Joo Lydia** for the joy that she has brought into our lives during last two years.

Above all, I thank my God and the Lord Jesus Christ. His words provided me heavenly peace and wisdom at all times: "I am with you and will watch over you wherever you go, and I will bring you back to this land. I will not leave you until I have done what I have promised you." (Genesis 28:15).

IMAGE EVALUATION TEST TARGET (QA-3)



APPLIED IMAGE, Inc
1653 East Main Street
Rochester, NY 14609 USA
Phone: 716/482-0300
Fax: 716/288-5989

© 1993, Applied Image, Inc., All Rights Reserved